LIGAND-GATED CALCIUM MOBILISATION IN HIGHER PLANTS

By

George David Dickinson

A thesis submitted in part fulfilment of the degree of Doctor of Philosophy

Department of Biology

University of York

York

September 2002

Abstract

Ligand-gated Calcium Mobilisation in Higher Plants

George D. Dickinson

Calcium release from intracellular stores in plant cells is responsible for coupling a range of stimuli to specific responses. Cyclic ADP-ribose (cADPR) and nicotinamide adenine dinucleotide phosphate (NAADP), metabolites of NAD with Ca^{2+} mobilising activity, have recently been nominated as second messengers in plant cells with similar roles to that of inositol 1,4,5- trisphosphate ($InsP_3$). Little is known about the routes of metabolism of these compounds in plant cells or the nature, or means of regulation of the Ca^{2+}-permeable channels they act upon.

Using HPLC and a radioimmunoassay with antibodies raised against cADPR, the basal level of cADPR in red beet was determined to be in the pmol/mg range. A screen of plant tissue monitoring the formation of cyclic GDP-ribose (cGDPR) (a fluorescent analogue of cADPR) indicated that red beet, maize, *Arabidopsis* and cauliflower possess ADP-ribosyl cyclase activity. Characterisation of cauliflower cyclase activity indicated that cGDPR formation was dose-dependent (V_{max} = 2.8 mmol/g.h and K_m = 130.4 μM). Soluble and membrane activities varied and were differentially stimulated by cGMP suggesting the presence of soluble and membrane cyclases. The membrane cyclase was pH dependent with maximal activity at pH 10 and was half-maximally inhibited by 10 mM nicotinamide. Partial purification of solubilised cauliflower microsomes by column chromatography resulted in a 49-fold enrichment in activity.

Ligand-gated release channels in ER-enriched cauliflower microsomes were found to be modulated by pH and redox agents with H_2O_2 demonstrating biphasic regulation. Ligand-specific differences in modulation by pH and redox agents were observed that provide a potential mechanism for plant cells to generate specificity in Ca^{2+} signalling pathways.

A BLAST search of the *Arabidopsis* protein database uncovered several proteins containing SPRY domains indicative of ryanodine receptors. However, none of these sequences, or any others in the database, displayed significant homology to the ligand-gated Ca^{2+}-release channels of animals.

Contents

List of Figures

List of tables

Acknowledgements

I would like to thank Professor Dale Sanders for his supervision and encouragement over the course of this project and also for having the patience to proof read the draft copy of this thesis.

Special thanks are owed to Drs Anna Amtmann and Sandip Patel and the Sanders Lab for helpful discussions, expert advice, friendship and general support given.

Many thanks to my parents for their support over the years.

At long last, thanks to Helen and Michael for telling me to, "Get on with it."

List of Abbreviations

ABA	abscisic acid
ADPR	adenosine 5'-diphosphate-ribose
ATP	adenosine 5'-triphosphate
BAPTA	1,2-Bis(2-aminophenoxy)ethane-N,N,N',N'-tetraacetic acid
BLAST	basic local alignment search tool
BSA	bovine serum albumin
BTP	1,3-bis[tris(hydroxymethyl)methylamino]-propane
$[Ca^{2+}]_c$	cytosolic-free calcium ion concentration
$[Ca^{2+}]_v$	vacuolar calcium ion concentration
cADPR	cyclic adenosine 5'-diphosphribose
CaM	calmodulin
cAMP	adenosine 3',5'-cyclic monophosphate
CDPK	calcium-dependent protein kinase
cGDPR	cyclic GDP ribose
cGMP	cyclic Guanine monophasphate
CICR	calcium-induced calcium release
cIDPR	cyclic inosine diphosphate-ribose
DACC channel	depolarisation-activated channel
DAG	diacylgylcerol

DAPI	4',6-Diamidino-2-phenylindole
DEAE	diethylaminoethyl
DMSO	dimethyl suphoxide
DTT	dithioletheritol
EDTA	diaminoethanetetra-acetic acid
EGTA	ethyleneglycol-bis-(β-aminoethyl ether) N,N,N',N'-tetraacetic acid
ER	endoplasmic reticulum
EST	expressed sequence tag
FCCP	carbonyl cyanide *p*-(trifluoromethoxy)phenyl-hydrazone
GFP	green fluorescent protein
GNSO	S-nitrosoglutathione
GSH	reduced glutathione
GSSG	oxidised glutathione
HB	homogenisation buffer
HPLC	high pressure liquid chromatography
$InsP_3$	inositol 1,4,5-trisphosphate
$InsP_3R$	inositol 1,4,5-trisphosphate receptor
$InsP_6$	phytic acid
LEAC channel	large-conductance elicitor-activated channel
L-NMMA	N^G-monomethyl-L-arginine monoacetate

MES	2-[N-morpholino]ethanesulphonic acid
NAAD	nicotinic acid adenine dinucleotide
NAADP	nicotinic acid adenine dinucleotide phosphate
NAD	nicotinamide adenine dinucleotide
NADP	nicotinamide adenine dinucleotide phosphate
NGD	nicotinamide guanine dinucleotide
NO	nitric oxide
NOS	nitric oxide synthase
ODQ	1H-[1,2,4]Oxadiazole[4,3-a]quinoxalin-1-one
PA	perchloric acid
PCR	polymerase chain reaction
PIP_2	phosphatidylinositol 4,5 bisphosphate
PKC	protein kinase C
PLC	phospholipase C
PTIO	2-(4-Carboxyphenyl)-4,4,5,5-tetramethylimidazoline-1-oxyl-3-oxide
$Pt(4,5)IP_2$	phosphatidylinositol 4,5 bisphosphate
PMCA	plasma membrane calcium-ATPase
PMSF	phenylmethylsulfonylfluoride
PVP	polyvinyl pyrolidine
RIA	radioimmunoassay
ROC	receptor-operated channel

RyR	ryanodine receptor
SBTI	soybean trypsin inhibitor
SERCA	sarcoplasmic/endoplasmic reticulum calcium-ATPase
SEM	standard error of the mean
SHAM	salicylhydroxamic acid
SNAP	S-nitoso-N-acetyl-D,L-penacillamine
SNP	sodium nitroprusside
SOC	store-operated channel
SOD	super oxide dismutase
SV channel	slowly activating vacuolar channel
TCA	trichloroacetic acid
TFA	trifluoroacetic acid
TLC	thin layer chromatography
TMB-8	8-(N,N-di-methyamino)octyl 3,4,5-trimethoxybenzoate
TnC	troponin C
VDCC2 channel	voltage-dependent cation channel
VOC	voltage-operated channel
VK channel	calcium-activated K^+ channel
VVCa channel	vacuolar voltage-gated calcium channel
W-7	N-(6-Aminohexyl)-5-chloro-1-naphthalenesulfonamide hydrochloride

1. Introduction

1.1. Ca^{2+} as a second messenger in plants

In order to respond to their environment, combat stress, obtain nutrients and successfully develop and grow, complex multicellular organisms need to be able to link an array of stimuli to appropriate responses. Plants, being sessile, have not developed a nervous system for the rapid transduction of signals: they do, however, possess a complex hormone and peptide based system of signal transduction. While comparative analysis between the recently sequenced genomes of *Arabidopsis*, *Drosophila* and *Caenorhabditis* has suggested that the signalling pathways of plants contain several unique signalling cascades and protein receptor types, biochemical studies indicate that some signalling pathways in plants bare a resemblance to the endocrine system of animals in that they utilise second messengers, such as: calcium, cyclic nucleotides, pH and inositol 1,4,5-trisphosphate ($InsP_3$), to amplify signals and generate signal specificity (Bush, 1995; McCarty & Chory, 2000; The *Arabidopsis* Genome Initiative, 2000, Sanders *et al.*, 2002). Calcium, one of the essential plant nutrients, is of particular interest as it appears to act as a convergence point, linking a range of highly diverse stimuli to specific responses (Sanders *et al.*, 1999; 2002). The widespread role calcium plays in disparate stimulus-response pathways has raised an important question (McAinsh & Hetherington, 1998): how are changes in the concentration of a single ion within a plant cell able simultaneously to transduce signals between diverse stimuli and appropriate, specific, responses?

In mammalian cells, where calcium has become established as a second messenger, characteristic calcium signals, i.e. repetitive, transient elevations in cytosolic calcium concentration, have been recorded in a variety of cell types (Berridge, 2000). It is becoming increasingly clear that the spatio-temporal characteristics of these calcium signals are vital to their specificity and that these characteristics are modulated by other second messengers, in particular $InsP_3$ and the more recently discovered calcium-mobilising agents cyclic adenosine 5'-diphosphribose (cADPR) and nicotinic acid adenine dinucleotide phosphate (NAADP) (Berridge, 1997; Guse, 2002). Recently, it has been demonstrated that $InsP_3$, cADPR and NAADP are also capable of releasing calcium from intracellular

stores in plant cells (reviewed in Sanders *et al.*, 2002). Although, in comparison to the work in animals, the study of second messengers and calcium signals in plants is at an early stage, research carried out over the last ten years indicates that plant cells may also use $InsP_3$, cADPR and NAADP to impart specificity to a calcium signal.

The aim of this of this chapter is to review calcium physiology in plants, focusing on evidence supporting the role of calcium as a second messenger, the mechanisms used in generating a calcium signal and the current views on the manner in which plant cells use calcium to couple divergent stimuli to specific responses. This is used as a background for examining probable roles of $InsP_3$, cADPR and NAADP in signalling pathways in plant cells and ways in which these pathways, and their regulation, may lead to signal specificity. Brief comparisons to calcium signalling in animal cells are made where they are considered to be useful.

1.2. Ca^{2+} and plant physiology

Calcium is the second most abundant metal ion found in the majority of plant tissues (Epstein, 1972). Absorbed by the roots, millimolar concentrations of calcium ions (Ca^{2+}) are accumulated in tissues throughout a plant and a constant supply of 1-10 mM Ca^{2+} is required to maintain normal growth and development (Clarkson & Hanson, 1980). Such is its importance that even relatively brief Ca^{2+} starvation leads to the death of apical meristem cells and cessation of growth, whilst concentrations as high as 10% of the dry weight can be reached in mature leaves without signs of toxicity in some plant species (such as calcicoles which thrive in calcareous soils) because Ca^{2+} homeostasis is tightly regulated (Marschner, 1995).

1.2.1. Structural properties and compartmentation of Ca^{2+}

Most Ca^{2+} accumulated by a plant is found in the cell wall (Bush & McColl, 1987) and the vacuole (Clarkson & Hanson, 1980). The ion is thought to have a structural role in the cell wall, strengthening it by cross-linking carboxyl groups of pectic polymers (Cleland *et al.*, 1990). It is also believed that a high concentration of Ca^{2+} is required on the outside of the plasma membrane (PM) for it to maintain its function and integrity. In this case Ca^{2+} is considered to act by connecting phosphate and carboxylate groups of phospholipids and proteins (Cleland *et al.*, 1990). These structural roles are thought to arise from the ability of Ca^{2+} to form

reversible, yet stable, intermolecular linkages resulting from the high capacity of the Ca^{2+} ion coordination (McPhalen *et al.*, 1991).

The cytosol of plant cells contains a variety of high affinity Ca^{2+}-binding proteins such as calmodulin (CaM). The combined action of these proteins and Ca^{2+} homeostasis (transport) mechanisms results in a concentration of cytosolic free Ca^{2+} ($[Ca^{2+}]_c$) of 100-200 nM (Bush, 1995). The Ca^{2+}-binding proteins also restrict the rate of diffusion of Ca^{2+} in the cytosol.

Various organelles within the cell are able to sequester Ca^{2+} from the cytosol through the action of Ca^{2+}-pumps (see below). These organelles include the ER, vacuoles, chloroplasts and mitochondria. The relatively large volume of the vacuole in mature plant cells results in it being the principal accumulator of Ca^{2+} in many cells. Inside the vacuole, Ca^{2+} exists mainly as insoluble oxalic, phytic, and phosphoric salts. Never-the-less, mechanisms exist for releasing the ion into the cytosol, when required, from the vacuole and other organelles and thus these organelles act as internal stores of, potentially, millimolar concentrations of mobilizable Ca^{2+} for Ca^{2+} signalling (Marschner, 1995).

1.2.2. Ca^{2+} as a signalling ion

The low $[Ca^{2+}]_c$ levels measured in both plant and animal cells arise from tightly regulated Ca^{2+} homeostasis mechanisms that are believed to have evolved to limit the cytotoxic effects of Ca^{2+} - that is its ability to form lethal calcium phosphates and compete for enzyme Mg^{2+}-binding sites (Carafoli, 1987; Trump & Berezesky, 1995; Marschner, 1995). Low baseline $[Ca^{2+}]_c$ gives rise to the possibility of a rapid, manifold, increase in ion concentration upon the transport of a relatively small amount of Ca^{2+} into the cytoplasm and thus a minimal effect on the osmotic balance of the cell. This change in $[Ca^{2+}]_c$ is localised as a result of the calcium-buffering capacity of the cytoplasm and the action of Ca^{2+} pumps (Carafoli, 1994; Sanders *et al.*, 1999). The large, inward, electrochemical potential difference of Ca^{2+} resulting from homeostasis, combined with the low diffusibility and cytotoxicity of Ca^{2+} in the cytoplasm, has been attributed to the evolution of a mechanism of Ca^{2+} signalling in which brief elevations in $[Ca^{2+}]_c$ (spikes), arising from Ca^{2+} released across the PM or membranes of internal stores, are used as a signal (reviewed in Bootman & Berridge, 1995; Clapham, 1995; Berridge, 1997), modifying the activity of downstream Ca^{2+}-responsive elements.

Although spikes of Ca^{2+} are able to modify the activity of proteins close to the site of entry of Ca^{2+} into the cytoplasm, Cheng *et al.* (1993) demonstrated with muscle cells that Ca^{2+} can also act as a more global signal. These authors were able to record a wave of elevated Ca^{2+} moving through the cytoplasm of cells overloaded with Ca^{2+} that arose from the temporary activation of Ca^{2+}-permeable channels by Ca^{2+}, referred to as Ca^{2+}-induced Ca^{2+}-release (CICR). In animals, best characterised in the model systems of *Xenopus* oocytes and sea urchin eggs (Galione *et al.*, 1991; Parker & Yao, 1996), CICR allows a calcium signal to be transmitted throughout the cell using members of the $InsP_3$ receptor ($InsP_3R$) or ryanodine receptor (RyR) families. These two families of proteins are intracellular Ca^{2+}-permeable channels. The activity of $InsP_3R$ is modulated by $InsP_3$ and, in the case of at least two isoforms (see section 1.3.3.5), the activity of RyR is modulated by cADPR (Galione *et al.* 1991; Taylor & Traynor, 1995). The frequency of activity of these receptors can be modulated by their agonist and, thus, allow Ca^{2+}-waves to oscillate repetitively (Goldbeter *et al.*, 1990). Waves and oscillations of Ca^{2+} are believed to provide a means for plant and animal cells to encode information into both localised and global Ca^{2+} signals. This information can be used to generate signal specificity while maintaining $[Ca^{2+}]_c$ below cytotoxic levels (Berridge, 1997; Bootman & Berridge, 1997; Malhó *et al.* 1998).

1.2.3. Ca^{2+} signals in plant cells

1.2.3.1. Measuring changes in $[Ca^{2+}]_c$ in living plant cells

Experiments by Williamson & Ashley (1982) using the calcium-sensitive photoprotein aequorin first demonstrated a transient rise in $[Ca^{2+}]_c$ in plants during the action potential of the alga *Chara*. The large size of *Chara* cells made them amenable to microinjection and provided the first plant system where an increase in $[Ca^{2+}]_c$ was correlated with a response, in this case the cessation of cytoplasmic streaming that follows the action potential. Subsequently, measurements of changes in $[Ca^{2+}]_c$ have been carried out with Ca^{2+}-sensitive micro-electrodes in which two electrodes, a Ca^{2+}-sensitive electrode and a reference, were impaled into the cytoplasm of a cell (Brownlee & Wood, 1986; Miller & Sanders, 1987; reviewed in Felle, 1989). Thus, micro-electrodes were successfully used to monitor a tip-focused elevation in $[Ca_{2+}]_c$ in *Fucus* cells by Brownlee & Wood (1986) and by Miller & Sanders (1987) to measure light-induced changes in $[Ca^{2+}]_c$ in the alga *Nitellopsis*. While micro-electrodes continue to be used (often bound together as a

double-barrelled electrode) in investigations into Ca^{2+} homeostasis, they have a major drawback in that they can only measure Ca^{2+} at point locations within the cell.

The development of Ca^{2+}-sensitive fluorescent dyes, such as Calcium Green and Fura-2, provided a means for investigating the spatial and temporal distribution of Ca^{2+} throughout a cell (reviewed in Read *et al.*, 1993). Both single wavelength and ratiometric dyes, which allow the determination of $[Ca^{2+}]_c$, have been successfully used to visualise Ca^{2+} dynamics in plant cells (Gilroy *et al.*, 1991; Gilroy & Jones 1992; McAinsh *et al.*, 1997). Problems with loading Ca^{2+}-sensitive dyes into plant cells and sequestration of the dyes into intracellular organelles prompted the development of non-invasive recombinant technology in which aequorin (Read *et al.*, 1993; Knight *et al.*, 1991, 1992) and cameleon, a green fluorescent protein (GFP)-based Ca^{2+} indicator (Allen, 1999), have been expressed in transgenic plants. Even though cameleon technology has only recently been applied to plants and animals it has already proved to be a powerful technique for dissecting calcium signals (see below), overcoming difficulties with low-intensity light emission from aequorin that prevented resolution of Ca^{2+} signals at the single cell level (Takahashi *et al.*, 1999).

1.2.3.2. Coupling changes in $[Ca^{2+}]_c$ to stimulus-response pathways

The technical advances in monitoring Ca^{2+} in living cells have resulted in changes in $[Ca^{2+}]_c$ being implicated in the transduction of a rapidly growing list of stimuli in plants (Table 1.1). This evidence, however, is circumstantial with respect to whether Ca^{2+} is acting as a *bona fide* second messenger. For changes in $[Ca^{2+}]_c$ to be supported as coupling a specific stimulus to a response, three fundamental experimental criteria defined by Hepler & Wayne (1985) must be met: (1) a stimulus must induce a change in $[Ca^{2+}]_c$, (2) the change in $[Ca^{2+}]_c$ must precede the cellular response, and (3) the response can be blocked by inhibiting changes in $[Ca^{2+}]_c$. So far the number of systems in which these criteria have been met is far fewer than the number of systems in which changes in Ca^{2+} have been detected (Evans *et al.*, 2001; Rudd & Franklin Tong, 2001) as, in practice, inhibiting changes in $[Ca^{2+}]_c$ has proved to be difficult when intracellular stores are involved. For example, the action of antagonists of calcium release channels in animal cells, such as ruthenium red or heparin, are difficult to validate in plant cells (Marshall *et al.*, 1994). In addition the presence of the vacuole in a plant cell generally reduces the cytosol to a thin peripheral layer, complicating the detection of subtle changes in $[Ca^{2+}]_c$ (Malhó *et al*, 1998).

Table 1.1. Partial list of stimulus-response couples that involve an elevation in $[Ca^{2+}]_c$ in plant cells

Changes (↑↓) in $[Ca^{2+}]_c$ have been detected using injection of fluorescent dyes or transgenic plants expressing aequorin. Table adapted from Sanders *et al.* (1999) & Reddy (2001).

Stimulus	Response	Effect on $[Ca^{2+}]_c$	Reference
Red Light	Photomorphogenesis	↑	Shacklock *et al.* (1992)
Abscisic acid	Stomatal closure	↑,↓	McAinsh *et al.* (1990)
Auxin	Cell elongation and division	↑	Legue *et al.* (1997)
Gibberellin	α- Amylase secretion	↑	Bush & Jones (1988)
Salinity	Gene activation & Proline synthesis	↑	Knight *et al.* (1997)
Drought	Gene expression, synthesis of osmoprotectants & osmotolerance	↑	Knight *et al.* (1997) Johansson *et al.* (1996)
Gravity	Gravitropism	↑	Gehring *et al.* (1990)
Hypoosmotic stress	Osmoadaptation	↑	Taylor *et al.* (1996)
Touch	Growth retardation, thigmomorphogenesis.	↑	Knight *et al.* (1991)
Fungal elicitors	Phytoalexin synthesis	↑	Knight *et al.* (1991)
Cold	*COR* & *KIN1* gene expression, proline synthesis, changes in membrane lipids & cold acclimatization.	↑	Knight *et al.* (1996) Knight *et al.* (1999) Campell *et al.* (1996) Thomashow (1998)
Heat shock	Thermotolerance	↑	Gong *et al.* (1998)
Anoxia	Gene activation, adaptation to oxygen deprivation	↑	Subbaiah *et al.* (1994)
Oxidative stress	Free radical scavenger induction	↑	Price *et al.* (1994)
Ozone stress	Production of active oxygen species	↑	Clayton *et al.* (1999)
NOD factors	Root hair curling	↑	Ehrhardt *et al.* (1996)
Aluminium	Ion imbalance	↑,↓	Lindberg & Strid (1997)
Pathogens and elicitors	Phytoalexin biosynthesis and induction of hypersensitive response.	↑	Knight *et al.* (1991) Levine *et al.* (1996) Blume *et al.* (2000)

One example of a system where changes in $[Ca^{2+}]_c$ have been shown to be part of a signal transduction pathway is described by Bowler *et al.* (1994). Using micro-injection they introduced into *aurea* mutant tomato seedlings (in which phytochrome A is inactive) and wildtype seedlings both promoters of light-sensitive genes fused with β-glucuronidase (GUS) and a variety of signalling intermediates. Their experiments identified three calcium and/or cyclic guanine monophosphate (cGMP)-dependent pathways linking phytochrome activation to the stimulation of genes such as chalcone synthase (*CHS*), chlorophyll a,b binding protein (CAB) genes and genes encoding photosystem I (PSI). In a subsequent paper, Neuhaus *et al.* (1997) demonstrated that activation of phytochrome A also utilises a Ca^{2+}/cGMP dependent pathway to inhibit a negatively light-regulated gene (*ASI1*) encoding asparagine synthetase. The authors suggested that a family of promoter-repressor proteins with specific requirements for Ca^{2+} and cGMP would allow different responses to share a common signal transduction pathway.

Stomatal closure also involves changes in $[Ca^{2+}]_c$ in guard cells in response to various stimuli (Irving *et al.*, 1990; Irving *et al.*, 1992; MacRobbie, 1997) and has been used extensively to study the role Ca^{2+} plays as a second messenger in plant cells. Many aspects of Ca^{2+} signal transduction during abscisic acid (ABA)-induced stomatal closure in guard cells have been elucidated: ABA has been shown to elevate $[Ca^{2+}]_c$ in guard cells preceding stomatal closure (McAinsh *et al.*, 1990, 1992), inhibition of $[Ca^{2+}]_c$ elevation by microinjection of BAPTA has been demonstrated to inhibit stomatal closure (Webb *et al.*, 2001) and ABA-induced oscillations in $[Ca^{2+}]_c$ have been correlated with both ABA concentrations and stomatal aperture (Staxen *et al.*, 1999; Allen *et al.*, 2001). The impact guard cell Ca^{2+} signalling studies has had on our understanding of Ca^{2+}-signal specificity is discussed below.

Another area in which $[Ca^{2+}]_c$ has been identified as playing a central role is in polarised (tip) growth, following a report by Brownlee & Wood (1986) into the distribution of Ca^{2+} in germinating *Fucus serratus* zygotes. Using Ca^{2+}-selective microelectrodes they measured values of 2.47± 0.8 μM and 0.28± 0.06 μM $[Ca^{2+}]_c$ for tip and sub-tip regions of rhizoid cells. Fluorescence microscopy of zygotes that had been ester loaded with the fluorescent dye Quin-2 supported the evidence of the microelectrodes for a longitudinal gradient of $[Ca^{2+}]_c$. Brownlee & Wood suggested that the gradient was maintained by a flux of Ca^{2+} that enters the rhizoid tip through Ca^{2+}-channels and exits at the thallus end of the zygote and would

regulate cytoskeletal processes, exocytosis, ATPase activity and CaM-regulated processes. Since then $[Ca^{2+}]_c$ gradients have been shown to be important in the growth of root hairs of *Arabidopsis* (Wymer *et* al., 1997) and pollen tubes of *Lillium longiflorum* (Nobiling & Reiss, 1987; Holdaway-Clarke *et al.*, 1997; 1998) and *Papaver* (Franklin-Tong *et al.*, 1996).

1.2.4. Ca^{2+} signal specificity

Signalling events such as repetitive transient increases in Ca^{2+} (oscillations) and regenerative, progressive release of Ca^{2+} from internal stores (waves) (Kiegle *et al.*, 2000) have been detected alongside spatially localised Ca^{2+} signals and gradients in plants (Cessna *et al.*, 1998; Holdaway-Clark *et al.*, 1997; reviewed in Webb *et al.*, 1996, Trewavas, 1999). The Ca^{2+} waves and oscillations in plant cells are similar in nature to Ca^{2+} waves of *Xenopus* oocytes (Lechletter *et al.*, 1991) and Ca^{2+} oscillations of stimulated hepatocytes (Thomas *et al.*, 1991) and are thus thought to be responsible for determining the specificity of a signal by allowing a Ca^{2+} signal to be spatially and temporally localised with respect to Ca^{2+}-responsive elements (Malhó *et al.*, 1998).

1.2.4.1. Ca^{2+} waves

The main body of evidence for the existence of Ca^{2+} waves in plants arises from studies of the alga *Fucus*. In *Fucus* rhizoid cells hypo-osmotically induced Ca^{2+} transients originating from intracellular stores display spatial patterns that vary depending on the degree of hypo-osmotic treatment applied. A weak hypo-osmotic shock induced a wave of elevated $[Ca^{2+}]$ originating in the rhizoid apex (Taylor *et al.*, 1996). The application of a stronger hypo-osmotic shock, however, was followed by a brief elevation in apical Ca^{2+} and then a bi-directional wave of elevated Ca^{2+} propagating from the nuclear region (Goddard *et al.*, 2000). Importantly Goddard *et al.* observed that photorelease of caged $InsP_3$ was also able to generate elevations in $[Ca^{2+}]_c$ in a rhizoid cell. The photorelease of caged $InsP_3$ has also been reported to induce Ca^{2+} waves in *Papaver* pollen tubes (Malhó *et al.*, 1994, 1996). This suggests the existence of a similar mechanism of agonist induced Ca^{2+} wave propagation in plants as occurs for CICR in animal cells. A characteristic feature of these waves in animal cells is that they can be constrained to specific areas of the cell. Thus, different regions of the cytoplasm can be differentially regulated and different physiological processes controlled in the same cell by the same ion (Meyer, 1991; Berridge, 1997). This type of localised release of Ca^{2+} from internal stores

requires the existence of both an agonist-sensitive Ca^{2+}-release channel and an agonist. The evidence for the presence of $InsP_3$ and cADPR and their receptors in plants is discussed below.

1.2.4.2. Ca^{2+} oscillations

Stomatal guard cells have been used extensively to study $[Ca^{2+}]_c$ oscillations in plants as this cell type exhibits $[Ca^{2+}]_c$ oscillations induced by changes in external $[Ca^{2+}]$ and ABA (McAinsh *et al.*, 1995, Staxen *et al.*, 1996). The magnitude and frequency of the oscillations have also been correlated with the stomatal aperture of guard cells. This has provided a means for assessing the coupling of stimulus to an important functional response.

In an attempt to understand the mechanism by which Ca^{2+} oscillations link stimuli to stomatal closure various experimental methodologies have been employed. One strategy has been to examine the effects of manipulating elements of the Ca^{2+} entry and efflux pathways of guard cells or by damping $[Ca^{2+}]_c$ elevations through enhancing the cytosolic buffer capacity. For example, by microinjection of BAPTA into *Commelina communis* guard cells, Webb *et al.* (2001) have shown that inhibition of elevations in $[Ca^{2+}]_c$ resulted in inhibition of ABA-induced stomatal closure. Conversely, transient Ca^{2+} elevations have been induced by activation of plasma membrane Ca^{2+}-permeable channels by hyperpolarisation (Grabov & Blatt, 1998a) or application of H_2O_2 (Pei *et al.*, 2000) and linked to stimulation of stomatal closure. Changes in Ca^{2+} oscillations in guard cells coupled to changes in stomatal aperture have also been shown to be mediated by cADPR or $InsP_3$ (Leckie *et al.*, 1998, Staxen *et al.*, 1999). The role of cADPR and $InsP_3$ in the ABA signalling pathway is described in more detail below.

Another strategy for dissecting Ca^{2+} oscillations in guard cells has been to develop *Arabidopsis* guard cells transformed with the GFP-based Ca^{2+} sensor cameleon. This method, coupled with the manipulation of Ca^{2+} channel activity with membrane hyperpolarisation, confirmed that Ca^{2+} oscillations control both the stomatal closure response and the resting state of the aperture (Allen *et al.*, 2000, 2001). Furthermore, by combining the use of mutants defective in Ca^{2+} signalling components with cameleons it was demonstrated that the patterning of the oscillations is important in generating signal specificity. The mutant *det3* did not respond with the characteristic repetitive oscillations of Ca^{2+} seen in wild-type plants upon treatment with an increase in external Ca^{2+} or oxidative stress (Allen *et al.*,

2000) and its stomata did not close in response to the stimuli, as happens in the wild-type. Stomatal closure induced by cold or ABA, however, was unaffected and both the mutant and the wild-type plants displayed similar oscillatory Ca^{2+} patterns. In addition by artificially inducing a specific pattern of Ca^{2+} oscillations through manipulation of membrane polarization, stomatal closure could be induced in the mutant and wildtype plants. It is not known how the *det3* mutation was able to muddle the pattern of Ca^{2+} oscillation required to induce stomatal closure. The mutant is defective in a vacuolar proton pump, the V-type H^+-ATPase (Schumacher *et al.*, 1999). It has been hypothesised that the mutant is disrupted in the proton motive force across the vacuolar membrane and hence defective in H^+-driven vacuolar Ca^{2+} sequestration (see 1.3.2). This could prevent the necessary oscillations from occurring (Harper, 2001). A follow up study of the *gca2* mutant, a variant that does not close its stomata in response to ABA or Ca^{2+}, indicated that it too did not exhibit normal patterns of Ca^{2+} oscillations when stimulated (Allen *et al.*, 2001, reviewed in Sanders *et al.*, 2002).

Two other cell types that have been shown to demonstrate downstream responses to Ca^{2+} oscillations are *Arabidopsis* roots and pollen tubes. Using transgenic plants expressing aequorin, Sedbrook *et al.* (1996) observed that anoxic gene expression in *Arabidopsis* roots subjected to anaerobic conditions is preceded by repetitive Ca^{2+} spikes. Pollen tube growth rates have been linked to oscillations in Ca^{2+} gradients found in their tips (Rathore *et al.*, 1991, Miller *et al.*, 1992). Furthermore, Malhó & Trewavas (1996) have reported a correlation between the oscillation in the orientation of growth of a pollen tube and the oscillation in the $[Ca^{2+}]_c$ in the apical dome of pollen tubes displaying exaggerated oscillations in growth. However, as pollen tubes are also able to grow in the absence of detectable Ca^{2+} oscillations (Holdaway-Clarke *et al.*, 1997) it is difficult to determine the significance of the relationship between the oscillations and growth (Sanders *et al.*, 1999).

Ca^{2+} waves and oscillations have been described as being spatial and temporal manifestations of the same phenomenon (Malhó *et al.* 1998). Due to the limited diffusion of Ca^{2+} in the cytosol, both mechanisms rely on intracellular stores of Ca^{2+} to propagate and thus the distribution of intracellular stores has an impact on the spatial features of a signal. By varying in frequency or in amplitude, Ca^{2+} oscillations encode a signal with further information, and allow it to target specific responsive elements. A mechanism for decoding different patterns of Ca^{2+} oscillations has been put forward by Goldbeter *et al.* (1990) and McAinsh & Hetherington (1998). Based

on the action of Ca^{2+}-dependent kinases, such as calcinerurin B-like interacting protein kinases (CIPK), recently identified by Shi *et al.* (1999) and calcium-dependent protein kinase (CDPK) (Cheng *et al.*, 2002), and Ca^{2+}-independent phosphatases the model relies on differences in Ca^{2+} oscillations inducing differential phosphorylation of target proteins and thus different responses (reviewed Sanders *et al.*, 1999).

1.2.5. $InsP_3$ and calcium signalling

In animal cells, $InsP_3$ signalling is initiated through the action of an environmental stimulus (e.g. a hormone such as vasopressin or thyrotropin) which binds to a G-protein-coupled receptor (GPCR) located in the PM. Upon binding, the receptor-hormone complex catalyses the activation of a heterotrimeric G-protein that is able to stimulate phospholipase C (PLC) to hydrolyse phosphatidylinositol 4,5-bisphosphate (PIP_2) located in the PM, liberating the two second messengers diacylglycerol (DAG) and $InsP_3$. While DAG remains in the membrane activating protein kinase C (PKC) $InsP_3$, being soluble in water, diffuses into the cytosol and activates $InsP_3$-gated Ca^{2+} channels, elevating $[Ca^{2+}]_c$ and modulating the activity of Ca^{2+} binding proteins (for review see Berridge, 1989, 1993; Connor, 1993; Miyazaki, 1995).

Although the seven-membrane spanning GPCRs make up a major family of proteins in mammalian tissue there is no direct evidence for their having a role in $InsP_3$ metabolism in plants. The only seven-membrane spanning proteins thus far identified in plants are of the mildew resistance (MlO) class of proteins, which were identified through sequence analysis of the *Arabidopsis* genome and have not been assigned a physiological role (The *Arabidopsis* Genome Initiative, 2000). A superfamilly of putative GPCRs has been identified by screening an *Arabidopsis* cDNA library using a probe obtained by comparing plant expressed sequence tags (ESTs) and known GPCR sequences (Josefsson & Rask, 1997). However, this family is poorly conserved with established GPCRs.

The heterotrimeric G-protein of animals consists of the subunits Gα, Gβ and Gγ. G-protein α- and β-subunits have been isolated from plant tissue (reviewed by Ma, 1994) and biochemical studies by Ma indicate a protein displaying properties of γ-subunit is likely to exist (The *Arabidopsis* Genome Initiative, 2000). Furthermore, ABA-induced inhibition of guard cell opening has been shown to involve G-protein

regulation of K^+-influx (Wang *et al.*, 2001). However, analysis of the *Arabidopsis* genome suggests that plants may display far less variation in their subunits than animals. Whilst animals possess 23 different Gα, six Gβ and 12 Gγ subunits *Arabidopsis* contains single Gα and Gβ subunits and two putative Gγ subunits (Jones, 2002). Thus, the number of heterotrimeric complexes that a plant can produce appears to be far fewer than that of animals. As the variety of G-protein complexes formed in animals is thought to be vital to the generation of specificity in a G-protein-coupled signal the function of G-protein complexes in plant cells remains to be elucidated.

The most convincing evidence for the conservation of a PLC signalling system in plant cells comes from reports of $InsP_3$-induced Ca^{2+} release, from hypocotyl microsomes (Drøbak & Ferguson, 1985) and other internal membranes (Muir *et al.* 1997), with a pharmacological profile analogous to that of animal systems. The existence of $InsP_3$ responsive elements in plant cells, corroborated by the identification of an $InsP_3$ binding protein with similar properties to animal $InsP_3$Rs by Brosnan & Sanders (1993), implicates $InsP_3$ as a second messenger. This view has been strengthened by reports that stimuli such as ABA (Lee *et al.*, 1994), osmotic stress (Drøbak & Watkins, 2000), light (Kim *et al.*, 1996), fungal elicitors (Walton, 1995) and ethanol (Musgrave *et al.*, 1992) can increase intracellular levels of $InsP_3$ in plant tissue. Additionally the experiments of Blatt *et al.*, (1990) and Thiel *et al.*, (1990) have suggested that increases in guard cell and characean algal cell $[Ca^{2+}]_c$ can be elicited by increases in levels of cytosolic $InsP_3$, experimentally generated by micro-injection.

1.2.5.1. $InsP_3$ and stomatal movements

Stress induced stomatal closure is one of the physiological responses attributed to $InsP_3$ in plants (Assman, 1993). $InsP_3$ levels have also been demonstrated to increase in response to treatment with ABA as mentioned above (Coté & Crain, 1994). In addition, artificially increasing the concentration of $InsP_3$ in the cytosol of guard cells by intracellular injection and photorelease of caged $InsP_3$ (Gilroy *et al.*, 1990; Blatt *et al.*, 1990) has been shown to induce an increase in $[Ca^{2+}]_c$ preceding stomatal closure. The increase in $[Ca^{2+}]_c$ is thought to induce stomatal closure through the reversible activation of anion channels and inactivation of K^+ channels, a response seen upon treatment with ABA, both in cells where levels of $InsP_3$ have been stimulated by photolysis of caged $InsP_3$ (Blatt *et al.*, 1990) or through application of blue light (Kim *et al.*, 1996). Kim *et al.* also demonstrated that an

inhibitor of polyphosphoinositide hydrolysis (neomycin) was able to inhibit the accumulation of $InsP_3$ induced by blue light and K^+-channel closure and that a G-protein activator (mastoporan) was able to increase $InsP_3$ and close K^+-channels suggesting that phospholipase C-catalyzed hydrolysis of phosphoinositides, potentially mediated by a G-protein, may be involved in the signal-transduction pathway by which blue light closes K^+ channels.

Staxen *et al.* (1999) have recently provided further evidence for the role of $InsP_3$ in ABA-induced stomatal closure by showing that ABA-induced oscillations in guard cell $[Ca^{2+}]_c$ could involve a phosphoinositide-specific phospholipase C (PI-PLC) that was identified in a guard cell-enriched cDNA library. Staxen *et al.* microinjected guard cells of *C. communis* with fura-2. They observed that the pattern of ABA-induced oscillations in $[Ca^{2+}]_c$ was dependent on the concentration of ABA the guard cell was exposed to and also that the pattern correlated with the final stomatal aperture. They also observed that U-73122, a specific inhibitor of PI-PLC-dependent processes in animals which also inhibited recombinant PI-PLC activity isolated from the guard cell-enriched cDNA library, could inhibit both $[Ca^{2+}]_c$ oscillations and stomatal closure. From their experiments the authors concluded that PI-PLC plays a physiological role in the generation of ABA-induced oscillations and that the oscillations were involved in the maintenance of the stomatal aperture.

1.2.5.2. $InsP_3$ metabolism

Little is known about the metabolism of $InsP_3$ in plant cells (for recent review see Munnik, *et al.*, 1998). Attempts to measure endogenous levels of inositol phosphates in plant tissue using co-migration of [^{3}H]inositol-labelled compounds with standards on HPLC have been hindered in the past by the role of inositol in plant cells as a precursor for a wide range of interfering metabolic products (discussed in Coté & Crain, 1993). Further complicating the attempts to elucidate the metabolism of $InsP_3$ are the extremely low levels of $InsP_3$ and PIP_2 in plant tissue examined up to now (Munnik *et al.*, 1998; Brearley & Hanke, 2000). To some extent, these apparently low levels of $InsP_3$ and PIP_2 might be a reflection of the relatively small contribution to cell volume made by the cytosol in mature plant cells.

In vitro soluble and membrane-associated PLC activity with substrate specificity sufficient for a role in signalling has been reported in plant cells (Irvine *et al.*, 1980; Huang *et al.*, 1995; Tate *et al.*, 1989) and a gene encoding a phosphatidylinositol-specific Ca^{2+}-dependent PLC with significant homology to the mammalian PLC-δ

isoform has been isolated from *Arabidopsis* (Hirayama *et al.*, 1995). However, the phospholipase C-induced production of $InsP_3$ has only recently been demonstrated *in vivo* (Brearley *et al.*, 1997). As in animal cells, the activities of plant PLCs are dependent on Ca^{2+}, with an increase over a physiological range stimulating activity. As Ca^{2+} concentrations increase the substrate preference of PLCs is also altered, with higher concentrations of Ca^{2+} favouring hydrolysis of phosphatidylinositol over its mono- or bis-phosphates (reviewed in Munnik *et al.*, 1998). This represents a possible means of *in vivo* regulation of PLC activity.

Early studies following the fate of radio-labelled inositol phosphates incubated with various plant homogenates or cell fractions indicated that plants are able to metabolise $InsP_3$: Drøbak *et al.* (1991) and Martinoia *et al.* (1993) demonstrated that soluble extracts from pea roots and barley mesophyll could dephosphorylate $InsP_3$ back to 1,4- and 4,5- bisphosphates. A recent report by DeWald *et al.* (2001) indicates that, although levels of PIP_2 in *Arabidopsis* plant tissue are very low in comparison with yeast, algae and mammalian cells, upon salt or osmotic stress both PIP_2 and $InsP_3$ levels rapidly increase. These findings compliment earlier studies by Hirayama *et al.* (1995) and Mikami *et al.* (1998) who showed that *Arabidopsis* phosphatidylinositol-4-phosphate 5-kinase (PIP5K) (responsible for the production of PIP_2) and a PI-PLC are transcriptionally up-regulated in response to both water stress and ABA. This is consistent with a stress activated, phosphoinositide-based, signalling pathway similar to that seen in animal cells.

Another route of metabolism for $InsP_3$ is for it to be phosphorylated by $InsP_3$ 3-kinase to inositol 1,3,4,5-tetrakisphosphate ($Ins(1,3,4,5)P_4$), an important regulator of signal transduction in animals. $Ins(1,3,4,5)P_4$ can, in turn, be dephosphorylated to form inositol 1,3-bisphosphate ($Ins(1,3)P_2$) from which various isomers of tetrakis-, pentakis-, as well as hexakisphosphate are synthesised (reviewed in Coté & Crain, 1993; Munnik *et al.*, 1998). Whether $InsP_4$ has an important signalling role in plants is unknown. Although higher plants cells have been shown to be able to phosphorylate $InsP_3$ it is to $Ins(1,4,5,6)P_4$, via 6-kinase activity, not $Ins(1,3,4,5)P_4$ (Chattaway *et al.*, 1992). $InsP_3$ 3-kinase activity has been described in the alga *Chlamydomonas* but its physiological relevance has not been deduced (Irvine *et al.*, 1992) and there have been no reports of 3-kinase activity in higher plants.

DePass *et al.* (2001) recently attempted to determine the preferential pathway of $InsP_3$ degradation in higher plant cells. They microinjected stamen hairs of

Tradescantia virginiana L. with the calcium sensitive dye fura-2-dextran and either $InsP_3$ or analogs that were selectively resistant to either the 5-phosphatase or 3-kinase activity. Following microinjection of $InsP_3$ they observed a transient Ca^{2+} signal. A similar transient signal was seen upon injection of the 3-kinase insensitive 3-fluoro-3deoxy $InsP_3$. However following injection of a 5-monophosphorothioate derivative of $InsP_3$, a signal was observed that remained elevated for significantly longer. From this they suggest that the 5-phosphate pathway for $InsP_3$ metabolism is the preferred pathway in vivo in stamen hair cells of *Tradescantia*, and possibly other plant species.

1.2.6. cADPR and Ca^{2+} signalling

cADPR was discovered in 1987, during investigations of Ca^{2+} mobilisation in sea urchin eggs. This compound functions, in animal cells, as an endogenous regulator of the CICR mechanism, apparently by increasing the sensitivity of RyR isoforms 2 and 3 to Ca^{2+} (Mészáros *et al.*, 1993; Lee *et al.*, 1995a; Sonnleitner *et al.*, 1998). The Ca^{2+} mobilising activity of cADPR has also been described in over 40 other cell systems (Lee *et al.,* 1995b), including plants and the primitive, unicellular protist *Euglena gracilis* (Masuda *et al.*, 1997), suggesting that it, like $InsP_3$, regulates a global, conserved Ca^{2+} signalling mechanism.

cADPR was first reported to mobilise Ca^{2+} from the vacuoles of plants by Allen *et al.* (1995). The authors used a $^{45}Ca^{2+}$ flux assay with vacuole-enriched microsomes and patch-clamp analysis of intact vacuoles prepared from the storage root of red beet. By carrying out cross-desensitisation studies they were able to demonstrate that cADPR releases Ca^{2+} using a different pathway to $InsP_3$ and thus a cADPR signalling pathway co-exists with an $InsP_3$ signalling pathway at the vacuolar membrane. It was hypothesised that both cADPR- and $InsP_3$-gated Ca^{2+} release was likely to act as a trigger for CICR. Further studies by Muir & Sanders (1996) indicated that cADPR-induced release was also modulated by agonists and antagonists of the ryanodine receptor. Taken together this provides strong evidence that the release pathway was one likely to be conserved with that of animal cells.

1.2.6.1. The ABA/cADPR signalling pathway

Pioneering work from the lab of Chua (Wu *et al.*, 1997) made use of single-cell microinjection experiments to identify intermediates of ABA signal transduction pathways in tomato hypocotyl cells. The authors demonstrated that cADPR was not

only capable of regulating $[Ca^{2+}]_c$, but was a Ca^{2+}-mobilizing second messenger in its own right, acting separately to other ABA signalling steps. In this study, a bioassay for cADPR indicated that levels of cADPR increased following treatment with ABA. Furthermore, it was demonstrated that injection of cADPR could activate downstream ABA induced genes (GUS-linked *Kin2* and *rd29A*) in the absence of ABA and also that the pathway was both dependent upon Ca^{2+} and could be blocked by 8-amino-cADPR, a specific antagonist of the cADPR receptor (Walseth & Lee, 1993). Injection of ADP-ribosyl cyclase was able to mimic the effects of cADPR, presumably via the formation of cADPR from endogenous NAD. The data of Walseth & Lee also indicated that while $InsP_3$ could activate the same expression of the same genes as ABA and cADPR, its pathway could be blocked with heparin while that of ABA-cADPR was not, corroborating the suggestion of Allen *et al.* (1995) that cADPR- and $InsP_3$-induced Ca^{2+} release occurs through different pathways.

Further evidence for a role for cADPR in plant cell signalling came when Leckie *et al.* (1998) demonstrated that cADPR could elevate intracellular Ca^{2+} by mobilising intracellular stores. Microinjection of cADPR into the cytosol of guard cells of *C. communis* resulted both in an increase in $[Ca^{2+}]_c$ and in a decrease in cell turgor commensurate with stomatal closure induced by ABA. Patch-clamp analysis of vacuoles isolated from the guard cells indicated that they were competent to respond to cADPR but also that cADPR-induced Ca^{2+}-currents were inhibited by $[Ca^{2+}]_c$ above 600 nM. Additionally, these authors showed that microinjection of 8-amino-cADPR reduced the rate of turgor loss induced by ABA and that nicotinamide, an inhibitor of ADP-ribosyl cyclase, blocked ABA-induced stomatal closure in a dose dependent manner. Injection of ADPR, an analogue of cADPR with limited Ca^{2+}-mobilising activity did not affect ABA-induced changes in turgor. Together with the results of Wu *et al.* (1997), these data suggests that cADPR is a *bona fide* signalling molecule in plants. The data also highlight an unexpected difference between the cADPR-induced Ca^{2+} mobilisation pathways of plant guard cells and animals: as cADPR-induced Ca^{2+} release was inhibited by $[Ca^{2+}]_c$ above 600 nM, the cADPR-pathway is unlikely to directly involved in CICR. It has been proposed that CICR may instead be regulated by voltage-activated cation channels identified in red beet vacuolar vesicles (Bewell *et al.*, 1999) that are probably identical to the ubiquitous slow-vacuolar (SV) channel (Hedrich *et al.*, 1988; Ward & Schroeder, 1994).

1.2.6.2. Nitric oxide/cADPR pathway

In addition to the activation of ABA inducible genes, cADPR has also been implicated in the mediation of gene expression in plants as part of a nitric oxide (NO)/cADPR-pathway homologous to one previously identified in animal cells. Initially characterised in sea urchin eggs (Galione *et al.*, 1993), the NO pathway links Ca^{2+} mobilisation to NO through cGMP activation of ADP-ribosyl cyclase and has been observed in various cell types including neurosecretory cells (Clementi *et al.*, 1996) and rat hippocampal cells (Reyes-Harde *et al.*, 1999). Plants have been known to accumulate and metabolise NO since 1986 (Nishimura *et al.*, 1986). NO levels are increased during pathogen attack (Delledonde *et al.*, 1998) via the activation of NO synthase (NOS) as part of their disease resistance response. Increases in NO arising from addition of gaseous NO or from the addition of exogenous NO donors, like sodium nitroprusside (SNP), have been demonstrated: (1) to cause transient elevations in cGMP levels in cells from spruce needles (Pfeiffer *et al.*, 1994), bean (Brown & Newton, 1992) and barley aleurone (Penson *et al.*, 1996) and (2) to induce in tobacco plants or cell suspensions the expression of the plant defence genes *PAL* and *PR-1* (encoding phenylalanine ammonia lyase and pathogensis-related (PR)-1 protein, respectively). The induction of *PAL* and *PR-1* can be mimicked by cADPR and cGMP, and is blocked by ruthenium red (Durner *et al.*, 1998), 8-bromo-cADPR and inhibitors of NOS such as N^G-monomethyl-L-arginine monacetate (L-NMMA) (Klessig *et al.*, 2000). The evidence suggests that NO acts by elevating cGMP which in turn elevates cADPR, presumably as in animal cells via ADP-ribosyl cyclase (Wilmott *et al.*, 1996), mobilising internal Ca^{2+} and activating defence gene induction. Salicylic acid has also been found to be crucial for NO- and cADPR-induced activation of *PR-1* expression, but not that of *PAL*, indicating that NO/cADPR activation of defence responses has salicylic acid-dependent and independent pathways (Klessig *et al.*, 2000).

1.2.7. NAADP and Ca^{2+} signalling

The finding that NAADP is a potent mobiliser of Ca^{2+} from $InsP_3$- and cADPR-independent stores in: sea urchin eggs (Lee & Aarhus, 1995); brain (Bak *et al.*, 1999) and pancreatic acinar cells (Cancela *et al.*, 1999), prompted an investigation into the role of this compound in plant tissue. Initial desensitisation experiments with *Arabidopsis*, carried out by Wu *et al.* (1997), provided the first evidence that plant tissue contains endogenous NAADP. Later the ability of NAADP to mobilise Ca^{2+} in plants was assessed by Navazio *et al.* (2000) using vesicles prepared from red beet

tap roots and cauliflower inflorescences. These data indicated that NAADP released Ca^{2+} from red beet microsomes through a pathway independent of that of both cADPR and $InsP_3$. Fractionation studies of the microsomes demonstrated that NAADP could not release Ca^{2+} from vacuolar membranes. Further investigation of the membrane location using fractionated cauliflower microsomes indicated that the NAADP-sensitive vesicles were derived from the ER. The pharmacology of NAADP release also demonstrated similarity to that of animal cells: pre-treatment with sub-threshold doses of NAADP inhibited further NAADP-induced release and the release was insensitive to heparin and 8-amino-cADPR. In addition the NAADP-induced release was also insensitive to changes in $[Ca^{2+}]_c$, indicating that it also is not involved in CICR. In contrast to the release described in animal cells, the release pathway of plants is not inhibited by the L-type channel antagonists verapamil or diltiazem. Since the NAADP-induced release pathway is also insensitive to inhibitors of $InsP_3$- and cADPR-mechanisms and is localised to the ER, the NAADP-pathway appears to be distinct from those of $InsP_3$ and cADPR, in principle providing a mechanism for the mediation of spatially localised Ca^{2+} changes.

1.2.8. Metabolism of cADPR and NAADP

1.2.8.1. ADP-ribosyl cyclase activity in animals, protests and prokaryotes

In animals, both cADPR and NAADP are synthesised by ADP-ribosyl cyclase from the pyridine nucleotides NAD and NADP, respectively (Lee, 1997). The enzyme was initially purified from eggs of the sea slug *Aplysia californica* (Lee & Aarhus, 1991; Hellmich *et al.*, 1991), and several types of ADP-ribosyl cyclase activity have now been characterised in depth including: (1) a soluble, cyclic guanine monophosphate (cGMP)-activated cyclase and a membrane-bound cGMP-insensitive cyclase in sea urchin eggs (Graeff *et al.*, 1998); (2) CD38 and BST-1, a lymphocyte antigen and a bone marrow surface marker that demonstrate both cADPR synthesising and hydrolytic activity in mammalian tissue (Takasawa *et al.*, 1993; Inageda *et al.*, 1995; Hirata *et al.*, 1994); (3) a NAD-glycohydrolase of *Streptococcus pyogenes* that has been determined to possess cyclase and hydrolase activity (Karasawa *et al.*, 1995); and (4) a 40 kDa protein with cyclase activity purified from the unicellular protist *Euglena gracilis* (Masuda *et al.*, 1997; 1999). The soluble cyclase purified from *Aplysia* has had its three-dimensional structure determined by X-ray crystallography. Cyclic ADPR hydrolase, the enzyme that degrades cADPR to ADP-ribose (ADPR), has also been discovered in a wide range of animal cells (Kim *et al.*, 1993). The

ubiquitous nature of the cyclase indicates that cADPR levels are tightly regulated by most cells, as would be expected for a second messenger.

ADP-ribosyl cyclase is unusual in that it is multifunctional: it is capable of catalysing the formation of structurally discrete products including cADPR, NAADP and other Ca^{2+} mobilising metabolites such as 2,-P-cADPR from different substrates (see Figure 1.1). The catalysed reaction produces cADPR by cyclisation of the terminal ribose of NAD at the N-1 position with the release of nicotinamide. The cyclic structure can be converted to ADPR by hydrolysis of the N-1 to ribose bound through the action of heat or of ADP-ribosyl hydrolase (Lee *et al.*, 1989). Dual-functional enzymes, such as the lymphocyte antigen CD38 (Howard *et al.*, 1993) and the bone marrow stromal cell surface marker BST-1 (Hirata *et al.*, 1994) are capable of catalysing both cyclisation and hydrolysis. Interestingly, the ADP-ribosyl cyclase enzyme first purified from *Aplysia* does not exhibit significant hydrolase activity (Lee & Aarhus, 1991).

NAADP is produced when the substrates for the enzyme are NADP and nicotinic acid. In these conditions the exchange of the nicotinamide group with nicotinic acid is catalysed. This base-exchange reaction occurs preferentially at acidic pH and produces a linear molecule that, while structurally different from cADPR, is more potent at mobilising Ca^{2+} (Aarhus *et al.*, 1995).

1.2.8.2. ADP-ribosyl cyclase activity in plants

Having been discovered in three different kingdoms (animal, protist and prokaryote) ADP-ribosyl cyclase activity appears to be highly conserved. As the machinery for cADPR and NAADP signalling has been shown to be present in plant cells it has been hypothesised that plants would also possess ADP-ribosyl cyclase activity. Evidence for ADP-ribosyl cyclase activity in plant cells has been shown by microinjection studies of NAD into the stamen hair cells of *Tradescantia virginiana*. Following the injection a delayed wave in Ca^{2+} was visualised using fura-2-dextran (DePass & Hepler, 1998), indicating the production of an active product, presumably cADPR, following enzymatic conversion of NAD.

The synthesis of NAADP has recently been demonstrated in cauliflower florets by Navazio *et al.* (2000). After incubating homogenised cauliflower tissue with the precursors of NAADP (i.e. nicotinic acid and NADP) extracts of the tissue were assayed for NAADP using the sea urchin microsome Ca^{2+}-release bioassay.

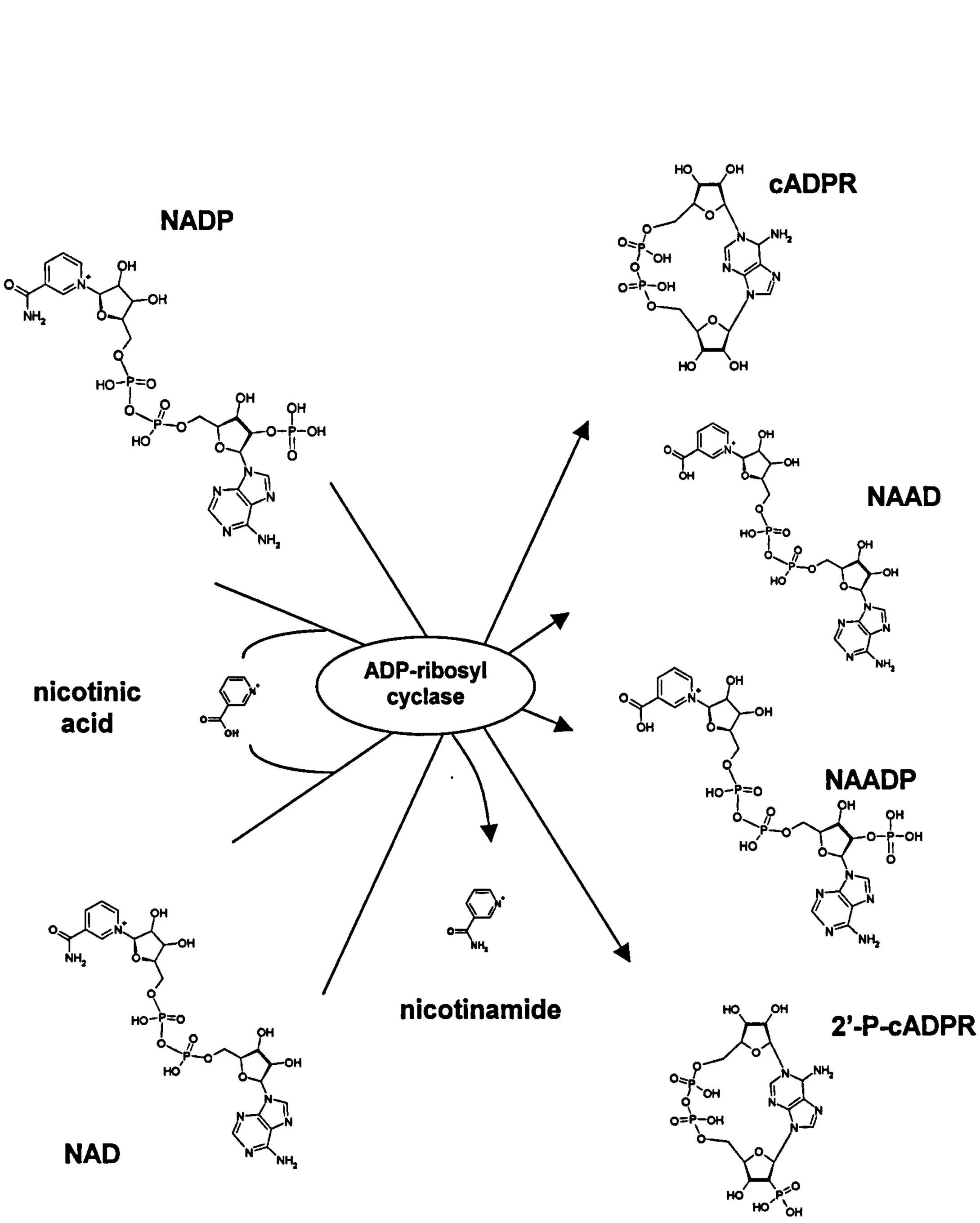

Figure 1.1. Pyridine nucleotide metabolites with Ca^{2+} mobilising activity

The chemical structures of pyridine nucleotides that are capable of mobilising Ca^{2+} are depicted along with the compounds they are derived from. ADP-ribosyl cyclase is a multifunctional enzyme that is capable of synthesising various Ca^{2+} mobilising compounds from different substrates. Figure based on Genazzani & Galione (1997).

NAADP was synthesised at a rate of 6.5 pmol/mg – comparable with values of animals. Whether this activity is due to ADP-ribosyl cyclase has not been determined

1.3. Calcium homeostasis

Changes in $[Ca^{2+}]_c$ need to be strictly regulated and linked to downstream processes, both to maintain Ca^{2+} homeostasis and for Ca^{2+} to work effectively as a second messenger. The effectiveness of Ca^{2+} a signalling element and the importance of maintaining its homeostasis has favoured the evolution of a range of proteins that utilise the flexible coordination number and large radius of Ca^{2+} to regulate their activity via conformational changes arising from the binding of Ca^{2+} to remote domains (McPhalen *et al.*, 1991). Proteins directly involved in Ca^{2+} signalling can thus be divided into three groups: Ca^{2+} sensors, Ca^{2+} transporters, and Ca^{2+}-permeable ion channels.

1.3.1. Calcium sensors

Proteins concerned with the detection and transduction of Ca^{2+} signals in plants have been divided into two broad categories (Sanders *et al.*, 2002): (1) relay sensors, such as calmodulin and calcineurin B-like proteins, that mediate the action of downstream targets in response to a conformational change induced by Ca^{2+}, and (2) sensor responders that have their own activity directly regulated by a Ca^{2+} induced change in conformation, such as calcium-dependent protein kinases (CDPKs).

CaM, known as a prototypical calcium sensor in animal cells (Chin & Means, 2000), is thought to be one of the chief Ca^{2+} sensors in plants. CaM has been shown to modulate a wide scope of cellular activities by interacting with a variety of proteins, for example the SV channel (Bethke & Jones, 1994), NAD kinase (Muto & Miyachi, 1977), glutamate decarboxylase (Baum *et al.*, 1993), heat shock inducible proteins (Lu *et al.*, 1995), glyoxalase I (Veena *et al.*, 1999), and Ca^{2+}-ATPase (Harper *et al.*, 1998). Furthermore, recent evidence has indicated that plants contain far more isoforms of CaM than animals (Zielinskii, 1998) and that these isoforms differ in their affinity to target proteins, adding a further level of complexity to the Ca^{2+}-signalling network – especially as expression of these divergent CaM isoforms also appears to be differentially regulated by stimuli such as pathogens or fungal elicitors (Heo *et al.*, 1999).

Ca^{2+}/calmodulin-dependent kinase activity has been reported in plants (Ranjeva, *et al.*, 1983), however, the majority of Ca^{2+}-dependent kinase activity is currently thought to be controlled by CDPKs (Harmon *et al.*, 2000), which are not directly regulated by CaM (Harmon *et al.*, 1987). These proteins possess a C-terminal CaM-like regulatory domain with four calcium-binding EF-hands, following a protein kinase catalytic domain, and are unique to plants and protists. There is an abundance of isoforms - over 40 *CDPKs* in the *Arabidopsis* genome (Harmon *et al.*, 2000) - and as these are found in different cellular locations, including the cytosol, nucleus, cytoskeleton and associated to membranes (for review see Sanders *et al.*, 2002), the pathways and substrates acted upon by CDPKs are likely to be substantial. This speculation is substantiated by recent work into the identification of potential CDPK targets via protein-protein interactions carried out by Patharkar & Cushman (2000).

Apart from CaMs and CDPKs, various work, including the *Arabidopsis* genome project, points to the existence of a range of CaM-like proteins (proteins with EF-hands) in plants (Reddy *et al.*, 2002). The function of these proteins has not yet been determined. However, they are presumed to be Ca^{2+} sensors that are functionally distinct from CaM and thus involved in the regulation of different Ca^{2+}-mediated cellular functions. One example of a CaM-like protein in animals is calcineurin, which is responsible for regulating protein phosphatase activity (Cohen, & Cohen, 1989). It has recently been reported that a family Ca^{2+} sensors resembling the regulatory B-subunit of calcineurin have been identified in *Arabidopsis* – known as calcineurin B-like (CBL) proteins (Kudla *et al.*, 1999). It has also been observed that K^+ currents in guard cells and the activity of SV channels in barley aleurone cells can be regulated by calcineurin (Allen & Sanders, 1995; MacRobbie, 1998; Bethke & Jones, 1997). This has opened up two possible functions for CBL-like proteins. Firstly, through regulation of K^+ and/or Na^+ transport systems, they could play a role in salt stress signalling. This possibility has been confirmed through studies of salt-overly-sensitive (*sos*) mutants of *Arabidopsis* where the *SOS3* gene has been shown to encode a CBL-like product (Liu & Zhu, 1998). Secondly, if SV channels are involved in CICR, as described above, then CBLs could also act as regulators of oscillation frequency, or as a negative feedback mechanism preventing the cytosol from being flooded by the vacuolar Ca^{2+} pool.

Calcium sensors without EF-hands have also been described in plants and include calreticulin, annexins and pistil-expressed Ca^{2+}-binding proteins. Calreticulin has

been reported as acting as a chaperone in the ER of plant cells (Baluska *et al.*, 1999) and is thus thought to be involved in Ca^{2+} homeostasis in a similar manner to that of animal cells where it has been observed that calreticulin modulates ER Ca^{2+} storage and transport (Michalak *et al.*, 1998).

Several cDNA clones for annexins have been purified from various plants including *Arabidopsis* and have been shown to possess Ca^{2+}-binding motifs (reviewed in Delmer & Potikha, 1997). It has been suggested that plant annexins may be involved in regulating secretory processes as they bind phospholipids in a Ca^{2+} dependent manner like their animal counterparts (Raynal & Pollard, 1994; Delmer & Potikha, 1997) and high levels of annexins have been measured in the tips of growing pollen tubes where vesicle secretion is highly active (Blackbourne *et al.*, 1993). A unique feature of some plant annexins is that they possess peroxidase activity (Gidrol *et al.*, 1996), and because the motif assumed to be responsible for the activity is situated in a region of the protein that is predicted to bind Ca^{2+}, it has been speculated that the peroxidase activity may be Ca^{2+} dependent (Delmer & Potikha, 1997). Interestingly several animal annexins (I, V, VI and VII) have been documented as displaying voltage-gated Ca^{2+} channel activity *in vitro* (Pollard *et al.*, 1992). Although no such activity has been reported for plant annexins, hydropathy plots indicate a high degree of resemblance between human annexin V and a cotton annexin (Delmer & Potikha, 1997) raising the possibility that some annexins may also act as Ca^{2+}-permeable channels.

A novel low affinity Ca^{2+}-binding protein has been reported that is expressed in *Brassica* pistils and anthers (Furuyama & Dzelzkalns, 1999). The authors isolated the clone for an estimated 19.1 kDa protein from a cDNA library that was enriched in transcripts present in the pistil late in flower development. From the pattern of expression of mRNA, which was predominantly found in the stigma and style of the pistils, they concluded that this protein plays a role in either pollen-pistil interactions or pistil development.

1.3.2. Calcium transport systems

A variety of plant Ca^{2+} transporters have been identified (Figure 5), they are categorised into (1) energised transport systems that remove Ca^{2+} from the cytosol and (2) Ca^{2+}-permeable channels through which Ca^{2+} diffuses passively along its electrochemical gradient (for review see Sanders *et al.*, 2002). The energised

transporters are powered by ATP hydrolysis or proton motive force and work in conjunction with Ca^{2+} binding proteins to terminate Ca^{2+} signals and maintain $[Ca^{2+}]_c$ at resting levels. These energised Ca^{2+} transport systems are the primary homeostatic devices for maintenance of low $[Ca^{2+}]_c$. By loading Ca^{2+} into intracellular organelles, these transport systems also keep Ca^{2+} stores filled and provide the Ca^{2+} necessary for normal organellar function. Traditionally such energised transporters have often been viewed as having a 'house-keeping' function. However, from the work of Camacho and Lechleiter (1993), who indicated that the frequency Ca^{2+} wave generation can be altered by the expression of a Ca^{2+}-ATPase in *Xenopus* oocytes, the possibility has been raised that energised efflux pathways may also be involved in Ca^{2+} signal dynamics along with Ca^{2+} channels. This possibility is reinforced for plant cells by the observation that *det3* mutants defective in a vacuolar H^+-pumping ATPase, also have defective Ca^{2+} signalling dynamics (Allen *et al.*, 2000). A generalised view of Ca^{2+} transport processes in plant cells is given in Figure 1.2 to serve as a basis for the following discussion.

1.3.2.1. Ca^{2+}-ATPases

Plant Ca^{2+}-ATPases are members of the P-type ATPase superfamily. Phylogenetic analysis indicates that plant Ca^{2+}-ATPases fall into two categories: type IIA and IIB (Axelsen & Palmgren, 1998). In *Arabidopsis* twelve Ca^{2+}-ATPases have been identified and it has been estimated from expressed sequence tag (EST) and genomic analysis that there are approximately four type IIA pumps and eight type IIB pumps (Geisler *et al.*, 2000). Genes for type IIA pumps have been identified in several plants including tomato (Wimmers *et al.*, 1992), tobacco (Perez-Prat *et al.*, 1992), *Arabidopsis* (Liang *et al.*, 1997), rice (Chen *et al.*, 1997) and the halotolerant alga *Dunaliella bioculata* (Raschke & Wolf, 1996). Sequence analysis of type IIA pumps indicates that they are homologues of the SERCA pumps of animals and, like the SERCA pumps, type II pumps do not appear to have CaM binding sites (Evans & Williams, 1998). However, in contrast to SERCA pumps, which are localised to the ER, all the isoforms of plant IIA pumps that have been so far studied, apart from ECA1/ACA3, have been assigned to membranes other than the ER (Evans, 1994). Immunoblotting of ECA1/ACA3 indicates that this pump is predominantly localised to ER membranes (Liang *et al.*, 1997). ECA1/ACA3 is also the only type IIA pump for which functional data are available. Other IIA pumps are classified as Ca^{2+}-ATPases based on sequence homology alone.

There are several models of the structure of plant type IIA ATPases with

Figure 1.2. Major Ca^{2+} transport pathways in an idealised plant cell

Areas with a deficiency of evidence and/or primarily based on animal models are indicated with an '?'.

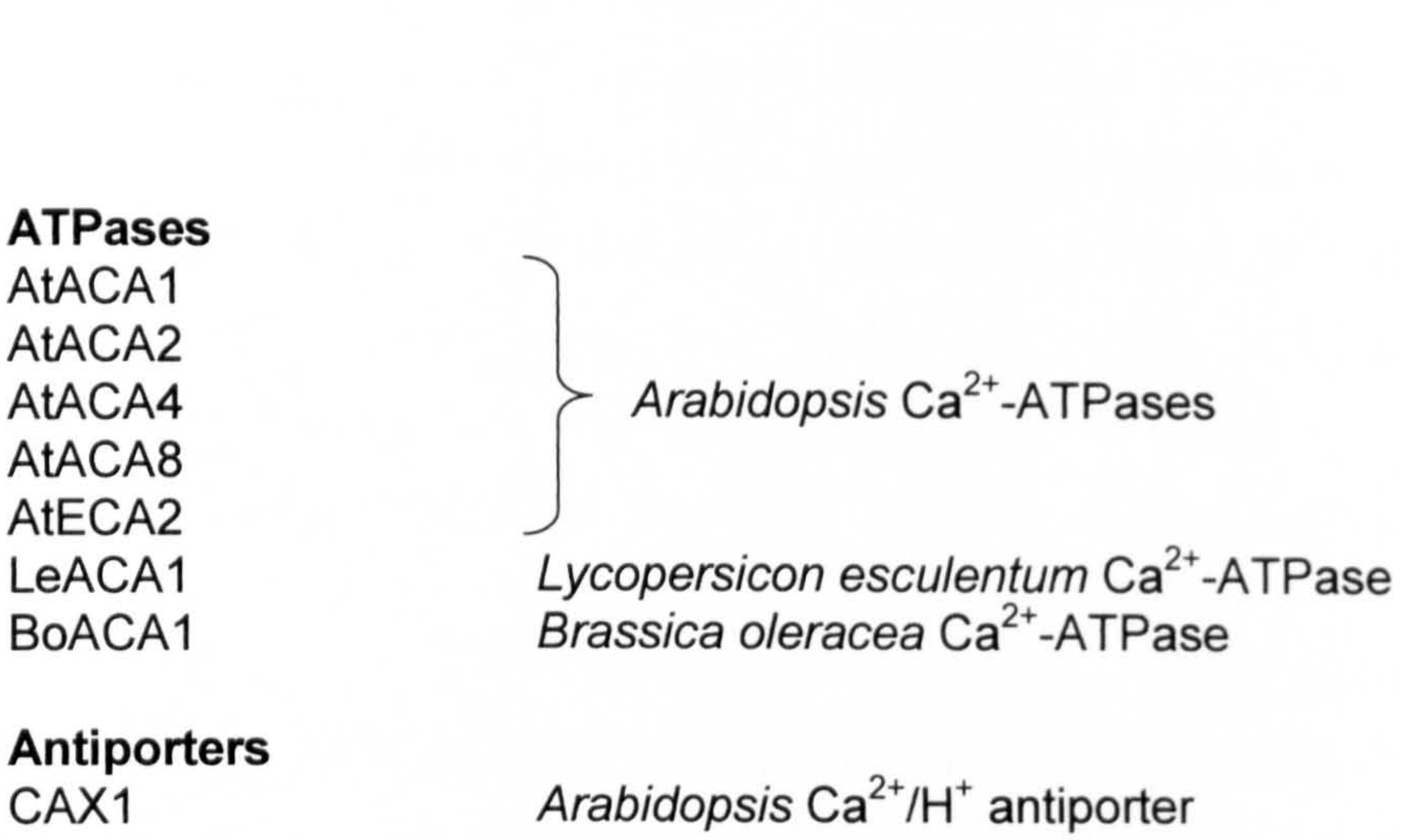

See text for more details.

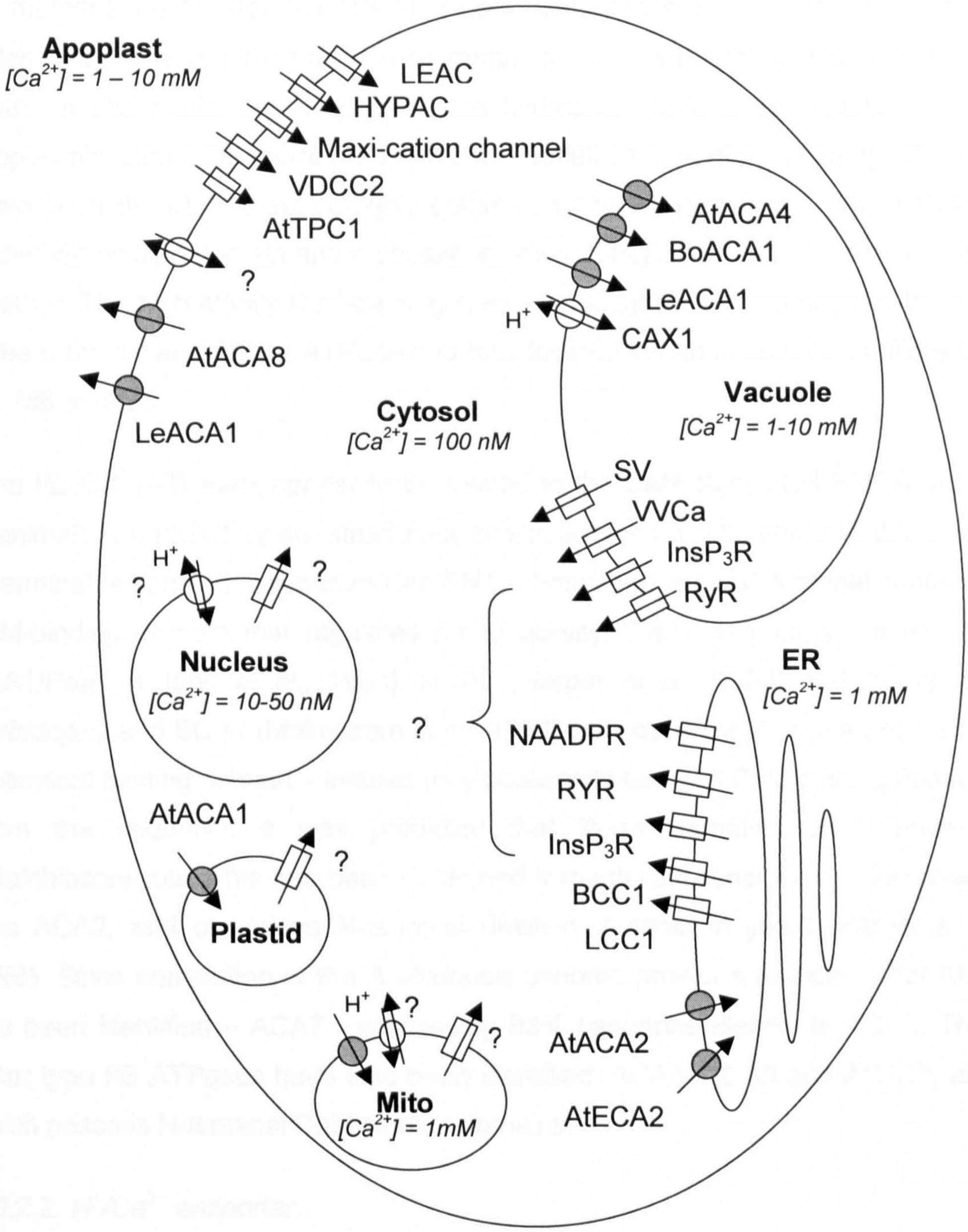

hydrophobicity analysis predicting between 8 and 10 transmembrane domains. At the moment the ten-domain model is commonly accepted, as this most closely matches the crystal structure of a mammalian SERCA homologue (Zhang *et al.*, 1998). In this model the majority of the hydrophilic regions are located on the cytoplasmic side of the membrane with only a small amount of the polypeptide chain showing on the other side. A highly conserved hinge region is thought to allow a nucleotide binding domain and a phosphorylation domain (the catalytic site) to come together. The high affinity Ca^{2+}-binding sites are thought to be homologous to those of the mammalian SERCA ATPase and thus located in transmembrane helices M4, M5, M6 and M8.

Type IIB Ca^{2+}-ATPases appear to be related to the CaM-stimulated PMCA pumps of animals to which they are structurally similar except for differences in the C- and N-terminal regions. In the mammalian PMCA homologues the C-terminal contains a CaM-binding domain that regulates pump activity. Type IIB pumps, for example ACA1/Pea1 (Huang *et al.*, 1993), ACA2 (Harper *et al.*, 1998) and ACA4 from *Arabidopsis* and BCA1 (Malmstrom *et al.*, 1997) from cauliflower, lack a well defined C-terminal binding domain – instead they possess N-terminal CaM binding domains. From the sequence it was predicted that these domains would have an autoinhibitory role. This has been confirmed through functional expression of wild-type ACA2, and of various N-terminal deletion mutants in yeast (Harper *et al.*, 1998). Since completion of the *Arabidopsis* genome project a homologue of ACA2 has been identified – ACA7 - possessing 93% sequence identity to ACA2. Three other type IIB ATPases have also been identified: ACA8, ACA9 and ACA10, all of which possess N-terminal CaM binding domains.

1.3.2.2. H^+/Ca^{2+} antiporter

In contrast with the Na^+ driven transport systems of animal cells, the primary driving force for the transport of most solutes in plant cells arises from a proton motive force (PMF) generated by H^+-ATPase pumps in the plasma membrane and tonoplast (PMF is approximately -270 mV and -200 mV, respectively, assuming membrane potentials of -150 mV and -20 mV) (Morsomme & Boutry, 2000; Maeshima, 2001). H^+/Ca^{2+} antiporters, such as the *Arabidopsis* Ca^{2+}/H^+ antiporter CAX1 (calcium exchanger 1; cloned and expressed by Hirschi *et al.*, 1996) make use of this gradient to remove Ca^{2+} from the cytosol. Although CAX1 activity in *Arabidopsis* and antiporters identified on the basis of biochemical activity in other plants (e.g. carrot (Bush & Sze, 1986), oat (Schumaker & Sze, 1990), sugar beet (Andreev *et al.*,

1990) and maize (Chanson, 1991)) are localised to the tonoplast, antiporter activity has also been reported in several other membranes, including the plasma membrane (Kasai & Muto, 1990).

The predicted membrane topology of CAX1 determined from hydropathy plots suggests the existence of a possible 8-11 transmembrane domains (Hirschi *et al.*, 1996). The activity of CAX1 has recently been established as being under the regulation of an autoinhibitory N-terminal sequence (Pittman & Hirschi, 2001) occurring prior to the first transmembrane domain. The specificity of transport for cations is determined, at least in part, by a 9-amino acid sequence occurring just after the first transmembrane domain (Shigaki *et al.*, 2001).

1.3.3. Ca^{2+}-permeable channels

Passive entry of Ca^{2+} into the cytosol is mediated by ion channels whose physiological role is to mediate transport of Ca^{2+} across cellular membranes. The origin of the Ca^{2+} that enters the cytosol in response to a given stimulus can be either intracellular, extracellular or both (Marschner, 1995) and the type and location of channel involved is thought to be pivotal in encoding specificity to the signal. Calcium permeable channels have been characterised on the PM, tonoplast, ER, nuclear and plastid membranes of plant cells (recently reviewed by White, 1998; 2000 and Sanders *et al.*, 2001, 2002) where they are thought to play a role in generating Ca^{2+} signal specificity by providing a mechanism through which different pools of Ca^{2+} can be accessed by different stimuli and characteristic Ca^{2+} oscillations and waves can be produced.

1.3.3.1. PM Ca^{2+} channels

Various investigations, using both patch clamp and planar lipid bilayer techniques, have uncovered three major classes of Ca^{2+}-permeable channel in the PM of plant cells (White, 2000). They have been classified based on their voltage-sensitivity into depolarisation-activated, hyperpolarisation-activated and voltage-independent.

The first class, depolarisation-activated channels, are activated by membrane potentials generally more positive than –140 mV (the approximate resting membrane potential of the PM). They are considered to transduce general stress-related signals. They include: maxi-cation channels - channels that possess high single-channel conductances whilst being relatively nonselective toward cation

passage (White, 1993) - and voltage-dependent cation channels which are more selective towards cations with a smaller single-channel conductance (White, 1994).

Depolarisation-activated channels have been extensively characterised in cereal roots (White, 2000), but are believed to exist in a wide variety of tissues, having also been detected in carrots (Thuleau *et al.*, 1994), *Arabidopsis* (Kiegle *et al.*, 1998) and *Vicia fabia* (Cosgrove & Hedrich, 1991). There is some evidence that depolarisation-activated channels can be regulated by cytoskeletal interactions based on the action of microtubule disrupters, such as colchicine and oryzalin, on depolarisation-activated Ca^{2+}-currents (Thion *et al.*, 1998) and the observation that in the *Arabidopsis ton2* mutant, which possesses microtubules that are not correctly bound to the PM, depolarisation-activated channels are recruited (Thion *et al.*, 1998).

A gene encoding a putative depolarisation-activated channel, AtTPC1, has recently been isolated from *Arabidopsis* (Furuichi *et al.*, 2001). AtPC1 comprises two Shaker-like domains, each with six putative transmembrane segments containing a pore loop. The two Shaker-like domains are connected by a hydrophilic region, made up of two EF-hand domains. AtTPC1 is closely homologous to a two-pore channel isolated from rat kidney (TPC1: Furuichi *et al.*, 2001). AtTPC1 was able to rescue Ca^{2+} uptake activity when expressed in yeast mutants deficient in the calcium channel CCH1 and was activated by membrane depolarisation, strong evidence that it is the first voltage-dependent channel with a high affinity for Ca^{2+} to be identified at a genetic level in plants (reviewed in White *et al.*, 2002).

The second class of PM Ca^{2+}-permeable channel is hyperpolarisation-activated. Examples have been reported in a variety of different cell types and exhibit activation when the PM is in a hyperpolarized state (about –200 mV: Gelli *et al.*, 1997; Grabov & Blatt, 1998a; Hamilton *et al.*, 2000). One group of hyperpolarisation-activated Ca^{2+} channel, including examples from broad bean (*Vicia fabia*) guard cells (Cosgrove & Hedrich, 1991) and onion bulb epidermal cells (Ding & Pickard, 1993), are also stretch-activated and are predicted to act as mechanoreceptors, regulating turgor and transducing mechanical stress induced by flexure, touch and gravity (Ding & Pickard, 1993). Hyperpolarisation-activated channels found in guard cells appear to coordinate the loss of solutes by initiating PM depolarisation and stomatal closure and have been linked with ABA signalling (Grabov & Blatt, 1998b; Hamilton *et al.*, 2000). Similar channels in root endodermal cells are believed to

mediate mineral nutrition (Kiegle *et al.*, 1998) while others found in tomato protoplasts respond to elicitors and are thought to play a role in pathogenic defence responses (Gelli & Blumwald, 1997). Immature root hair cells have also been described as demonstrating hyperpolarisation-activated channel activity in their tips. Such activity is thought to be involved with the generation of Ca^{2+} gradients essential for growth (Véry & Davies, 2000).

The third class of Ca^{2+} channel identified in the PM is voltage-independent. Only one has been reported, a large-conductance elicitor-activated channel (LEAC) (Zimmermman *et al.*, 1997). The activity of this channel is not affected by changes in membrane potential between –30 and –150 mV and can be activated by an oligopeptide elicitor derived from a cell wall protein of the pathogenic fungus *Phytophthora sojae*. This channel is currently accepted as playing a role in pathogenic defence responses.

Recently, homologues of animal cyclic nucleotide-gated channel (CNGC) genes have been identified in plants (Köhler & Neuhaus, 1998; Schuurink *et al.*, 1998; Mäser *et al.*, 2001). The CNGCs of animals are permeable to Ca^{2+} raising the possibility that plant CNGCs may comprise an additional class of Ca^{2+} permeable PM channel in plants. Indeed, an elevation in cAMP or cGMP in the cytoplasm of a plant cell has been reported to elicit an increase in both the influx of Ca^{2+} and $[Ca^{2+}]_c$ (Kurosaki *et al.*, 1994; Volotovski *et al.*, 1998). Sequence analysis of plant CNGC homologues indicates that they contain Shaker-like domains (Arazi *et al.*, 2000), much like AtTPC1. The homologues also contain and N-terminal domains that are able to bind both cyclic nucleotides and CaM (Kohler & Neuhaus, 2000). The pore structure of plant and animal CNGCs differ sufficiently to prevent the selectivity of animal CNGCs to be predicted from sequence homology alone (White *et al.*, 2002). However, plant CNGCs seem to be permeable to both monovalent and divalent cations. For example, following injection of AtCNGC2 cRNA into *Xenopus* oocytes inward currents of K^+, Rb^+, Cs^+ and Ca^{2+} could be induced by elevation of cytosolic cyclic nucleotide monophosphates (cNMP) (Leng *et al.*, 1999; 2002). Furthermore, Leng *et al.* (2002) also reported that human embryonic kidney cells transfected with AtCNGC2 cDNA demonstrate an increase in Ca^{2+} permeability when treated with lipophilic cNMPs.

1.3.3.2. Endomembrane voltage gating channels

The vacuole accounts for between 85-90% of the total volume of a mature plant cell and is thus, by far, the largest intracellular compartment. This has made it amenable both to electrophysiological and biochemical studies and a range of Ca^{2+}-selective channels have been characterised at vacuolar membranes (Gelli & Blumwald, 1993; Allen & Sanders, 1997). The voltage-gated channels fall into two categories: (1) hyperpolarisation activated channels (inward rectifiers), e.g. the vacuolar voltage-gated Ca^{2+} (VVCa) channel and (2) depolarisation-activated channels (outward rectifiers), e.g. the slowly activating vacuolar (SV) channel.

Hyperpolarisation channels located on the tonoplast instantaneously open at negative voltages between –20 and –70 mV (compared with the resting membrane potential of the tonoplast which is only slightly negative) and have been detected in vacuoles from red beet (*Beta vulgaris*) taproot (Johannes *et al.*, 1992), *Commelina communis* (Johannes *et al.*, 1994) and broad bean (*Vicia faba)* (Allen & Sanders, 1994a) guard cells. All the channels characterised possess single-channel conductances in the range 4-27 pS and moderate Ca^{2+} selectivity over K^+. These channels do, however, display differential sensitivity to Ca^{2+}. For example, voltage patch-clamp experiments performed by Gelli & Blumwald (1993) at whole-vacuole and single channel levels identified a dihydropyridine (DHP)-sensitive channel similar to the DHP-sensitive L-type Ca^{2+} channels of animal cells. Whilst this channel allowed movement of Ca^{2+} out of the vacuole under physiological conditions of pH, $[Ca^{2+}]_c$, vacuolar Ca^{2+} ($[Ca^{2+}]_v$) and vacuolar membrane potential, it was completely inhibited by $[Ca^{2+}]_c$ greater than 1 μM. In contrast, patch clamp experiments reported by Johannes & Sanders (1995) identified a Ca^{2+} release channel in the vacuole of sugar beet tap roots that is insensitive to $[Ca^{2+}]_c$. but is affected by luminal pH and $[Ca^{2+}]_v$, with an increase in $[Ca^{2+}]_v$ favouring channel opening via Ca^{2+}-induced lowering of the threshold of the voltage required for activation. Kinetic analysis of the channel activity reported by Johannes & Sanders led them to construct a model of channel function in which a dynamic pore is able to allow passage of multiple ions when opened by the binding of two Ca^{2+} ions. VVCa channels have not yet been assigned definitive physiological roles.

SV channels, so named because they activate over a period of several hundred milliseconds (Hedrich & Neher, 1987) have been detected in red beet root (Coyaud *et al.*, 1987) and *Vicia fabia* guard cells (Allen & Sanders, 1996) with conductances of 40 pS and 240-280 pS respectively. The property of SV channels that has

attracted the most interest is the ability of the channel to be activated by $[Ca^{2+}]_c$ over a physiological range (0.1-1.0 μM: Hedrich & Neher, 1987; Bethke & Jones, 1994; Allen & Sanders, 1996). The dependence of SV channels on $[Ca^{2+}]_c$ over a physiological range is indicative that SV channels might have a role in Ca^{2+}-signal transduction and raises the possibility that the channel could form part of the mechanism of CICR. Thus, Ca^{2+} could be supplied by the opening of another channel type, such as the ligand-gated channels described below, and thereby act as a trigger for activation of the SV channel. This proposal has met with some controversy as SV channels have not been demonstrated to be active at physiological (negative) membrane potentials and the response to Ca^{2+} alone is not sufficient to enable CICR (Pottosin *et al.*, 1997). However, it has been argued that there are at least two circumstances where conditions might be permissive for activation. First, during the opening of Ca^{2+}-selective ligand-gated channels or Ca^{2+}-activated K^+ channels (VK channels), which would temporarily shift the membrane potential positive, in the direction of the equilibrium potential for Ca^{2+} or K^+ (Sanders *et al.*, 1995). Second, in the presence of Mg^{2+} ions at physiological concentrations, which were absent in the experiments of Pottosin *et al.* (1997). Mg^{2+} ions have been shown to enhance the probability of the SV channel being open in conditions that would allow CICR to operate at relatively negative potentials (Pei *et al.*, 1999).

Voltage-sensitive Ca^{2+} channels have been detected in the ER of *Bryonica dioica* (BCC1: Klüsener *et al.*, 1995) and the root tips of *Lepidium satvium* (LCC1: Klüsener & Weiler, 1999). Both of the voltage-sensitive Ca^{2+}-channels demonstrated selectivity for Ca^{2+} over K^+ whilst being strongly rectifying and open at positive voltages. The channels were also activated by increases in luminal $[Ca^{2+}]$ and the conductance of BCC1 increased in response to cytoplasmic acidification. It has been argued that the physiological activity of BCC1 is governed primarily by luminal $[Ca^{2+}]$ or possibly by cytoplasmic pH in such a way as to generate transient elevations of $[Ca^{2+}]_c$ of varying frequency. As the frequency of the transients could be modulated by Ca^{2+}-ATPases, Ca^{2+} gradients across the ER or pH this channel may provide another mechanism for generating Ca^{2+}-signalling specificity.

1.3.3.3. Ligand-gated Ca^{2+}-channels in plants

The evidence for the existence of ligand-gated channels in plants relies on data from biochemical and electrophysiological studies. Early work on tonoplast-enriched vesicles prepared from oat roots and vacuoles isolated from *Acer* cells indicated that Ca^{2+} could be released from the vesicles by concentrations of $InsP_3$ similar to those

active in animal systems (Schumaker & Sze, 1987; Ranjeva *et al.*, 1988). Patch clamp experiments, reporting whole membrane currents in red beet vacuoles, substantiated this work and demonstrated that $InsP_3$ could elicit currents selective for Ca^{2+} across the tonoplast over a physiological range of membrane potentials (-20 to -50 mV: Alexandre *et al.*, 1990; Allen & Sanders, 1994b). Comparison of whole vacuole with single channel currents yielded an estimate of approximately 1200 $InsP_3$-dependent Ca^{2+} channels in each red beet vacuole (Alexandre *et al.*, 1990). Further patch clamp and Ca^{2+}-release studies indicated that cADPR could also mobilise Ca^{2+} from red beet vacuoles, accessing different pools of Ca^{2+} than $InsP_3$ (Allen *et al.*, 1995).

The ability of ligands to access different pools of Ca^{2+} in plant cells is important as it potentially provides a mechanism for the generation of signal specificity similar to that suggested for animal cells (Berridge & Galione, 1988). Initial membrane fractionation studies on carrot suspension cultures and zucchini hypocotyls were unable to identify any membranes other than the tonoplast that were sensitive to $InsP_3$ (Canut *et al.*, 1993; Lew *et al.*, 1986). Since then, fractionated cauliflower inflorescences, using tissue sections that are rich in ER, have indicated that both $InsP_3$ and cADPR can release Ca^{2+} from distinct populations of microsome vesicles separated on sucrose gradients (Muir & Sanders, 1997; Navazio *et al.*, 2001). The fractionation studies were unable to distinguish conclusively whether $InsP_3$ was acting at the PM or ER due to the close association of cortical ER and the PM. The authors tentatively designated the ER as being the $InsP_3$-sensitive membrane as no evidence for $InsP_3$ on PM Ca^{2+} conductance has been reported and previous micro-injection studies in pollen tubes have indicated that $InsP_3$-release is associated with ER (Franklin-Tong *et al.*, 1996). By monitoring the distribution of ER and vacuolar marker enzyme activities, the cADPR-sensitive population of microsomal vesicles have been confirmed as originating from the ER (Navazio *et al.*, 2001). This technique has also indicated that NAADP can also release Ca^{2+} from ER Ca^{2+}-stores but not vacuolar stores, at least in cauliflower (Navazio *et al.*, 2000). These studies point to the existence of multiple Ca^{2+} release sites and mobilization pathways that can contribute to stimulus-specific Ca^{2+} signals.

The data from ligand-gated Ca^{2+}-release experiments indicate that the Ca^{2+} release pathways of in plants share a similarity with respective pathways in the ER of animals. In both animals and plants the three ligand-gated pathways detected demonstrate a high degree of specificity for their respective ligands and a similar

pharmacological profile. For example, $InsP_3$-gated release from plant vacuolar vesicles is blocked by inhibitors of $InsP_3$Rs including low molecular weight heparin and 8-(N,N-di-methylamino)octyl 3,4,5-trimethoxybenzoate (TMB-8), while not being affected by antagonists of the RyR (Muir *et al.*, 1997). Conversely, cADPR-gated release is inhibited by inhibitors of RyRs, procaine and ruthenium red, but not by antagonists of the $InsP_3$Rs (Navazio *et al.*, 2001). Furthermore inhibitors of the $InsP_3$ and cADPR release pathways had no effect on NAADP-induced release. In addition the self-inactivation of NAADP-gated release upon pre-treatment of sea urchin eggs with subthreshold doses of NAADP, which is unique to the NAADP release pathway, is also observed with NAADP-induced release in plant cells (Nazvazio *et al.*, 2000).

A major difference between plant vacuolar ligand-gated Ca^{2+} release and that of animals is that plant Ca^{2+} release pathways do not appear to be modulated by $[Ca^{2+}]_c$. Even though waves, oscillations and spikes, indicative of CICR, have been detected in plants, neither $InsP_3$- nor cADPR-gated currents have been demonstrated to be activated by Ca^{2+} as they are in animal systems during CICR. As mentioned previously, this has led to the suggestion that the ligand-gated pathways are linked to the SV channel, which is Ca^{2+} -activated (Hedrich & Neher, 1987), to allow CICR to occur at the vacuole – with the putative ligand-gated Ca^{2+} channels acting as triggers for SV activation.

The evidence for the existence of ligand-gated channels in plants is compelling. Indeed, although $InsP_3$ binding studies on red beet have indicated a very low binding site density (B_{max}) of 840 fmol/mg (compared to $5x10^3$ fmol/mg in rat cerebellum), a 400 kDa $InsP_3$-binding protein has been reported as being purified to homogeneity from mung-bean embryos (Biswas *et al.*, 1995). These authors also reported that $InsP_3$-gated Ca^{2+}-release could be recorded when the protein was reconstituted into liposomes (Biswas *et al.*, 1995). In denaturing conditions the molecular mass of the binding protein was 110 kDa (compared with 300 kDa reported for most animal systems) and the authors therefore suggested that the protein was a homotetramer in its native form. So far, no ligand-gated channel has been characterised at the molecular level in plants, and thus little is known about structure, function or means of regulation of these channels. However, the similarities of the Ca^{2+}-release pathways and of the binding properties of the $InsP_3$-binding proteins of plants and animals have led to the suggestion that the putative receptors in plants responsible for gating Ca^{2+} release are analogous to the $InsP_3$Rs

and RyR isoforms sensitive to cADPR (Brosnan & Sanders, 1993; Allen *et al.*, 1995). No NAADP receptor has yet been identified in any cell.

1.3.3.4. $InsP_3Rs$ in animals

Since $InsP_3$-binding proteins were first identified in mammalian hepatocytes by Burgess *et al.* (1984), $InsP_3Rs$ have been purified (Supattapone *et al.*, 1988), functionally reconstituted into proteoliposomes (Ferris *et al.*, 1989) and bilayers - from which currents have been measured (Watras *et al.*, 1991) - and cloned to determine their primary structure (Furuichi *et al.*, 1989; Mignery *et al.*, 1989). The human $InsP_3R$ family so far encompasses three different full-length genes (I-III) with further heterogeneity of gene products arising from gene splicing (Südhof *et al.*, 1991; Ross *et al.*, 1992; Patel *et al.*, 1999). The members of the $InsP_3R$ family share considerable sequence homology with each other and exhibit some regions of similarity with the other major family of intracellular Ca^{2+} channels, the RyRs (Berridge, 1993). As with RyRs, $InsP_3Rs$ form homotetrameric structures with native molecular weights in excess of 1000 kDa. In each subunit a very large cytoplasmic N-terminal regulatory domain is joined to a C-terminal domain comprised of membrane spanning regions. These transmembrane regions form the Ca^{2+} channel (Furuichi *et al.*, 1989). Deletion analysis has indicated that the $InsP_3$ binding site is located at the end of the N-terminal domain (Yoshikawa *et al.*, 1996). Upon ligand binding, the receptor undergoes a large conformational change believed to be coupled to the opening of the channel (Berridge, 1993).

Between the ligand-binding domain and the Ca^{2+} channel region is a portion of the $InsP_3R$ known as the regulatory domain as it contains consensus sequences for accessory protein, adenine nucleotide-binding and multiple phosphorylation sites. Two accessory proteins that are known to regulate the activity of $InsP_3Rs$ are calmodulin (Patel *et al.*, 1997) and the immunophilin FKBP12 (Cameron *et al.*, 1995). Although calmodulin is a mediator for indirect Ca^{2+} action on $InsP_3Rs$, it is also reported that Ca^{2+} can directly regulate the activity of the receptor by binding to one of seven binding sites (Sienaert, 1997). The multiple means by which Ca^{2+} interacts with the receptor reflect the complex regulatory effects of the ion: low concentrations of Ca^{2+} potentiate $InsP_3$-induced Ca^{2+} mobilisation (Lino, 1990), while higher concentrations (millimolar) inhibit the effect of $InsP_3$ (Hirata *et al.*, 1984). This biphasic regulation is thought to allow negative feedback inhibition of the receptor by Ca^{2+} release during CICR (Lino, 1990). ATP also displays a biphasic regulatory effect on $InsP_3R$ activity arising from its interaction with two ATP-binding

sites at micromolar concentrations (Bezprozvanny & Ehrlich, 1993) and competitive interaction with the $InsP_3$ binding site at higher concentrations (Nunn & Taylor, 1990). $InsP_3$ receptors act as substrates for phosphorylation by a wide range of kinases. These include PKA, cyclic GMP-dependent protein kinase (PKG), PKC and Ca^{2+}-calmodulin dependent protein kinase II (CamKII). IP_3Rs can also undergo auotophosphorylation (Ferris *et al.*, 1992). The effects of phosphorylation can be either inhibitory or excitatory depending on cell type (reviewed in Patel *et al.*, 1999).

1.3.3.5. RyRs in animals

Three different isoforms of RyR were initially identified in mammals: skeletal (RyR1) (Takeshima *et al.*, 1989), cardiac (RyR2) (Nakai *et al.*, 1990) and brain (RyR3) (Hakamata *et al.*, 1992), encoded for by the genes *ryr1*, *ryr2* and *ryr3* respectively. PCR analysis of the distribution of RyR mRNA in porcine tissue has indicated that the various isoforms are located throughout the body and not just to the tissues in which they were first identified. RyR1 RT-PCR products were located in skeletal muscle and the oesophagus, RyR2 RT-PCR products in cardiac muscle, aora and oesophagus and RyR3 RT-PCR products in skeletal and cardiac muscle, aorta, oesophagus, adrenal gland, small intestine and lung. All three RyR isoforms were identified throughout the brain (Ledbetter *et al.*, 1994).

As the receptors can undergo alternative splicing, the actual number of forms possible is believed to be 5-8 (Hakamata *et al.*, 1992). As with the $InsP_3R$ the three major isoforms have been purified and cloned and their secondary structure predicted based on sequence analysis (Sorrentino, 1995). Although almost twice as large as $InsP_3Rs$ they are thought to have a similar architecture. Thus, functional RyRs are homotetramers with each subunit possessing a regulatory N-terminal domain and a C-terminal domain of 4 or 10 transmembrane spanning segments that create the Ca^{2+}-channel. The majority of the cytoplasmic N-terminal domain is believed to form a foot-like structure involved in excitation-contraction coupling of the RyR to the DHP receptor – a PM/T-tubule voltage sensor. The three-dimensional structure of the calcium channel and the foot domain has been resolved to 3.7 nm via electron microscopy (Wagenknect *et al.*, 1989) and confirms the presence of separate calcium channel and foot domains.

RyR1 and RyR2 are the most studied of the isoforms and have been demonstrated to be activated by Ca^{2+}, ATP and caffeine and inhibited by ruthenium red and Mg^{2+} (Marks, 1996; Laver *et al.*, 2001; Blazev & Lamb, 1999; Pessah *et al.*, 1995). RyR3

possesses a much shorter N-terminal domain and although it binds ryanodine is not activated by caffeine. Electrophysiological studies have indicated that only type 2 and type 3 RyRs respond to cADPR (Meszaros *et al.*, 1993; Sitsapesan & Williams, 1995). Two other types of RyR (α-RyR and β-RyR) have been identified in the skeletal muscle of birds, amphibians and fish (reviewed in Airey *et al.*, 1991). These isoforms have significantly different sequences to the RyR of mammals, and while they have similar pharmacological properties, are differentially activated by protein kinases and CaM.

1.4. Aims

The aim of this project was to further elucidate the role ligand-gated Ca^{2+} mobilisation plays in plant cells. It has been conjectured that plant cells use ligand-gated Ca^{2+} release to encode information in Ca^{2+} signals in an analagous manner to the Ca^{2+}-signalling system of animal cells (Figure 1.3 shows a possible model in which $InsP_3$, cADPR and NAADP act as second messengers mediating Ca^{2+} release from internal stores in response to stimuli such as NO and osmotic stress). For cADPR and NAADP to be accepted as second messengers in plant cells plants need to be shown to be capable of metabolising the ligands. Chapters 2 and 3 address the metabolism of cADPR. Chapter 2 describes the preliminary analysis of various plant extracts for cADPR, using chromatographic techniques, and for ADP-ribosyl cyclase activity via a spectrofluorescence assay. The aim of the work detailed in this chapter was to develop a methodology for monitoring metabolism of cADPR in plant tissue. Chapter 3 reports how the assays developed in Chapter 2 were utilised in the characterisation of ADP-ribosyl cyclase activity in cauliflower meristematic tissue and in the partial extraction of ADP-ribosyl cyclase activity from cauliflower microsomes.

Little is known about how the Ca^{2+}-mobilisation channels of plants are regulated. One possibility, that ligand-gated channels are modulated by other signalling compounds (i.e. pH, Ca^{2+}, CaM, redox state, and phosphoylation agents) is considered here. The aim of the work in Chapter 4 was to assess the effect of these compounds on Ca^{2+} release from cauliflower microsome vesicals loaded with $^{45}Ca^{2+}$. The assay was also used to screen several putative, novel, Ca^{2+} release agents.

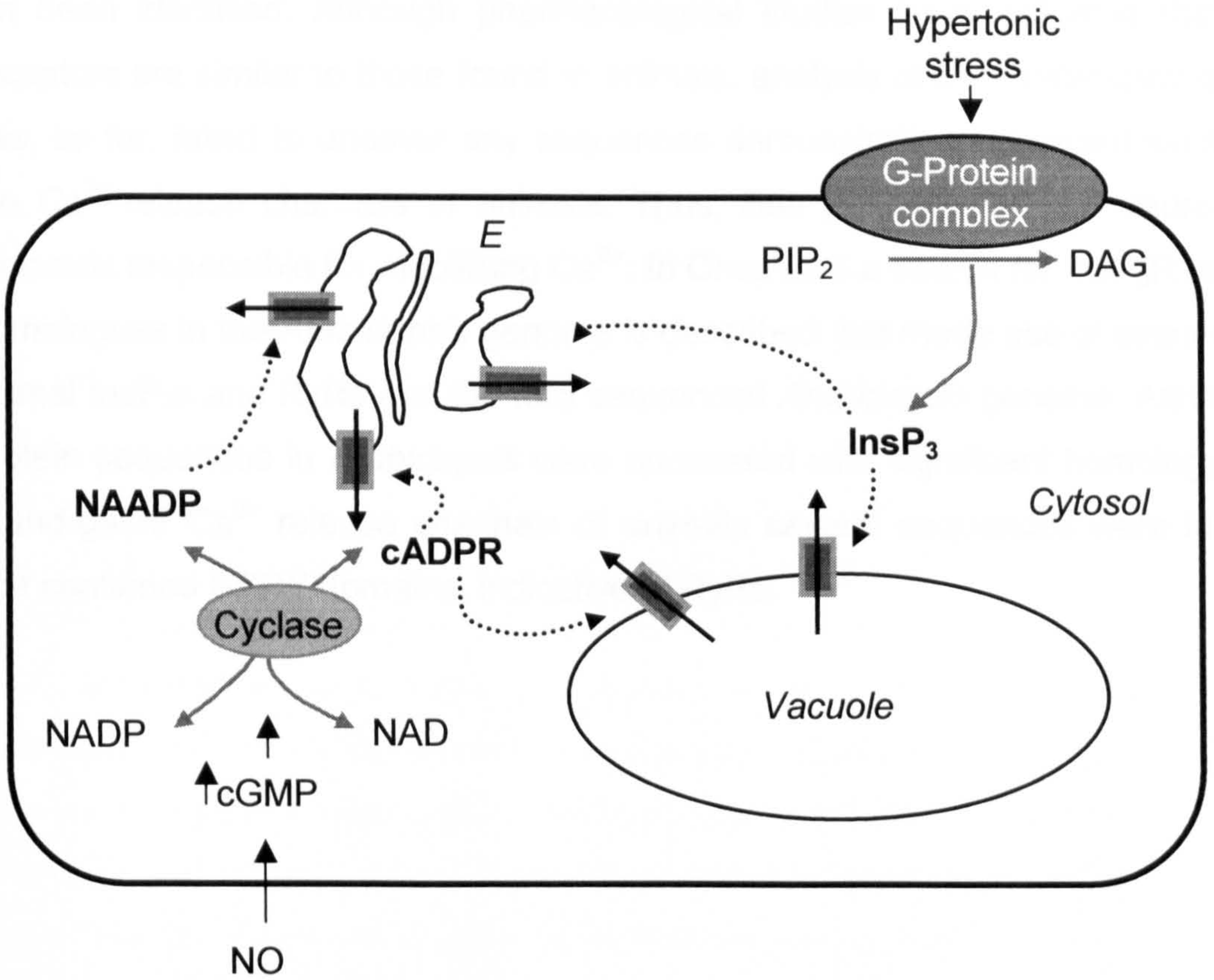

Figure1.3. Ligand gated Ca^{2+} signalling in an idealised plant cell

Both $InsP_3$ and cADPR signalling pathways are believed to be initiated by extracellular signals. Prominent extracellular signals might be NO via cGMP, in the case of cADPR, and hypertonic stress via G-protein mediated release of $InsP_3$ from PIP_2 (which also releases DAG). With various ion-channels discovered in the tonoplast it is thought that calcium waves regularly move over the surface of the vacuole. $InsP_3$, cADPR and NAADP (which may be synthesised from the same enzyme as cADPR) have been reported to mobilise Ca^{2+} from non-vacuolar sources such as the ER.

The genes that encode the putative $InsP_3$, cADPR and NAADP receptors have not yet been identified. Although pharmacological studies have indicated that these receptors are similar to those found in animals, analysis of the *Arabidopsis* genome has, so far, failed to uncover any sequences demonstrating significant similarity to the Ca^{2+}-release channels of animals. Thus, little is known of the nature of the channels responsible for mobilising Ca^{2+}. In Chapter 5 a search for $InsP_3R$ and RyR homologues in the *Arabidopsis* genome is described that made use of sequences of animal $InsP_3$s and RyRs and the fully sequenced *Arabidopsis* genome. Although no protein sequences in *Arabidopsis* were uncovered with significant homology to the ligand-gated Ca^{2+} release channels of animals several sequences were identified that contained SPRY domains, indicative of RyRs.

2. Endogenous cADPR

2.1. Introduction

As detailed in the preceding chapter it is well established that a variety of environmental stimuli are transduced in plants by changes in $[Ca^{2+}]_c$ and that $InsP_3$, cADPR and NAADP are able to mobilise Ca^{2+} stores within plant cells. For cADPR to be shown to have a physiological role as a second messenger in plants it is necessary to demonstrate that plant cells are capable both of cADPR synthesis and hydrolysis. This necessitates the development of an assay capable of detecting nano-Molar quantities of cADPR in plant tissue, since the basal level of cADPR in various animal cell types has been estimated to be 100-200 nM (Walseth *et al.*, 1991). An indirect method for assessing ADP-ribosyl cyclase/hydrolase activity was developed by Graeff *et al.* (1994). This assay monitors cyclic guanine diphosphoribose (cGDPR), a fluorescent analogue of cADPR. ADP-ribosyl cyclase is able to catalyse the formation of cADPR and cGDPR via cyclisation of NAD or its guanine substituted analogue NGD, respectively. Unlike cADPR, which is cyclised at the N-1 position of the purine ring, cGDPR is cyclised at the N-7 position resulting in a fluorescent product (Graeff *et al.*, 1996). As cGDPR is also resistant to hydrolysis it is suitable for monitoring ADP-ribosyl cyclase activity in a variety of tissue preparations. (Figure 2.1) cGDPR can be easily detected using fluorescent spectrophotometry.

To date, there is little information on basal cADPR levels and ADP-ribosyl cylase activity in plant cells. This chapter reports the detection of cADPR and of ADP-ribosyl cyclase activity in plant tissue. Endogenous cADPR was detected in perchloric acid (PA) extracts from red beet tap roots using a radioimmunoassay (RIA) based on that of Takahashi *et al.* (1995). Reverse phase HPLC confirmed the presence of cADPR in red beet tap root acid extracts that had been treated with nucleotide degrading enzymes to remove interfering nucleotides. A comparison is made between the results obtained with the two techniques. ADP-ribosyl cyclase activity was also monitored in red beet and maize roots, cauliflower florets and isolated *Arabidopsis* nuclei using the spectrofluorimetric assay based on cGDPR formation as described by Graeff *et al.* (1994). These experiments provide further evidence for endogenous cADPR in plant tissue and strengthen the argument for its role as a second messenger.

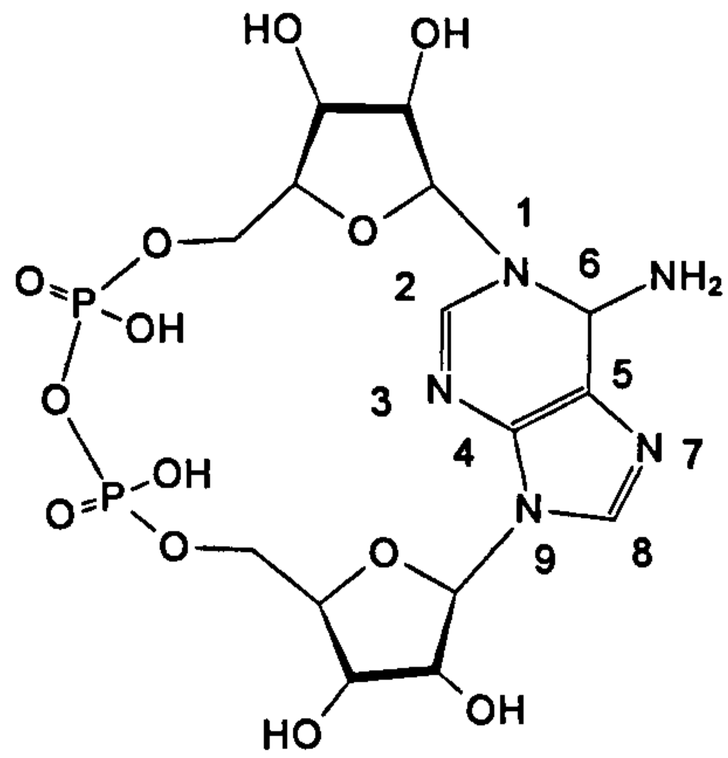

cADPR

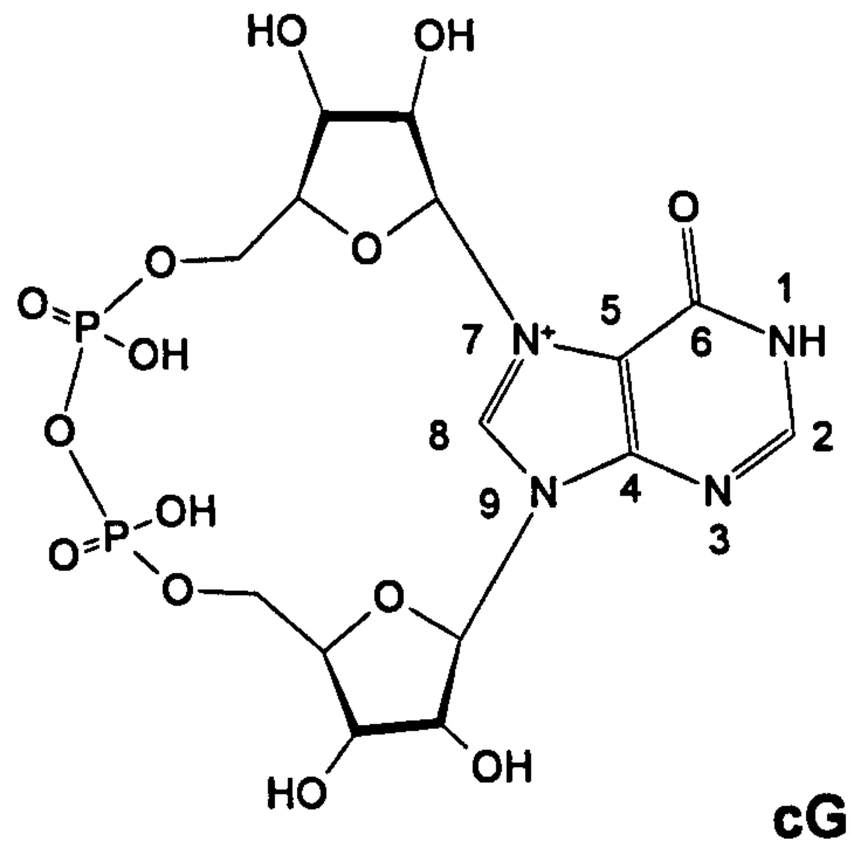

cGDPR

Figure 2.1. The chemical structures of cADPR and cGDPR

2.2. Materials and Methods

2.2.1. Plant material and chemicals

Fresh, greenhouse-grown red beets (*Beta vulgaris* L.) were briefly washed in running tap water before the roots were removed from the plant. The storage root was peeled while the tap root was stripped of lateral roots before use. Seeds of maize (*Zea mays* L.) were imbibed overnight in distilled water, before being transferred to trays of vermiculite. Distilled water was used to keep the vermiculite moist. Maize seedlings were grown in a 12h/day 12h/night cycle at 24 °C/15 °C and an irradiance of 150 μmol m^{-2} sec^{-1}. Plants were harvested after 5-7 days when roots were typically 4-8 cm in length. The roots were briefly rinsed in running tap water before being excised from the plant. Cauliflowers were purchased locally, stored at 4 °C and used within 24 h.

The anti-cADPR antibody serum used in initial experiments was a generous gift from Dr K. Katada (University of Tokyo, Japan). Later experiments made use of serum obtained from Chemicon International Inc. Other reagents, unless indicated to the contrary, were obtained from Sigma.

2.2.2. Preparation and extraction of tissue samples

Two nucleotide extraction methods were used in the preparation of samples for the radioimmunoassay and for HPLC analysis of cADPR. Protocols employed either trichloroacetic acid (TCA) or perchloric acid (PA).

2.2.2.1. TCA extraction

The nucleotide extraction protocol of Takahashi *et al.* (1995) was used as a basis to prepare tissue for the cADPR assay. Red beet tap root or storage root (5 g) was finely sliced in 20 ml of a 4% (w/v) TCA solution (ice cold). The solution was sonicated, 3 x 10 s bursts, on ice using a 100W ultrasonic tip-probe disintegrator (MSE, Crawley, Surrey, U.K.), incubated on ice for 20 min and centrifuged at 15,000 x g for 10 min at 4 °C. The supernatant was neutralised by stepwise addition of 2 M Tris-base to give a pH of approximately 7.5. The extract was lyophilised and stored at –80 °C prior to further purification and HPLC analysis.

2.2.2.2. PA extraction

A modification of the protocol described by Walseth *et al.* (1991) was used to prepare tissue for the cADPR assay. Red beet storage root (5 g) was finely sliced, immediately frozen using liquid nitrogen, and ground to a fine powder in a pre-

cooled porcelain mortar. The frozen powder was added to 2 ml of frozen 3 M PA and allowed to thaw, on ice, to the melting point of PA (approximately –10 °C). The powder was allowed to mix into the liquefied perchlorate and then rapidly diluted to 0.5 M acid with the addition of 10 ml of ice-cold water. Extracts were sonicated as described for TCA extraction and centrifuged at 15,000 x g for 10 min at 4 °C to remove aggregated protein. The supernatant was neutralised by the addition of 2 M $KHCO_3$ and the potassium perchlorate precipitate was removed by centrifugation at 15,000 x g for 10 min. The neutralised supernatant was lyophilised and stored at –80 °C prior to further purification and HPLC analysis.

2.2.2.3. Stimulation of red beet tissue

To investigate whether the signalling compound cGMP is able to stimulate cADPR synthesis in plant cells, red beet tissue was treated with a membrane-permeable analogue of cGMP prior to acid extraction of nucleotides and HPLC analysis. 15 g of red beet tap root was finely sliced and incubated for 30 min at room temperature, with shaking, in 50 mM Tris-Mes (pH 7.5), 1 mM $CaCl_2$ containing 500 μM dibutryl cGMP (DB-cGMP). Unstimulated control tissue was incubated in media that did not contain DB-cGMP under identical conditions. Following incubation, TCA extraction was carried out as described above.

2.2.2.4. Red beet protoplast isolation

Red beet storage or tap root (approximately 1 g) was finely sliced and incubated at 35°C, with gentle shaking, for 1 h, in 10 ml of an enzyme cocktail containing 150 mg cellulase (Onozuka RS, Yakult Honsha Co. Ltd, Tokyo), 80 mg hemicellulase, 10 mg pectolyase, 10 mM KCl, 2 mM $CaCl_2$, 2 mM $MgCl_2$, 600 mM sorbitol, and 0.1% (w/v) bovine serum albumin (BSA), pH brought to 5.5 with HCl. The protoplasts were washed gently through a nylon mesh (50 μm pore diameter) with a solution containing 10 mM KCl, 2 mM $CaCl_2$, 2 mM $MgCl_2$, and 300 mM sorbitol, and collected in a petri-dish over ice. Numbers of protoplasts produced were assessed using a haemocytometer and a light microscope. Early experiments indicated that protoplast yield could be increased by vacuum infiltrating the enzyme cocktail into sliced root material. Thus vacuum infiltration was performed out in later experiments.

2.2.2.5. Maize protoplast isolation

Protoplasts were prepared based on the protocol of Gronwald *et al.* (1982). The tissue was finely chopped in a solution containing 500 mM sorbitol, 1 mM $CaCl_2$, 5

mM 2-[N-morpholino]ethanesulphonic acid (MES)/KOH, pH 6.0), 0.5% (w/v) polyvinyl pyrolidine (PVP, 10,000 MW), 0.5 % (w/v) BSA, 0.8% (w/v) cellulase and 0.08% (w/v) pectolyase. The chopped tissue was agitated at 28 °C in the dark for 3 h. The digest was filtered through 50 μm pore diamter nylon mesh and stored on ice.

2.2.2.6. Protoplast homogenisation

Red beet and maize protoplasts (approximately 30-50 x 10^6 protoplasts/ml) were centrifuged at 150 x g for 5 min, 4°C. The pellet was resuspended in 5 ml of homogenisation buffer A or B (see below), and homogenised in a handheld glass homogeniser, centrifuged at 100 g for 5 min, 4 °C and rinsed with 5 ml of homogenisation buffer. Once rinsed the homogenised protoplasts were re-pelleted by centrifugation at 100 x g for 5 min, 4 °C. The supernatant was tested for cyclase activity immediately.

Two homogenisation buffers were tested during experimentation, Buffer A, and Buffer B. Buffer A was based on the homogenisation buffer used by Graeff *et al.* (1994) containing 340 mM glucose, 20 mM Hepes, 1 mM $MgCl_2$, 10 mM mercaptoethanol, 50 μg/ml soybean trypsin inhibitor (SBTI), 10 μg/ml leupeptin, and 10 μg/ml aprotinin, pH 7.2 with KOH. Buffer B contained 50 mM Tris-MES, 10 mM EDTA, 2 mM DTT, 1 mM benzamine.HCl, 1 μg/ml BSA, 0.5% (w/v) PVP, and 10 μg/ml leupeptin, pH 7.4.

2.2.2.7. Preparation of red beet extracts enriched in tonoplast

A red beet sample rich in tonoplast membrane was prepared from storage root material using sucrose density gradient centrifugation of a microsomal preparation according to Blumwald *et al.* (1986) with the following modifications: 1μg/ml SBTI, 1 μg/ml leupeptin, 0.5 mM phenylmethylsulfonylfluoride (PMSF) and 5 mM benzamidine.HCl were added to the Homogenisation Medium replacing nupercain. 1 μg/ml SBTI and 1 μg/ml leupeptin were also included in the Suspension Medium. After separation of the membranes on a sucrose step-gradient the pink band at the 10-23% (w/w) sucrose interface was removed, diluted 10-fold in Homogenisation Buffer A, and centrifuged at 80,000 x g for 30 min, 4°C. The final pellet was resuspended in the same buffer and stored at –80 °C.

2.2.2.8. Preparation of cauliflower extract

5 mm of the outermost layer of cauliflower inflorescences (approximately 10g) were homogenised in 27.5 ml of 0.33 M sucrose, 5 mM Na_2-EDTA, 5 mM DTT, 0.2% (w/v) BSA, 0.2% (w/v) casein (boiled enzymatic hydrolysate), 0.6% (w/v) PVP-40, 1 mM benzamidine.HCl, 0.5 mM PMSF, 2 μg / ml leupeptin and 50 mM Mops / BTP, pH 7.5, supplemented with 1.7% (w/v) Protease and Phosphatase Inhibitor Cocktail (for plant cell extracts; Sigma, P6599). The homogenate was filtered through four layers of muslin and centrifuged at 10,000 g for 15 min at 4 °C to remove cell debris. Extracts were used immediately.

2.2.3. Isolation of intact nuclei

2.2.3.1. Homogenisation

A modification of the method of Folta and Kaufman (2000) was used to isolate nuclei from light-grown *Arabidopsis*. Ten to 15 g of *Arabidopsis* leaves were harvested and immersed in 4 volumes (approximately 100 – 150 ml) of ice-cold anhydrous ethyl ether. The tissue was chopped with scissors for 5 min while on ice. The ether was poured off and the tissue was rinsed twice with 3 volumes (approximately 25 - 30 ml) of extraction buffer, comprising 1.0 M hexylene glycol (2-methyl-2,4-pentandiol), 0.5 M PIPES-KOH (pH 7.0), 10 mM $MgCl_2$, 5 mM 2-mercaptoethanol. The tissue was resuspended in 2 volumes (approximately 15 – 20 ml) of extraction buffer and homogenised with a Polytron tissue homogeniser set to 19,000 rpm. Homogenisation was carried out for 15 min, on ice. All the following procedures were carried out at 4 °C. Particulate matter was removed from the homogenate by passing it through a double layer of muslin, pre-soaked in extraction buffer. Twenty five percent (v/v) Triton X-100 was added dropwise to the homogenate, with constant stirring, until a final concentration of 1 % (v/v) was reached, to lyse organelles other than the nuclei.

2.2.3.2. Purification of nuclei

The homogenate was made up to 40 ml with extraction buffer containing 1% (v/v) Triton X-100 and centrifuged at 2,000 x g for 30 min at 4 °C. The supernatant was gently removed and the nuclei, visible as a layer of non-clumping material on the top of the pellet, were resuspended in 5 ml of ice-cold gradient buffer, 0.5 M hexylene glycol, 0.5 M PIPES-KOH (pH 7.0), 10 mM $MgCl_2$, 5 mM 2-mercaptoethanol, 1% (v/v) Triton X-100. Resulting nuclei were gently resuspended by swirling the gradient buffer in the tube with a soft hair paintbrush. Care was taken not to disturb any non-

homogenised plant material, cell debris or starch visible as layers of denser material under the nuclei.

Once resuspended the nuclei-containing fraction was removed and made up to 40 ml with ice-cold gradient buffer. This suspension was centrifuged at 2,000 x g for 5 min at 4 °C to remove any remaining non-nuclear material. The supernatant was removed and the nuclei once again resuspended in 5 ml of gradient buffer as described above. This nuclei-enriched fraction was centrifuged at 2,000 x g for 5 min at 4 °C, the supernatant was removed and the pellet was resuspended in 800 µl of nuclear storage buffer, comprising 50 mM Tris-HCl (pH 7.8), 10 mM 2-mercaptoethanol, 20% (v/v) glycerol, 5 mM $MgCl_2$ and 0.44 M sucrose, with extremely gentle pipetting. Nuclei were stored at –80 °C until use.

2.2.4. HPLC

Modifications of the methods of Graeff *et al.* (1997) and Ziegler *et al.* (1997), respectively, were used to prepare and analyse tissue extracts for cADPR. For initial experiments lyophilised TCA and PA extracts prepared from red beet storage root were reconstituted in dH_2O (10x volume) and incubated at 37°C for 2 h to break down potentially interfering nucleotides, such as NAD, NADP, ATP and ADP, with an enzyme cocktail of NADase from *N. crassa* (0.25 U/ml), nucleotide pyrophosphatase from *C. atrox* venom (1.75 U/ml), bovine alkaline phosphatase (50 U/ml) and apyrase from potato (5 U/ml) in 100 mM Hepes (pH 7.5) and 5 mM $MgCl_2$. The enzyme-treated extract was filtered (0.2 µm pore diameter filters; Whatman), applied to an AG MP-1 mini-column (a macroporous Dowex-1 anion-exchange resin, 200-400 mesh, Cl^- form purchased from Bio-Rad and converted to the trifluoroacetate following the manufacturers instructions; 0.6 ml bed volume) that had been equilibrated with water. The column was washed with 3 ml water, and bound cADPR was eluted with 30 mM trifluoroacetic acid (TFA). Fractions eluting at the same time as cADPR standards were applied to a reverse phase column (4.6 x 250 mm; Genesis C18 (4 µm); Jones Chromatography) fitted with the appropriate guard column. Elution was carried out at a flow rate of 1 ml/min with phosphate buffer containing 100 mM potassium phosphate and 5% (v/v) MeOH, taken to pH 6 with KOH. Absorbance at 254 nm was monitored.

The elution times of authentic cADPR, ADPR, NAD, nicotinamide and adenosine triphosphate (ATP) standards were determined on the reverse phase column described above to aid in peak identification and to verify that adequate separation

was achieved. To determine whether the elution times of the nucleotides of interest were the same under experimental conditions, acid extract samples were spiked with 100 μM of the compound and applied to the HPLC column as described.

For later experiments acid extracts were reconstituted in 1x volume of dH_2O. The analysis was otherwise the same except a larger AG MP-1 column was used (2 ml bed volume). It was washed and eluted with twice the volumes described above. Fractions believed to contain cADPR were split. Half were heated to 100°C for 30 min. They were then analysed by HPLC.

2.2.5. Radioimmunoassay for cADPR

A modification of the RIA of Takahashi *et al.* (1995) was used to detect cADPR in red beet tissue.

2.2.5.1. Preparation of [^{32}P]cADPR

Aplysia ADP-ribosyl cyclase was used to prepare [^{32}P]cADPR from [^{32}P]NAD as follows. 18 μl of 6.3μM [α-^{32}P]NAD (NEG-023X, 29.6 TBq/mmol, 185 MBq/ml) was combined with 2 μl of 0.2 M Hepes-Na (pH 7.4) and 0.33 μl of 200 μg/ml *Aplysia* ADP-ribosyl cyclase (Sigma, A8950) and incubated at 25 °C for 35 min. The reaction was terminated with the addition of 2 μl of 50 % (w/v) TCA, neutralised with 5 μl of 2 M Tris-base solution and diluted 10-fold with ultrapure water. The reaction mix was applied to an AG MP-1 mini-column (Cl^- form, 0.4 ml bed volume) equilibrated with water. The column was washed with 1 ml of water and bound [^{32}P]cADPR was eluted with 30 mM trifluoroacetic acid.

2.2.5.2 Binding assay

Lyophilised TCA or PA extracts were reconstituted in dH_2O (10x volume) and incubated with 50 U/ml of bovine alkaline phosphatase and 2 U/ml of venom phosphodiesterase in 100 mM imidazole.HCl (pH 7.5), 2 mM $MgCl_2$, 100 mM NaCl and 400 mM KCl to degrade any nucleotides that may cross react with anti-cADPR antiserum. 15 μl of the enzyme-treated sample was mixed with 10 μl of 1.5 nM [^{32}P]cADPR (20,000 cpm; approximately 0.6 kBq) in 0.2 M imidazole.HCl (pH 7.5) containing 10 mg/ml of bovine γ-globulin, followed by the addition of 5 μl of the anti-cADPR antiserum diluted with PBS containing 15 mg/ml of bovine γ-globulin. Following incubation at 25°C for 2 h, 60 μl of 20% (w/v) polyethylene glycol (MW; 6,000) in 0.1 M imidazole.HCl (pH 7.5) was added to the reaction mixture. The immune complex of [^{32}P]cADPR-bound antibodies together with γ-globulin added as

a carrier for precipitation. The precipitate was removed from the solution by centrifugation at 15,000 x g for 10 min, and the supernatant (60 μl) was counted for the unbound form of [^{32}P]cADPR in a liquid scintillation counter.

A standard curve was prepared by replacing enzyme treated extracts with known concentrations of cADPR (1-1000 nM). A sigmoid curve was fitted to the data using the equation:

$$Y = \frac{A}{1+10^{(\log(K_{0.5})-\log[L]).\text{Slope Factor}}} + \text{Nonspecific Binding}$$

where **Y** is the free [^{32}P]cADPR, **A** is the free [^{32}P]cADPR in the presence of the competing ligand, the **Slope Factor** is the Hill coefficient, **[L]** is the concentration of unlabelled cADPR and $\mathbf{K_{0.5}}$ is the concentration of unlabelled cADPR giving half-maximal displacement of [^{32}P]cADPR. **Nonspecific Binding** is defined as the free [^{32}P]cADPR in the absence of competing ligand.

2.2.6. Spectrofluorimetric assay of ADP-ribosyl cyclase

The conversion of nicotinamide guanine dinucleotide (NGD) to cyclic GDP-ribose (cGDPR) was used to detect ADP-ribosyl cyclase activity based on the assay described by Graeff *et al.* (1994). The structure of cGDPR is identical to cADPR except the adenine is replaced by guanine (Figure 2.1). Spectroscopic analysis has indicated that cGDPR is fluorescent while the substrate NGD, the hydrolysis product, GDP-ribose, and cADPR are not. The accumulation of cGDPR is thus an indication of cyclase activity and can be easily monitored as the reaction progresses by exciting the reaction mix at 300 nm and measuring the resultant fluorescence changes emitted at 410nm.

Maize root and red beet protoplasts, cauliflower meristematic tissue or root tissue from maize and red beet were homogenised in ice cold buffer containing 340 mM glucose, 20 mM Hepes, 1 mM $MgCl_2$, 50 μg/ml soybean trypsin inhibitor (SBTI), 10 μg/ml leupeptin, and 10 μg/ml aprotinin, pH 7.2 with KOH (1 g of tissue in 10 ml of buffer or approximately 30-50 protoplasts x 10^6/ml) and cell debris was removed by centrifugation at 10,000 x g for 15 min at 4 °C. 600 μl aliquots of homogenised plant material were incubated separately with 40 μM NGD or NAD at ambient

temperature with stirring. The resultant fluorescence changes at 410 nm (excited at 300 nm) were measured using a luminescence spectrofluorimeter (Perkin-Elmer Model LS-5). Homogenate that had been incubated at 95 °C for 2 h to inactivate enzyme activity was assayed as a negative control.

To determine the rate of formation of cGDPR the fluorescence changes were converted to concentrations of cGDPR by comparison with cGDPR standards. cGDPR standards were prepared by incubating 40 μM NGD with Aplysia ADP-ribosyl cyclase for 30 min. The reaction was monitored to ensure it went to completion. It was assumed that 100% of the NGD was converted to cGDPR and a range of concentrations of cGDPR was prepared by serial dilution.

2.2.7. Protein determination

Protein concentration was determined with a Bio-Rad assay kit based on the dye binding method of Bradford (1976). Bovine serum albumin was used as a standard.

2.3. Results

2.3.1. Endogenous cADPR in beet and cauliflower

Both red beet and cauliflower tissue have been previously shown to be responsive to Ca^{2+}-mobilising ligands such as cADPR (see section 1.3.3.3). If cADPR acts as a second messenger in plants in a homologous manner to that of animal cells its level in the cell will be strictly regulated via the action of ADP-ribosyl cyclases and hydrolases. One way to assess the role of cADPR in plants is to determine the levels of endogenous cADPR in resting and stimulated tissue. In animals values for basal levels of cADPR vary depending on the tissue investigated and the extraction system/assay used. However, in unstimulated tissue the concentration of cADPR has generally found to be in the picomolar range, for example 1 pmol/mg protein in rat heart and 3 pmol/mg protein in rat liver (Walseth *et al.*, 1991). Two methods that have been utilised by investigators to measure endogenous levels of cADPR in this range in animal tissue are RIA (Takahashi *et al.*, 1995) and HPLC analysis of purine nucleotides in tissue extracts (Axleson *et* al., 1981; Zeigler *et al.*, 1997). Both of these methods were examined here to assess their effectiveness in measuring cADPR in plant tissue.

2.3.1.1. RIA

The cADPR content of tissue extracts was determined using the RIA described by Takahashi *et al.* (1995). This assay is sensitive down to 100 pmol of cADPR and makes use of anti-cADPR antibody raised in rabbits and [^{32}P]-labelled cADPR. [^{32}P]cADPR was prepared here by incubating [^{32}P]NAD with purified *Aplysia* ADP-ribosyl cyclase. The [^{32}P]cADPR was purified on an AG-MP 1 anion exchange mini-column (Cl^- form, 0.6 ml bed volume) and then added to an extract to be tested. When the anti-cADPR antibody was added to the extract it competitively bound both radioactively labelled (hot) and unlabelled (cold) cADPR. By comparisons with standards the proportion of cold cADPR bound and thus the amount of cADPR in the extract was estimated. The presence of cross-reacting nucleotides required both samples and standards to be treated with enzymes prior to use in order to degrade nucleotides other than cADPR into inactive compounds. An assay with improved sensitivity to cADPR has been reported that makes use of anti-cADPR antibodies raised in chickens (Graeff *et al.*, 1998), however the antibody is not commercially available.

A standard curve for the RIA of cADPR was prepared. Figure 2.1A indicates that as the concentration of unlabelled cADPR was increased the amount of unbound [^{32}P]cADPR in solution increased, reflecting a decrease in the binding of [^{32}P]cADPR. Throughout the experiments consistently high background cpm values were measured. This is manifested in the high value measured in the presence of 1 nM cADPR. The high background values are indicative of non-specific binding. While a sigmoid curve was obtained upon plotting the data on a log scale, as expected for this assay, it was flattened in comparison to previous standard curves (Dr K. Katada, personal communication). This problem was not resolved and led to a severe reduction in the accuracy of the assay, particularly when attempting to deduce concentrations of cADPR within the lower range of the standard curve.

Two methods for extracting nucleotides from red beet tap root were investigated, one utilising TCA the other PA. Using the RIA no cADPR was detected in TCA extracts. The PA extracts, however, demonstrated 10.0 ±2.4 pmol of cADPR / mg protein (Figure 2.2B). In an attempt to validate the assay, red beet extracts were heat treated to convert cADPR to its linear analogue ADPR to which the assay is not sensitive. In PA extracts that had been boiled for 30 min the amount of cADPR detected decreased to 3.95±2.0 pmol/mg (Figure 2.2B).

2.3.1.2. HPLC

The red beet acid extracts were also examined by HPLC to evaluate their cADPR content. Various HPLC methods have been used to detect cADPR in acid extracts from animal tissue which make use of anion exchange (Axleson *et al*, 1981), or reverse phase chromatography (Ziegler *et al.*, 1997) or a combination of the two (Pawlikowska *et al.*, 1996; Kim *et al.*, 1993). Here isocratic reverse phase chromatography was initially used to examine extracts that had been enzyme treated to remove interfering nucleotides. Initial optimisation of the HPLC indicated that the greatest degree of separation of nucleotides with a Genesis C18 column, without excessive peak spreading, could be achieved using eluting buffer of pH 6 containing 5% (v/v) MeOH and a flow rate of 1ml/min (data not shown). Figure 2.3 indicates that in these conditions the resolution of separation of the acid extract constituents was insufficient to distinguish peaks that corresponded to endogenous cADPR. To clean up the samples they were further purified using an anion exchange mini-column. Enzyme treated acid extracts were loaded onto an AG-MP1 column. The column was washed with buffer and bound compounds eluted with 30 mM TFA. Authentic nucleotides run on the column under identical conditions

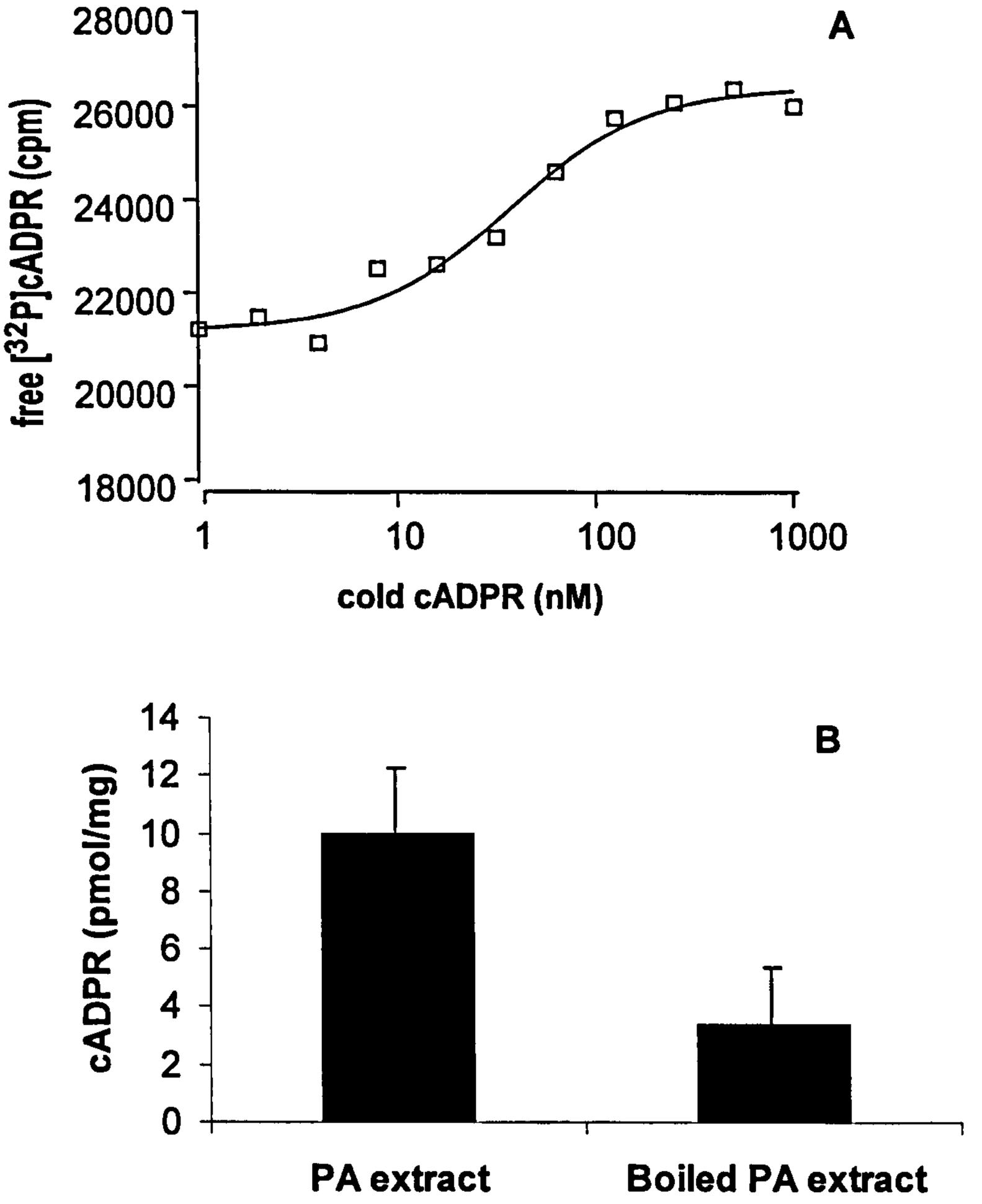

Figure 2.2. Endogenous cADPR detected in red beet by RIA

A. A standard curve for the radioimmunoassay of cADPR was generated through the displacement of [^{32}P]cADPR from the antibody by cold cADPR as described in Materials and Methods. The result from one experiment is depicted. **B.** The assay of endogenous cADPR was carried out for PA extracts of red beet tissue prepared as described in Materials and Methods. Tissue that had been boiled for 20 min to break down cADPR was used as a negative control. Values derived from comparison to the standard curve are shown. Mean values for three experiments are shown with SEM.

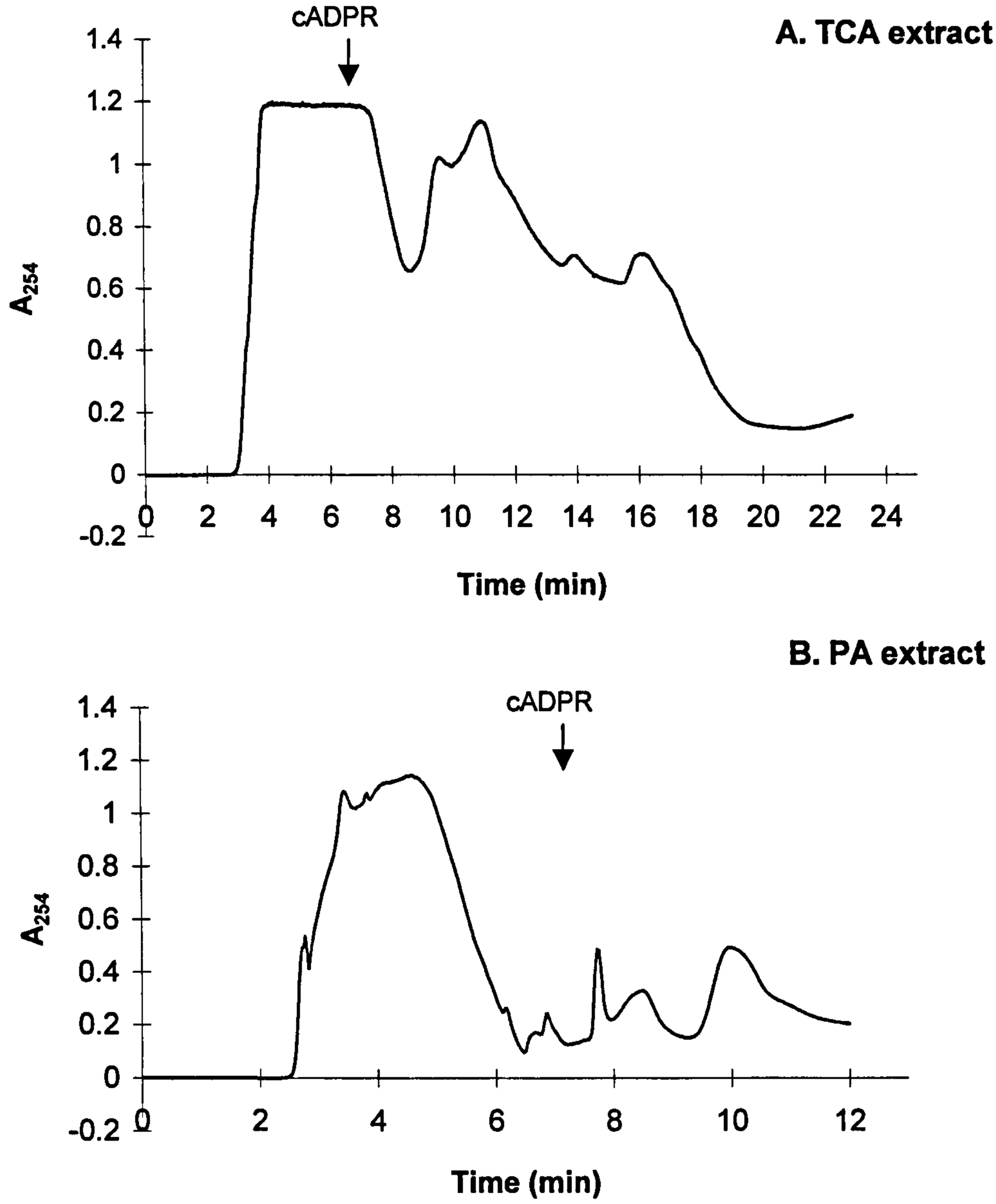

Figure 2.3. HPLC analysis of acid extracts from red beet tap root

Nucleotides were purified from homogenised red beet tap root by acid extraction with TCA (**A**) or PA (**B**). The extracts were neutralised and separated on a reverse phase column with an isocratic gradient of 100 mM potassium phosphate (pH 6) containing 5% (v/v) MeOH. The absorbance at 254 nm was monitored. The time of elution of authentic cADPR is indicated by the arrows.

demonstrated different elution times indicating chromatographic separation was occurring (data not shown). Fractions coelluting with cADPR standards were neutralised, combined and analysed by HPLC. As Figure 2.4 indicates, in TCA extracts a peak could be detected at 7.5 min, corresponding to the elution time of the cADPR standard. NAD and ADPR eluted at 10.7 min and 8.9 min respectively under the same conditions. PA extracts retained interfering compounds that eluted at 7.5 min, masking smaller peaks that may have corresponded to cADPR.

By comparing the areas of peaks attributed to cADPR in TCA extracts with the area of known concentrations of cADPR standards an estimation of the concentration of cADPR in the extracts was made. In three separate extractions a peak of sufficient size to be measured was detected. From these peak areas a mean value of 0.12 ± 0.09 pmol of cADPR / mg of protein was calculated. Figure 2.5 shows that while the peak seen at 7.4 min could be diminished by heat treatment the corresponding increase in ADPR that would be expected for a sample containing cADPR was not observed. Thus, the authenticity of the cADPR peak could not be confirmed.

The signalling agent cGMP has been proposed to stimulate cADPR production in plants (see section 1.6.2). To further investigate this proposition and test the efficacy of the HPLC assay for monitoring physiological changes in cADPR in plant cells red beet tissue was incubated with DB-cGMP for 30 min prior to acid extraction. The tissue was purified and analysed via HPLC for cADPR. Figure 2.6 illustrates that in comparison to untreated tissue, several components of the extract changed following cyclic nucleotide treatment suggesting that various compounds in the cell may be affected by cGMP. Although there was a general increase in the broad peak corresponding to cADPR it was not ascertained whether this was due to an increase in cADPR, or other components of the extract eluting at a similar time.

2.3.2. ADP-ribosyl cyclase activity

To determine whether different plant tissues possess ADP-ribosyl cyclase activity homogenised maize roots, protoplast released from maize roots, cauliflower inflorescences, red beet tap root and protoplast released from red beet tap roots were incubated with 40 μM NGD, based on the protocol of Graeff *et al.* (1996). The change in fluorescence was monitored (Excitation: 300 nm; Emission: 410 nm) and recorded. As shown in Figure 2.7 an increase in fluorescence over the time of incubation was observed in homogenised maize and beet protoplasts and in cauliflower as would be expected during the generation and accumulation of the

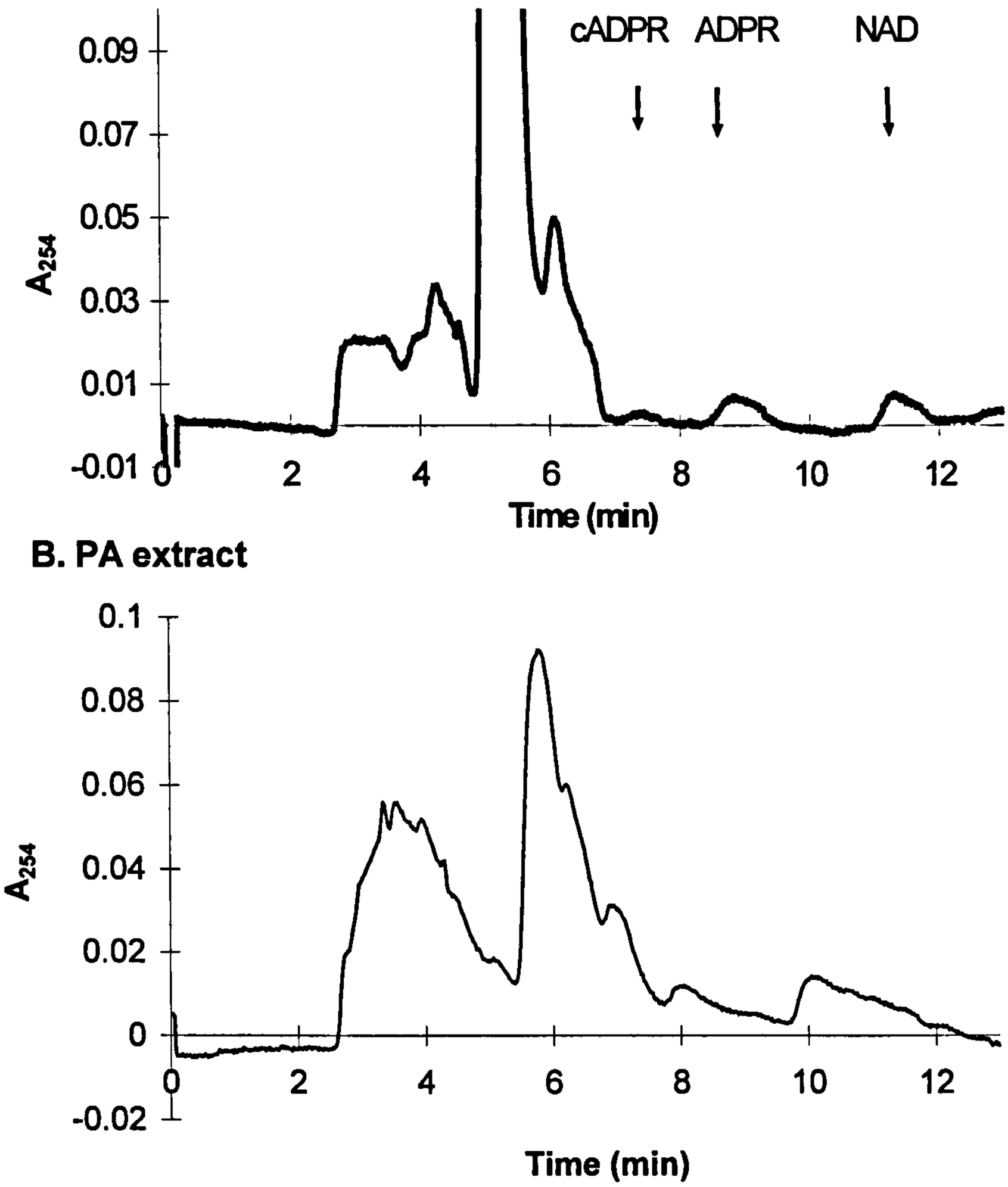

Figure 2.4. Endogenous cADPR detected in red beet extract using HPLC

Nucleotides were purified from homogenised red beet tap root by acid extraction with TCA (**A**) or PA (**B**). The extracts were further purified by means of AG–MP1 column chromatography as described in Materials and Methods. Fractions eluting at the same time as cADPR standards were analysed by reverse phase HPLC to assess whether cADPR was present. The absorbance at 254 nm was monitored. The time of elution of authentic nucleotides are indicated by arrows.

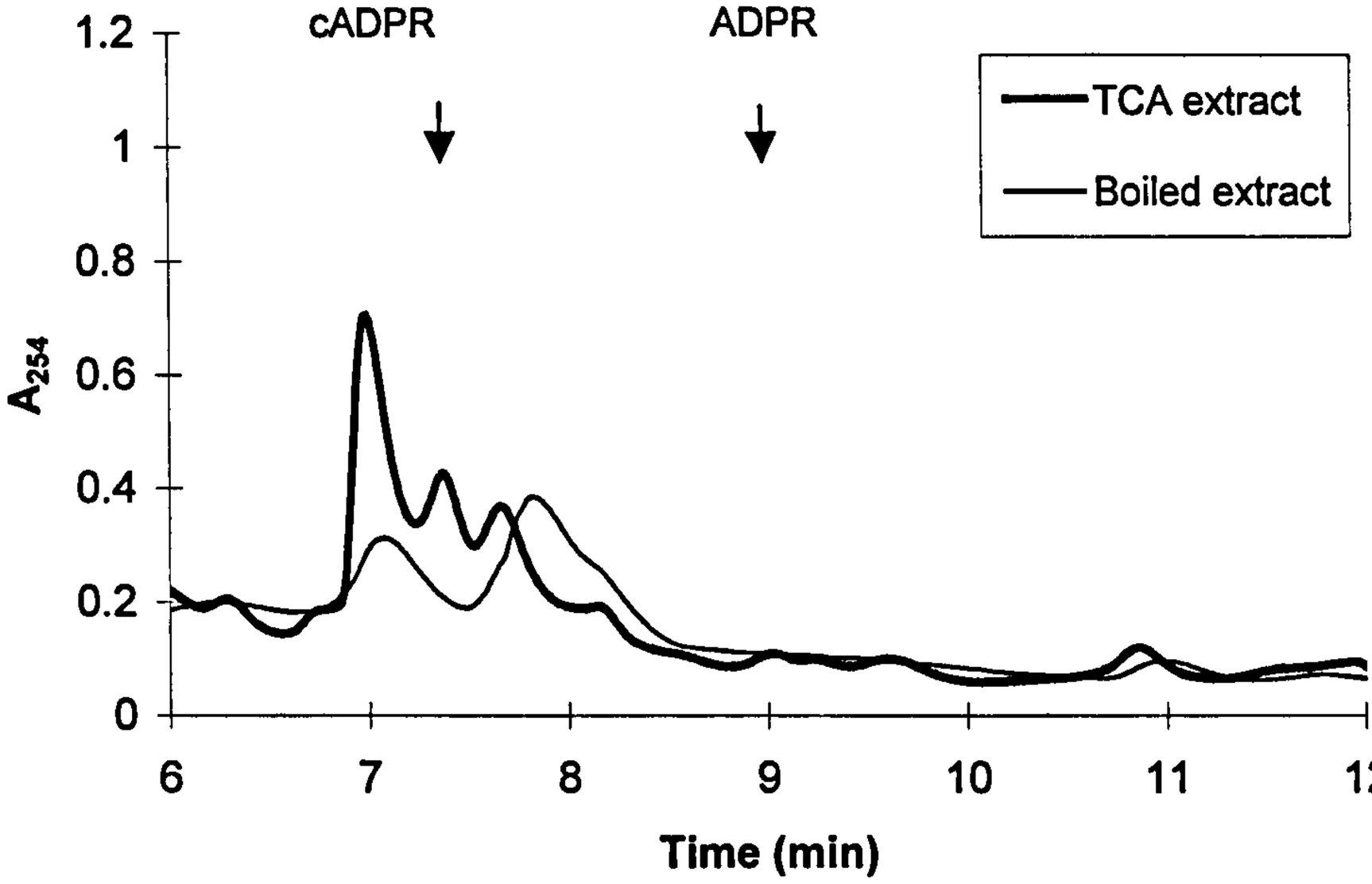

Figure 2.5. HPLC analysis of heat treated TCA extract

Nucleotides were purified from homogenised red beet tap root by acid extraction with TCA. The extracts were further purified by means of AG–MP1 column chromatography, as described in Materials and Methods. Fractions eluting at the same time as cADPR standards were combined and split. Half of the purified extract was boiled for 30 min convert cADPR to ADPR. The extracts were analysed by reverse phase HPLC to assess whether cADPR was present. The absorbance at 254 nm was monitored. The time of elution of authentic cADPR and ADPR are indicated by arrows.

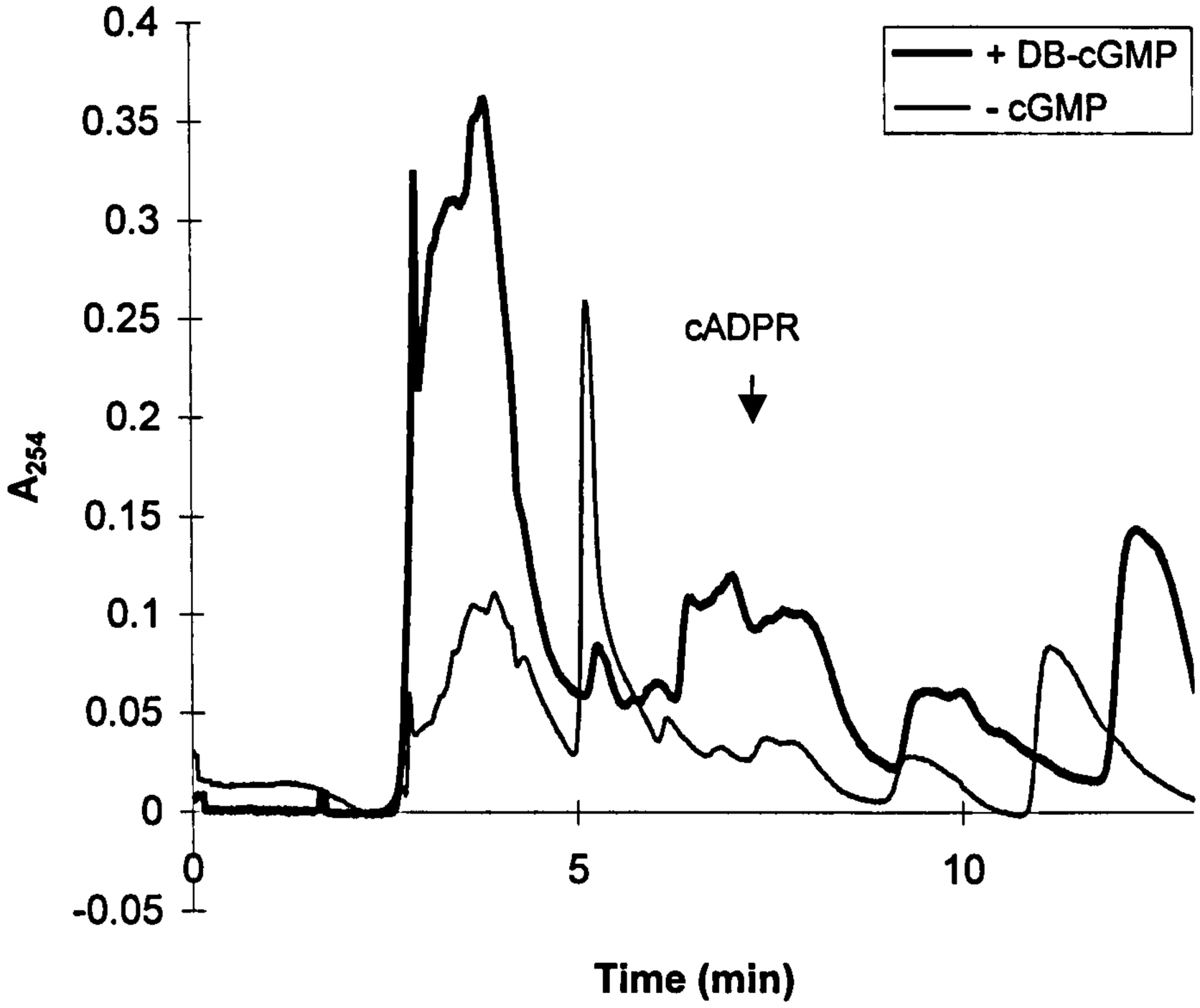

Figure 2.6. HPLC analysis of DB-cGMP stimulated beet extract

Sliced red beet tap root was incubated with or without DB-cGMP. The tissue was homogenised and nucleotides acid extracted, purified and analysed by HPLC as described in Materials and Methods. The time of elution of authentic cADPR is indicated.

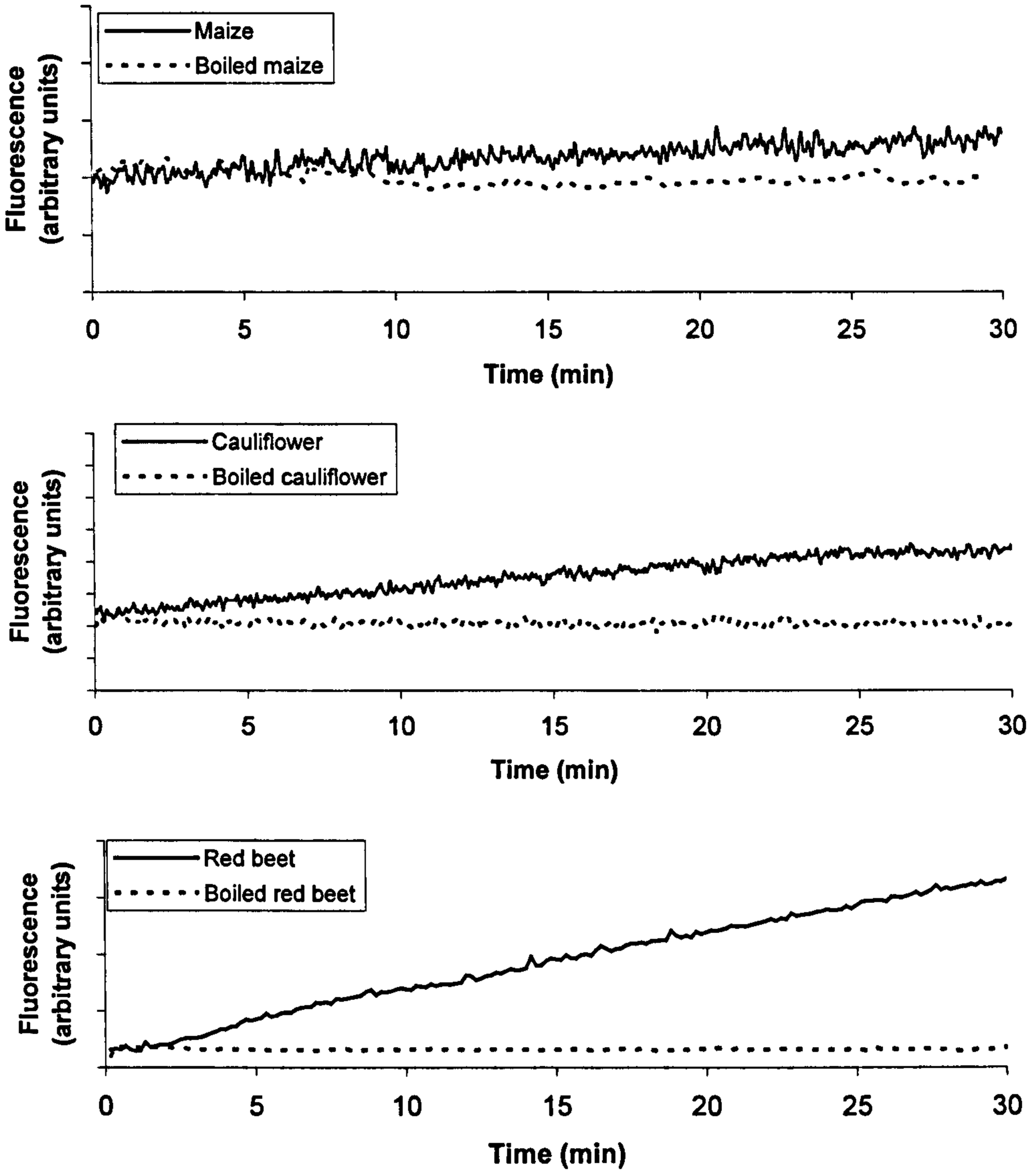

Figure 2.7. Various plant tissues demonstrate ADP-ribocyclase activity

Homogenised maize root protoplasts (**A**), cauliflower meristematic tissue (**B**) and red beet protoplasts (**C**) were assayed for ADP-ribosyl cyclase activity by incubating them with 40 μM NGD in assay buffer, at room temperature, as described in Materials and Methods. Changes in fluorescence were monitored with a luminescence spectrofluorimeter. Tissue boiled for two hours was also assayed as a negative control.

fluorescent product cGDPR. Tissue that had been boiled for two hours did not demonstrate an increase in fluorescence indicating that the change in fluorescence was an enzyme mediated process.

Following reports that ADP-ribosyl cyclase activity had been measured in the nuclear membranes of MC3T3.E1 cells (Adebanjo *et al.*, 1999) and that plant nuclei contain elements of Ca^{2+}-signal transduction machinery (Downie *et al.*, 1998; Bunney *et al.*, 2000) nuclei isolated from *Arabidopsis* were also investigated for ADP-ribosyl cyclase activity. Purified nuclei were isolated (Figure 2.8). The nuclei were demonstrated to be transcriptionally competent by their ability to incorporate [^{32}P]-UDP into mRNA (Dr B. Stanchev, University of York, personal communication). The nuclei were incubated with NGD and the change in fluorescence monitored. The increase in fluorescence detected is consistent with the synthesis of cGDPR and could be abolished by heat treatment (Figure 2.9). The samples monitored all demonstrated large fluctuations in fluorescence over the course of the experiment. This noise may be due to inconsistencies in the stirring. The nuclei were observed to clump together and could have also attached themselves to the cuvette wall or stir bar. Isolated nuclei or *Arabidopsis* leaf tissue homogenised with a pestle and mortar did not demonstrate an increase in fluorescence when assayed (data not shown).

By using a calibration curve to convert the changes in fluorescence to concentrations of cGDPR, as described in Materials and Methods, the rates of CGDPR synthesis were determined (Table 2.1).

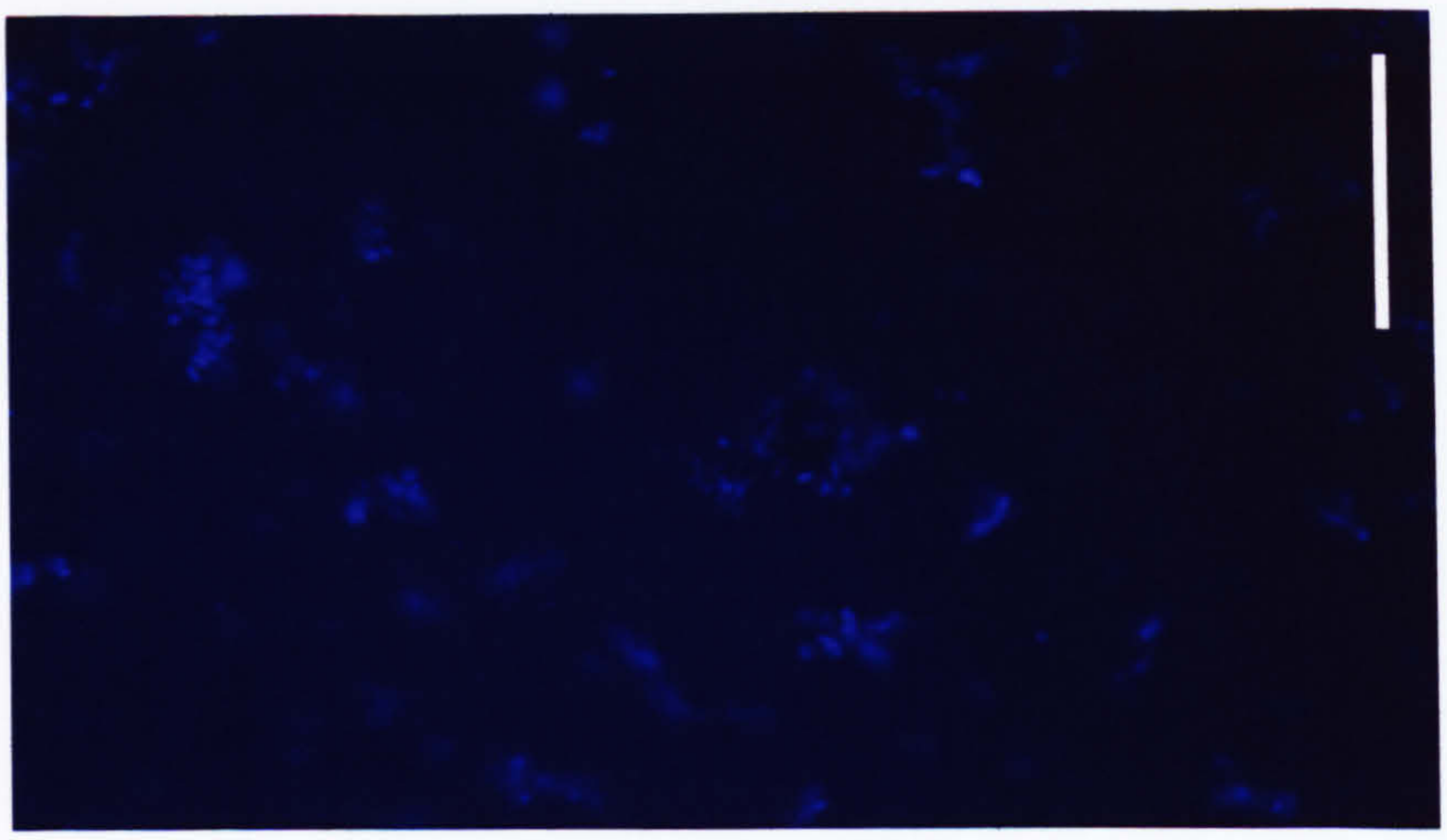

Figure 2.8. Isolated nuclei stained with DAPI

Nuclei of *Arabidopsis* leaf cells were isolated as described in Materials and Methods. The nuclei were viewed with fluorescence microscopy following treatment with DAPI (10 μg/ml) to enhance identification (**A** and **C**) and under bright field (**B**). The bar in A is 200 μM, the bars in B and C are 10 μM.

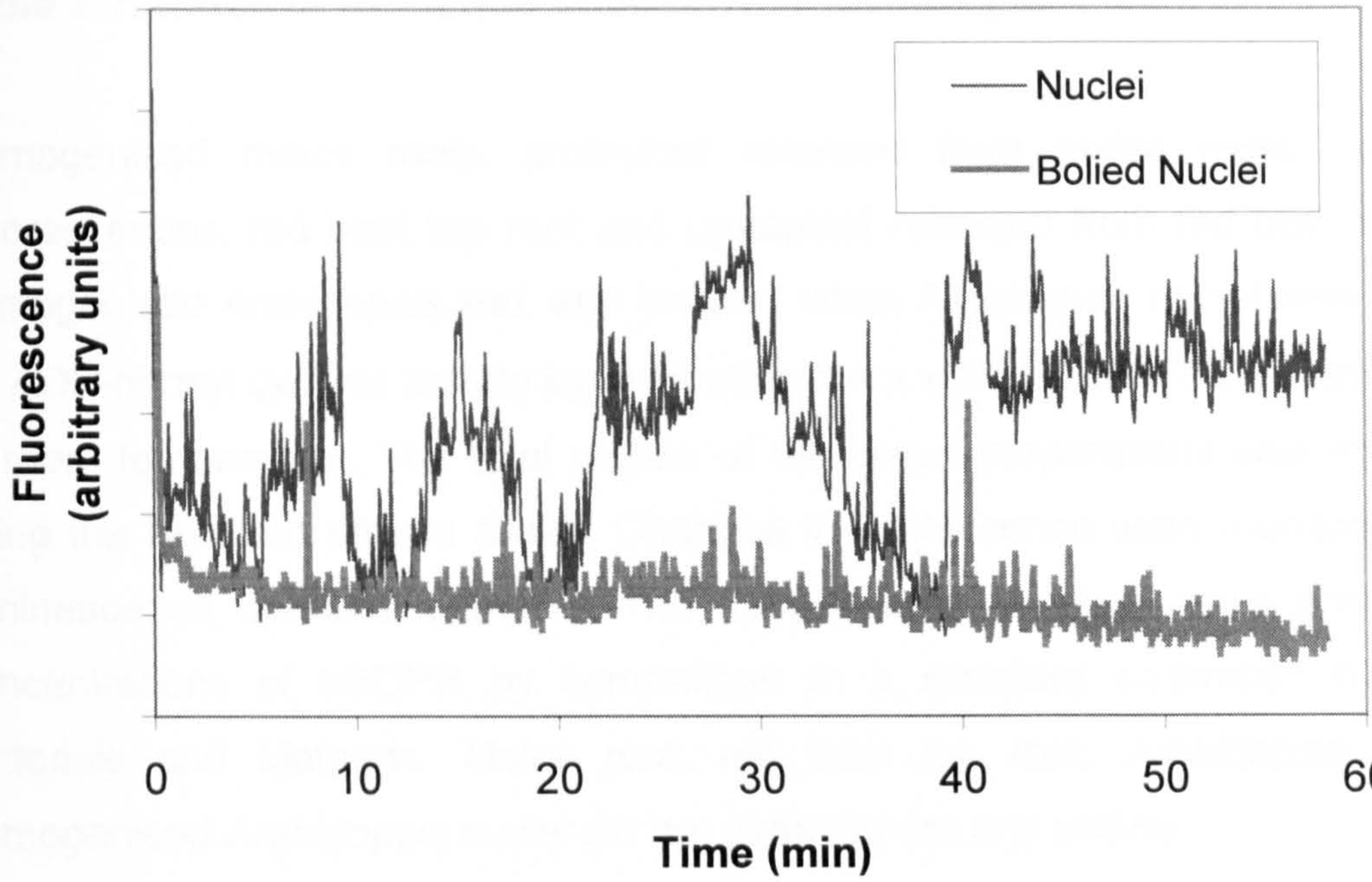

Figure 2.9. Nuclear ADP-ribosyl cyclase activity

Isolated *Arabidopsis* nuclei were assayed for ADP-ribosyl cyclase activity by incubating them with 40 mM NGD in assay buffer at room temperature, as described in Materials and Methods. Changes in fluorescence were monitored with a luminescence spectrofluorimeter. Nuclei boiled for one hour were also assayed as a negative control.

Table 2.1. Rates of formation of cGDPR in various plant tissues

Homogenised maize roots, protoplast released from maize roots, cauliflower inflorescences, red beet tap root and protoplast released from red beet tap roots, homogenised *Arabidopsis* leaf, and isolated intact *Arabidopsis* nuclei were assayed for ADP-ribosyl cyclase activity by incubating them with 40 μM NGD in assay buffer, at room temperature. The total protein of the tissue preparations was determined using the Bradford protein assay. Changes in fluorescence were monitored with a luminescence spectrofluorimeter. The fluorescence changes were converted to concentrations of cGDPR by comparison to a standard calibration curve, see Materials and Methods. Maize root, red beet tap root, *Arabidopsis* leaf and homogenised *Arabidopsis* nuclei did not demonstrate any activity.

Tissue	**Specific activity (nmol/mg.h)**
Maize protoplasts	0.2±0.1
Cauliflower meristem	0.5±0.2
Red beet protoplasts	0.8±0.4
Arabidopsis nuclei	0.4±0.4

2.4. Discussion

2.4.1. Endogenous cADPR

It has been hypothesised that plant cells use cADPR as a second messenger in a similar manner to that of animal cells even though the evidence for endogenous cADPR in plant cells is limited to two previously described reports from Wu *et al.* (1997) and Bewell (1999). The RIA and HPLC analysis carried out here substantiate these reports. However, the techniques were not consistent in the amount of cADPR they measured. The RIA indicated that 10.0 ±2.4 pmol/mg protein of cADPR could be extracted from red beet root using PA, but did not detect cADPR in TCA extracts. The value for the cADPR concentration detected via RIA was similar to that reported in animal cells (1-3 pmol/mg in rat tissue). However, the high background values of radioactivity observed while performing the RIA cast some doubt on the accuracy of the reading. Later experiments with the RIA monitoring the effects of regulators, such as cGMP, on endogenous cADPR (data not shown) demonstrated a large degree of variance and were unsuitable for assessing changes in cADPR over a physiological range of concentrations. Whether the variance was due to the high background and unspecific binding or other factors, such as degradation of the antibody, could not be determined.

Although reverse phase HPLC analysis suggested that cADPR could be acid-extracted from plant tissue, this method was not suitable for accurately determining the quantity of cADPR in the samples as the amount of cADPR extracted was close to the detection limit. The limitations on the quantity of cADPR that could be extracted with TCA were exacerbated by losses of cADPR arising from the additional anion-exchange step required to clean up the sample and suggest that the derived value of 0.12 ± 0.09 pmol cADPR / mg of protein detected is likely to be an underestimate. A single-step chromatographic separation would be simpler to perform and would limit this loss. The reverse-phase HPLC carried out here did not possess sufficient resolving power to separate cADPR from other tissue extracts.

The results of these assays are consistent with the presence of endogenous cADPR but the problems of high background, inaccuracy and high cost of the RIA and the lack of resolving power of the reverse phase HPLC indicate that other techniques should be examined for the accurate determination of cADPR concentrations in plant tissue. More accurate methods are especially required for monitoring metabolic changes that might occur during signalling. While the preliminary data

obtained from HPLC analysis of tissue extracts treated with cGMP are suggestive of a cGMP-modulated increase in cADPR, improved chromatographic separation techniques are required to substantiate this.

2.4.2. ADP-ribosyl cyclase activity

For plant tissue to use cADPR as a second messenger it is necessary for it to possess the ability to synthesize cADPR. It has been hypothesised that plants possess ADP-ribosyl cyclase activity and some evidence has been reported that substantiates this, i.e. the bioassay of Wu *et al.* (1997), microinjection studies by DePass & Hepler *et al.* (1998) and cGDPR fluorescence assay/HPLC analysis carried out by Bewell (1999).

Bewell (1999) first reported the use of the cGDPR fluorescence assay in plant tissue for the detection of cyclase activity. The results presented here are in accord with his data and demonstrate that in addition to red beet tap root, other plant tissues - maize root, cauliflower inflorescence and *Arabidopsis* nuclei - show a heat-labile increase in fluorescence when incubated with NGD. This fluorescence increase is consistent with the production of cGDPR and hence of ADP-ribosyl cyclase activity. The presence of cyclase activity in a variety of tissues supports the idea that cADPR is an important, universal second messenger. Of the tissues investigated cauliflower inflorescences demonstrated the most consistent activity with all samples tested being active. Approximately one in four samples prepared from both maize and red beet, either from whole tissue or protoplasts, were inactive.

The report of Adebanjo *et al.* (1999) describing ADP-ribosyl cyclase activity in the nuclei of CD38-positive MC3T3.E1 cells (a mouse cell line that differentiates to osetoblasts) prompted the examination of *Arabidopsis* nuclei for cyclase activity. Isolated nuclei, previously prepared for Ca^{2+} transport studies, were checked for purity by microscopy following DAPI staining, and tested for functional transcriptional activity through the incorporation of [^{32}P]-UDP into mRNA. As with the other plant tissue tested the increase in fluorescence occurring upon incubation of nuclei with NGD suggests that they possess cyclase activity. The problems with the noisiness of the signal could not be resolved

The existence of cyclase activity in various plant tissues, as indicated by the cGDPR fluorescence assay, is an exciting proposition as it strengthens the argument for cADPR as a second messenger in plant cells. As recent studies of Ca^{2+} transport in

plant nuclei indicate that Ca^{2+} flux across the nuclear pore is tightly controlled (Bunney *et al.*, 2000) and that gene expression can be regulated by changes in both the concentration of nuclear and cytoplasmic Ca^{2+} (Hardingham *et al.*, 1997; Carrion *et al.*, 1999) it would appear that Ca^{2+} may play a direct role in transducing cytoplasmic signals to gene expression. The presence of cyclase activity in the nuclei would implicate NAD as a regulator of nuclear Ca^{2+} homeostasis and gene expression, as has been hypothesised for animal cells where NAD metabolism is known to affect gene transcription (Biswas *et al.*, 1998).

The rates of formation of cGDPR in the plant tissues examined (Table 2.1) were low compared to the values for ADP-ribosyl cyclase reported for brain extracts (e.g. 62.7±6.2 μmol/g.h in dog brain; 20.6±2.8 μmol/g.h in chick brain), however, they are similar to the value reported for sea-urchin egg of 0.3±0.05 μmol/g.h (Lee & Aarhus, 1993). Although the experiments described here have proven useful for screening various plant tissues for cyclase activity, the activity is close to the detection limit of this technique. This makes it difficult to accurately estimate the rates of formation of cGDPR from the fluorescence changes measured and thus precludes a convenient method of analysis of enzyme kinetics, in which rates are determined as the reaction progresses (as described by Graeff *et al.*, 1994) and used to calculate K_m and V_{max} values. An alternative method for determining K_m and V_{max} values is to vary the concentration of the substrate experimentally and measure the initial rates of formation of the product. Graeff *et al.* (1994) have reported that the initial rates of formation of cGDPR by human CD38 are dependent on NGD concentration (up to 100 μM) and have successfully used the fluorescence assay to monitor cyclase activity of *Aplysia* with 1 mM NGD. It was hypothesised that plant ADP-ribosyl cyclase would demonstrate a similar dependence on substrate concentration. Chapter 3 describes the experimental determination of the K_m and V_{max} of cyclase activity using NGD up to 500 μM.

3. Purification and characterisation of cauliflower ADP-ribosyl cyclase

3.1. Introduction

Cauliflower microsomes prepared from meristematic tissue of the inflorescences have been used as a model system for the study of Ca^{2+} transport. They have previously been demonstrated to possess active Ca^{2+} sequestration mechanisms and Ca^{2+} channels and are responsive to Ca^{2+} mobilising ligands such as cADPR, $InsP_3$, and NAADP (Muir *et al.*, 1997; Muir & Sanders, 1997; Navazio *et al.*, 2000) Recent work by Navazio *et al.* (2000) indicates that extracts of homogenised cauliflower inflorescences are able to synthesize NAADP when presented with the substrates NADP and nicotinic acid. Taken together with the results of the fluorimetric assay presented in Chapter 2, this suggests that cauliflower tissue possesses ADP-ribosyl cyclase activity and thus may use cADPR as a second messenger in a similar manner to animal cells. In this chapter the ADP-ribosyl cyclase and hydrolase activities of cauliflower tissue are examined in more detail and the partial purification of cyclase activity from cauliflower florets is described.

There were two main objectives to the work described in this chapter: (1) to confirm the presence of, and further characterise the cyclase activity observed in microsomes prepared from cauliflower inflorescences using the cGDPR fluorescence assay and (2) purify the cyclase activity via column chromatography. The work described here indicates that:

1. Incubating cauliflower tissue with NAD/NGD results in the synthesis of cADPR/cGDPR.
2. The rate of synthesis of cGDPR is dependent on the concentration of NGD.
3. Cauliflower ADP-ribosyl cyclase activity is segregated to different subcellular locations.
4. Cauliflower tissue demonstrates cADP-ribosyl hydrolase activity.
5. Cauliflower cyclase activity is inhibited by nicotinamide.
6. Cauliflower cyclase activity is modulated by physiological regulators such as cAMP, cGMP, pH, ATP, Ca^{2+} and Mg^{2+}.

Furthermore by utilising the cGDPR fluorescence assay to monitor cyclase activity in fractions eluted from successive chromatographic columns, a partially purified preparation enriched in cyclase activity was obtained.

3.2. Materials and Methods

3.2.1. HPLC assay for cADPR

Cauliflower microsomes were diluted to 2 mg/ml in Buffer A, comprised of 340 mM glucose, 20 mM Hepes, 1 mM $MgCl_2$, 10 mM mercaptoethanol, 50 μg/ml soybean trypsin inhibitor (SBTI), 10 μg/ml leupeptin, and 10 μg/ml aprotinin, pH 7.2 with KOH supplemented with 0.1 mM EDTA. 10 mM NAD spiked with [^{32}P]NAD (Amersham, 37 TBq/mmol) was added to a specific activity of 0.185 MBq/ml. The reaction mix was incubated at ambient temperature with 1 ml aliquots removed at 1 min, 60 min and 20 hours. The reaction was terminated by incubating the mix on ice for 20 min with 20% (w/v) TCA. The microsomes were pelleted by centrifugation (400,000 x g for 20 min at 4 °C) and the supernatant removed. The supernatant was neutralised by the addition of 400 mM Tris and analysed by reverse phase HPLC using a Genesis C18 column (4.6 x 250 mm; Jones Chromatography) fitted with a guard column. Elution was carried out with an isocratic gradient of 100 mM phosphate buffer and 5 % (v/v) methanol (pH adjusted to 6.0 with KOH) at a flow rate of 1 ml/min. Absorbance at 254 nm was monitored and fractions were collected and tested for the presence of ^{32}P by Cerenkov counting.

3.2.2. Spectrofluorimetric assay of cauliflower microsomes for cyclase activity.

The spectrofluorimetric assay of the cyclase reaction described in Chapter 2 was used to monitor the production of cGDPR with time in cauliflower microsomes and to determine the effect of NGD concentration on cyclase activity. Microsomes (20 mg/ml total protein) were incubated with 20 – 500 μM NGD in buffered solution containing 20 mM Hepes, pH 7.2. The change in fluorescence was followed (excitation 300 nm; emission 410 nm, in a Perkin Elmer LS-5 luminescence spectrofluorimeter. A standard curve of cGDPR fluorescence as a function of cGDPR concentration was constructed, to enable quantification of cGDPR production by cauliflower extracts, as described in 2.2.6. Initial rates were estimated graphically by fitting a straight line through the data (0-60 min).

The Michaelis-Menton equation was used to fit the data with a non-linear least squares fitting routine and determine K_m and V_{max} values for cauliflower ADP-ribsyl cyclase activity. The Michaelis-Menton equation used is as follows:

$$v = \frac{V_{max} * [S]}{K_m + [S]}$$

where **v**= reaction rate, V_{max} = maximum rate, K_m = Michaelis-Menten constant and **[S]** = substrate concentration.

The assay was also used to assess the activity of cauliflower fractions at various stages of purification, described below, as well as the effects of pH, 100 μM cGMP, 1 mM ATP, 10 mM nicotinamide, 100 μM cAMP and 10 mM EDTA on cyclase activity in membrane-derived fractions produced during the purification procedure that followed ultracentrifugation. To determine the effect of pH, the reaction buffer was acidified with HCl and the fluorescence of the reaction buffer blank at various pH values was determined and subtracted from all readings. For the pharmacological experiments the compound under investigation was added to the reaction buffer prior to NGD at the appropriate concentration. 200 μM NGD was added in all cases to start the reaction.

3.2.3. Spectrofluorimetric assay of cauliflower microsomes for hydrolase activity

A fluorimetric assay was used for monitoring the cADPR hydrolase activity of cauliflower microsomes based on the method of Graeff *et al.* (1996). Hydrolysis can be followed by measuring the decrease in fluorescence of cGDPR as it is converted to its nucleoside diphosphoribose. However, as cGDPR is resistant to hydrolysis (Graeff *et al.*, 1994) it is convenient to use another fluorescent analogue of cADPR, cyclic inosine diphosphoribose (cIDPR). Graeff *et al.* (1996) demonstrated that cIDPR can be readily hydrolysed by CD38 and that the rate of hydrolysis is proportional to the concentration of CD38 used, making it ideally suited for screening tissues for hydrolase activity. The ADP ribosyl hydrolase activity of cauliflower was measured by adding 50 μM cIDPR to cauliflower microsomes (20 mg/ml total protein) in buffer containing 20 mM Hepes, pH 7.2. Over the course of a 20 min incubation, at room temperature with constant stirring, changes in fluorescence were monitored, as previously described for the spectrofluorimetric cyclase assay.

3.2.4. Purification of cauliflower ADP-ribosyl cyclase activity

A procedure, similar to that described by Masuda *et al.* (1999) for purifying ADP-ribosyl cyclase activity from *Euglena gracilis,* was used to attempt purification of ADP-ribosyl cyclase activity from cauliflower. Cauliflower meristematic tissue was collected, as described in section 2.2.2.8, and homogenised in a blender (3 x 30s pulses) in Homogenisation Buffer comprising 20 mM Hepes-Tris (pH 7), 1 mM $MgCl_2$, 0.1 mM EDTA and 0.1 mM EGTA and supplemented with 0.34 M Glucose, 12.5 mM benzamidine, 0.1 mM PMSF, 10 μM leupeptin and 20 mg/ml soybean trypsin inhibitor. Cell debris was removed by centrifugation (10,000 x g, 5 min). The supernatant was tested for ADP-ribosyl cyclase activity using the spectrofluorimetric assay described above. The extract was diluted to give a final protein concentration of approximately 20 mg/ml.

The cauliflower extract was separated into membrane and cytosolic fractions by centrifugation (400,000 x g, 60 min, 4 °C). The membrane pellet was resuspended in Homogenisation Buffer supplemented with 0.1 mM PMSF, 10 μM leupeptin and 20 μg/ml soybean trypsin inhibitor and the fractions were assayed for ADP-ribosyl cyclase activity. The membrane fraction was treated with 0.25% (v/v) deoxycholate on ice for 60 min to solubilize membrane bound proteins and again assayed for ADP-ribosyl cyclase activity.

The membrane fraction was applied to a DEAE-Sepharose column (1 x 20 cm) previously equilibrated with Purification Buffer consisting of 20 mM Hepes-Tris (pH 7), 1 mM $MgCl_2$, 0.1 mM PMSF, 10 μM leupeptin and supplemented with 0.25 % deoxycholate. The column was washed with 30 ml of this buffer and bound proteins eluted with 80 ml of a linear concentration gradient of 0-1 M NaCl in the buffer. The fractions were assayed and active fractions were combined, dialysed overnight against Purification Buffer at 4°C and loaded onto a DEAE-Toyopearl column (1 x 4 cm) that had been equilibrated with Purification Buffer. The column was washed with 10 ml of Purification Buffer and protein was eluted with 30 ml of a linear gradient of 0-1 M NaCl in the buffer. The fractions were assayed for cyclase activity and protein content (by monitoring absorbance at 280 nm) and dialysed overnight against Purification Buffer at 4°C. Aliquots of active fractions were stored at -20°C for protein analysis. Active fractions were further purified using a Q-sepharose column (0.5 x 5 cm), washed with 3 ml of Purification Buffer and eluted with a

gradient of 0-2 M NaCl. Fractions were analysed for cyclase activity and protein content.

3.2.4.1. SDS-Polyacrylamide Gel Electrophoresis (SDS-PAGE)

SDS-PAGE was carried out on the various fractions recovered from using precast Gradi Gels (8-16%, Gradipore), as described by Laemmli (1970). Dialysed fractions recovered from the various stages of cyclase purification were diluted with an equal volume of SDS Denaturation Buffer comprised of 4% (w/v) SDS (electrophoresis grade), 20% (w/v) glycerol, 0.004% Bromophenol Blue buffered to pH 6.8 with 0.13 M Tris-HCl. Mercaptoethanol was added to a final concentration of 5% (v/v) and the samples were denatured by heating at 95 °C for 5 min. Protein gels electrophoresis was performed on a Bio-Rad Mini-Protean Electrophoresis Cell for approximately 45 min at 200 V in Running Buffer containing 25 mM Tris, 192 mM glycine, 0.1% SDS (approximate pH of 8.3).

3.2.4.2. Visualisation of protein with Coomassie Blue Stain

Following electrophoresis gels were incubated with gentle shaking for 2 h in Coomassie Stain containing 0.25% (w/v) Coomassie Brilliant Blue R, 40% (v/v) methanol and 7% acetic acid. Gels were destained overnight by incubation, with shaking, in Destain containing 15% methanol and 7% (v/v) acetic acid.

3.3. Results

3.3.1. Measurement of cADPR synthesis via HPLC

Microsomes prepared from cauliflower inflorescences were incubated with [^{32}P]NAD. At times of 1 min, 60 min and 20 h aliquots (1ml) were centrifuged to pellet insoluble material and the supernatant was separated on a reverse phase HPLC column. As shown in Figure 3.1 the separation profile of the radioactivity of fractions collected from the column was dependent on time of collection. For material recovered at 1 min the majority of the radioactive material eluted at the same time as the standard for NAD (7.5 min). Material recovered after 20 h eluted mainly at the time of the standard for cADPR (3.5 min). At 1 h, the radioactivity profile was largely in accord with that at 1 min, but with indications of a peak shift from NAD to cADPR. These results are consistent with the conversion of [^{32}P]NAD to [^{32}P]cADPR by ADP-ribosyl cyclase activity. The absorbance was also monitored at 254 nm. However, the separation was not sufficient to identify peaks of cADPR or NAD against the background of contaminating material. Even so, changes in absorbance that are suggestive of an increase in cADPR and a decrease in NAD over time were detected.

3.3.2. Measurement of cGDPR production with the NGD assay

The spectrofluorimetic assay monitoring the conversion of NGD to cGDPR was used to investigate further the ADP-ribosyl cyclase activity of cauliflower tissue. As Figure 3.2 illustrates incubation of homogenised cauliflower meristematic tissue with NGD results in an increase in fluorescence consistent with the formation of cGDPR. This reaction is an enzyme-based as it is heat labile. Figure 3.3 shows that the activity of the tissue is dependent on the concentration of NGD, with a V_{max} of 2.8 μmol/g.h., and a K_m of 130.4 μM.

3.3.2.1. Distribution of ADP-ribosyl cyclase activity

Figure 3.4 shows that upon fractionation of cauliflower meristematic tissue by centrifugation at 400,000 x g for 60 min, the majority of ADP-ribosyl cyclase activity can be found in the membrane fraction. Significantly less activity is present in the supernatant, which also demonstrates a decrease in fluorescence consistent with hydrolase activity. Heat treatment eliminated the activity in both fractions. The hydrolase activity of the soluble fraction was assessed further by incubating the fractions with cIDPR (a less stable, fluorescent analogue of cGDPR) and monitoring

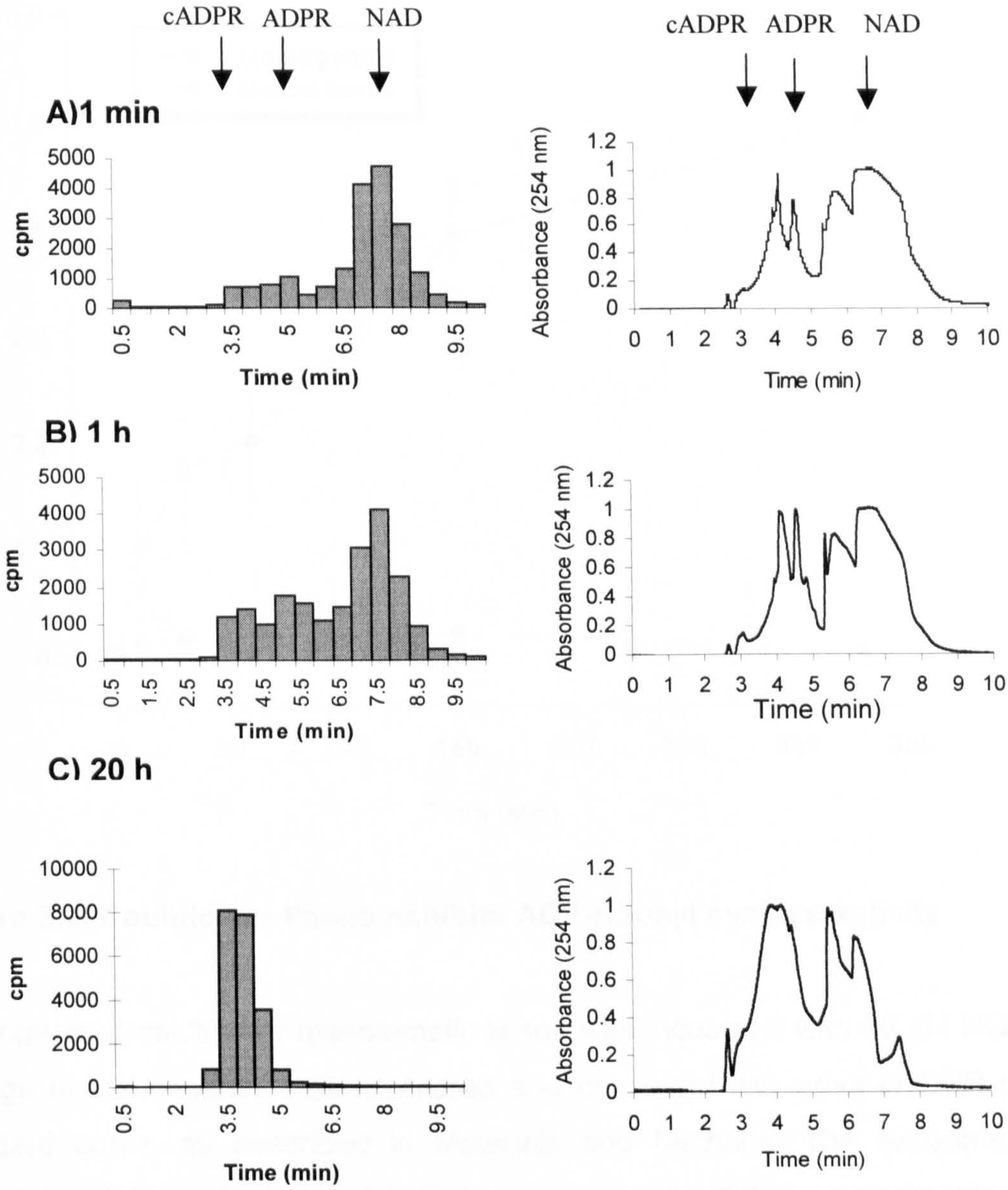

Figure 3.1. HPLC analysis of cauliflower cyclase activity

Cauliflower microsomes were incubated with 10 mM NAD spiked with [^{32}P]NAD overnight. After A) 1 min, B) 1 h and C) 20 h, aliquots were removed and analysed by reverse phase HPLC, as described in Materials and Methods. Absorbance at 254 nm was monitored, fractions were collected and their radioactivity measured by Cerenkov counting.

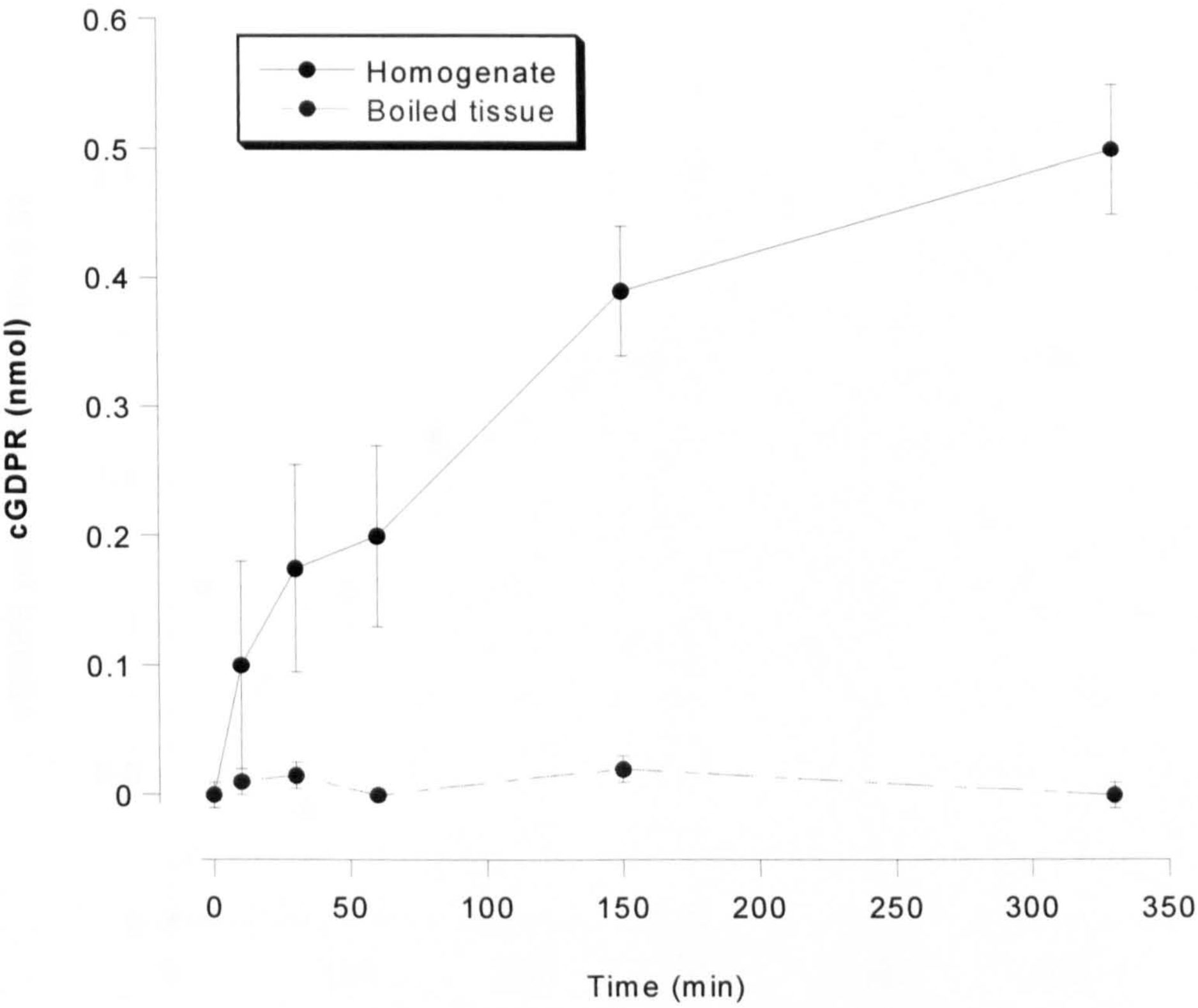

Figure 3.2. Cauliflower tissue exhibits ADP-ribosyl cyclase activity

Homogenised cauliflower meristematic tissue was incubated with 40 μM NGD. The change in fluorescence was monitored and converted into nmol cGDPR using a standard curve, as described in Materials and Methods. The experiment was repeated with tissue boiled for 2 h. Data are the means of three experiments ± SEM.

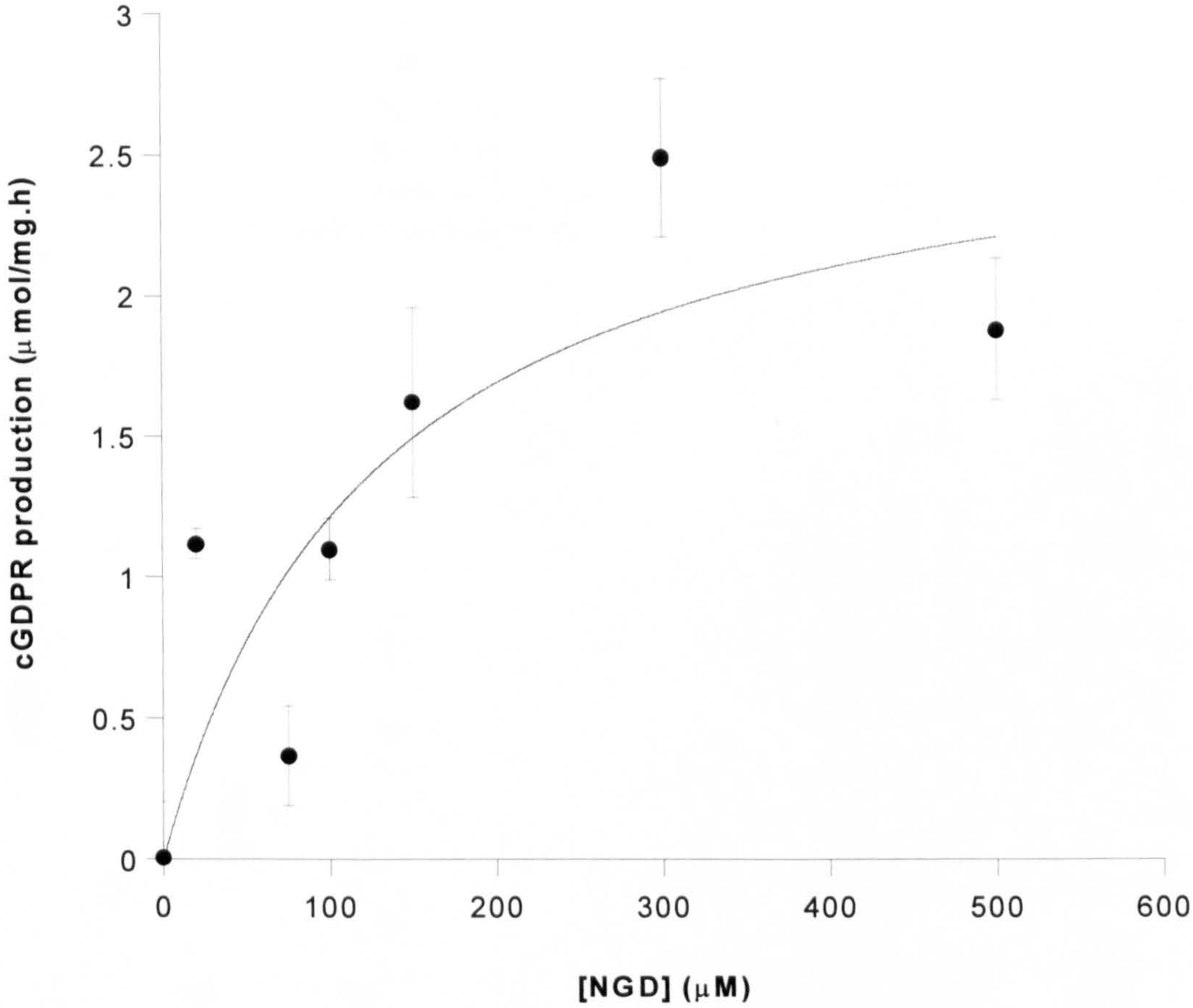

Figure 3.3. Cauliflower ADP-ribosyl cyclase activity is dependent on NGD concentration

Homogenised cauliflower meristematic tissue was incubated with NGD for 60 min, over a range of concentrations, and the change in fluorescence was monitored, as described in Materials and Methods. A standard curve of cGDPR fluorescence enabled the amount of cGDPR formed to be determined. Initial rates were estimated by fitting a line through a plot of the change in cGDPR formed. Data are the mean of three experiments ± SEM. The data were fitted by non-linear least squares to a Michaelis-Menton function yielding a V_{max} of 2.8 μmol/g.h., and a K_m of 130.4 μM.

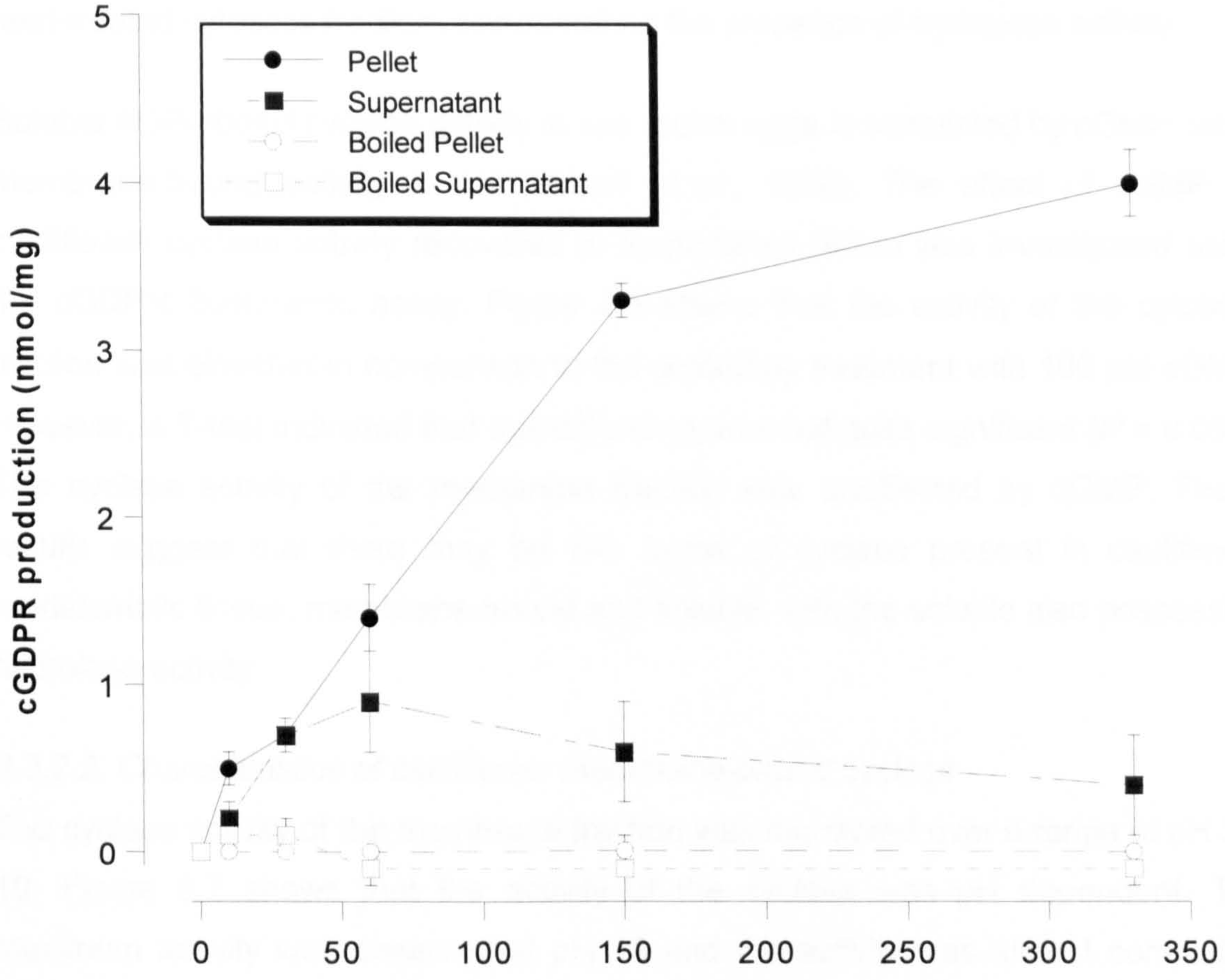

Figure 3.4. Membrane and cytosolic fractions of cauliflower tissue demonstrate different ADP-ribosyl cyclase activities

Cauliflower meristematic tissue was homogenised, fractionated by centrifugation into supernatant and membrane pellet fractions and assayed for ADP-ribosyl cyclase activity by incubation with 200 μM NGD as described in Materials and Methods. A standard curve of cGDPR fluorescence enabled the amount of cGDPR formed to be determined. Tissue boiled for 2 h was also assayed. Data are the means of three or more experiments ± SEM.

the change in fluorescence. Figure 3.5 shows that hydrolysis of cIDPR occurs more rapidly when incubated with membrane or cytosolic fractions, in comparison to the heat-treated cytosolic fraction, corroborating the presence of hydrolase activity.

Soluble ADP-ribosyl cyclase activity in sea urchin eggs is stimulated by cGMP, while membrane-bound activity is not (Graeff *et al.*, 1998). The effect of cGMP on cauliflower cyclase activity recovered in fractionated tissue was investigated using the cGDPR fluorimetric assay. Figure 3.6 shows that the activity of the cytosolic fraction was elevated in comparison to the control by treatment with 100 μM cGMP. However, a T-test indicated that this difference was not quite significant ($P = 0.051$). The cyclase activity of the membrane fraction was unaffected by cGMP. These results suggest that there may be two forms of cyclase present in cauliflower meristematic tissue, membrane-bound and soluble, with the soluble also possessing hydrolase activity.

3.3.2.2. Characteristics of cauliflower membrane-bound cyclase.

The cyclase activity of the membrane fraction was monitored over a range of pH 3 – 10. Figure 3.7 shows that the activity of the cyclase was pH dependent. The maximum activity was observed at pH 10 and the activity was almost completely abolished at pH 3. The influence of other potential regulators of cyclase activity was also examined. Figure 3.6 demonstrates that the activity was unaffected by 1 mM ATP or 100 μM cAMP and inhibited slightly by 10 mM EDTA. Nicotinamide demonstrated the greatest inhibition, reducing the activity approximately 2-fold.

3.3.3. Purification of ADP-ribosyl cyclase activity

Microsomes prepared from cauliflower meristematic tissue were treated with 0.25% (w/v) deoxycholate for 60 min to solubilise the membrane-bound cyclase. The solubilised protein was separated from cell debris by centrifugation at 400,000 x g for 60 min. The supernatant was assayed for cyclase activity using the cGDPR fluorimetric assay. As indicated in Figure 3.9 the solubilised protein retained cyclase activity. The solubilised microsomes were purified sequentially by DEAE-Sepharose, DEAE-toyopearl and Q-sepharose column chromatography with a final yield of 13% and a 49-fold purification (Table 3.1). Active fractions were collected at each stage and analysed by SDS-PAGE (Figures 3.10-3.14). Analysis of the final fractions indicated the sample had not been purified to homogeneity as several bands could be detected. Candidate bands in fractions demonstrating enrichment were identified with sizes of approximately 35, 40, 55, and 60 kDa.

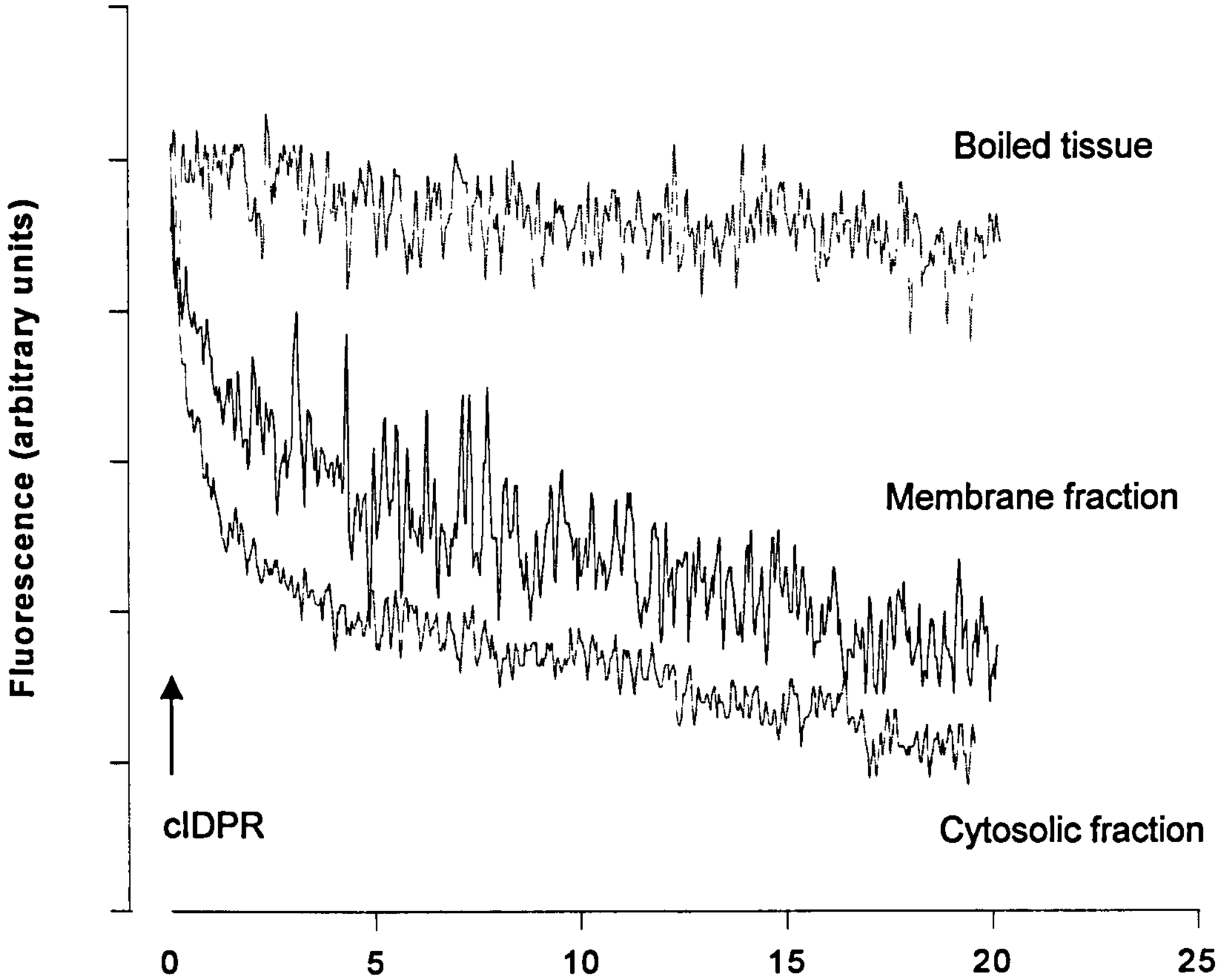

Figure 3.5. Hydrolase activity in fractionated cauliflower tissue

Cauliflower meristematic tissue was homogenised and fractionated by centrifugation as described in Materials and Methods. The membrane and cytosolic fractions were assayed for ADP ribosyl hydrolase activity by incubation with 50 μM cIDPR. Changes in fluorescence (excitation 300, emission 410) were monitored. Tissue heat-treated for 2 h was also assayed as a control. Data representative of two or more experiments are shown.

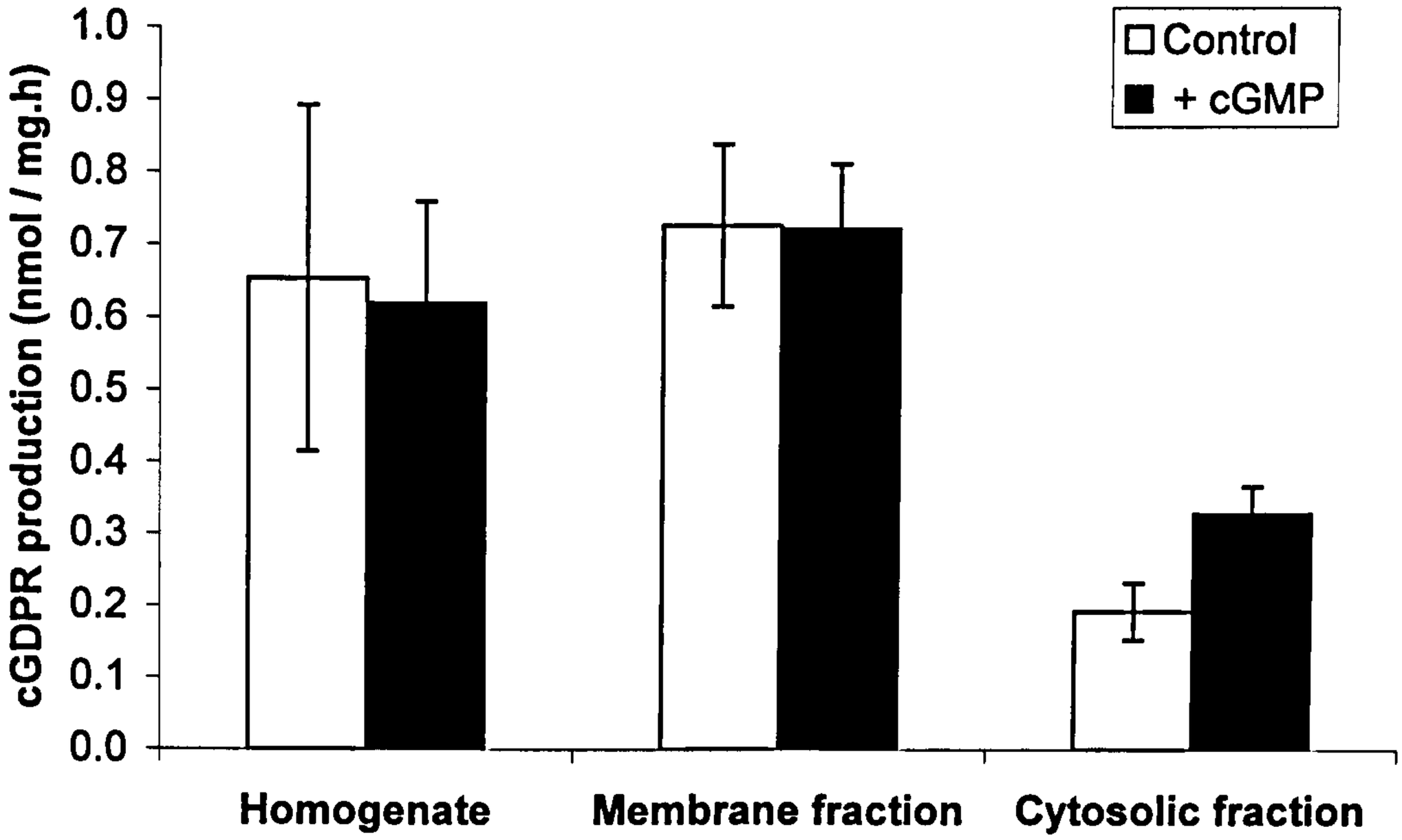

Figure 3.6. Effect of cGMP on ADP-ribosyl cyclase activity

Cauliflower meristematic tissue was homogenised, fractionated by centrifugation into supernatant and membrane pellet fractions and assayed for ADP-ribosyl cyclase activity by incubation with 200 μM NGD in the presence of 100 μM cGMP (+ cGMP) or water (- cGMP), as described in Materials and Methods. A standard curve of cGDPR fluorescence enabled the amount of cGDPR formed to be determined. Initial rates were estimated by fitting a line through a plot of the change in cGDPR formed. Data are the means of three or more experiments ± SEM. T-test results indicate that there is no significant difference between treatment and control ($P > 0.05$).

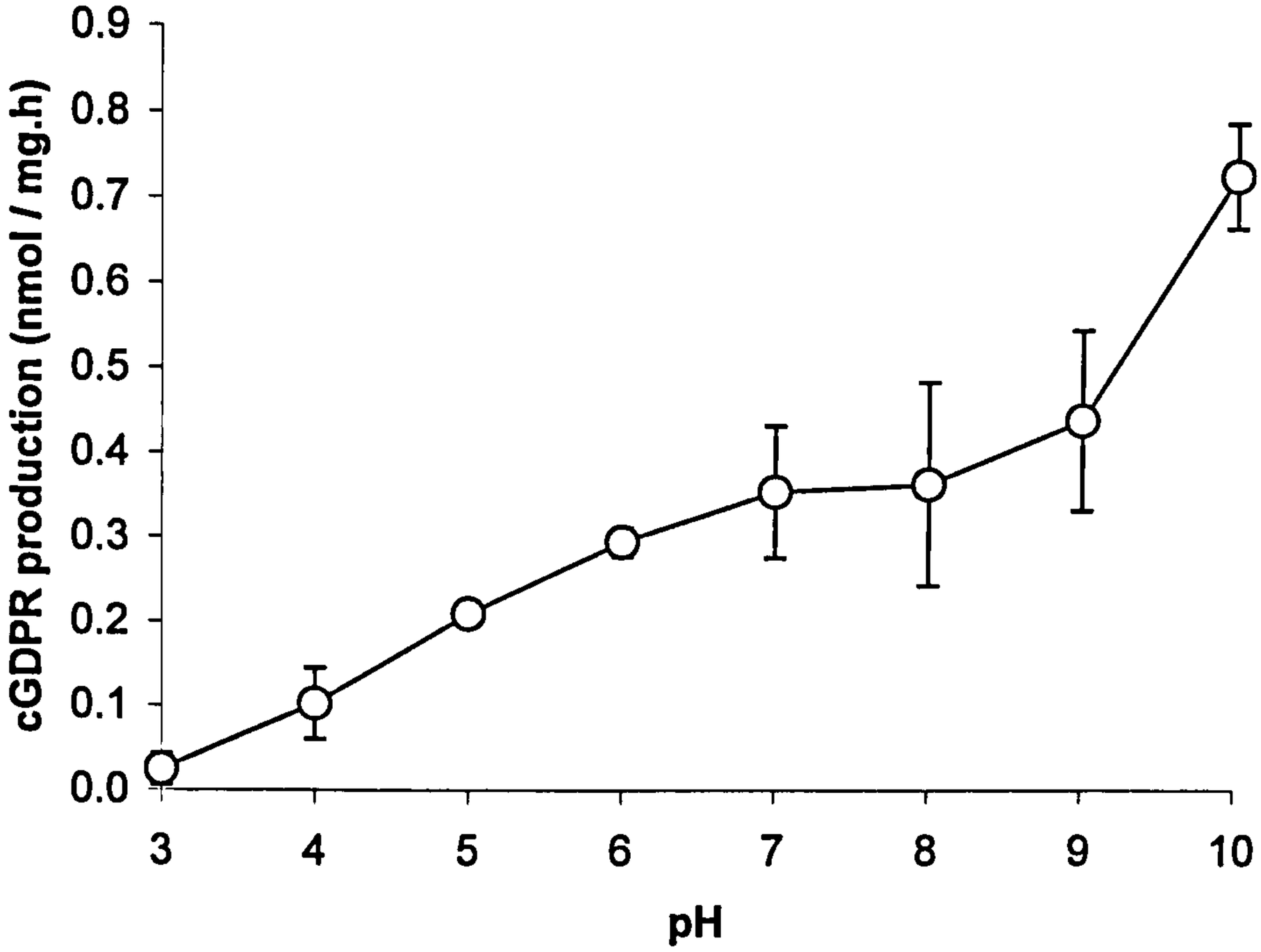

Figure 3.7. pH dependence of membrane fraction ADP-ribosyl cyclase activity

Cauliflower meristematic tissue was homogenised, fractionated by centrifugation into supernatant and membrane pellet fractions. The membrane pellet fraction was assayed for ADP-ribosyl cyclase activity by incubation with 200 μM NGD over a range of pH, as described in Materials and Methods. A standard curve of cGDPR fluorescence enabled the amount of cGDPR formed to be determined. Initial rates were estimated by fitting a line through a plot of the change in cGDPR formed. Data are the means of three or more experiments ± SEM.

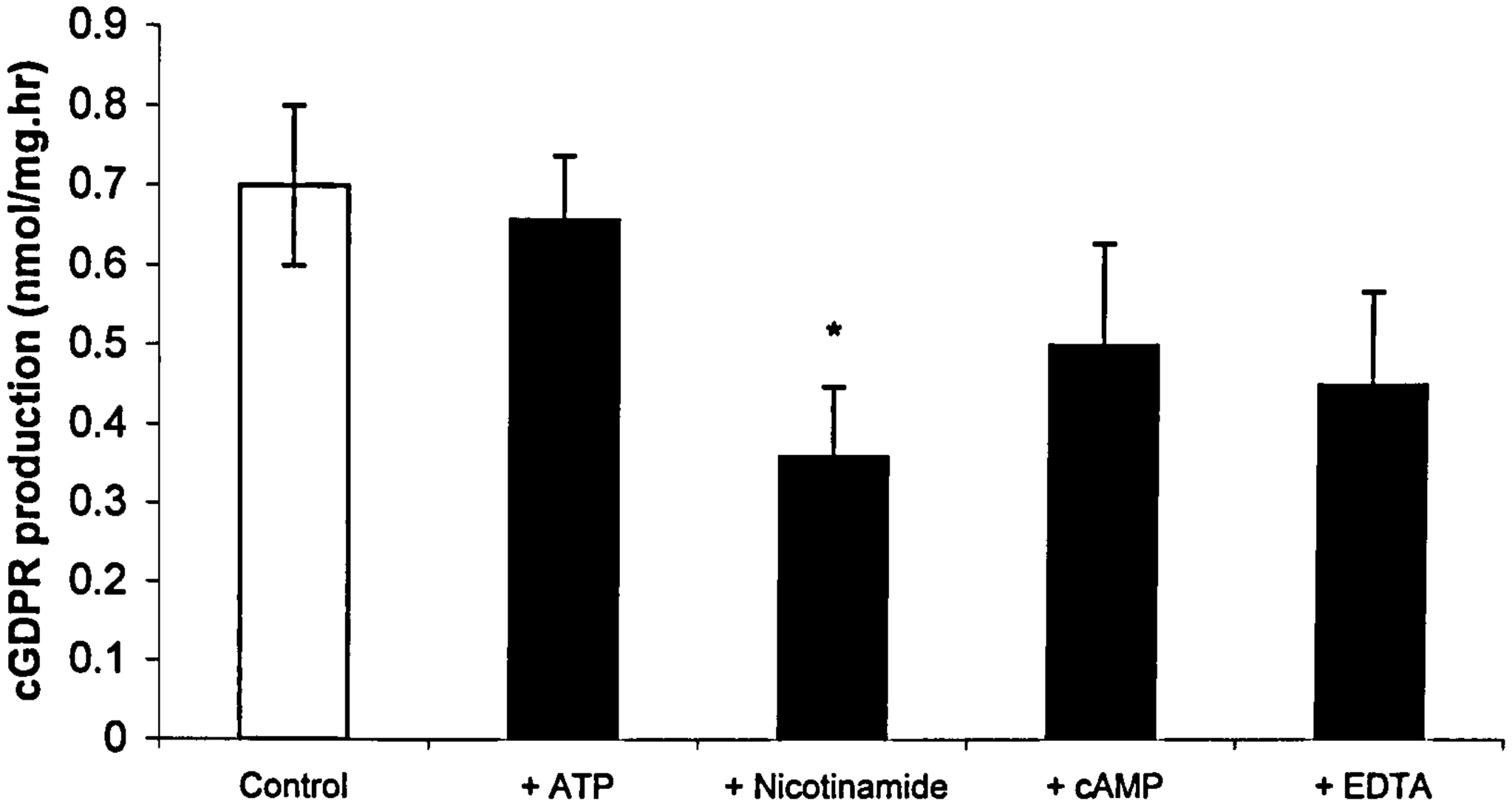

Figure 3.8. Influence of potential regulators on membrane fraction ADP-ribosyl-cyclase activity

Cauliflower meristematic tissue was homogenised, fractionated by centrifugation into supernatant and membrane pellet fractions. The membrane pellet fraction was assayed for ADP-ribosyl cyclase activity by incubation with 200 μM in the presence of ATP (1 mM), Nicotinamide (10 mM), cAMP (100 μM), EDTA (10 mM) or water (control) as described in Materials and Methods. A standard curve of cGDPR fluorescence enabled the amount of cGDPR formed to be determined. Initial rates were estimated by fitting a line through a plot of the change in cGDPR formed Data are the means of three or more experiments ± SEM. An asterisk (*) indicates significant difference between the control and the treatment ($P < 0.05$).

Table 3.1. Purification of cauliflower ADP-ribosyl cyclase activity

ADP-ribosyl cyclase was purified from solublised cauliflower membrane fractions as described in Materials and Methods.

	Total activity (nmol/h)	Protein (mg)	Specific activity (nmol/mg.h)	Yield (%)	Purification factor
Homogenate	5.6	47.52	0.12	100	1
DEAE-Sepharose	2.6	6.42	0.41	47	3
DEAE-Toyopearl	0.9	0.72	1.22	16	10
Q-Sepharose	0.7	0.13	5.77	13	49

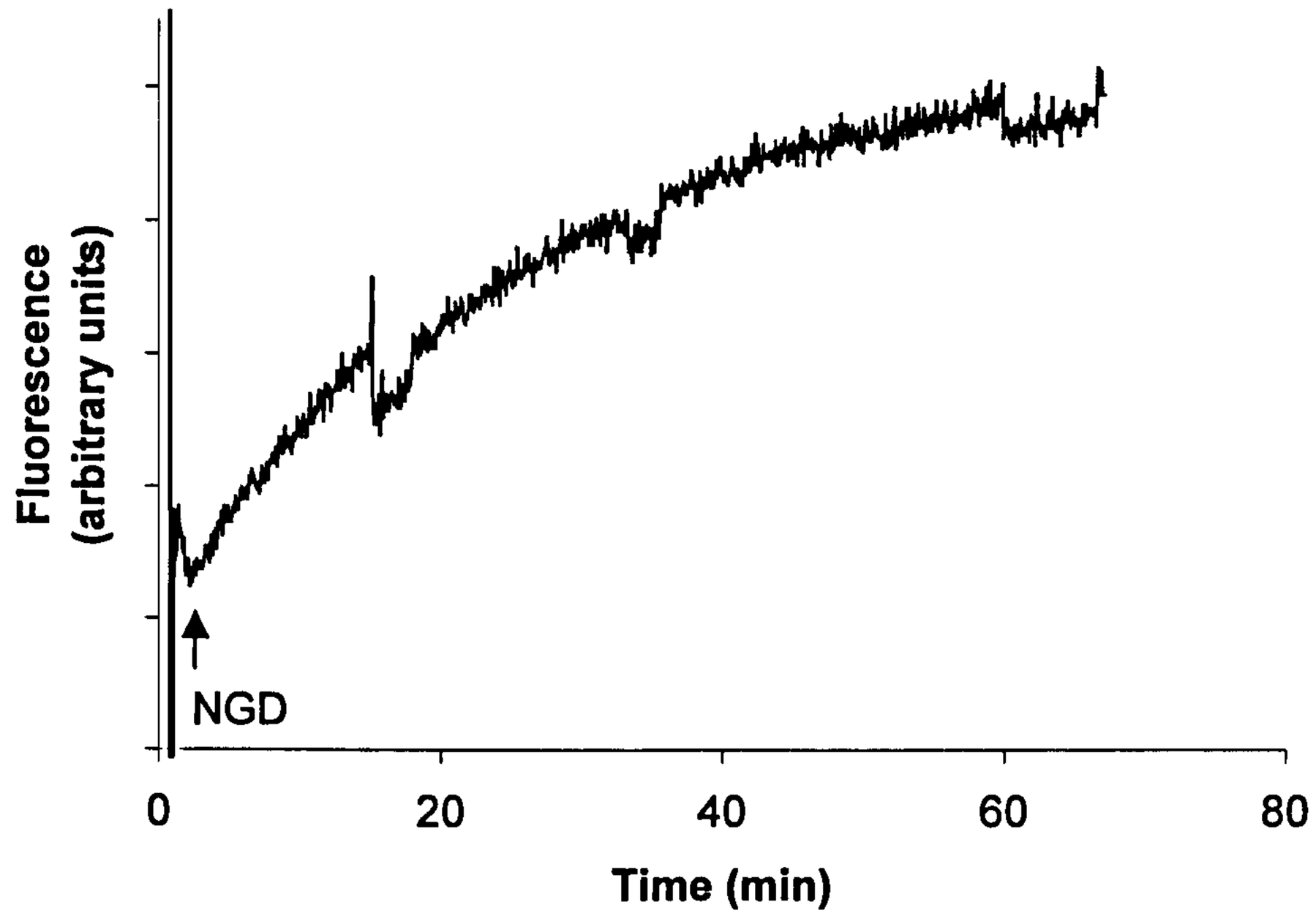

Figure 3.9. Solubilised cauliflower microsomes demonstrate ADP-ribosyl cyclase activity

Cauliflower microsomes were prepared as described in Materials and Methods. The microsomes were incubated with 0.25 % (w/v) deoxycholate at 4°C for 60 min. After centrifugation 400,000 x g for 60 min, the supernatant was assayed for ADP-ribosyl cyclase activity by incubating it with 100 μM NGD and monitoring fluorescence, as described.

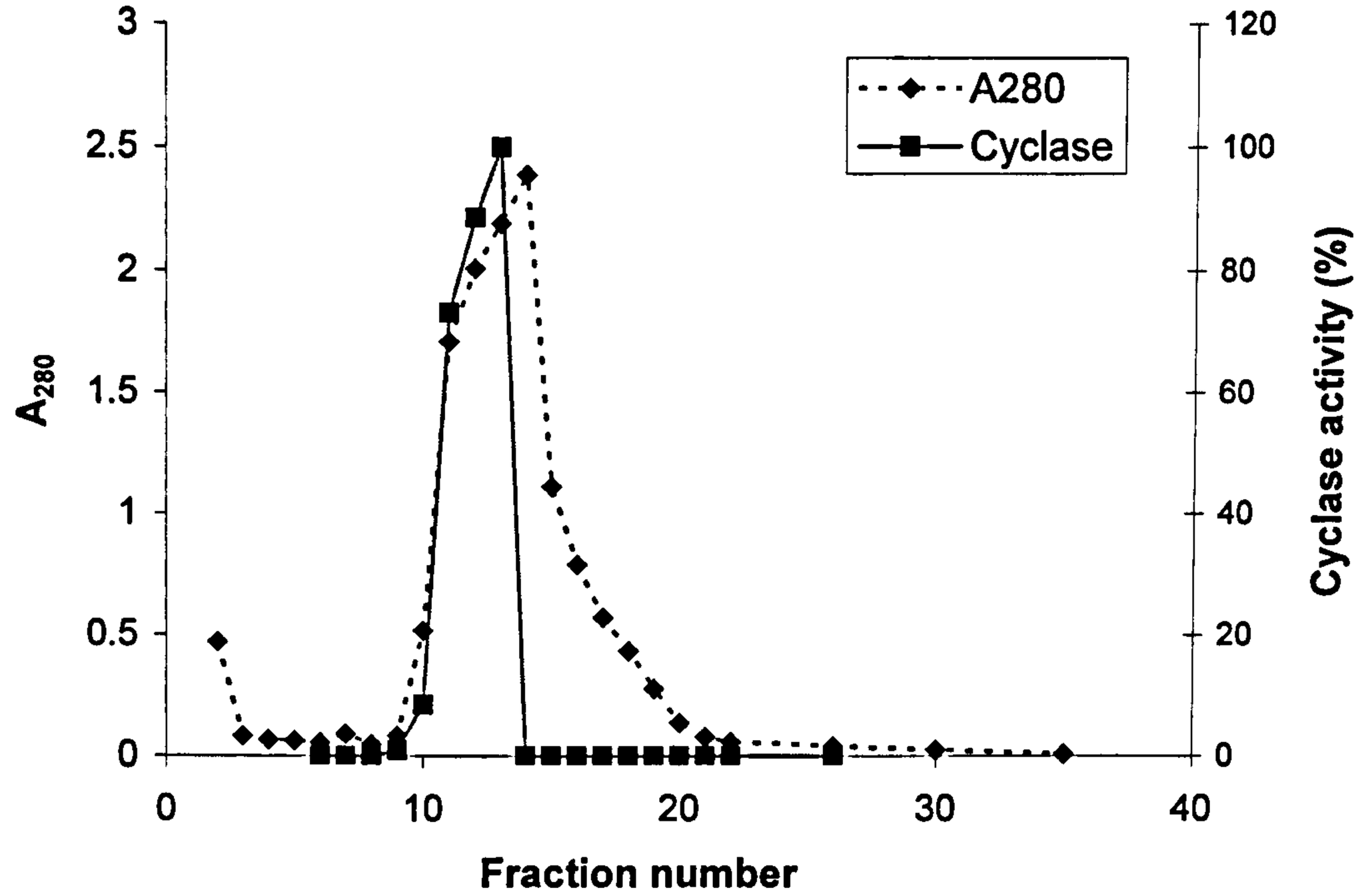

Figure 3.10. Purification of ADP-ribosyl cyclase activity via DEAE-sepharose chromatography

Solubilised cauliflower microsomes were applied to a DEAE-sepharose column and eluted with a gradient of 0-1 M NaCl, as described in Materials and Methods. Fractions were collected and monitored for absorbance at 280 nm and for ADP-ribosyl cyclase activity by incubating them with 100 μM NGD for 25 min, as described.

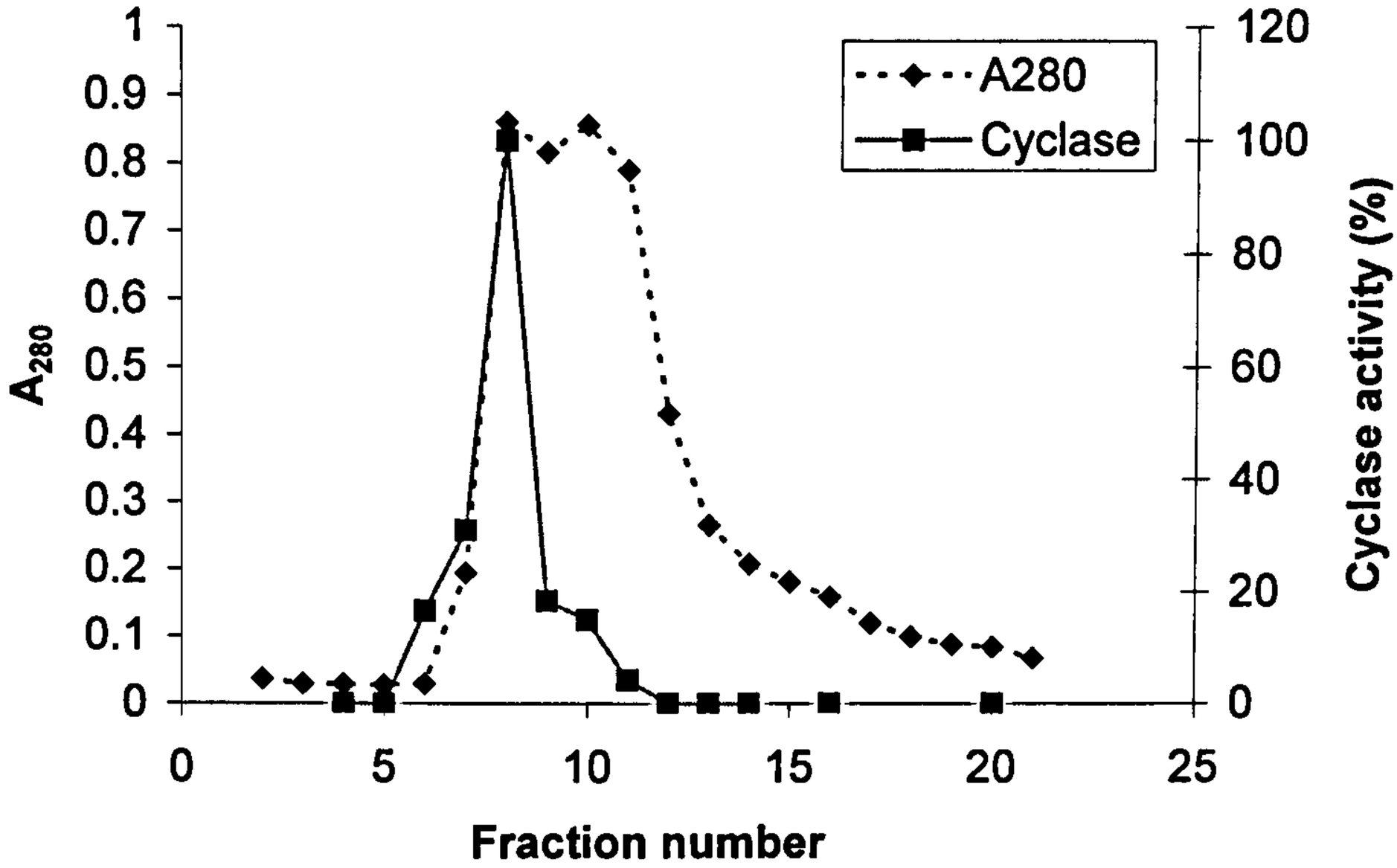

Figure 3.11. Purification of ADP-ribosyl cyclase activity via DEAE-Toyopearl chromatography

Active fractions (11-13) eluted from a DEAE-sepharose column (see Figure 3.10) were combined, dialysed, applied to a DEAE-Toyopearl column and eluted with a gradient of 0-1 M NaCl, as described in Materials and Methods. Fractions were collected and monitored for absorbance at 280 nm and for ADP-ribosyl cyclase activity by incubating them with 100 μM NGD for 25 min, as described.

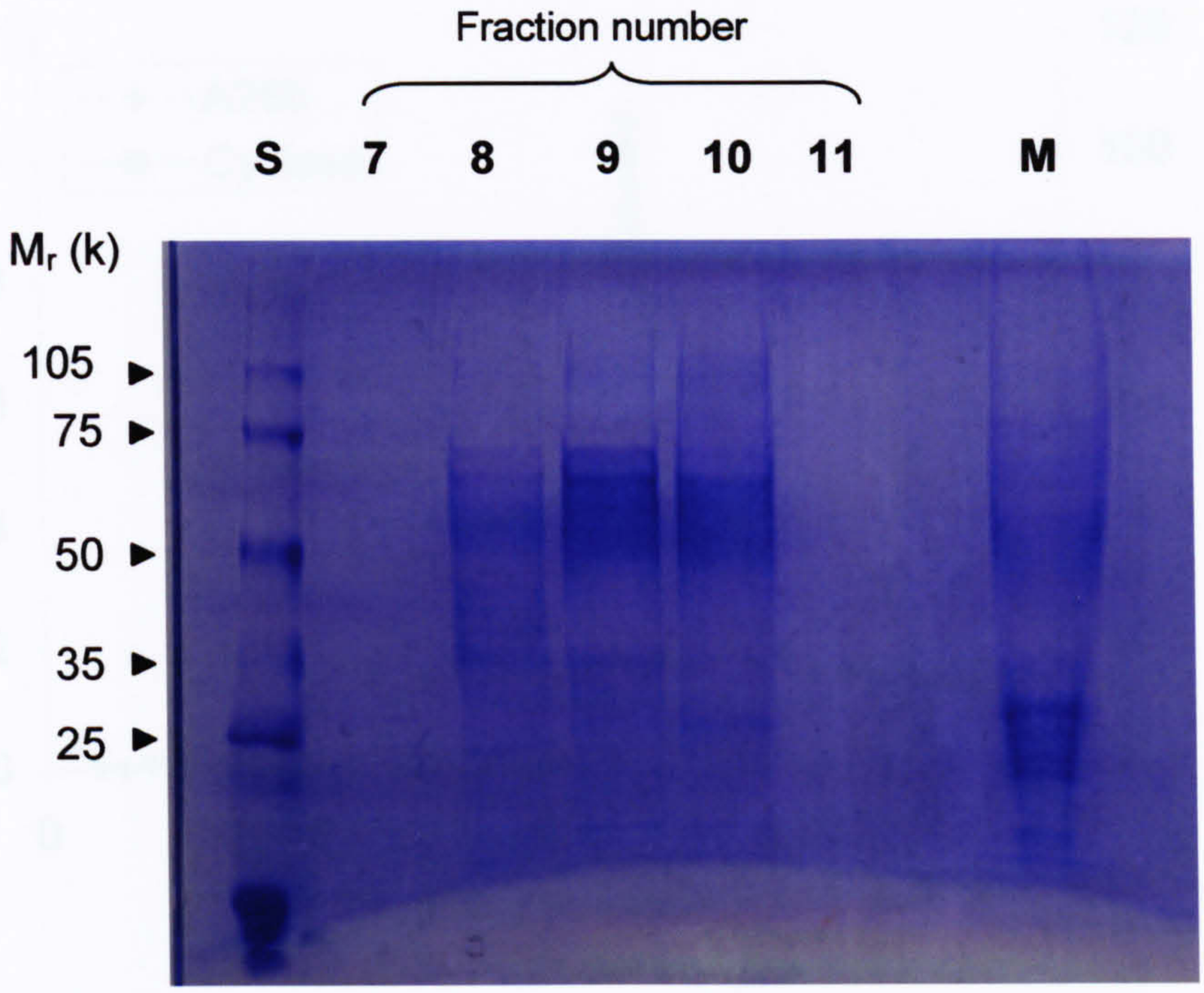

Figure 3.12. SDS-PAGE of cauliflower fractions from DEAE-toyopearl column demonstrating ADP-ribosyl cyclase activity

Fractions (7-11) of solubilised cauliflower membrane proteins eluted from a DEAE-toyopearl column and solubilised cauliflower microsomes (**M**) (diluted 1:10 with Purification Buffer) were analysed by SDS-PAGE (8-16% gradient gel) and visualised by coomassie blue staining. Molecular mass is shown on the left based on calibrated standards (**S**) (Bio-Rad, Low-range Prestained SDS-PAGE Standards).

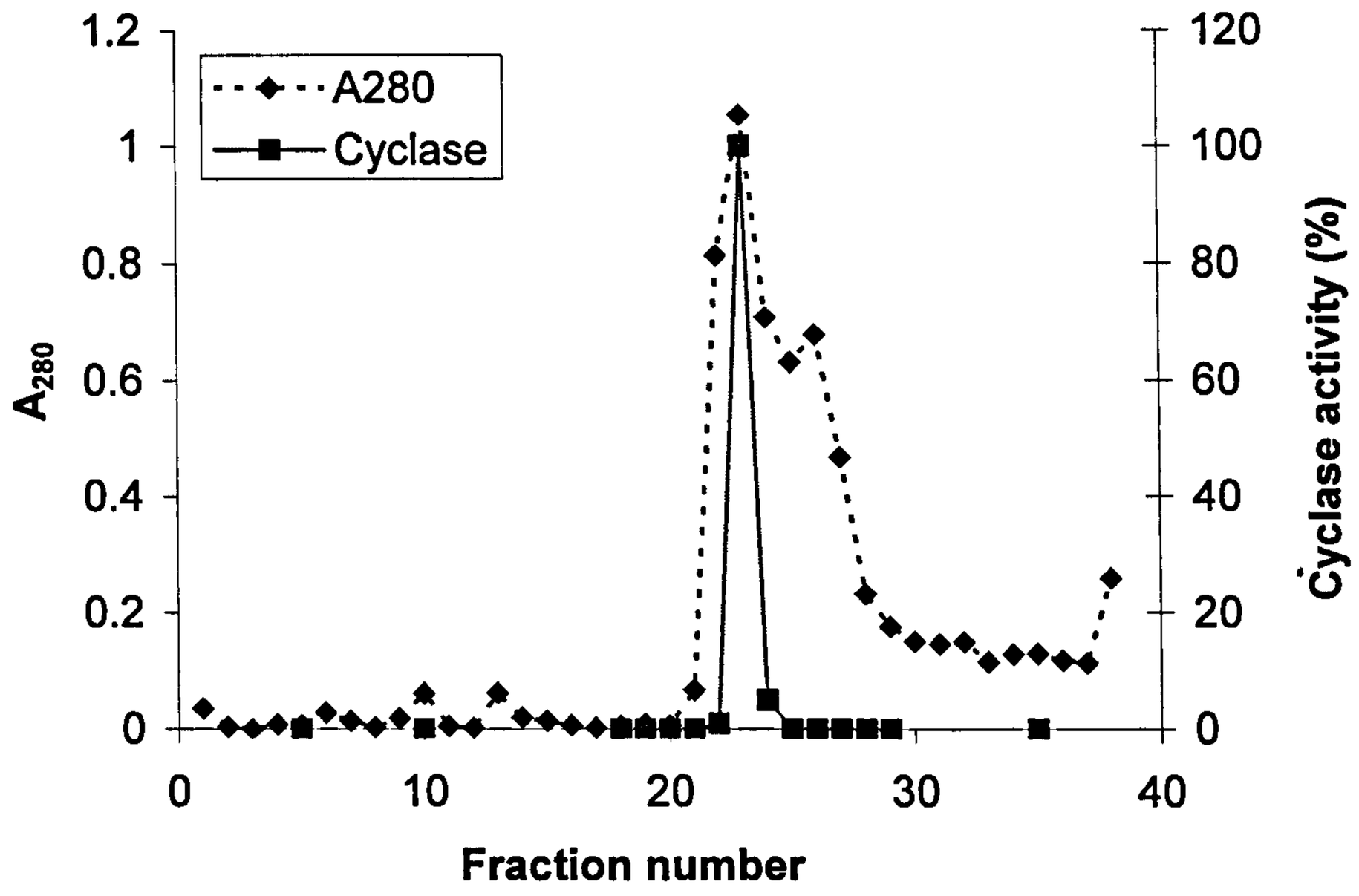

Figure 3.13. Purification of ADP-ribosyl cyclase activity via DEAE-Q-sepharose chromatography

Active fractions (7 and 8) eluted from a DEAE-toyopearl column (see Figure 3.11) were combined, dialysed, applied to a Q-sepharose column and eluted with a gradient of 0-2 M NaCl, as described in Materials and Methods. Fractions were collected and monitored for absorbance at 280 nm and for ADP-ribosyl cyclase activity by incubating them with 100 μM NGD for 25 min, as described.

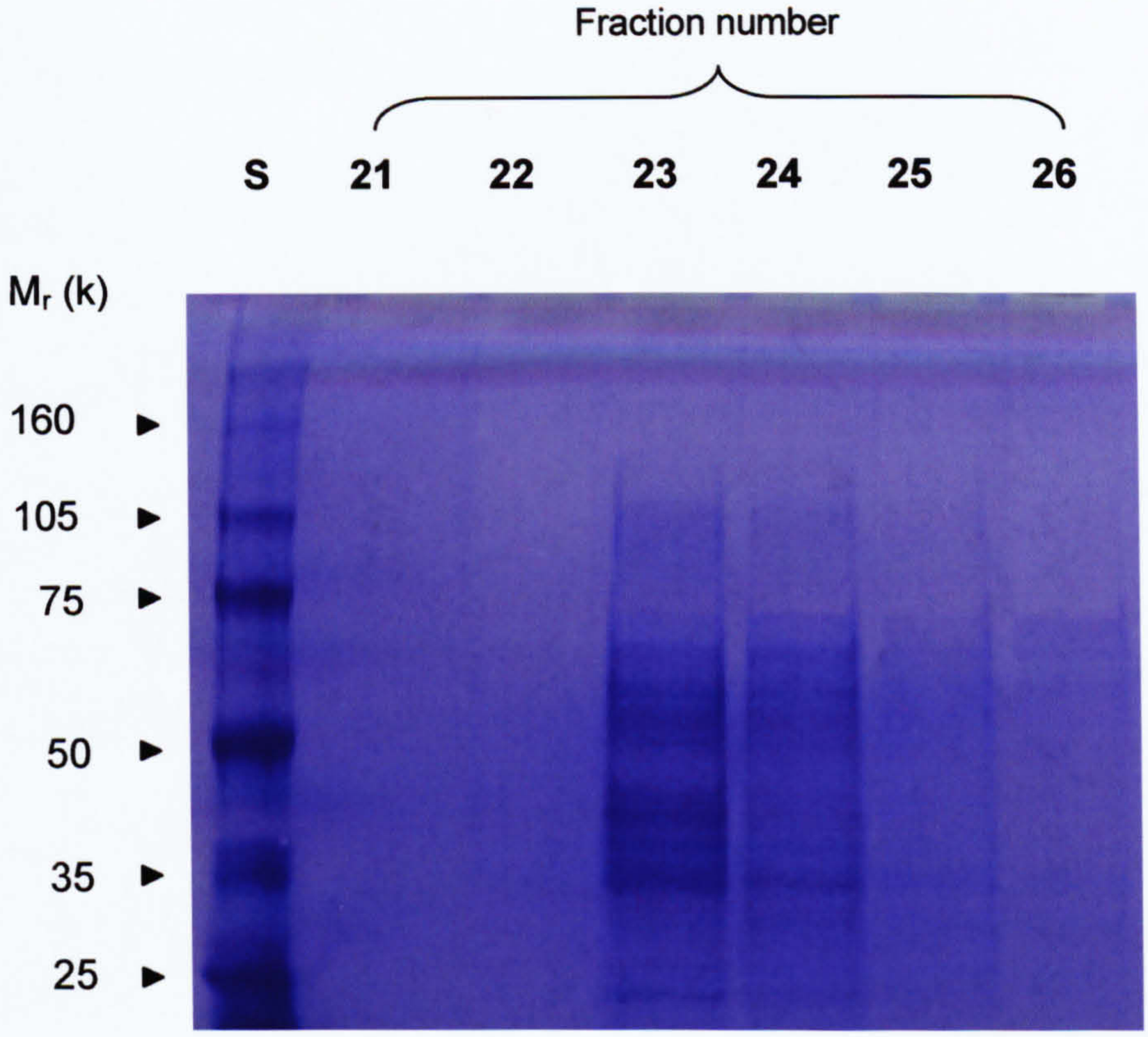

Figure 3.14. SDS-PAGE of cauliflower fractions from Q-sepharose column demonstrating ADP-ribosyl cyclase activity

Fractions (21-26) of solubilised cauliflower membrane proteins eluted from a Q-sepharose column were analysed by SDS-PAGE (8-16% gradient gel) and visualised by coomassie blue staining. Molecular mass is shown on the left based on calibrated standards (**S**) (Bio-Rad, Low-range Prestained SDS-PAGE Standards).

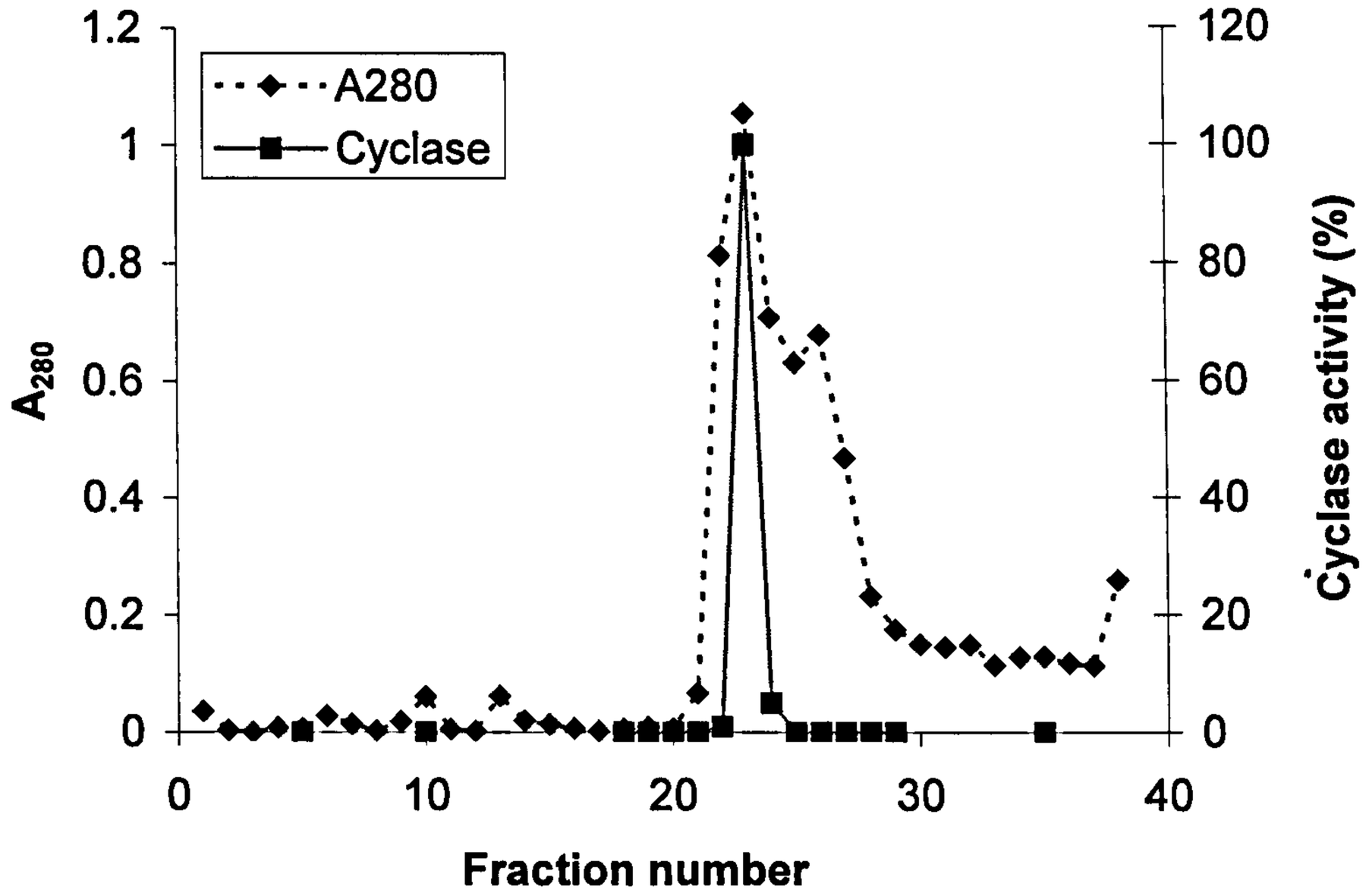

Figure 3.13. Purification of ADP-ribosyl cyclase activity via DEAE-Q-sepharose chromatography

Active fractions (7 and 8) eluted from a DEAE-toyopearl column (see Figure 3.11) were combined, dialysed, applied to a Q-sepharose column and eluted with a gradient of 0-2 M NaCl, as described in Materials and Methods. Fractions were collected and monitored for absorbance at 280 nm and for ADP-ribosyl cyclase activity by incubating them with 100 μM NGD for 25 min, as described.

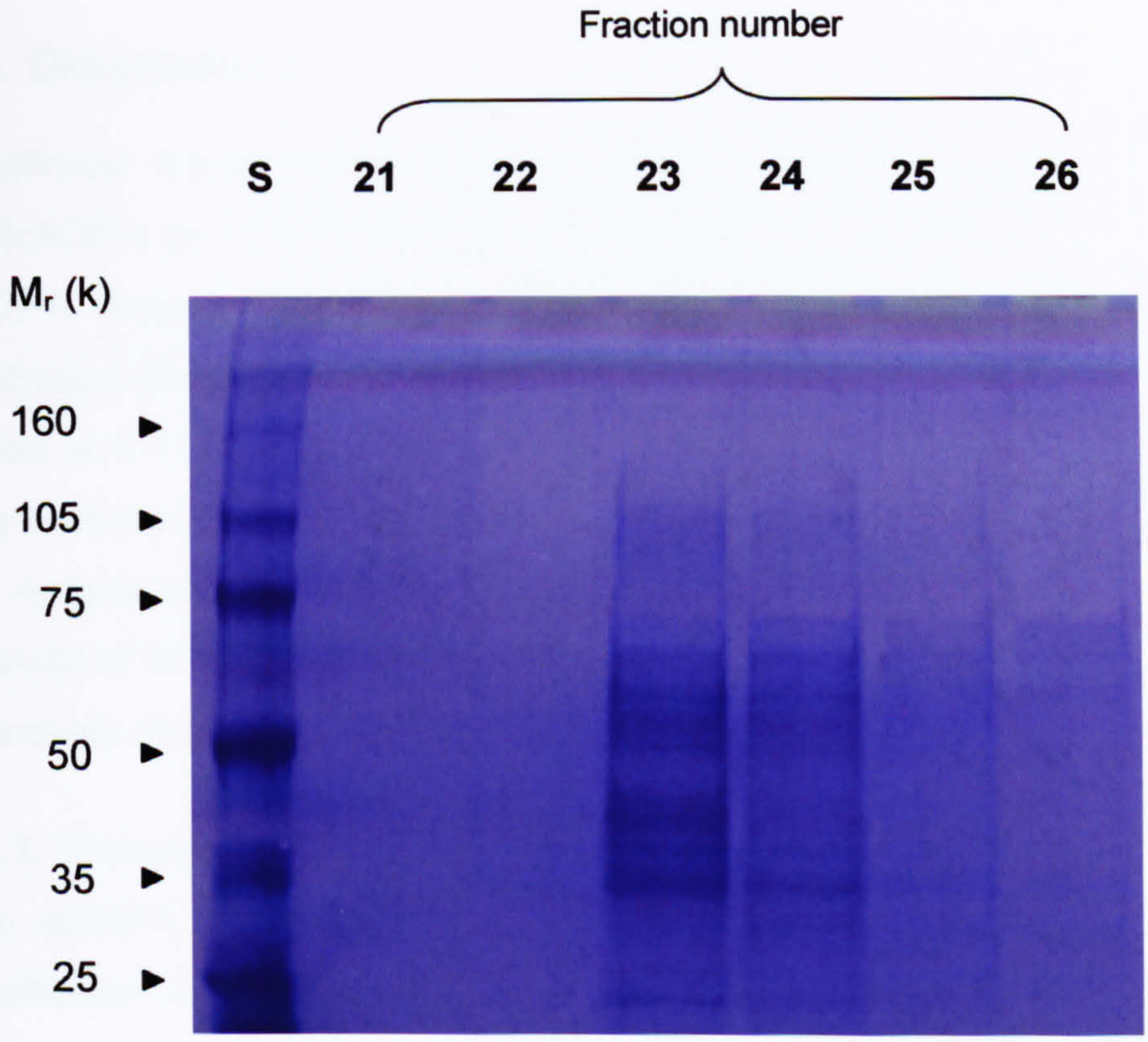

Figure 3.14. SDS-PAGE of cauliflower fractions from Q-sepharose column demonstrating ADP-ribosyl cyclase activity

Fractions (21-26) of solubilised cauliflower membrane proteins eluted from a Q-sepharose column were analysed by SDS-PAGE (8-16% gradient gel) and visualised by coomassie blue staining. Molecular mass is shown on the left based on calibrated standards (**S**) (Bio-Rad, Low-range Prestained SDS-PAGE Standards).

3.4. Discussion

Cauliflower microsomes incubated with [^{32}P]NAD and analysed for synthesis of [^{32}P]cADPR by HPLC confirmed the presence of cyclase activity indicated by the cGDPR fluorescence assay described in Chapter 2. Following an overnight incubation the majority of the [^{32}P]NAD appeared to be converted to a product that eluted at 3.5 min, the same time as the standard for cADPR (Figure 13). No peak was detected at 5 min, where the standard for ADPR eluted, suggesting that, like the *Aplysia* enzyme and the activity described for *E. gracilis* (Lee & Aarhus, 1991; Masuda *et al.*, 1999), membrane-bound cyclase in cauliflower does not catalyse the hydrolysis of cADPR.

3.4.1. Characterisation of cauliflower ADP-ribosyl cyclase activity

The cGDPR assay was used to characterise further the cyclase activity of the cauliflower tissue. Incubation of homogenised cauliflower meristematic tissue with NGD resulted in an increase in fluorescence over time that was heat labile and consistent with cyclase activity. The activity was dose dependent, exhibiting a V_{max} of 2.8 μmol/g.h and a K_m of 130.4 μM (Figure 3.3). From Table 3.2 it can be seen that the activity of cauliflower ADP-ribosyl cyclase is most similar to those reported for sea urchin eggs which have the lowest level of activity of any tissue yet examined (Lee & Aarhus, 1993). The K_m determined for cauliflower ADP-ribosyl cyclase is higher than the reported K_m for *Aplysia* cyclase for NGD of 2.8±0.2 μM (Graeff *et al.*, 1994), suggesting cauliflower ADP-ribosyl cyclase has a lower affinity for NGD. However, it is lower than the K_m reported for *Euglena* ADP-ribosyl cylase of 400 μM (Masuda *et al.*, 1999).

Cauliflower meristematic tissue was fractionated by centrifugation into soluble and membrane fractions which were assessed for cyclase activity to determine if, like sea urchin eggs, the cyclase activity is located in specific subcellular locations. The insoluble fraction demonstrated 4-fold higher activity than the soluble fraction suggesting that the majority of the cyclase activity was membrane bound (Figure 3.4). Whether the cyclase activity of the soluble fraction resulted from a discrete soluble form of the cyclase or arose from contamination from the insoluble fraction could not be determined. Both fractions also appeared to demonstrate hydrolase activity, since fluorescence decreased over time. Incubation of the fractions with cIDPR indicated that the decrease in fluorescence was heat labile and hence enzymic in nature and consistent with hydrolase activity (Figure 3.5).

Table 3.2. Comparison of ADP-ribosyl cyclase in various tissues

The activies of ADP-ribosyl cyclases in various tissues are indicated. The activities shown are for crude tissues and are for qualitative comparison as the assays were performed under different conditions. The table was modified from Lee *et al.* (1994).

Tissue	ADP-ribosyl cyclase (μmol/g.h)	Reference
Human RBC ghosts	8.4	Lee *et al.* (1993)
Dog brain	62.7±6.2	Lee & Aarhus (1993)
Chick embryonic brain	20.6±2.8	Lee & Aarhus (1993)
Salamander brain	4.5±0.1	Lee & Arrhus (1993)
Sea urchin egg	0.3±0.005	Lee & Aarhus (1993)
Aplysia ovotestis	1.3×10^6	Lee & Aarhus (1991)
Euglena extract	28.8	Masuda *et al.* (1999)
Cauliflower meristem	2.8	-

The demonstration of elevated cyclase activity and diminished hydrolase activity in the membrane fraction has two explanations: (1) that centrifugation of the tissue resulted in fractionation of inhibitory/stimulatory factors affecting cyclase/hydrolase activity and (2) two membrane-bound forms of ADP-ribosyl cyclase are present in cauliflower. These explanations are not mutually incompatible, however, when the two fractions were incubated with cGMP the activity of the soluble fraction was slightly stimulated while that of the insoluble fraction was not (Figure 3.6). Although the increase in activity was not quite significant the trend of activation is analogous to the cGMP stimulation reported for sea urchin egg homogenates (Graeff *et al.*, 1998) in which two forms of cyclase have been identified. The soluble cyclase of sea urchin was half-maximally stimulated by cGMP at 100 μM while the membrane-bound cyclase was not. In contrast to the activity of sea urchin eggs the soluble cyclase in cauliflower appears to demonstrate greater hydrolase activity than the membrane-bound form.

The pH-dependence of the insoluble cyclase indicates that its activity is higher at alkaline pH than acidic pH (Figure 3.7). Interestingly, these results are almost identical to the pH-dependence reported for the cyclase activity (with NGD as a substrate) of the *Aplysia* cyclase, and in contrast to the pH-dependence of the bifunctional enzyme CD38 which displays both cyclase and hydrolase activity and has the opposite pH-dependence (Graeff *et al.*, 1996). A study of the insoluble fraction cyclase indicated that ATP, even at 1 mM concentration, had no effect on activity (Figure 3.8). ATP is believed to stimulate the cyclase activity of CD38 by inhibiting its hydrolase activity (Takasawa *et al.*, 1993). Thus, an absence of stimulation by ATP is consistent with a monofunctional cyclase. Together, the pH dependence and the lack of action of ATP support the idea that the membrane fraction possesses only cyclase activity and not hydrolase activity.

Nicotinamide inhibited the cyclase activity, as expected for a product of the enzyme reaction. cAMP did not demonstrate any significant effect, but surprisingly EDTA (10 mM) slightly inhibited the cyclase. The enzymatic activitvities of other ADP-ribosyl cyclases have been determined not to require exogenous cofactors and they are unaffected by Ca^{2+} and Mg^{2+}.

3.4.2. Purification of cauliflower cyclase activity

Column chromatography was used to attempt purification of cyclase activity from solubilised cauliflower meristematic tissue. Following solubilsation with deoxycholate

the tissue was centrifuged at 400,000 x g and the soluble fraction was assayed for cyclase activity (Figure 3.9). Enzyme activity was further purified by DEAE-sepharose (Figure 3.10), DEAE-toyopearl (Figure 3.11) and Q-sepharose (Figure 3.13) column chromatography. The cyclase activity was purified 49-fold in a yield of 13% (Table 3.1). SDS-PAGE analysis of the active fractions indicated that although purification to homogeneity was not achieved, there was enrichment of several bands (approximately 35, 40 55 and 60 kDa). The band of molecular mass of 40 kDa (Figure 3.12 and Figure 3.14) is similar in size to mammalian CD38 and BST-1 (Mehta, *et* al., 1996; Hirata *et al.*, 1994) and the *Euglena* ADP-ribosyl cyclase (Masuda *et al.*, 1999) which are membrane-bound proteins of ~40 kDa, but not the soluble *Aplysia* ADP-ribosyl cyclase which is significantly smaller at ~30 kDa. The results indicate that the cauliflower cyclase most closely resembles *Euglena* ADP-ribosyl cyclase with possibly a similar molecular mass and a lack of hydrolase activity. The activity of the enzyme, however, is closer to that of sea urchin eggs.

4. Regulation of ligand-gated Ca^{2+}channels

4.1. Introduction

It has been shown that $InsP_3$, cADPR and NAADP are capable of releasing Ca^{2+} from intracellular stores within plant cells (see Chapter 1). Little, however, is known about how the Ca^{2+} release pathways activated by these ligands are modulated. Studies into the regulation of ligand-gated channels in animals (reviewed in Berridge, 1993; Taylor & Traynor, 1995; Lee, 1997) and functional studies of other ion channels in plants, such as the regulation of vacuolar voltage- and calcium-activiated currents by redox agents (Carpaneto *et al.*, 1999; Grabov & Blatt, 1999; Thuleau *et al.*, 1998; Klüsner *et al.*, 1997) suggest that Ca^{2+}/CaM, pH, redox state, and phosphorylation state might directly modulate the functional properties of plant ligand-gated Ca^{2+} release pathways. These second messengers may also impact on the action of other signal transduction components, for example, kinases and phosphatases, which in turn affect the activity of a variety of downstream events including the Ca^{2+}-permeable channels, and are discussed in more detail below.

4.1.1. Ca^{2+} and CaM

Although, as described above, various proteins have been identified in plants that are sensitive to Ca^{2+} and CaM - including CaM-regulated Ca^{2+}-ATPases in plant endomembranes and the plasma membrane (Malmstrom *et al.*, 2000; Bonza *et al.*, 2000) - little is known about the role of Ca^{2+} and CaM in modulating the activity of ion channels in plants. One exception already discussed is the SV channel: it is stimulated by Ca^{2+} and has been shown to be inhibited by antagonists of CaM (Hedrich & Neher, 1987; Bethk & Jones, 1994; Allen & Sanders, 1996). Furthermore, the recently described family of CNG-like channels, identified in barley (Schuurink *et al.*, 1998), *Arabidopsis* (Köhler & Merkle, 1999) and tobacco (Arazi *et al.*, 1999), possess a high-affinity CaM binding site (Arazi *et al.*, 2000) and are thought to be modulated by CaM.

4.1.2. pH

Cytosolic pH has been identified as a signalling intermediate in plant cells for over ten years with increases in pH accompanying an increase in $[Ca^{2+}]_c$ prior to stomatal closure and following treatment with ABA (Blatt & Armstrong, 1993) or other growth regulators (Irving *et al.*, 1992). Changes in pH have been linked to different

responses in the same tissue. For example, using ion-selective microelectrodes, Felle *et al.* (2000) demonstrated that the signalling molecule, NodRm-IV (C16:2,S) (a lipochitooligosaccharide Nod factor extracted from *Rhizobium meliloti*), induces a rapid and persistent increase in cytosolic pH in the root hairs of alfalfa (*Medicago sativa*). Conversely, the authors also found that the chitooligosaccharide, $(GlcNAc)_8$ (chitooctaose), acidified the cytosol of the root hairs whilst $(GlcNAc)_4$ (chitotetraose – the glucosamine backbone of NodRm-IV (C16:2,S)) had no effect. The authors concluded from this that these signal molecules may activate different responses in root hairs, with Nod factors inducing nodule organogenesis and chitooligosaccharides eliciting defense reactions.

Changes in cytosolic Ca^{2+} also occur in root hairs in response to both Nod factors and $(GlcNac)_8$ (Erhardt *et al.*, 1996; Gehring *et al.*, 1997; Felle *et al.*, 2000), however, how Ca^{2+} and pH signal transduction pathways interact has not yet been established. Grabov & Blatt (1997) have reported that artificially lowering the pH of the cytosol can lead to an increase in $[Ca^{2+}]_c$. This increase in Ca^{2+} does not follow the time course of the change in pH suggesting a complex interaction between the two signalling pathways. Grabov & Blatt (1998) suggest that the acidification of the cytosol may influence the activity of Ca^{2+} gating mechanisms across the PM as well as ligand-gated Ca^{2+}-release from intracellular stores. As changes in pH have been reported to affect $InsP_3$-, cADPR- and NAADP-induced release in microsomes derived from sea urchins and cerebellum (Joesph *et al.*, 1989; Chini *et al.*, 1989), if similar Ca^{2+}-release pathways exist in plants, it seems likely that the pH of the cytosol may be able to indirectly influence $[Ca^{2+}]_c$ by mediating the release of Ca^{2+} from intracellular stores.

4.1.3. Redox

The involvement of oxygen in respiration and photosynthesis leads to the formation of hydrogen peroxide, superoxides, hydroxyl radicals and other reactive oxygen species (ROS) that react with, and often damage, proteins, lipids and DNA. This oxidative stress is regulated and protected against, by plants and other organisms, through the action of enzymes such as superoxide dismutase (SOD), which catalyses the destruction of superoxide (the O^{2-} free radical) by conversion to H_2O_2, free radical scavengers (such as carotenoids, glutathione (GSH) and ascorbate) and enzymes that catalyse the break down of H_2O_2, including ascorbate peroxidase and catalase (Chaudière & Ferrari-Iliou, 1999; Noctor & Foyer, 1998; Noctor *et al.*, 2000). The redox state of a cell is under constant flux because the activities of the

protective mechanisms can alter dramatically when a plant experiences changes in environmental conditions. Conditions inducing the formation of ROS include chilling, pathogenic attack or exposure to ozone and other stresses, such as UV radiation or herbicide treatment (Prasad *et al.*, 1994; van Camp *et al.*, 1998; Grzelak *et al.*, 2001; Asada, 1994). The ways in which a plant cell perceives changes in redox state are not well understood but are thought to involve alterations in the ratio of reduced GSH to oxidised GSH (GSSG) (or the ratio of other pro- and antioxidants) as in animal cells (May *et al.*, 1998). GSH and GSSG are well suited to act as signalling compounds as they are tightly regulated by the cell and can be transported within and between cells (Foyer & Noctor, 2000). Furthermore, GSSG interacts with proteins to form disulphides by thiolation, which can modify protein activity (Thomas *et al.*, 1995). The effect of the redox state of the cell on constituents of signalling pathways, including ion channels is also likely to play a role in perception of redox state (for recent review see Foyer & Noctor, 2000).

4.1.4. Phosphorylation

Many signalling pathways involve protein phosphorylation and dephosphorylation reactions with phosphorylation commonly regulating the activity of ion channels in animal systems (for review see Levitan, 1994), including ligand-gated Ca^{2+} receptors (Orr *et al.*, 1996; Jayaraman *et al.*, 1996). While less is known about the role of phosphorylation events in plant cells there is a body of evidence accumulating that indicates that the activities of plant ion channels are similarly regulated by phosphorylation (Pei *et al.*, 1998). In guard cells, which have been a model for investigation of regulatory events, inward- and outward-rectifying K^+-channels and slow anion channels have been reported at the PM to be regulated by reversible phosphorylation (Armstrong *et al.*, 1994; Thiel & Blatt, 1994; Schmidt *et al.*, 1995) in a manner akin to that of the outward-rectifying K^+-channels at the PM of mesophyl-cells and pulvinar motor cells (Li *et al.*, 1994). A further example of the regulation of ion channel activity in plant cells by phosphorylation can be found in the tonoplast of broad bean guard cells. In the tonoplast of these cells SV channel activity has been shown to be modulated by the protein phosphatase calcineurin, i.e. the channels is activated by low concentrations of calcineurin and inhibited by high concentrations (Allen & Sanders, 1995). Similar results have been reported for the SV channel of barley aleurone protein storage vacuoles (Bethke & Jones, 1997).

4.1.5. Ca^{2+} release assay

This chapter describes the use of cauliflower meristematic vesicles as a model system for studying the effects of Ca^{2+}/CaM, pH, redox and phosphorylation on ligand-gated Ca^{2+} release. The effects of these compounds on Ca^{2+} release was assessed, by monitoring the flux of $^{45}Ca^{2+}$ from cauliflower vesicles, following loading of Ca^{2+} by endogenous Ca^{2+}-ATPases. The work presented here indicates that Ca^{2+}-release in plants cells is modulated by several of these signalling intermediates in an equivalent fashion to that seen in animal cells. Unexpectedly, the oxidative agent H_2O_2 demonstrated powerful inhibition of Ca^{2+} release induced by all three ligands - in contrast to recent experiments indicating it stimulates Ca^{2+} entry into guard cells (Pei *et al.*, 2000). This highlights the possibility that the redox state of a plant cell plays an important role in determining which Ca^{2+} stores are drawn upon during signalling.

The Ca^{2+} release assay was also used with the cauliflower model system to screen several putative Ca^{2+} release agents including, the cyclic nucleotides cAMP and cGMP, and analogues of NAADP and $InsP_3$. While none of the compounds tested were able to elicit Ca^{2+} release at expected physiological concentrations, $InsP_6$. and NADP demonstrated limited Ca^{2+} release when applied at concentrations 10-fold higher than a saturating dose of their analogues $InsP_3$ and NAADP. Surprisingly, the oxidising agent GSH, which was initially examined as a potential modulator of ligand-gated release, also demonstrated Ca^{2+}-release.

4.2. Materials and Methods

4.2.1. Plant material and chemicals

Cauliflowers were purchased locally, stored at 4°C and used within 24 h. $^{45}CaCl_2$ was obtained from Amersham. All other chemicals were from Sigma unless otherwise indicated.

4.2.2. Cauliflower membrane preparation

Microsomes were prepared from cauliflower inflorescences as described by Muir *et al.* (1997) with slight modification. Briefly, 5 mm of the outermost layer of cauliflower inflorescences (approximately 100g) were homogenised in 275 ml of 0.33 M sucrose, 5 mM Na_2-EDTA, 5 mM DTT, 0.2% (w/v) BSA, 0.2% (w/v) casein (boiled enzymatic hydrolysate), 0.6% (w/v) PVP-40, 1 mM benzamidine.HCl, 0.5 mM PMSF, 2 μg / ml leupeptin and 50 mM Mops / BTP, pH 7.5, supplemented with 1.7% (w/v) Protease and Phosphatase Inhibitor Cocktail (for plant cell extracts; Sigma, P6599). The homogenate was filtered through four layers of muslin and centrifuged at 10,000 g for 15 min at 4 °C. The supernatant was centrifuged at 40,000 g for 1 h at 4°C. The resulting membrane pellet was suspended in 25 ml of 0.33 M sucrose, 0.5 mM NaCl, 1 mM Na_2-EDTA, 5 mM DTT, 0.5 mM PMSF, 2 μg / ml leupeptin and 25 mM Mops / BTP, pH 7.5 and re-pelleted at 80,000 g for 45 min at 4 °C. The final pellet was resuspended (generally to a density of 35 mg protein /ml) in 0.33 M sucrose, 5 mM DTT, 0.5 mM PMSF, 2μg/ml leupeptin, 0.1% BSA and 25 mM Mops/BTP, pH 7.5, frozen in liquid nitrogen, and stored at –80 °C.

4.2.3. Protein determination

Protein concentration was determined with a Bio-Rad assay kit based on the dye binding method of Bradford (1976). Bovine serum albumin was used as a standard.

4.2.4. $^{45}Ca^{2+}$ transport assay

Cauliflower microsomes (50 μg) were diluted into 500 μl of calcium transport buffer that comprised: 400 mM glycerol, 5 mM BTP-Mes, pH 7.4, 25 mM KCl, 3 mM $MgSO_4$, 3 mM BTP-ATP and 0.3 mM NaN_3. Ca^{2+} uptake was started with the addition of 10 μM $CaCl_2$ containing 5.92 kBq $^{45}CaCl_2$ (original specific activity 74 MBq/ml) as a tracer. Ca^{2+} loading into the microsomes was driven by a combination of a Ca^{2+}/H^+ antiporter dependent upon V-type H^+-ATPase derived PMF and a P-type Ca^{2+}-ATPase (see Muir & Sanders, 1997). Loading was terminated after 60 min by the addition of the uncoupler, carbonyl cyanide *p*-(trifluoromethoxy)phenyl-

hydrazone (FCCP), to a final concentration of 10 μM and the P-type ATPase inhibitor, Na_3VO_4 to a concentration of 0.25 mM. For the release assays the completion of loading at 60 min was taken as time point zero. Uptake inhibitors were added at 0.25 min followed by treatments and then the appropriate ligand at various times, depending on the experiment. Typically release was induced by addition of the ligand at 1 min. Uptake and release of Ca^{2+} from the microsomes was monitored via a radiometric filtration assay using the Millipore filtration technique previously described (Muir & Sanders, 1997). 50 μl aliquots were removed from the reaction mix and placed onto nitocellulose filters (0.45 μm pore size: type WCN, Whatman) under vacuum. The filters had been prewetted with wash buffer (400 mM glycerol, 5 mM BTP-Mes, pH 7.4 and 0.2 mM $CaCl_2$). The filters were rapidly washed with 5 ml of ice-cold wash buffer, placed into scintillation vials and radioactivity measured by liquid scintillation counting. Radioactivity left on the filters after adding the Ca^{2+} ionophore, A23187 (10 μM), was defined as non-accumulated Ca^{2+} and was subtracted from all data. Generally, non-accumulated Ca^{2+} was equal to or less than 25% of the overall maximum Ca^{2+} accumulation and corresponds to non-specific binding of Ca^{2+} to the microsomes.

4.2.4.1. pH experiments

The effect of pH on Ca^{2+} uptake and release was investigated by adjusting the pH of the calcium transport buffer prior to loading. Uptake and release were monitored as described.

4.2.4.2. CaM experiments

To evaluate the effects of CaM on release Ca^{2+}, loading of vesicles proceeded as described above. Spinach CaM (Sigma) was added to 0.1 or 0.6 μM final concentration at 0.5 min. Release was then induced at 3 min with either a saturating dose (1μM) or a non-saturating dose (30 nM) of cADPR or NAADP. Release was monitored as described.

4.2.4.3. Redox experiments

The effect of the reducing agents DTT, GSH and oxidising agents thimerosal, chloramine-T, menadione and H_2O_2 on Ca^{2+} release was monitored by adding them, at varying final concentrations of 25 μM – 1 mM, to a release assay mix at 2 min. Release with saturating doses of cADPR (1μM), $InsP_3$ (10 μM) or NAADP (1μM) was induced at by adding the ligand at 3 min. The release assay was also used to

investigate whether the redox agents could induce calcium release by adding them in the place of cADPR, NAADP or $InsP_3$, as described above.

The effects of H_2O_2 were investigated in more detail. H_2O_2 was added to the reaction mix and release measured in response to non-saturating doses of cADPR (30 nM), $InsP_3$ (600 nM) or NAADP (100 nM) as previously described. The ability of DTT to protect the vesicles from the effect of H_2O_2 was monitored by adding 1 mM DTT 30 sec prior to 100 μM H_2O_2 and then inducing release with a saturating dose of release agent as described. The effect of H_2O_2 on uptake was also examined by adding H_2O_2 to a final concentration of 0-1 mM prior to loading. Uptake was monitored as described.

4.2.4.4. Phosphorylation experiments

The effect of phosphorylation on Ca^{2+} uptake was investigated by adding PKA (5 U/ml; catalytic subunit from bovine heart, Sigma P2645) or AP (100 U/ml, Type VII-S from bovine intestinal mucosa, Sigma P5521) to the calcium transport buffer prior to adding ATP to initiate loading (time 0). To monitor release they were added to the release assay mix, following loading, at 1 min. Release was induced by addition of saturating doses of cADPR, $InsP_3$ or NAADP at 3 min. Uptake and release were monitored as described.

4.2.4.5. Calcium experiments

To examine the possibility that $[Ca^{2+}]$ influences the activity of calcium release channels EGTA was added to a final concentration of 250 μM at 2 min. Release was induced with saturating doses of cADPR, $InsP_3$ or NAADP at 3 min. Release was monitored as described.

4.2.5. H^+ pumping assay

To assess the integrity of microsomes the formation of a trans-membrane pH gradient, generated by H^+-ATPase activity, was monitored using a pH sensitive dye and fluorescence spectroscopy. A modification of the method described by Blackford *et al.* (1990) was used.

Cauliflower microsomes (200 μg/ml) were incubated with 5 μM acridine orange in a reaction medium of 10 mM BTP-MES pH 7.4, 250 mM glycerol, 50 mM KCl, and 5 mM $MgCl_2$. Fluorescence was monitored in a Perkin-Elmer LS-5 luminescence spectrophotometer at room temperature with solutions under constant stirring and

the excitation and emission wavelengths set to 495 and 540 nm respectively. Both excitation and emission slit widths were set to 5 nm. Fluorescence was sampled at 1 s intervals and recorded by an IBM-PC using the program LSR (Jennings *et al.*, 1988).

Proton pumping was initiated by the addition of 1mM BTP-ATP (pH 7.4), generating a fluorescence quench. Once the pH gradient was fully formed, typically after 150 s, various oxidising and reducing agents were added to the reaction mix at different concentrations. A rapid collapse of the gradient, seen as quench recovery, was taken as an indication of loss of membrane integrity.

4.3. Results

4.3.1. Ca^{2+} release controls

Cauliflower microsomes that have been loaded with Ca^{2+} have previously been shown to release it in response to treatment with $InsP_3$, cADPR and NAADP (Muir *et al.*, 1997; Navazio *et al.*, 2000). In order to study how this Ca^{2+} release is regulated the same experimental system was used. Microsomes prepared from cauliflower meristematic tissue were initially tested to confirm that they were able to take up and release Ca^{2+}. Figure 4.1 demonstrates that the microsomes actively took up Ca^{2+} in the presence of ATP in a time dependent manner. Following abolition of Ca^{2+} uptake via treatment with P-type ATPase inhibitor vanadate and the protonophore FCCP Ca^{2+} release was induced with cADPR, $InsP_3$ and NAADP, as expected.

Table 4.1 shows that saturating doses of cADPR, $InsP_3$ and NAADP released Ca^{2+} as previously reported (Muir *et al.*, 1997; Navazio *et al.*, 2000; 2001). Ca^{2+} release was inhibited by procaine (with cADPR) and heparin (with $InsP_3$) and there was significantly less release when the microsomes were exposed to the negative controls of water or ADPR. The microsomes prepared had active uptake and release mechanisms with a pharmacology similar to that previously reported and thus were suitable for Ca^{2+} transport assays. The limited release of Ca^{2+} displayed by the negative controls was attributed to background leak from the vesicles.

4.3.2. Effect of pH on Ca^{2+} uptake and release

To determine whether pH promoted differential Ca^{2+} loading of the microsome vesicles cauliflower microsomes were incubated with $^{45}Ca^{2+}$ in media buffered to the same pH range used for the release experiments. The amount of $^{45}Ca^{2+}$ taken up by the vesicles over 60 min was determined as is shown in Figure 4.2. The experiments demonstrate that Ca^{2+} uptake is not affected by changes in pH over the range tested.

The effect of pH on cauliflower microsomal Ca^{2+}release induced by saturating doses of cADPR, $InsP_3$ and NAADP was investigated by altering the pH of the assay media (Figure 4.3). A stepwise increase of the pH from 7 to 8 had no effect on release stimulated by NAADP while it inhibited cADPR-induced release and stimulated $InsP_3$ release. An increase in pH above 7.4 reduced cADPR-induced Ca^{2+} release to a background level, whereas the release seen with $InsP_3$ at pH 7.8 is significantly higher than that demonstrated at pH 7.0. This is consistent with the effect of pH on Ca^{2+} release in sea urchin eggs described by Chini *et al.* (1989). The

Table 4.1. Mean Ca^{2+} release of controls

Ca^{2+} release data for $InsP_3$, cADPR and NAADP, the negative controls water and ADPR and release agents in the presence of inhibitors. Data are the means of three experiments ± SEM.

Reagent	Mean Ca^{2+} Release (%)
Negative controls	
Water	4.5 ± 1.3
ADPR (10 μM)	7.9 ± 1.4
Positive controls	
$InsP_3$ (10 μM)	14.3 ± 2.0
cADPR (1 μM)	18.1 ± 3.3
NAADP (1 μM)	16.5 ± 2.3
Inhibitors	
$InsP_3$ (10 μM) + heparin (10 μM)	2.8 ± 2.6
$InsP_3$ (10 μM) + procaine (1 mM)	13.1± 2.1
cADPR (1 μM) + procaine (1 mM)	6.3 ± 2.4
cADPR (1 μM) + heparin (10 μM)	17.5 ± 1.1

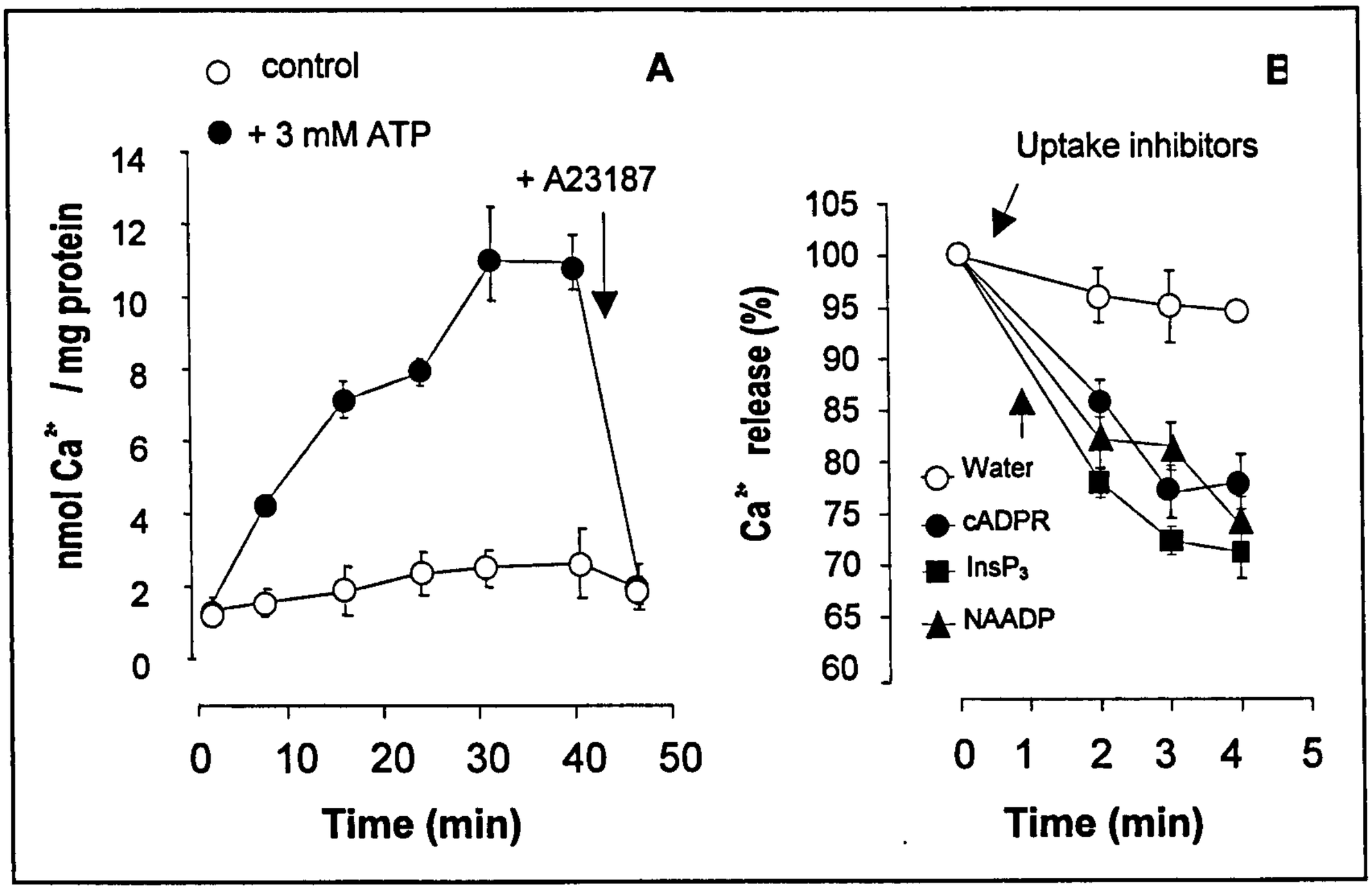

Figure 4.1. Microsomes prepared from cauliflower demonstrate Ca^{2+} uptake and release

A. Cauliflower microsomes were incubated with $^{45}Ca^{2+}$ in the presence or absence (control) of 3 mM ATP. After a steady state of loading was reached at 40 min the Ca^{2+} ionophore A23187 (10 μM) was added. **B.** Following loading of the vesicles with $^{45}Ca^{2+}$ to a steady state further uptake was inhibited 60 min after initiation of loading by addition of the uncoupler FCCP (10 μM) and the P-type ATPase inhibitor Na_3VO_4 (250 μM) data were standardised to the value of Ca^{2+} upake recorded just prior to inhibitor addition. Either water or cADPR, $InsP_3$ or NAADP, to a final concentration of 1, 10 and 1 μM respectively, were then added to the vesicles. Data are the means of three or more replicates ± SEM.

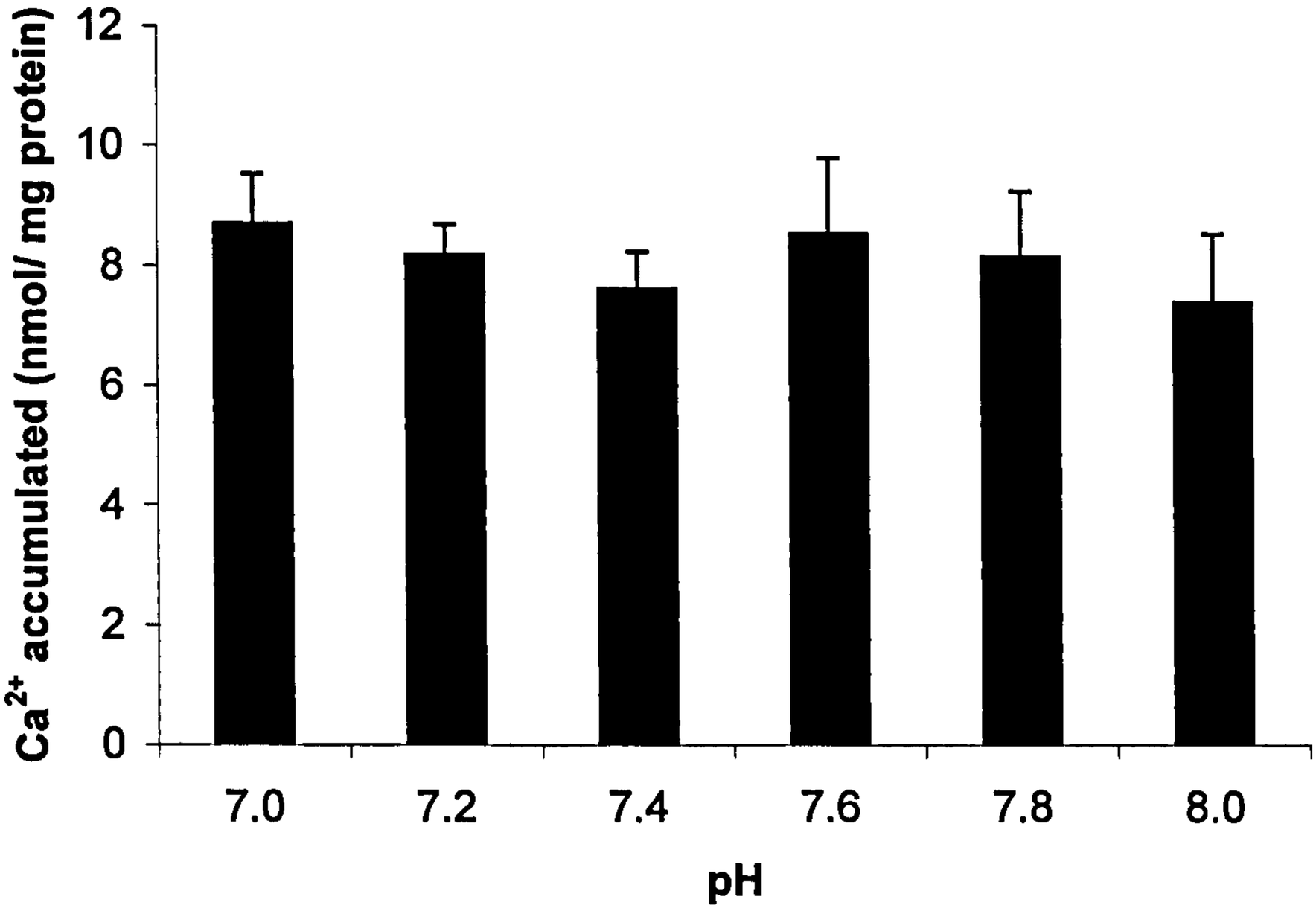

Figure 4.2. Over a physiological range pH has no effect on Ca^{2+} uptake into cauliflower microsomes

Cauliflower microsome vesicles were loaded with $^{45}Ca^{2+}$ for 60 min in calcium transport medium from pH 7.0 to 8.0. An aliquot was removed and filtered and the radioactivity counted by liquid scintillation to estimate the Ca^{2+} accumulated within the vesicles. Non-specific association of Ca^{2+} with vesicles was determined by addition of A23187. Data are the means of three experiments ± SEM. T-test results indicate no significant difference between any two treatments ($P > 0.05$).

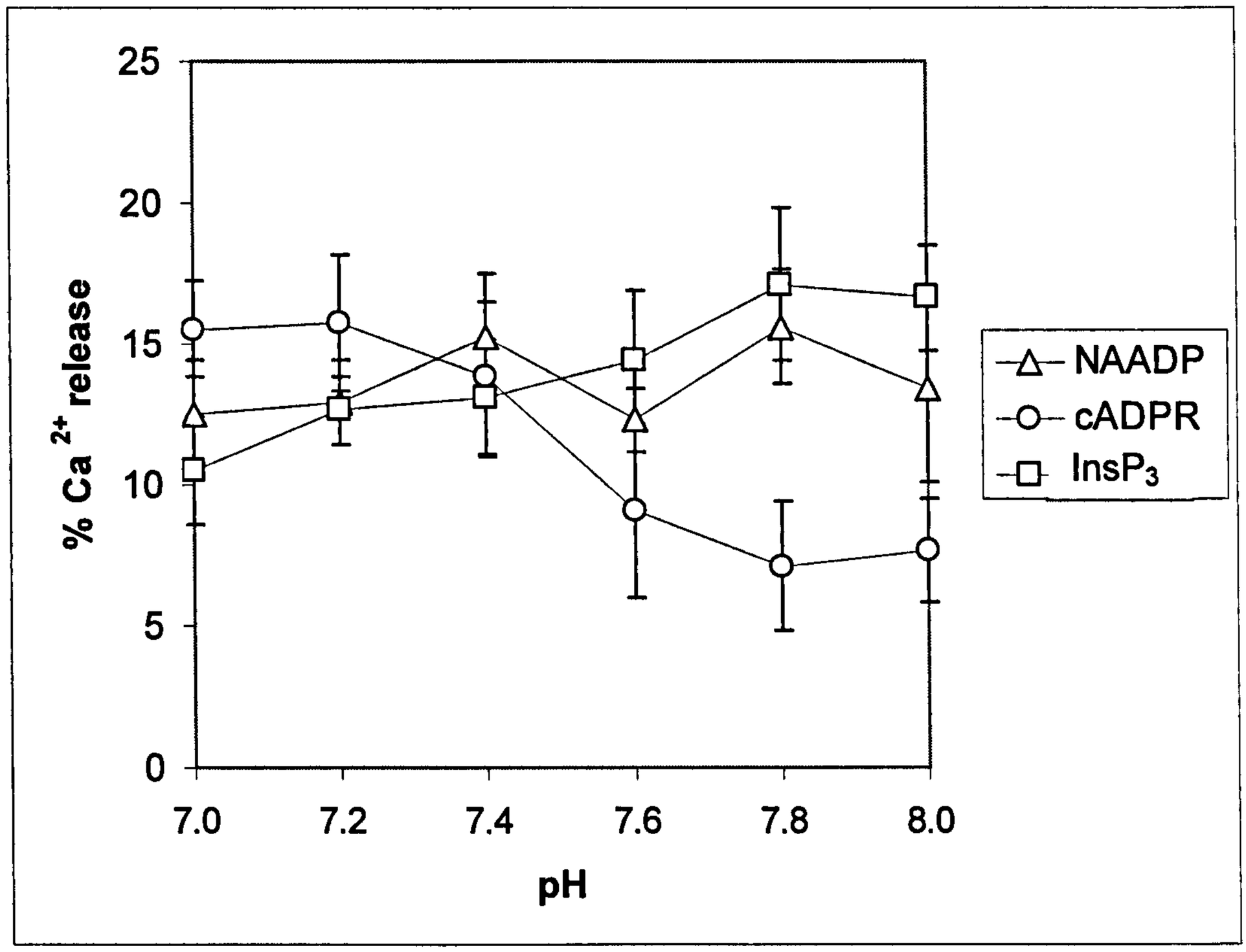

Figure 4.3. cADPR induced Ca^{2+} release from cauliflower microsomes is inhibited by an increase in pH

Cauliflower microsome vesicles were loaded with $^{45}Ca^{2+}$ for 60 min in calcium transport medium of pH from 7.0 to 8.0. Further uptake was inhibited with FCCP (10 μM) and Na_3VO_4 (200 μM). Subsequently either cADPR (1μM), $InsP_3$ (10 μM) or NAADP (1μM) were added and the change in accumulated Ca^{2+} measured. Data are the means of three experiments ± SEM.

authors demonstrated that pH has a differential effect upon the release induced by different ligands. Release induced by NAADP is almost pH-independent over a physiological range, cADPR-induced release is steeply reduced with increased alkalinization over a range of pH from 6.5 to 9.0, whereas $InsP_3$ induced release is optimal at pH 7.0. This effect is believed to arise from the dependence of ligand-binding on pH and direct activation of the channels involved by pharmacological agonists. These differential pH effects potentially link pH and Ca^{2+}-based signalling pathways and provide a possible mechanism by which signal specificity can arise.

4.3.3. Effect of [Ca^{2+}] and CaM on Ca^{2+} release

A Ca^{2+}-release assay was used to determine whether ligand-gated Ca^{2+} release channels are similarly modulated by Ca^{2+} and CaM.

4.3.3.1. Ca^{2+} regulation of Ca^{2+} release

The effect of Ca^{2+} on Ca^{2+}-release in cauliflower microsomes was studied by loading the microsomes with Ca^{2+} as described in Section 4.2.4. Release induced by saturating doses of cADPR, $InsP_3$ or NAADP was monitored 2 min after the addition of the calcium chelator EGTA (250 μM) or $CaCl_2$ (1 mM). As Figure 4.4 indicates, EGTA had no significant effect on the release induced by any of the different agents. 1 mM $CaCl_2$ had no effect on $InsP_3$- or NAADP-induced release, however, it activated cADPR-induced release.

4.3.3.2. CaM regulation of Ca^{2+} release

CaM is a ubiquitous Ca^{2+} binding protein: known to play a central role in Ca^{2+} signalling in eukaryotes and regulate calcium release channels in animals (Rodney *et al.*, 2000; Hirota *et al.*, 1999; Lee *et al.*, 1995). The effect of CaM on Ca^{2+} release induced by cADPR and NAADP from cauliflower microsomes was investigated by adding spinach CaM to the assay media 2 min prior to release. Figure 4.5 demonstrates that the release induced by a saturating dose of cADPR is inhibited by 0.6 μM CaM. While there also appears to be a trend of inhibition, with saturating doses of NAADP and non-saturating doses of both release agents, a Students T-test indicates that the difference between treatment with 0.6 μM CaM and water in these cases is not significant. The difference between the water control and treatment with 0.1 μM CaM followed by cADPR-induced release, with a non-saturating dose, indicates a trend of activation, similar to that previously reported (Bewell, 1999). Once again, the differences observed were not significant.

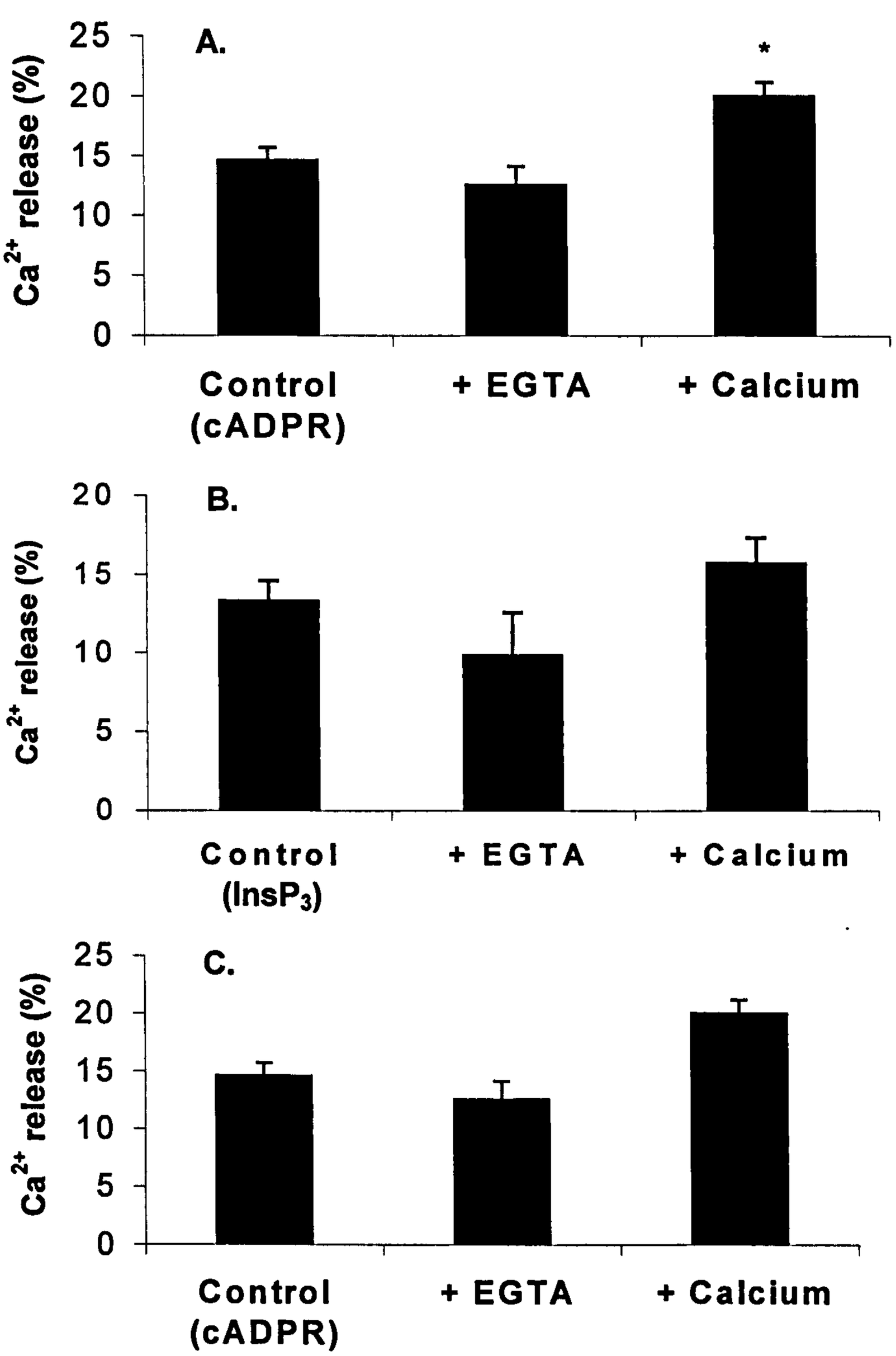

Figure 4.4. Calcium activates cADPR induced release

Cauliflower microsome vesicles were loaded with $^{45}Ca^{2+}$ for 60 min in calcium transport medium. Further uptake was inhibited with FCCP (10 μM) and Na_3VO_4 (200 μM) and EGTA (250 μM), $CaCl_2$ (1 mM) or water (control) were added. Subsequently either **A.** cADPR (1μM), **B.** $InsP_3$ (10 μM) or **C.** NAADP (1μM) were then added and the change in accumulated Ca^{2+} measured. Data are the means of three experiments ± SEM. An asterisk (*) indicates significant difference between the control and the treatment ($P < 0.05$).

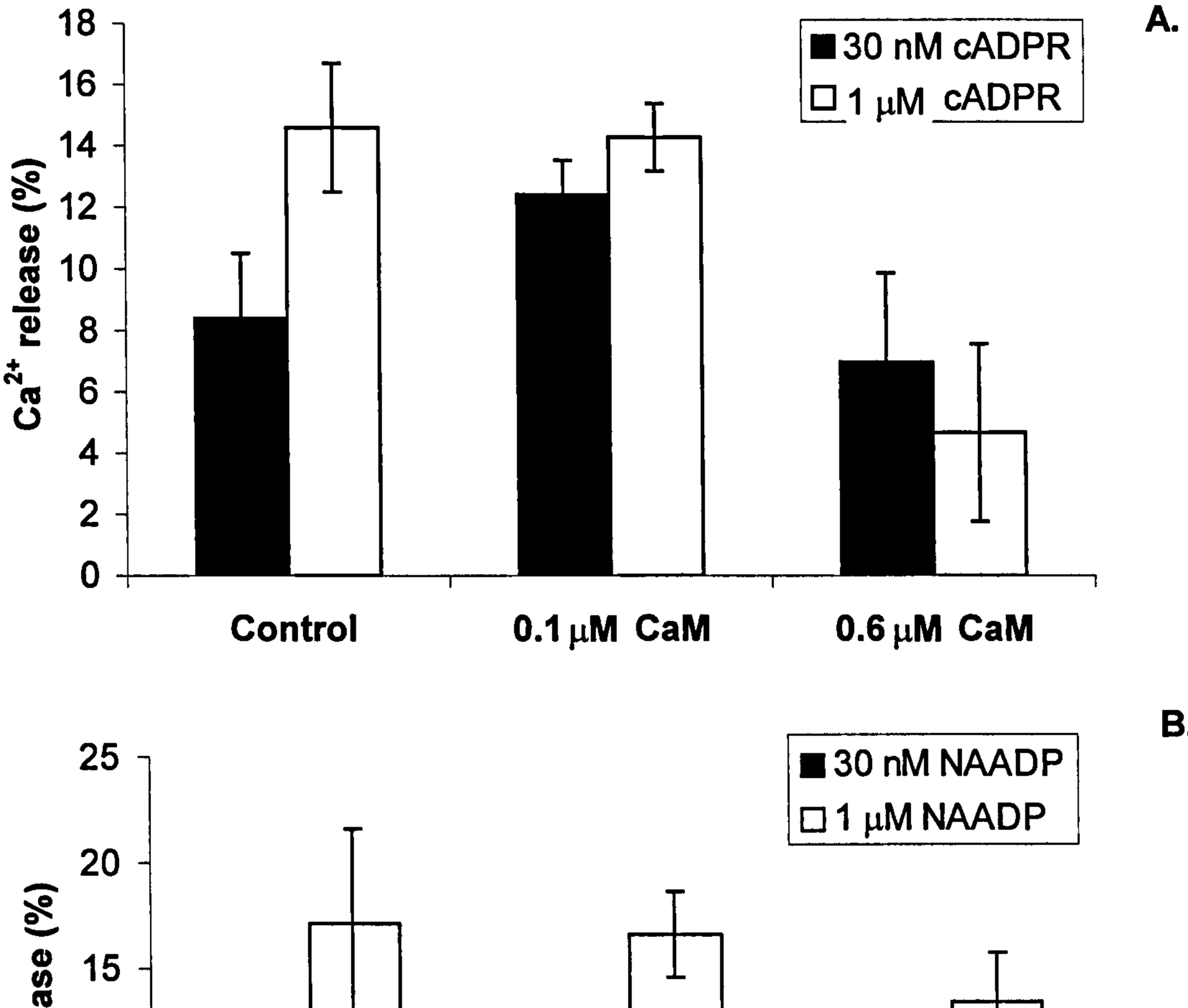

Figure 4.5. Effect of CaM on Ca^{2+} release induced by cADPR and NAADP

Cauliflower microsomal vesicles were loaded with $^{45}Ca^{2+}$ for as described in Section 3.4.4. CaM was added to a final concentration of 0.1 or 0.6 μM and release was induced with **A.** a saturating (1μM) or a non-saturating dose (30 nM) cADPR or **B.** a saturating (1μM) or non-saturating dose (30 nM) of NAADP. Data are the means of three experiments ± SEM. T-test results indicate no significant difference between the control and the treatments ($P > 0.05$).

To further investigate the role of calmodulin in regulating calcium release channels, W-7 was to be used to block any native calmodulin associated with the microsomes from sensitising or inhibiting the ligand-gated release. However, as Figure 4.6 illustrates, application of 150 μM W-7 to microsomes loaded with Ca^{2+} induced release of its own accord, making it unsuitable for use with the Ca^{2+} transport assay at an effective concentration.

4.3.4. Effect of redox agents on Ca^{2+} release

4.3.4.1. Ca^{2+} release properties of redox reagents

The effect of redox agents on the ion channels of higher plants has recently been investigated by Carpaneto *et al.* (1999). In tonoplast membranes isolated from the marine seagrass *Posidonia oceanica* and from the root of sugar beet, they were able to show, using the patch clamp technique, that various sulphydryl reducing agents, particularly dithiotheritol (DTT) and GSH, reversibly activated the SV channel when added to the cytoplasmic side of the vacuole. The oxidising agent chloramine-T irreversibly terminated any SV channel currents. To assess the modulation of Ca^{2+} release in plants by redox agents cauliflower microsomes were exposed to several concentrations of the reducing agents DTT and GSH and the oxidising agents thimerosal, chloramine-T and H_2O_2. Table 4.2 shows that exposure of cauliflower microsomes to different reducing and oxidising reagents induces a differential release of Ca^{2+}. DTT and H_2O_2 did not induce a release of Ca^{2+} significantly different from that of the negative control water, even at concentrations reaching 1 mM. However, concentrations of chloramines-T and thimerosal as low as 50 μM, however, were able to release significant amounts of Ca^{2+} from the vesicles. At higher concentrations (500 μM and above) menadione and GSH also elicited Ca^{2+} release. It is possible that part or all of the Ca^{2+} release observed with some redox agents results from the disruption of vesicle integrity. To determine whether this was indeed the case the ability of microsome vesicles to maintain a pH gradient in the presence of redox reagents was tested. As Figure 4.7 indicates, water and 1 mM H_2O_2 did not induce fluorescence quench recovery while 100 mM chloramine-T did. The quench recovery was presumed to arise from membrane damage and a loss of membrane integrity. The quench recoveries shown in Table 4.2 suggest that concentrations of chloramine T, thimerosal and menadione as low as 50 μM might damage the vesicle membranes. This suggests that the Ca^{2+} release observed with these reagents may be due to non-specific disruption of the vesicle membrane. GSH, DTT and H_2O_2 did not demonstrate any significant quench

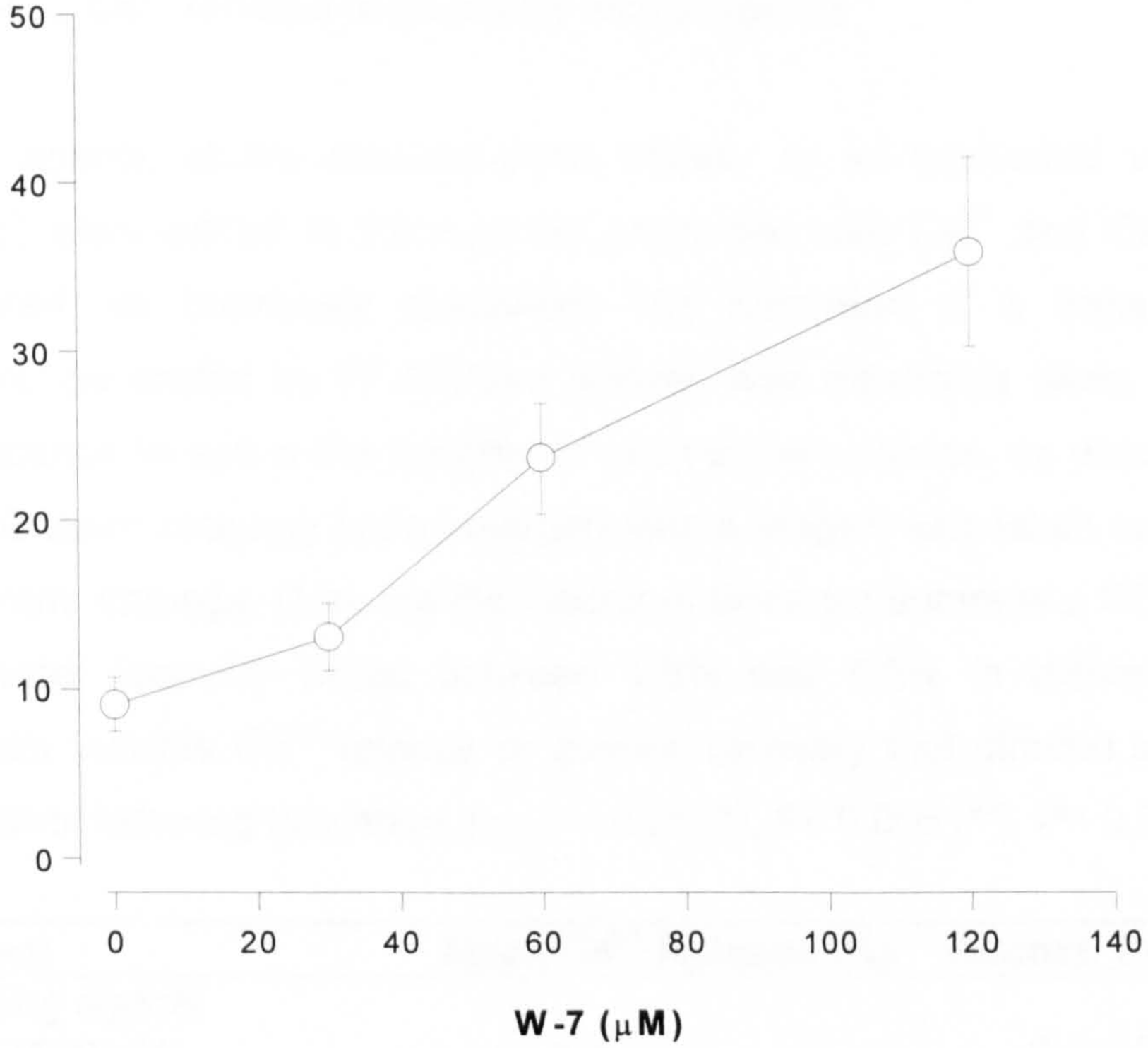

Figure 4.6. W-7 (a CaM antagonist) induces Ca^{2+} release

Cauliflower microsome vesicles were loaded with $^{45}Ca^{2+}$ as previously described. W-7 was added to a final concentration of up to 150 μM. The change in accumulated Ca^{2+} is shown. Data are the means of three experiments ± SEM.

Table 4.2. Ca^{2+} release induced by redox agents

Redox agents, at the concentrations shown, or an equivalent volume of water (control) were added to microsomes preloaded with Ca^{2+} and Ca^{2+} release was monitored, as previously described. The formation of a trans-membrane pH gradient, generated by H^+-ATPase activity, was monitored using acridine orange fluorescence to asses the integrity of microsomal vesicles, as described in section 4.2.5. Quench recovery upon treatment with a reagent was taken as an indication of membrane damage. Data are the means of three experiments ± SEM. Ca^{2+} release with water (control) varied between 1.8% and 5.5% in different experiments. Asterisks indicate Ca^{2+} release or quench recovery that differed significantly from the control following treatment, i.e. $P < 0.05$ (*), $P < 0.005$ (**), $P < 0.0005$ (***).

Reagent	Mean Ca^{2+} Release (%)		Quench Recovery (%)	
Reducing agents				
DTT (500 μM)	n.d.		-0.4 ± 0.2	
DTT (1 mM)	9.0 ± 1.6		-3.9 ± 0.2	**
GSH (500 μM)	9.6 ± 1.7		1.0 ± 0.1	
GSH (1 mM)	18.3 ± 3.2	*	2.2 ± 0.1	*
Oxidising agents				
GSSG (200 μM)	6.8 ± 2.2		n.d.	
GSSG (1 mM)	10.2 ± 1.1	*	0.2 ± 0.1	
thimerosal (25 μM)	5.8 ± 2.2		4.9 ± 1.2	*
thimerosal (50 μM)	7.3 ± 5.4		6.9 ± 0.5	***
thimerosal (100 μM)	20.1 ± 6.4	*	n.d.	
thimerosal (1 mM)	29.0 ± 5.3	*	20.2 ± 1.6	***
chloramine T (25 μM)	n.d.		2.1 ± 0.3	*
chloramine T (50 μM)	10.2 ± 1.8		4.0 ± 0.4	**
chloramine T (100 μM)	22.5 ± 3.3	**	21.1 ± 1.8	***
chloramine T (1 mM)	46.8 ± 6.9	**	n.d.	
menadione (50 μM)	5.1 ± 1.2		2.1 ± 0.6	
menadione (100 μM)	6.8 ± 1.2		8.9 ± 0.5	***
menadione (1 mM)	7.8 ± 1.4		n.d.	
H_2O_2 (50 μM)	4.5 ± 2.7		0.2 ± 0.2	
H_2O_2 (100 μM)	4.0 ± 3.0		1.2 ± 0.4	
H_2O_2 (1mM)	4.7 ± 1.2		1.1 ± 0.4	

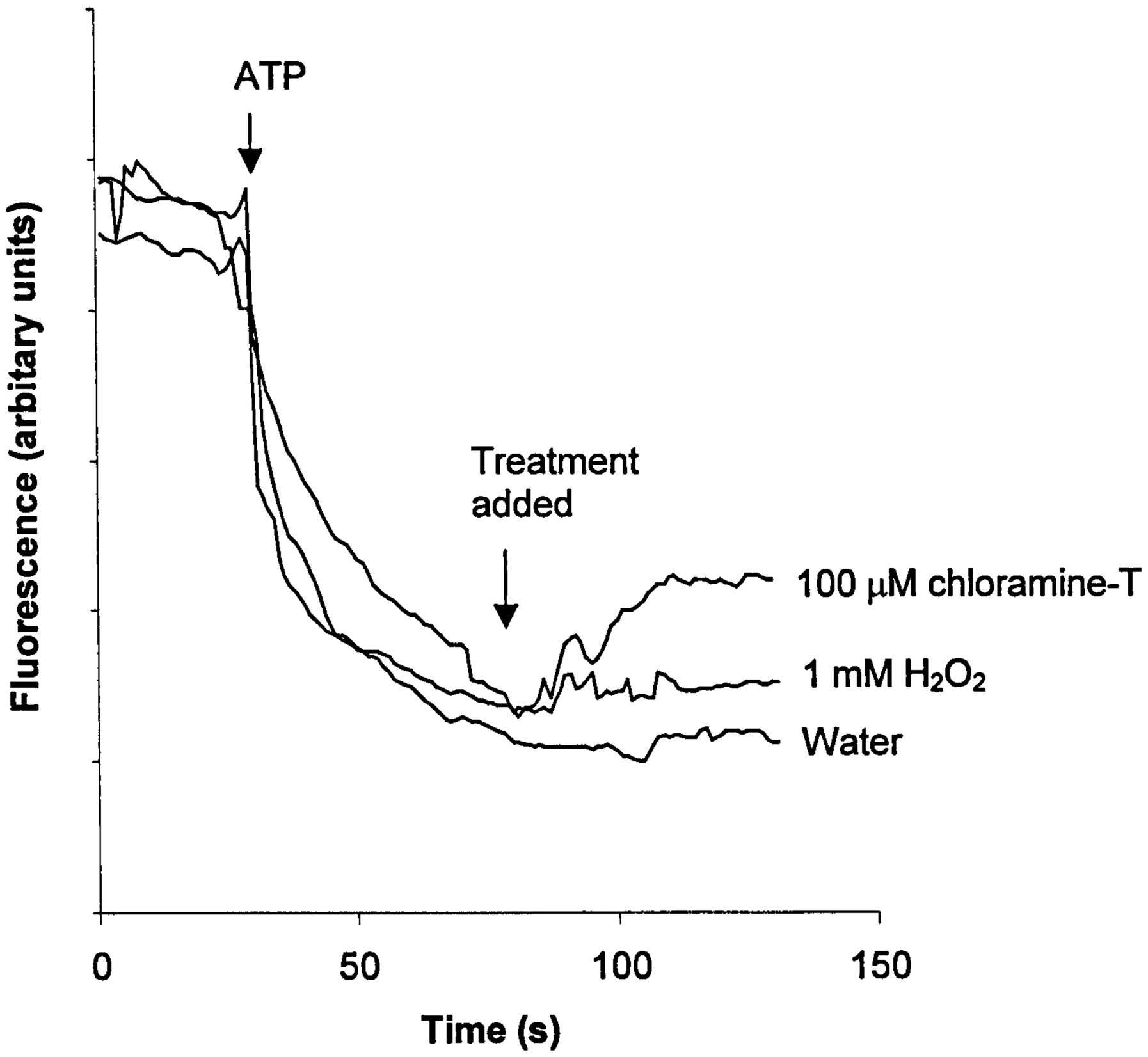

Figure 4.7. Membrane integrity assay using acridine orange

A trans-membrane proton gradient was generated in cauliflower microsome vesicles by incubating them with 1 mM ATP in the presence of acridine orange as described in section 4.2.5. Once a steady state was reached, various redox agents were added at a variety of concentrations and the quench recovery monitored. Typical data are depicted.

recovery at concentrations up to 1 mM. GSH was the only reagent tested that released Ca^{2+} without causing significant membrane integrity loss, indicating that GSH, at concentrations between 0.5 and 1.0 mM, may activate a calcium-permeable channel.

4.3.4.2. Ligand-gated Ca^{2+} release is attenuated by oxidising reagents

Having determined the concentrations at which various oxidising and reducing agents affect membrane integrity, the regulation of ligand-gated Ca^{2+} release by doses of redox agents not inducing integrity loss was examined. At concentrations up to 1 mM the reducing agents DTT and GSH were found to have no significant effect on cADPR-, $InsP_3$-and NAADP-induced Ca^{2+} release (Table 4.3). All of the oxidising reagents tested inhibited Ca^{2+} release induced with a maximal dose of ligand. The most potent inhibitor of Ca^{2+} release was H_2O_2. As shown in Figure 4.8 H_2O_2 concentrations of 50 μM inhibited the release of Ca^{2+} induced by a saturating dose of all three release agents by approximately 50%. Treatment with 100 μM H_2O_2 induced up to 97% inhibition.

4.3.4.3. H_2O_2 effects Ca^{2+} -mobilisation in cauliflower vesicles

As H_2O_2 has previously been shown to activate both ligand-gated calcium channels in animals (Anzai *et al.*, 1998; Oba *et al.*, 2000) and voltage-gated plasma membrane channels in plants (Pei *et al.*, 2000), the inhibitory effect of H_2O_2 on cauliflower vesicle Ca^{2+} release was unexpected and was examined in more detail. As Figure 4.9 depicts, H_2O_2 inhibits, in a dose-dependent manner, the Ca^{2+} release induced by concentrations of cADPR, NAADP and $InsP_3$ sufficient to effect maximal release (R_{max}). In each case, inhibition by H_2O_2 was half maximal at concentrations < 10 mM, although maximal inhibition of ligand-gated Ca^{2+} release did not exceed 85%. Hyperbolic curves were fitted to the data using the equation:

$$\mathbf{Y = V_{max}/(1+X/IC_{50})}$$

where **Y** is the Ca^{2+} released (%), $\mathbf{V_{max}}$ is the Ca^{2+} released (%) in absence of H_2O_2, **X** is the concentration of H_2O_2 (μM) and $\mathbf{IC_{50}}$ is the concentration of H_2O_2 at which Ca^{2+} released is 50% of V_{max} (μM). Examination of the IC_{50} values derived from the curves indicates that inhibition of Ca^{2+} release is greater at lower concentrations of H_2O_2 for release induced by NAADP (IC_{50} = 1.2 μM) and $InsP_3$ (IC_{50} = 1.3 μM) compared to cADPR (IC_{50} = 6.4 μM).

Table 4.3. Effect of redox agents on Ca^{2+} release induced by cADPR, $InsP_3$ and NAADP

Cauliflower microsomes were loaded with $^{45}Ca^{2+}$, and as described in Section 4.2.4, various redox agents were added to the reaction mix at different concentrations 2 min prior to induction of Ca^{2+} release with saturating doses of cADPR, $InsP_3$ and NAADP. The background release (leak of 4.5%) was subtracted from mean release values obtained with cADPR, $InsP_3$ and NAADP. Data are the means of three experiments ± SEM.

Treatment	cADPR (1 μM)		$InsP_3$ (10 μM)		NAADP (1 μM)	
	Mean Ca^{2+} release – background leak (%)	Inhibition (%)	Mean Ca^{2+} release – background leak (%)	Inhibition (%)	Mean Ca^{2+} release – background leak (%)	Inhibition (%)
Negative control						
Water	11.0 ± 2.2	0.0	9.8 ± 2.0	0.0	12.1 ± 2.5	0.0
Reducing agents						
DTT (1mM)	9.8 ± 2.6	10.9	11.6 ± 2.6	-18.4	8.7 ± 2.1	28.1
GSH (500 μM)	10.0 ± 1.1	9.1	9.6 ± 2.2	2.0	11.1 ± 2.0	8.3
Oxidising agents						
GSSG (200 μM)	2.2 ± 2.5	80.0	1.5 ± 0.6	84.7	2.0 ± 1.0	83.5
thimerosal (25μM)	6.3 ± 1.8	42.7	4.3 ± 1.2	56.1	9.3 ± 2.2	23.1
thimerosal (50 μM)	6.5 ± 2.4	40.9	3.1 ± 1.6	68.4	8.0 ± 2.2	33.9
chloramine T (25 μM)	6.9 ± 2.0	37.3	1.4 ± 3.1	85.7	10.8 ± 1.5	10.7
chloramine T (50 μM)	7.9 ± 2.3	28.2	1.8 ± 2.5	81.6	9.7 ± 2.7	80.2
menadione (50 μM)	6.0 ± 1.9	45.5	6.1 ± 1.6	37.8	4.8 ± 1.7	60.3
menadione (100 μM)	5.9 ± 1.5	46.4	7.3 ± 1.8	25.5	3.0 ± 1.9	75.2
H_2O_2 (50 μM)	3.5 ± 1.4	68.2	4.3 ± 1.5	56.1	2.9 ± 1.2	76.0
H_2O_2 (100 μM)	0.3 ± 1.0	97.3	3.2 ± 2.6	67.3	2.1 ± 1.7	82.6

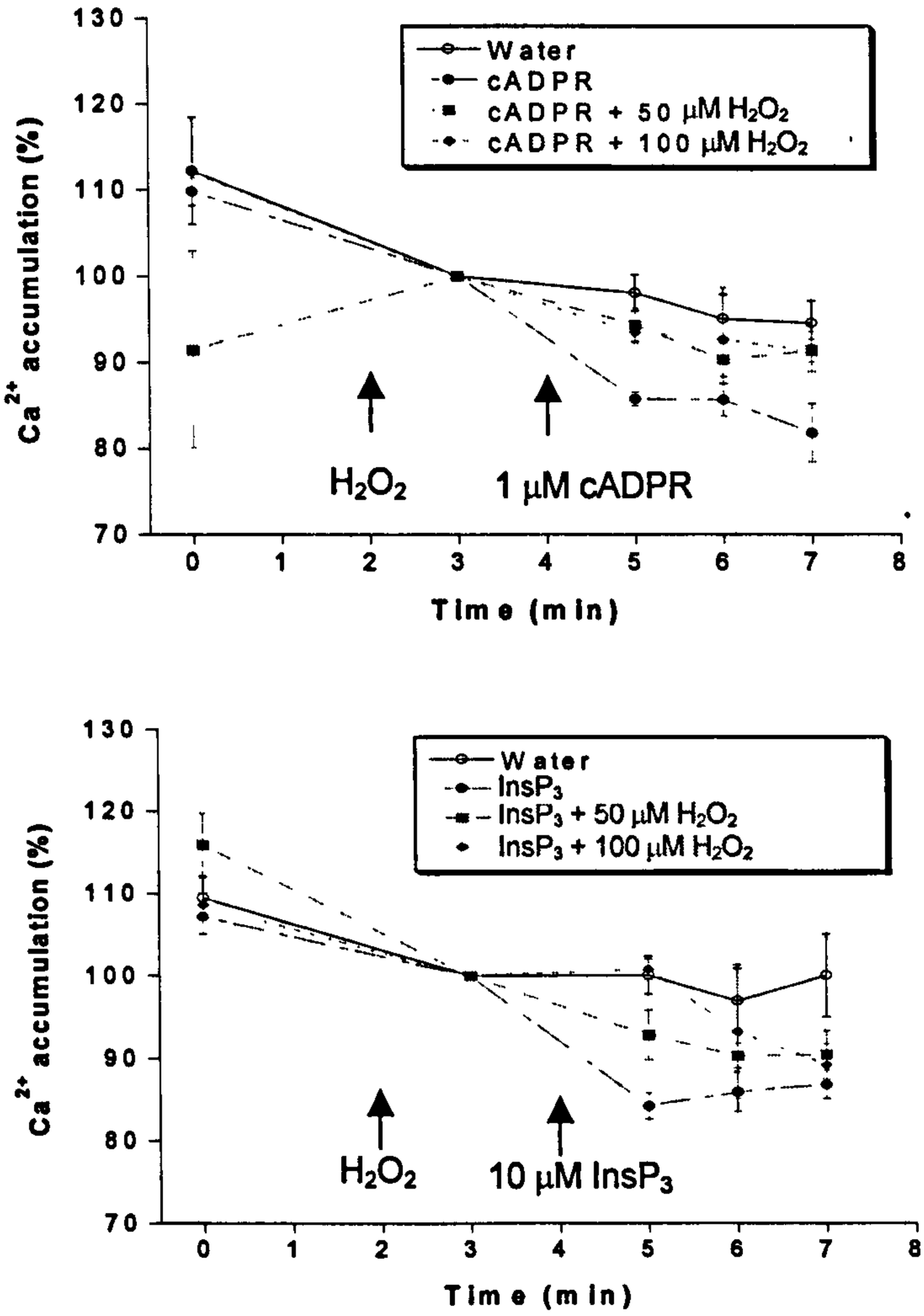

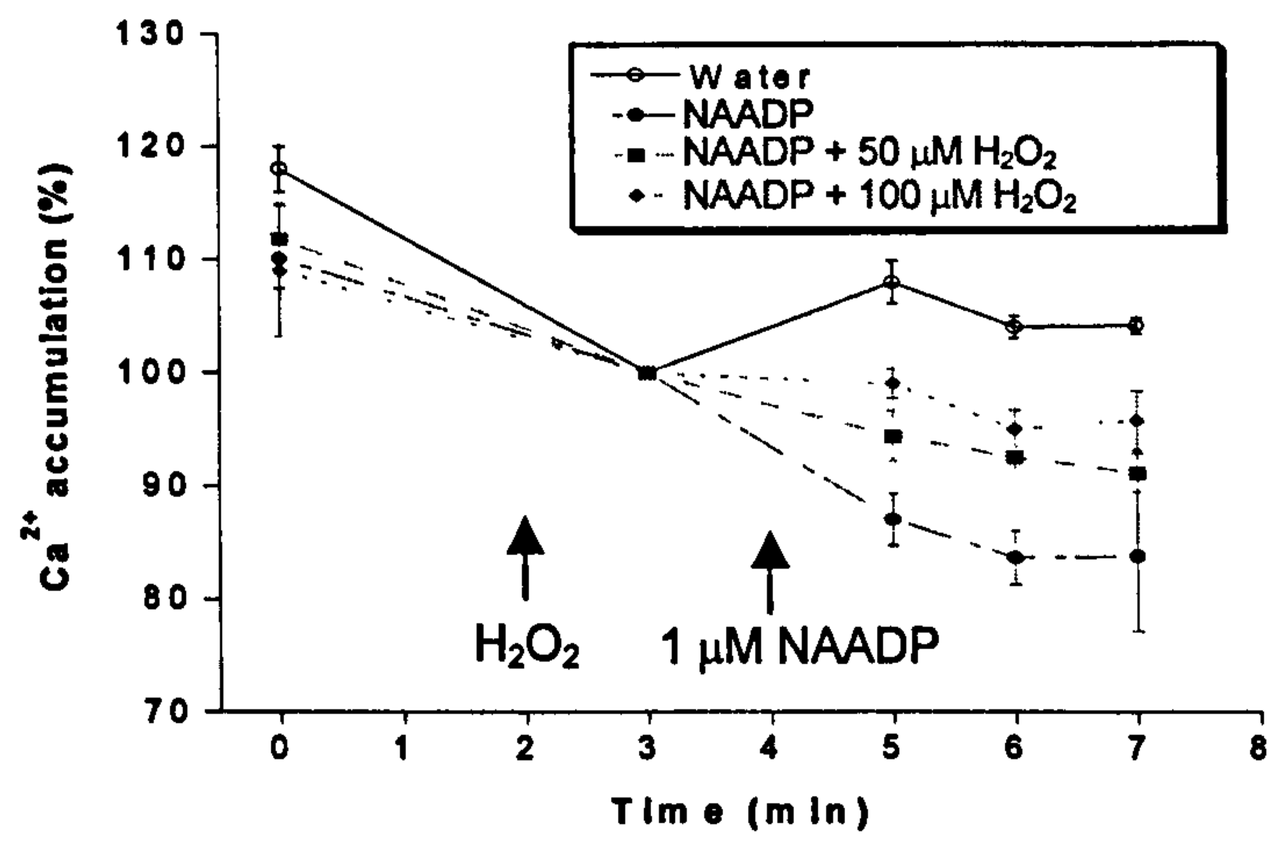

Figure 4.8. H_2O_2 inhibits Ca^{2+} release in cauliflower microsomes

Cauliflower microsomes were pre-loaded with $^{45}Ca^{2+}$ and further uptake was inhibited (at 0 min on the figures), as described in Section 4.2.4. H_2O_2 was then added to the reaction mix at 50 or 100 μM concentrations and release was induced with saturating doses of **A.** cADPR (1μM), **B.** $InsP_3$ (10 μM) or **C.** NAADP (1μM). Data are the means of three experiments ± SEM.

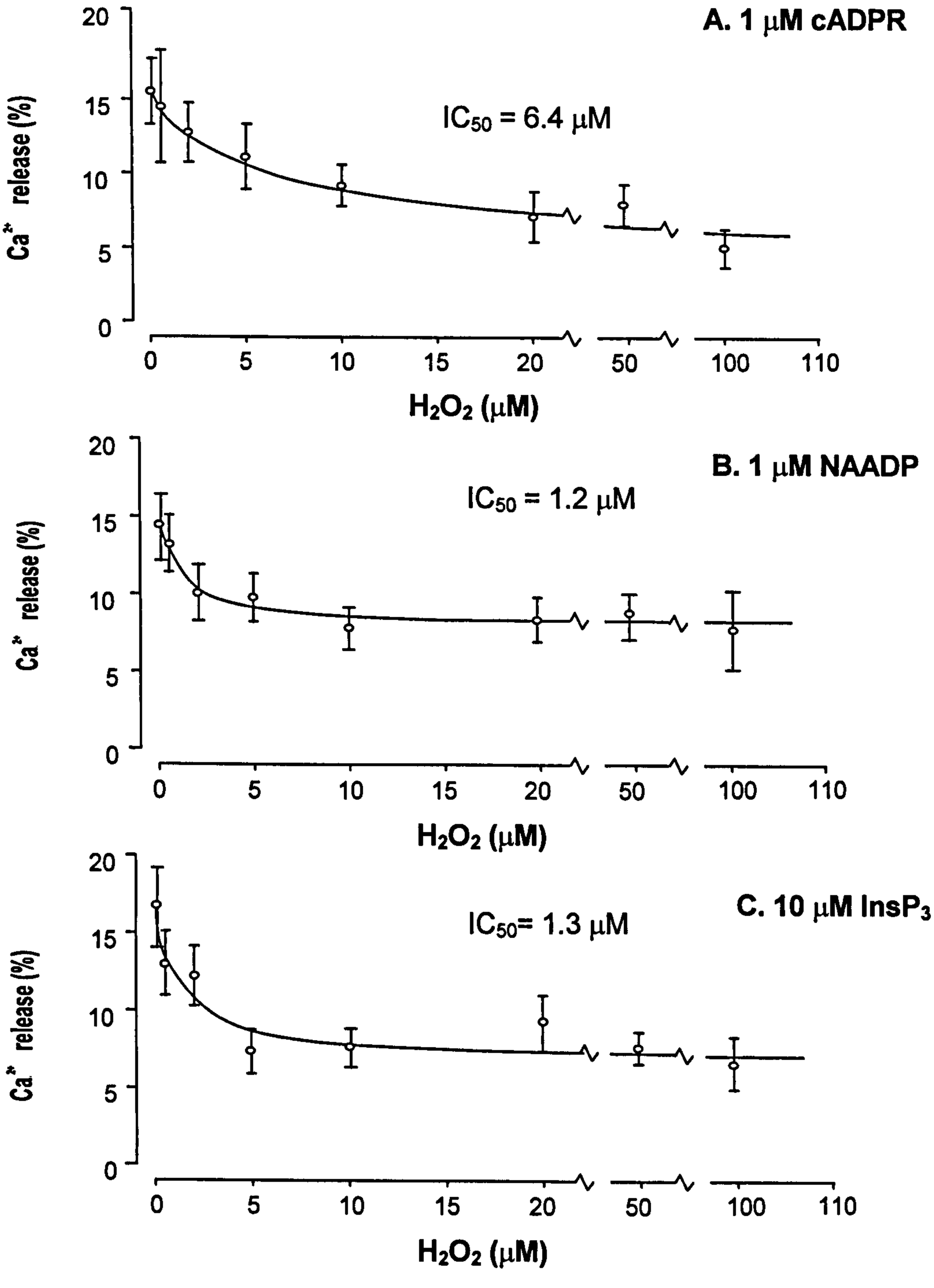

Figure 4.9. H_2O_2 mediates Ca^{2+}-release induced by $InsP_3$, cADPR and NAADP

Cauliflower microsomes were loaded with $^{45}Ca^{2+}$, as described in Section 4.2.4, H_2O_2 was added to the reaction mix at various concentrations and release was induced with saturating doses of **A.** cADPR (1μM), **B.** NAADP (1 μM) or **C.** $InsP_3$.(10 μM). Data are the means of three experiments ± SEM.

When the effect of H_2O_2 on Ca^{2+}-release was tested with a concentration of release agent sufficient to give approximately half-maximal activation of Ca^{2+} release ($K_{0.5}$), it was observed that relatively low concentrations of H_2O_2 potentiated ligand-gated release (Figure 4.10). At higher concentrations (greater than 5 μM), H_2O_2 inhibited the Ca^{2+} release in a similar manner to that seen in the presence of saturating doses of the release agent. Figure 4.11 indicates that pre-treatment of the microsomes with 1mM DTT protected them from the inhibitory effects of high concentrations of H_2O_2, suggesting that the inhibition arose from the oxidisation of sulphydryl groups present in cysteine residues.

Lipid peroxidation by H_2O_2 has previously been shown to inhibit Ca^{2+}-ATPases present in the ER (Racay *et al.*, 1997). In order to determine whether the inhibitory effects of H_2O_2 on ligand-induced Ca^{2+} release were related to effects on uptake, microsomal Ca^{2+} uptake was monitored as a function of time in the absence or presence of various concentrations of H_2O_2. Figure 4.12 indicates that 1 mM H_2O_2 significantly inhibits ATP driven uptake of Ca^{2+} into cauliflower microsomes. However, concentrations of H_2O_2 below 1 mM, in the range tested for the release experiments above, did not cause a significant change in Ca^{2+}-uptake. Figure 4.13 shows that uptake of Ca^{2+} into cauliflower vesicles was also inhibited by the reducing agent DTT but again, only at a very high concentration (40 mM).

4.3.5. Effect of phosphorylation agents on Ca^{2+} release

Figure 4.14 shows that treatment of cauliflower microsomes with the catalytic subunit of the serine/threonine kinase PKA or AP had no significant effect on release induced by cADPR-, $InsP_3$- and NAADP-induced release, compared to the water control. Figure 4.15 indicates that the loading of Ca^{2+} into the vesicles was unaffected by PKA.

4.3.6. Other calcium release agents

The cauliflower Ca^{2+}-release assay was used to investigate the Ca^{2+}-mobilisation potential of cyclic nucleotides, analogues of NAADP and: $InsP_6$. While these compounds have been identified as possible signalling elements their role (if any) in Ca^{2+} signalling in plants is poorly understood. The cauliflower microsomal Ca^{2+}-release assay provides a convenient means of assessing the ability of these compounds to induce Ca^{2+}-release from Ca^{2+} stores.

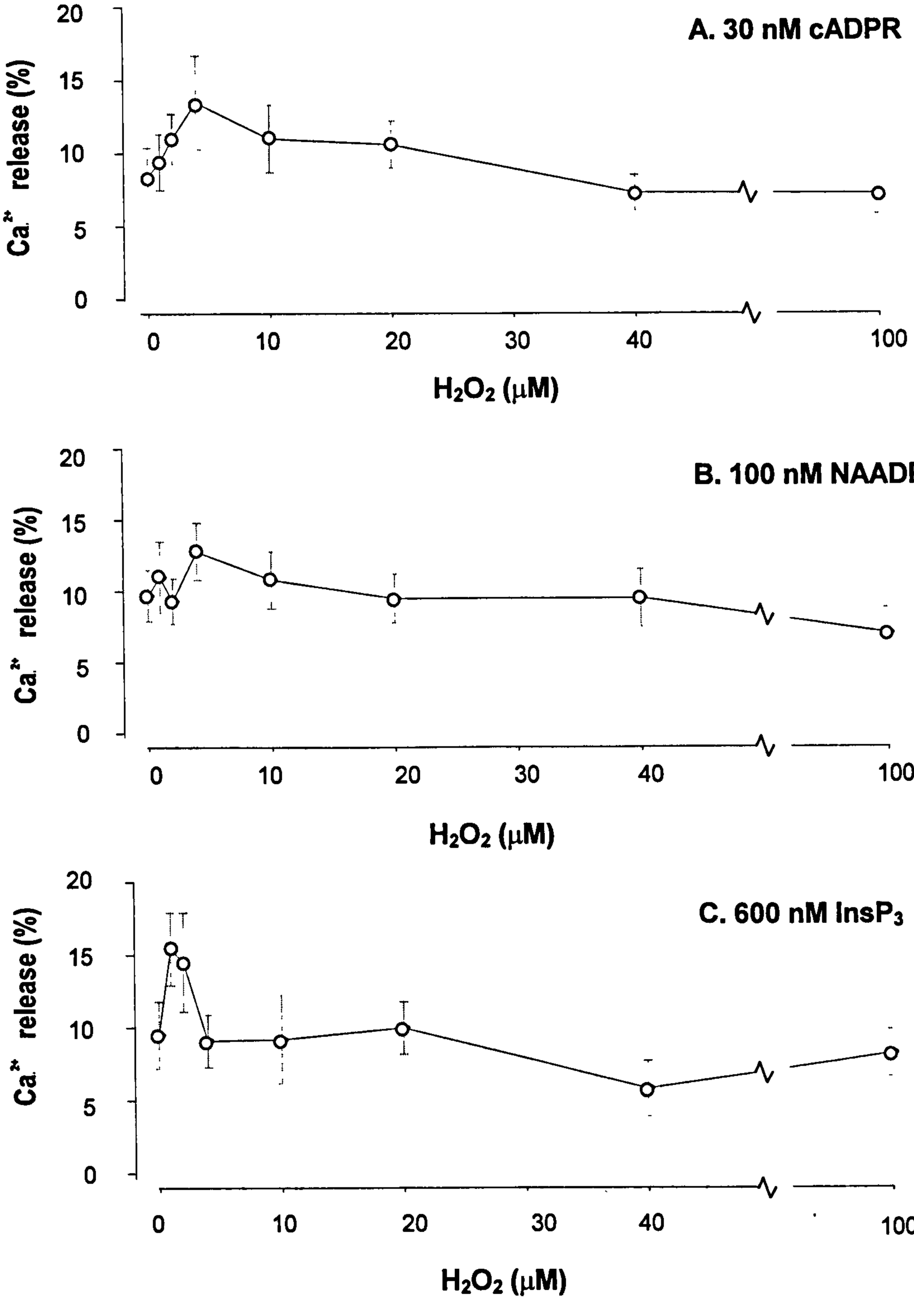

Figure 4.10. H_2O_2 mediates Ca^{2+}-release induced by $InsP_3$, cADPR and NAADP

Cauliflower microsomes were loaded with $^{45}Ca^{2+}$, as described in Section 4.2.4, H_2O_2 was added to the reaction mix at various concentrations and release was induced with non-saturating doses of **A.** cADPR (30 nM), **B.** NAADP (100 nM), or **C.** $InsP_3$ (600 nM). Data are the means of three experiments ± SEM.

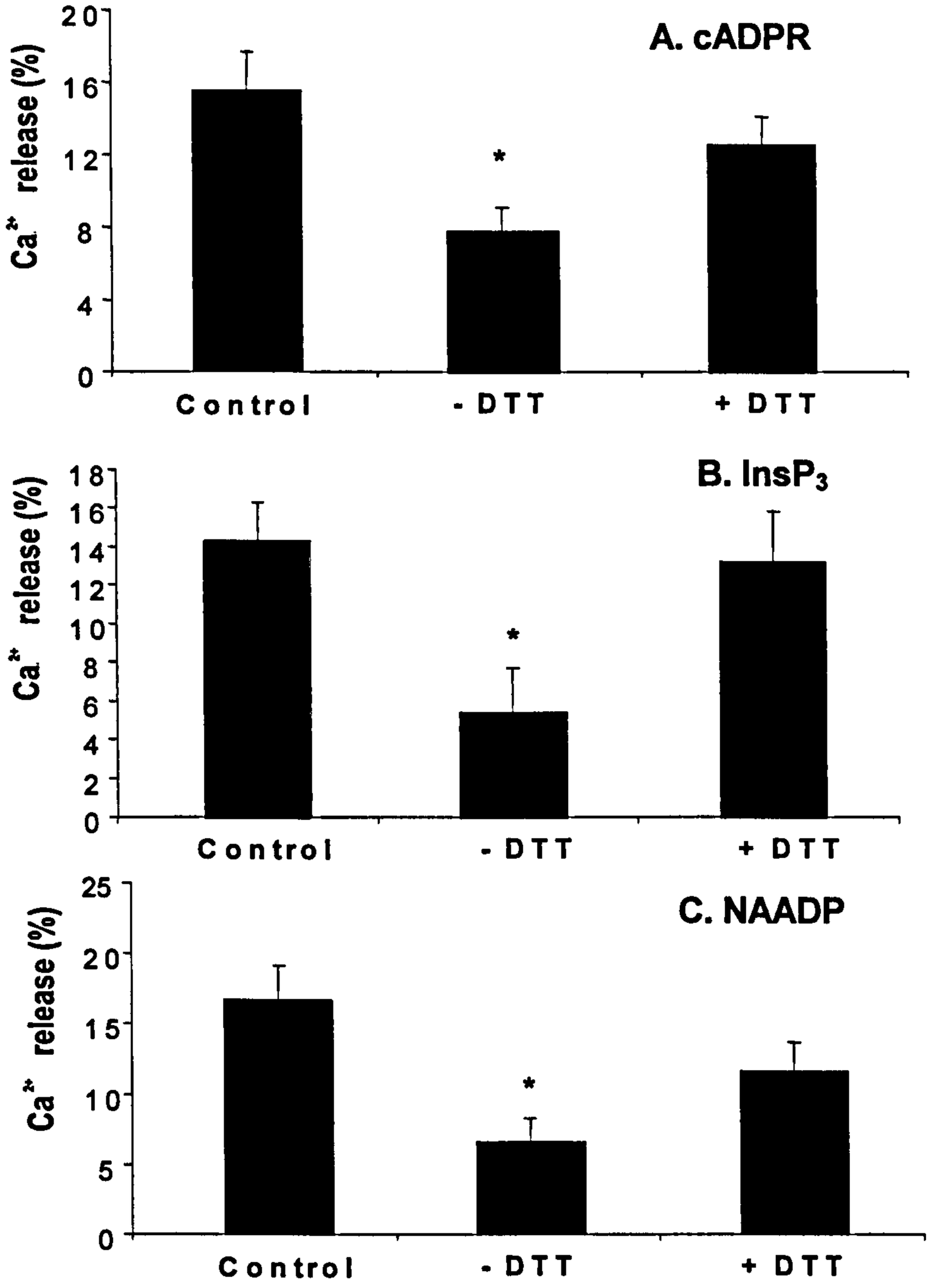

Figure 4.11. DTT prevents inhibition of Ca^{2+} release by H_2O_2

Cauliflower microsomes were pre-loaded with $^{45}Ca^{2+}$ for 60 min, as described in Section 4.2.4 and release induced in the presence of 100 μM H_2O_2 (- DTT), or 1 mM DTT and 100 μM H_2O_2 (+DTT) or water (control). Termination of loading was taken as time point 0. DTT or an equivalent volume of water was added at 1 min. H_2O_2 or an equivalent volume of water was added at 2 min. Release was induced with saturating doses of **A.** cADPR (1μM), **B.** $InsP_3$ (10 μM) or **C.** NAADP (1μM) at 4 min. Release Data are the means of three experiments ± SEM. Asterisks (*) indicate statistical significance between the control and the treatment ($P < 0.05$).

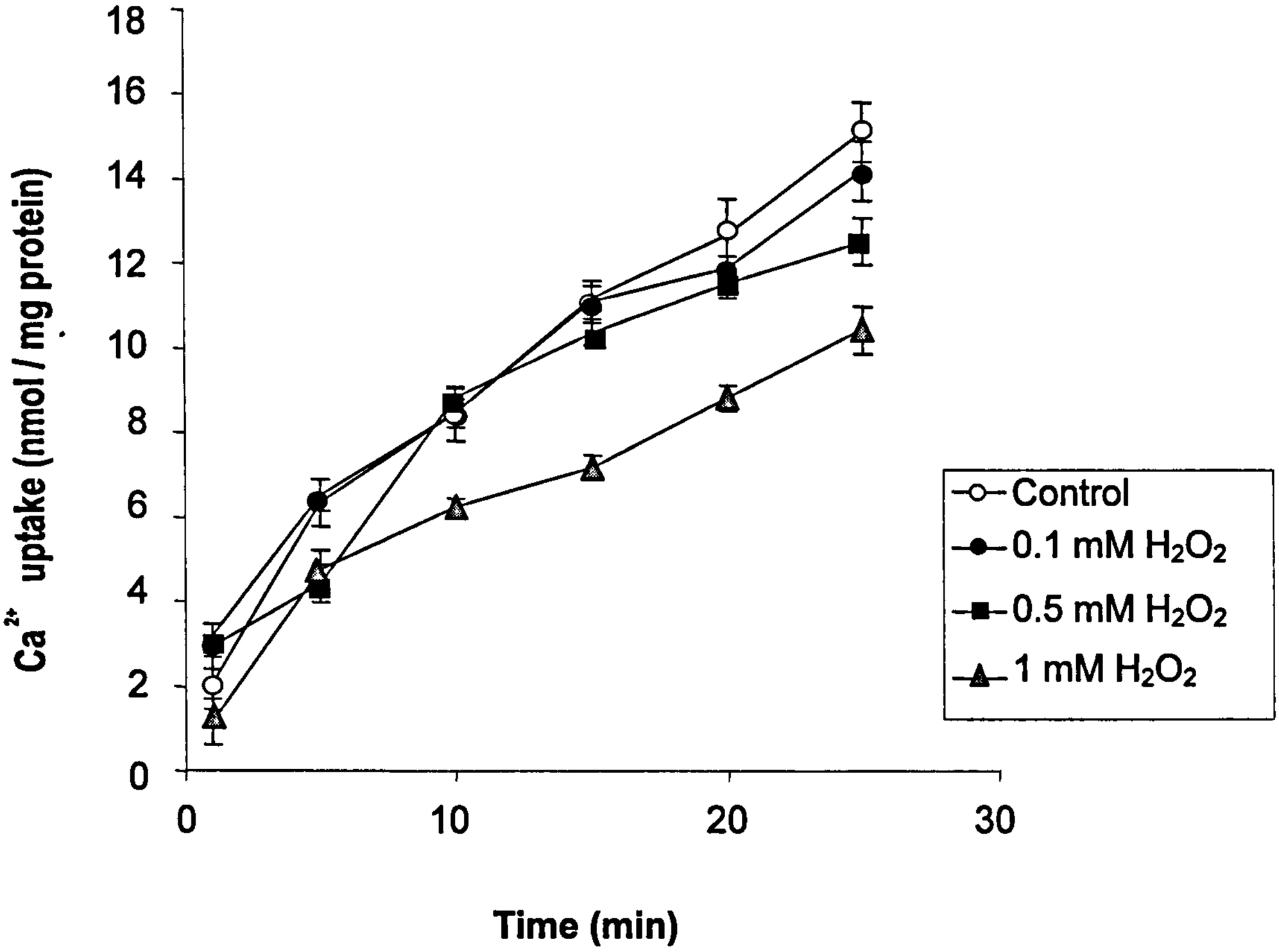

Figure 4.12. H_2O_2 inhibits Ca^{2+} uptake into cauliflower microsomes

Cauliflower microsomes were loaded with $^{45}Ca^{2+}$ for 60 min in calcium transport medium, in the presence of water (○), 0.1 (●), 0.5 (■) or 1 (▲) mM H_2O_2. An aliquot was removed and filtered and the radioactivity counted by liquid scintillation to estimate the Ca^{2+} accumulated within the vesicles. Non-specific association of Ca^{2+} with vesicles was determined by addition of A23187 and subtracted from data. Data are the means of three experiments ± SEM.

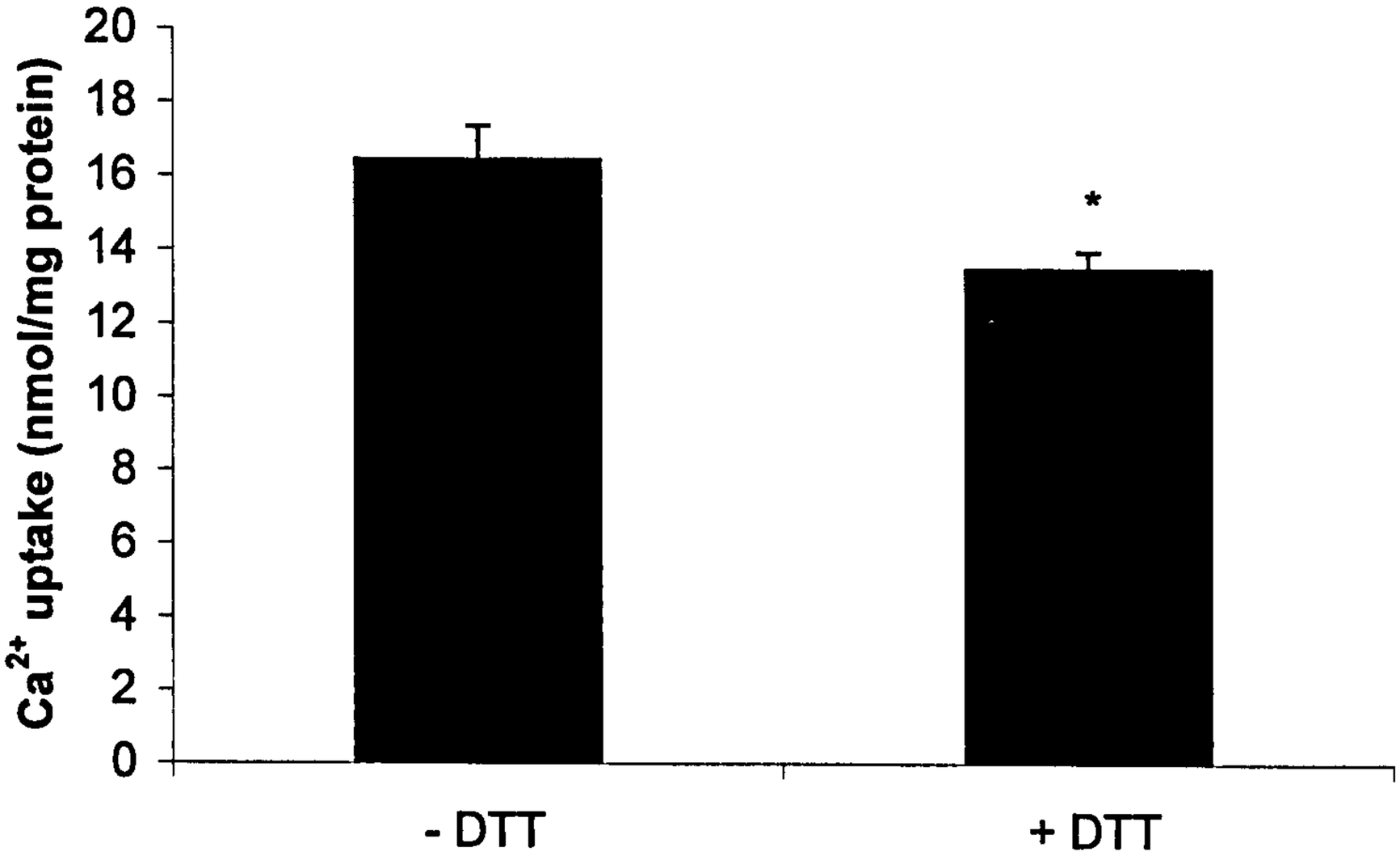

Figure 4.13. Ca^{2+} uptake into microsomes is inhibited by 40 mM DTT

Cauliflower microsomes were loaded with $^{45}Ca^{2+}$ for 60 min in calcium transport medium in the presence or absence of 40 mM DTT. An aliquot was removed and filtered and the radioactivity counted by liquid scintillation to estimate the Ca^{2+} accumulated within the vesicles. Non-specific association of Ca^{2+} with vesicles was determined by addition of A23187 and was subtracted from data. Data are the means of three experiments ± SEM. An asterisks (*) indicates statistical significance between the control and the treatment ($P < 0.05$).

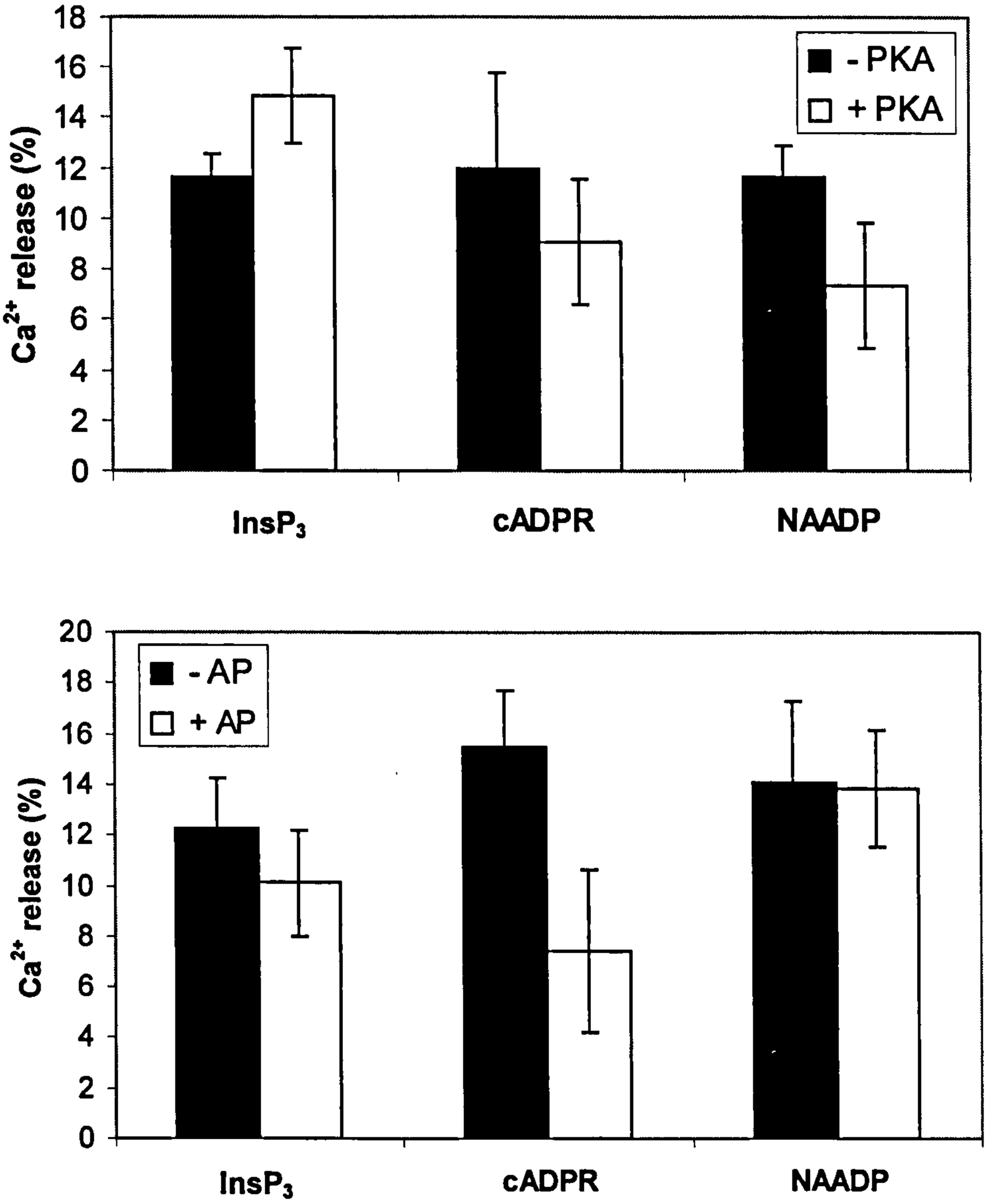

Figure 4.14. Effect of phosphorylation agents on Ca^{2+} release

Cauliflower microsomes were loaded with $^{45}Ca^{2+}$ for 60 min, as described in Section 4.2.4. Termination of loading was taken as time point 0. **A.** PKA (5 U/ml) or **B.** AP (100 U/ml) (filled bars) or an equivalent volume of water (control - open bars) was added at 1 min. Release was induced at 3 min with saturating doses of cADPR (1μM), NAADP (1μM) or $InsP_3$ (10 μM). Data are the mean of three experiments ± SEM. T-test results indicate no significant difference between the control and the treatments ($P > 0.05$).

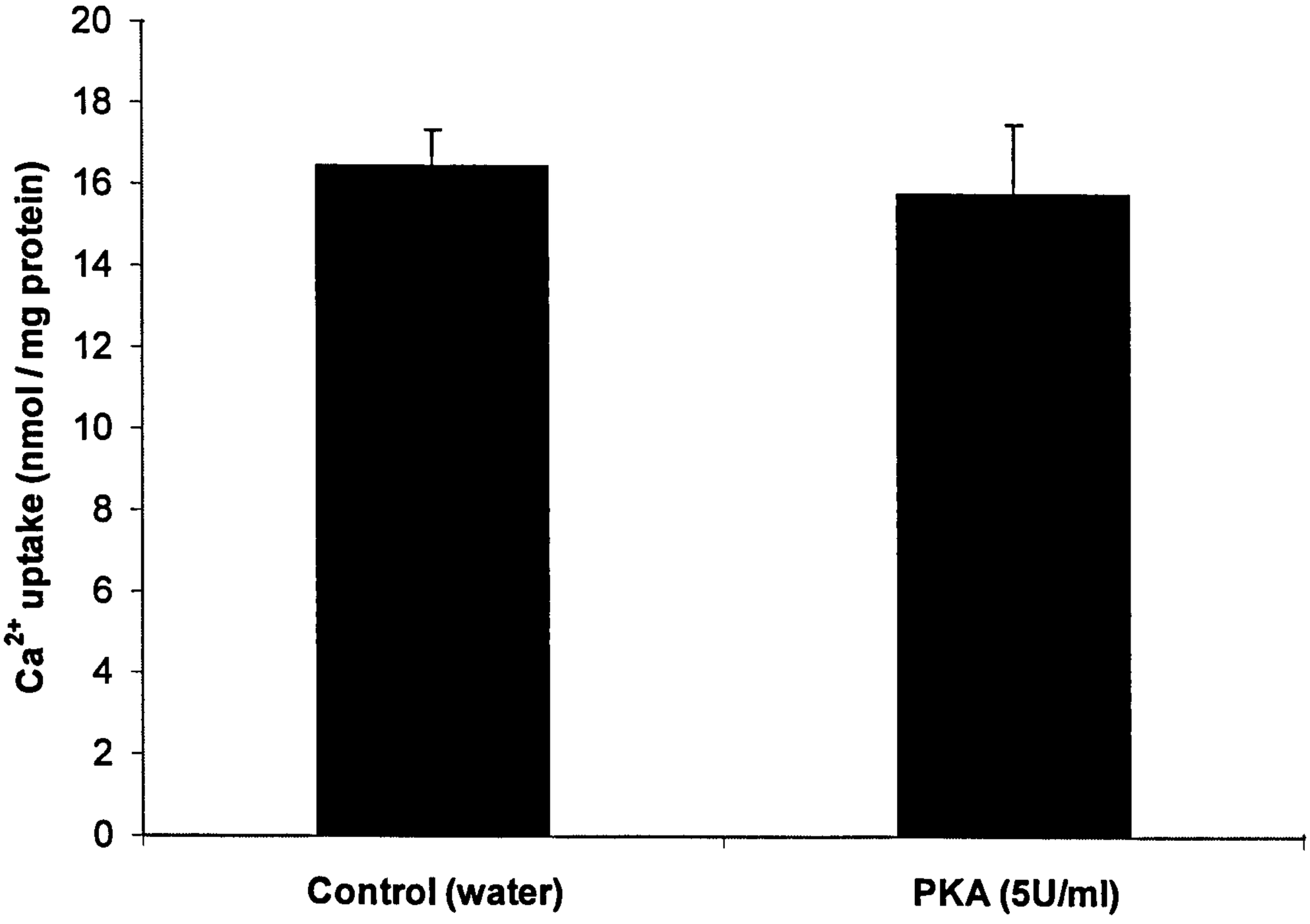

Figure 4.15. Effect of phosphorylation agents on Ca^{2+} uptake

Cauliflower microsomes were loaded with $^{45}Ca^{2+}$ for 60 min in calcium transport medium in the presence of PKA (5 U/ml), AP (100 U/ml) or water (control). An aliquot was removed and filtered and the radioactivity counted by liquid scintillation to estimate the Ca^{2+} accumulated within the vesicles. Non-specific association of Ca^{2+} with vesicles was determined by addition of A23187. Data are the means of three experiments ± SEM.

Figure 4.16 indicates that the cyclic nucleotides cAMP and cGMP and their membrane permeable analogues 8-Br-cAMP, 8-Br-cGMP and DT-cGMP were unable to induce Ca^{2+}-release from cauliflower when added to a final concentration of 100 μM. Based on animal studies, the analogues of NAADP were predicted not to induce Ca^{2+}-release from plant vesicles. In the case of NAAD Figure 4.17 shows that this was supported by the experimental evidence. NADP, however, induced almost as much Ca^{2+}-release as NAADP, albeit at a 10-fold higher concentration. A T-test indicated that this release was not quite significant compared to the water control. As shown in Figure 4.18, $InsP_6$ also induced Ca^{2+}-release similar to that of $InsP_3$, when applied at a 10-fold higher concentration. Once again, however, a T-test revealed that this release was not quite significant.

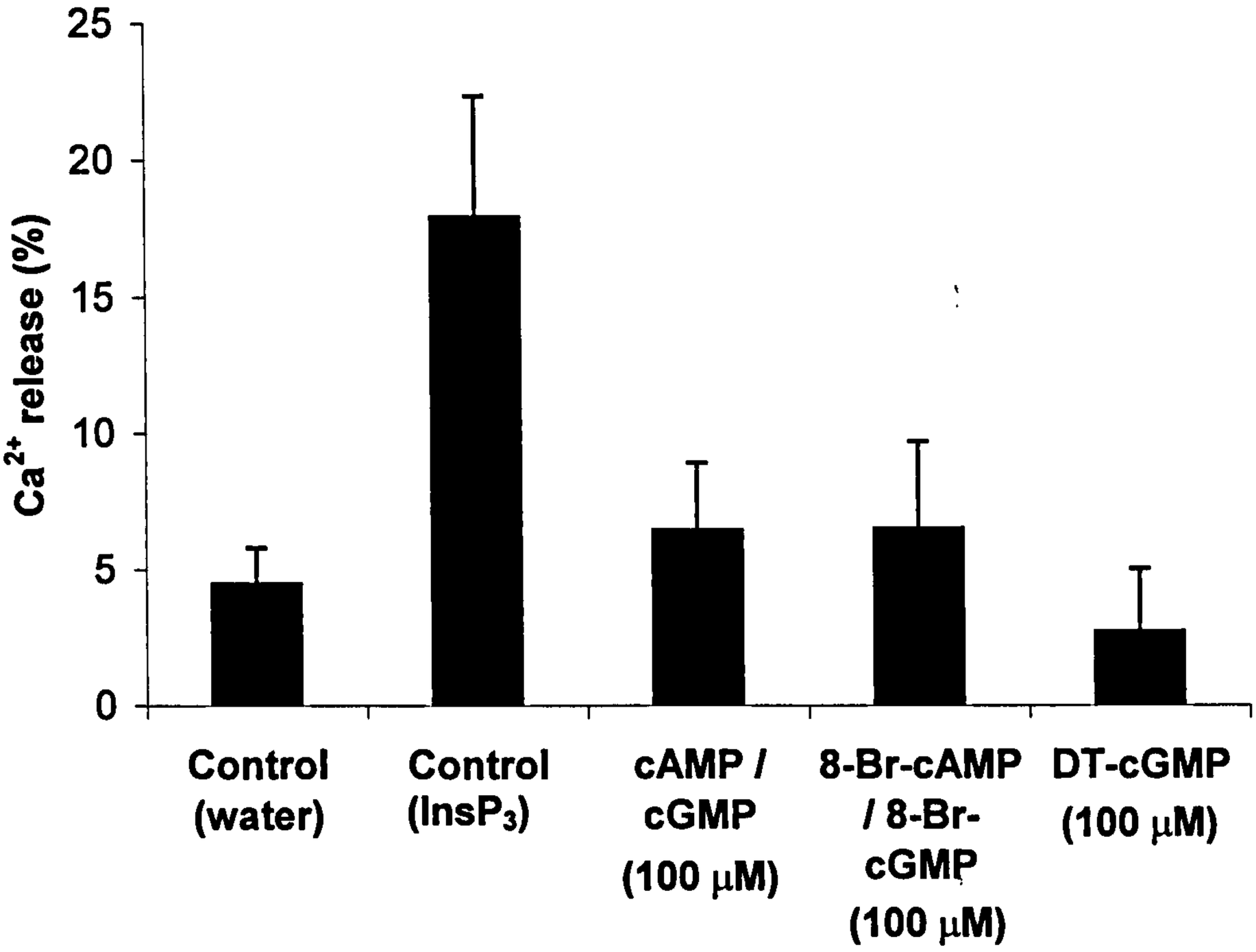

Figure 4.16. Cyclic nucleotides do not elicit Ca^{2+}-release from cauliflower microsomes

Cauliflower microsomes were loaded with $^{45}Ca^{2+}$ as previously described. Mixes of the cyclic nucleotides cAMP and cGMP, and of the membrane permeable analogues 8-Br-cAMP, 8-Br-cGMP as well as DT-cGMP were added to a final concentration of 100 μM for each compound. The change in accumulated Ca^{2+} is shown. Data are the means of three experiments ± SEM. T-test results indicate no significant difference between the negative control (water) and treatment with cyclic nucleotides ($P > 0.05$).

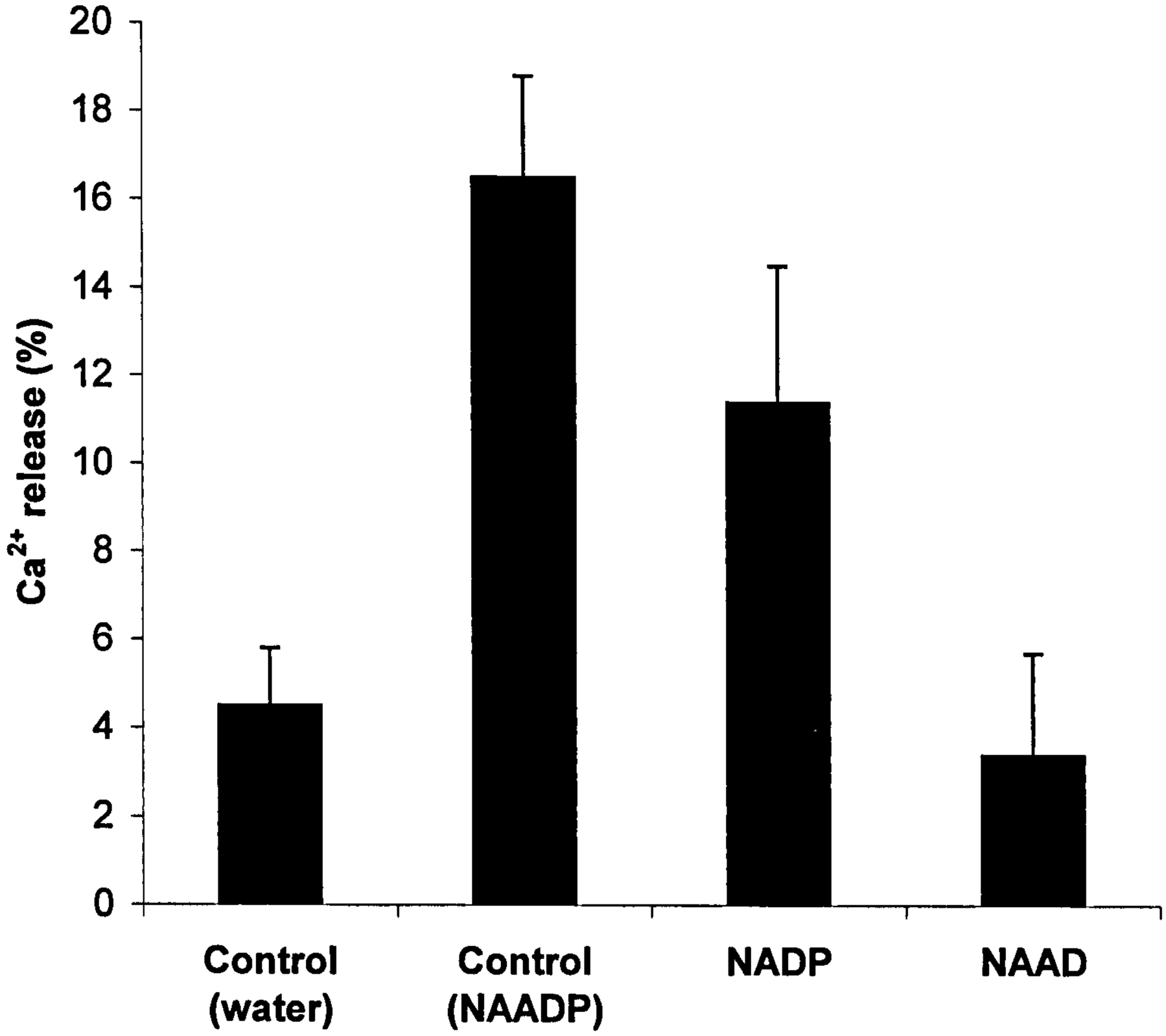

Figure 4.17. Ca^{2+} release with analogues of NAADP

Cauliflower microsomes were loaded with $^{45}Ca^{2+}$ as previously described. NAADP (1μM), NADP (10 μM) or NAAD (10 μM) or water (control) were added and the change in accumulated Ca^{2+} monitored and release induced assessed. Data are the means of three experiments ± SEM. T-test results indicate no significant difference between the negative control (water) and treatment with NADP or NAAD ($P > 0.05$).

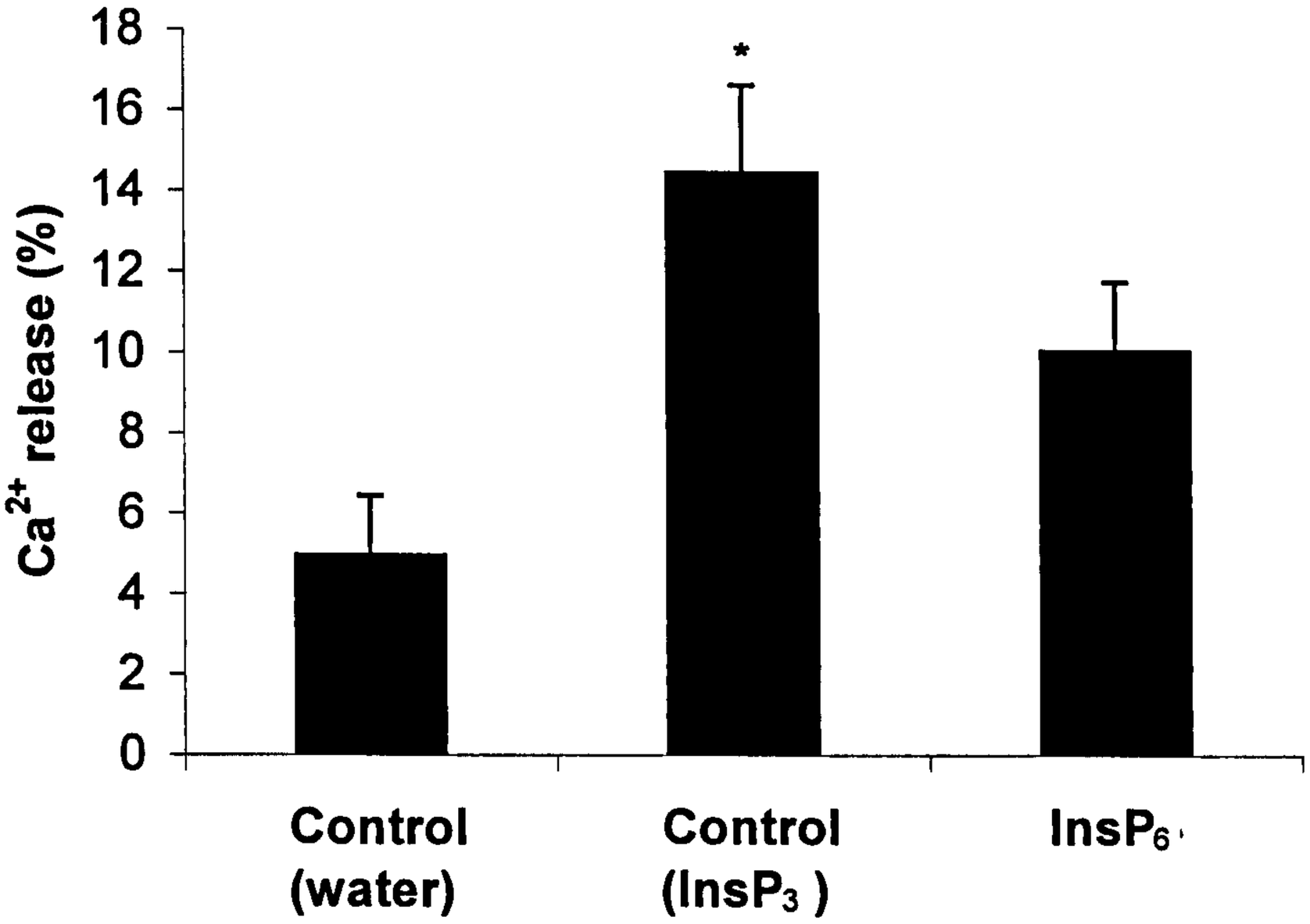

Figure 4.18. $InsP_6$ induces Ca^{2+} release in cauliflower microsomes

Cauliflower microsome vesicles were loaded with $^{45}Ca^{2+}$ as previously described. $InsP_3$ and $InsP_6$ were added to a final concentration of 10 and 100 μM respectively. The change in accumulated Ca^{2+} was monitored and total release assessed. Data are the mean of four experiments ± SEM. T-test results indicate that there is no significant difference between the negative control (water) and treatment with $InsP_6$ ($P > 0.05$).

4.4. Discussion

Membrane vesicles have been extensively used in the past to study transport phenomena as they allow transport processes to be separated from metabolic interference (Heinz & Weinstein, 1984). Cauliflower microsomes prepared from the ER-rich meristematic outer layer of the inflorescence were used here to assess the effects of pH, Ca^{2+}/calmodulin, redox agents and phosphorylation state on the activity of ligand-gated Ca^{2+} release and to determine whether potential Ca^{2+} release agents, such as cyclic nucleotides and $InsP_6$, act on cauliflower membranes independently of other ligands. Initial experiments indicated that the vesicle preparations were suitable for the study, demonstrating active Ca^{2+} loading in the presence of ATP, and release when treated with cADPR, $InsP_3$ and NAADP (Figure 4.1). Furthermore, release induced by cADPR and $InsP_3$ could be inhibited by the specific inhibitors heparin and procaine, respectively (Table 4.1) as previously reported in plants (Muir *et al.*, 1997; Muir & Sanders 1996).

4.4.1. pH modulation

Studies on animal systems have demonstrated that ligand-binding to $InsP_3R$ and RyR is modulated by pH resulting in changes to receptor activity. It has also been reported that $InsP_3$-binding to red beet microsomes is influenced by pH (Brosnan & Sanders, 1993). It was therefore been hypothesised that Ca^{2+} mobilisation via ligand-gated channels of plants is sensitive to changes in cytosolic pH. The experiments described in this chapter support this. Although T-tests did not indicate any significant difference between release at pH 7.4 and any other treatment, alkalinisation of the assay media demonstrated a trend of inhibition of cADPR-induced release above pH 7.4 (Figure 4.3). Release induced by cADPR at pH 8.0 was significantly different from the release measured at pH 7.0 (P = 0.0458). Conversely alkalisation of the assay media appeared to activate $InsP_3$-induced release at pH 7.6 and above. NAADP-induced release was independent of pH. These findings are remarkably similar to those described for the effect of pH on ligand-gated release in sea urchin egg homogenates (Chini *et al.*, 1989). The results also correspond to the binding studies on $InsP_3$ of Brosnan & Sanders (1993) that demonstrate optimum binding at pH 8.0, with a pronounced increase in binding above pH 7.0. Over the range of pH tested Ca^{2+} uptake was unaffected (Figure 4.2).

These results suggest that pH may act as an endogenous modulator of Ca^{2+} release and therefore provide a potential means for the generation of increased

signal specificity. An increase in pH from 7.0 to 7.8, for example, will inhibit cADPR induced Ca^{2+} release while activating $InsP_3$-induced Ca^{2+} release in accordance with changes in binding of the ligand to its receptor. Interestingly, the range over which the greatest change in cADPR induced release is observed is the same range of pH over which ABA induced alkalinisation of guard cell cytoplasm activates K^+_{out} channels (Roberts & Snowman, 2000). As cADPR and pH are both thought to act as second messengers in ABA promoted stomatal closure, this provides a means for cross talk between the Ca^{2+}- and pH-based transduction pathways and possibly the generation of increased signal specificity.

4.4.2. Ca^{2+}/calmodulin modulation

One of the distinguishing characteristics of both $InsP_3$Rs and RyRs in animals is their ability to be activated by increases in $[Ca^{2+}]_c$ – a property that is understood to form the basis of CICR (see section 1.2). Investigations into the effect of $[Ca^{2+}]$ on ligand-gated Ca^{2+} currents across the tonoplast of plants have indicated that their activities are independent of $[Ca^{2+}]_c$ (Allen & Sanders, 1994) even though $[Ca^{2+}]_c$ oscillations have been detected that are indicative of CICR. The addition of the calcium chelator EGTA (250 μM) to microsomes loaded with Ca^{2+} prior to treatment with a ligand did not have any significant effect on Ca^{2+} release, suggesting that the ligand-gated release was independent of changes in $[Ca^{2+}]$ over a normal physiological range (the assay media contained approximately 10 μM Ca^{2+}, and in the presence of 250 mM EGTA the free Ca^{2+} was calculated as 0.3 pM using the program WinMAXC (Bers *et al.*, 1994) and is consistent with the responses witnessed with cADPR- and $InsP_3$- gated currents across vacuolar membranes.

The addition of 1 mM $CaCl_2$ to the assay media had an unexpected result. All three ligands showed a trend towards increased activity, with cADPR-induced release exhibiting a significant increase (Figure 4.4). 1 mM Ca^{2+} is higher than the level $[Ca^{2+}]_c$ is normally thought to reach, at least in a global context. However, transient local increases in $[Ca^{2+}]_c$ occurring in the vicinity of a membrane when Ca^{2+} enters the cytosol from internal or external stores may come close to this, perhaps providing a direct mechanism for CICR that has not yet been considered in detail. Further research is required to examine this possibility, and also to determine whether there is a difference between the sensitivity of receptors of vacuolar and ER membranes. Cauliflower microsomes, being rich in ER, may display a different Ca^{2+} dependence to vacuolar preparations.

A shared property of the $InsP_3R$ and RyRs of animal cells is that they can be modulated by the Ca^{2+}-binding protein CaM (Hirota *et al.*, 1999; Balshaw *et al.*, 2001). Experiments with cauliflower microsomes indicate that with a non-saturating dose of cADPR, the inclusion of CaM in the assay media has a biphasic effect. When added to a final concentration of 0.1 μM, CaM activated cADPR-induced release. At 0.6 μM CaM inhibited cADPR-induced release. With a saturating dose of cADPR no activation was observed, although, 0.6 μM CaM also induced inhibition (Figure 4.5). NAADP-induced release was independent of CaM up to 0.6 μM. The biphasic nature of the effect of CaM on cADPR-induced release is similar to that reported for RyR1 (Hirota *et al.*, 1999; Rodney *et al.* (2000). Examining the effects of CaM on reconstituted $InsP_3R1$ and RyR1, respectively, indicates that CaM may have a biphasic effect on ligand-induced Ca^{2+} release. At nanoMolar concentrations of Ca^{2+}, the channels are minimally active and CaM further activates them. Conversely at micromolar concentrations of Ca^{2+}, where the channels are activated, CaM inhibits ligand-induced Ca^{2+} release. Binding experiments with RyR1 have indicated that Ca^{2+}-free CaM enhances the affinity of RYR1 for Ca^{2+}, thereby activating the receptor when Ca^{2+} binds to it. However, CaM itself converts from an activator to an inhibitor of the receptor when it binds Ca^{2+}. It has been speculated that this latter response forms part of a mechanism for negative feedback regulation of Ca^{2+} release. The data described here raises the possibility that CaM may modulate both the opening and the closing of the ligand-gated channels in a similar manner in plants.

The CaM antagonist W-7 was to be used to further investigate the role of CaM in modulating ligand-gated activity. Initial experiments indicated that W-7 induced release of Ca^{2+} from loaded cauliflower vesicles in a dose dependent manner (Figure 4.6). The reasons for the release are unclear, possibly arising from W-7's interaction with the CaM binding sites of ATPases or from decreased membrane stability. None-the-less W-7 was unsuitable for further investigations on CaM's role in modulating ligand-gated activity with the radiometric flux assay.

4.4.3. Redox modulation

Redox compounds have been found to regulate various ion channel types in animal cells including channel gating of $InsP_3Rs$ (Vanlingen *et al.*, 1999; Sayers *et al.*, 1993; 1999) and RyRs (Eager & Dulhunty, 1999). Recent patch clamp studies by Carpaneto *et al.* (1999) have indicated that voltage-gated ion channels located on

the tonoplast of plants can be regulated by redox agents. Price *et al.* (1994) and McAinsh *et al.* (1996) have previously shown that $[Ca^{2+}]_c$ is regulated by the redox state of the cytoplasm in tobacco seedlings expressing aequorin and guard cells, respectively. When treated with hydrogen peroxide a transient increase in $[Ca^{2+}]_c$ was detected which could be modified by changes in cellular glutathione levels and appeared to mobilise different pools of Ca^{2+} to signals involving cold shock or touch. Thus, the hypothesis that redox agents will modulate ligand-gated Ca^{2+} release in cauliflower microsomes was explored.

Various compounds were used to mimic oxidative stress or sensors of oxidative stress in the cell: GSSG, thimerosal, chloramine T, menadione and H_2O_2, or for reducing conditions, DTT and GSH. Following assessment of the ability of compounds to induce Ca^{2+}-release using the radiometric flux assay or to affect membrane integrity (Table 4.2) the compounds were included in the assay media, in concentrations not inducing Ca^{2+}-release or a loss of membrane integrity, prior to treatment with cADPR, $InsP_3$ or NAADP. Initial experiments with saturating doses of the ligands indicate that the oxidising agents inhibited release induced by all three ligands (Table 4.3). The reducing agents generally exhibited markedly less effect on release even at higher concentrations, although, 1 mM DTT activated $InsP_3$-induced release while inhibiting cADPR- and NAADP-induced release. 100 μM H_2O_2 generated the greatest inhibition of the compounds tested, with release by cADPR inhibited 97.3%, $InsP_3$ by 67.3%, and NAADP by 82.6%.

In contrast to these results exogenous hydrogen peroxide treatment of *Arabidopsis* guard cells has been shown to activate Ca^{2+} channels located in the plasma membrane (Pei *et al.*, 2000). Furthermore, as experiments carried out by Klüsner *et al.* (1997) indicate that hydrogen peroxide can also act as an inhibitor of the ER Ca^{2+} channel BCC1, it has been proposed that the redox state of the cell may influence which Ca^{2+} stores are utilised during signalling by differentially regulating channel activity. The inhibitory effect of H_2O_2 on ligand-gated Ca^{2+}-release demonstrated here (Figure 4.8) is of particular interest as it suggests that calcium channels on the PM may be differentially regulated in comparison with Ca^{2+} channels on internal membranes. Further investigations, using non-saturating doses of the ligands, revealed that H_2O_2 may have a biphasic effect on ligand-gated Ca^{2+}-release. With saturating doses of ligand, H_2O_2 inhibits release in a dose dependent manner with LC_{50} values of 6.4 μM for cADPR-induced release, 1.3 μM for $InsP_3$-induced release and 1.2 μM for NAADP-induced release. With non-saturating doses

of ligand there is an activation of Ca^{2+} release with concentrations of H_2O_2 below 5 μM. At higher concentrations the activity is inhibited (Figure 4.9). This is comparable to the effect of thimerosal on $InsP_3$-induced Ca^{2+} release in cerebellar microsomes (Sayers *et al.*, 1993) and indicates that the opening of the channels responsible for ligand-gated Ca^{2+}-release is a complex process.

The inhibitory effects of H_2O_2 can be protected against by 1 mM DTT (Figure 4.11) suggesting the involvement of cysteine residues that are sensitive to oxidation in the receptors responsible for Ca^{2+}-release. It is possible that cysteine residues with different sensitivities are present allowing H_2O_2 to have a biphasic effect: at low concentrations of H_2O_2 the channel becomes more sensitive to its ligand due to high sensitivity cysteine residues, at higher concentrations low sensitivity cysteine residues become modified and inhibit the channel. An alternative explanation is that the monophasic effect of H_2O_2 at a saturating dose of ligand may indicate protection of the lower affinity H_2O_2-sensitive site. Further investigations into the effects of H_2O_2 on the binding of the ligands to the receptor would be useful in elucidating the mechanism behind the effect.

The effect of H_2O_2 on Ca^{2+} uptake into cauliflower vesicles was also studied. Exposure of cauliflower microsome to 1 mM H_2O_2 for 10 min, or greater, or 0.5 mM H_2O_2 for 25 min produced a significantly inhibition of the uptake of Ca^{2+}. Concentrations of H_2O_2 below this did not display any effect over the time course examined (Figure 4.12). The inhibition of the ATPase activity is similar to the effect of H_2O_2 reported for the PMCA of animal cells (Zaidi & Michaelis, 1999). However, the Ca^{2+} uptake into cauliflower vesicles monitored here demonstrates a higher degree of resistance to the inhibitory effects of H_2O_2. Zaidi & Michaelis reported that treatment of synaptic plasma membranes with 200 μM and 700 μM H_2O_2 for 10 min inhibited PMCA activity by 40% and 90% respectively. At 10 min cauliflower Ca^{2+} uptake was inhibited by 30% by 1 mM H_2O_2 with no inhibition seen with lower concentrations of H_2O_2. At 25 min 500 μM H_2O_2 also inhibited cauliflower Ca^{2+} uptake, however only by 15%. High concentrations of DTT (40 mM) were also found to inhibit Ca^{2+} uptake, implicating cysteine residues as also being involved in regulation of the pump.

4.4.4. Modulation by phosphorylation

$InsP_3$Rs and RyRs of animals have been reported to be regulated by the action of the protein kinases A, G, C and by Ca^{2+}-CaM-dependent protein kinase (Takasago

et al., 1991; Yoshida *et al.*, 1992; Strand *et al.*, 1993; Ferris, *et al.*, 1991; Zhang *et al.*, 1993). However, cauliflower microsome vesicles did not display any significant change in ligand-gated Ca^{2+} release following treatment with 5 U / ml PKA (Figure 4.14). Although a trend for activation with $InsP_3$ and inactivation with cADPR and NAADP can be observed. This may indicate a lack of PKA phosphorylation sites in the receptors responsible for the release, or that the treatment incubation time (2.5 min) was not sufficient to fully stimulate / inactivate the receptors responsible. Although there is no direct evidence for the existence of PKA in plants recently the *in vivo* existence of cAMP has been reported (Bolwell, 1995), various genes with sequence homology to mammalian PKA have been identified (Biermann *et al.*, 1990; Lawton *et al.*, 1989) and cAMP stimulated phosphorylation events have been monitored (Janystin, 1989; Komatsu & Hirano, 1993) suggesting the existence of cAMP-dependent signalling pathways in plants. However, in experiments with plants where animal PKA has been used to activate downstream responses it has not yet been determined whether animal PKA mimics the action of a true plant PKA or is phosphorylating a substrate actually phosphorylated by a different plant serine/threonine kinase. If the receptor(s) responsible for the release monitored here do not possess a PKA phosphorylation site this doesn't preclude their modulation by other plant kinases. Treatment of cauliflower microsomes with 100 U / ml AP (Figure 4.14) did not demonstrate a significant effect on ligand-gated Ca^{2+} release suggesting that the microsomes were not prepared in a phosphorylated state.

Limited enquiries into the regulation of plant Ca^{2+}-ATPases by KF (a phosphatase inhibitor) have been conducted previously by Hsieh *et al.* (1991). The authors reported that CaM sensitive-Ca^{2+}-uptake, in vesicles prepared from carrot cells, was stimulated by KF, indicating that phosphorylation inhibits Ca^{2+}-ATPase activity. Treatment of cauliflower microsomes with PKA prior to Ca^{2+} loading indicated that PKA did not affect Ca^{2+}-ATPase activity (Figure 4.15). The deficiency of action of PKA on Ca^{2+} uptake into cauliflower microsomes described here is not consistent with the results of Hsieh *et al.* (1991). Taken with the lack of effect of PKA on Ca^{2+} release it suggests that either the conditions of the assay were not suitable for PKA to act (e.g. insufficient incubation time) or that phosphorylation sites for PKA are not present in the enzymes responsible for uptake and release and thus PKA has a limited role to play in Ca^{2+} homeostasis in plants. Further experimentation is required to clarify this.

4.4.5. Assessment of putative Ca^{2+}-release agents

The radiometric flux assay provided a convenient means for assessing whether cyclic nucleotides, NAADP analogues, and $InsP_6$ were able to activate Ca^{2+}-release from cauliflower microsome vesicles. These compounds are thought to have a role in signal transduction pathways but little is known about their action in plants. As the experiments described above indicated that GSH was capable of releasing Ca^{2+} from vesicles its activity was also investigated.

4.4.5.1. Cyclic nucleotides

Cyclic nucleotides have been found to be ubiquitous second messengers, reported in both eukaryotes and prokaryotes. The role of these second messengers in plants, however, is poorly understood. The cyclic nucleotide cAMP has recently been described as playing an important part in the control of the cell cycle in tobacco cultures (Ehsan *et al.*, 1998) and cGMP has been shown to regulate the activity of the inward rectifying K^+ channels KAT1 and AKT1 of *Arabidopsis* (Hoshi, 1995). Channels that are permeable for Ca^{2+} have also been reported, in the Electronic Plant Gene Register (http://www.tarweed.com/pgr/; entry PGR98-062) by Köhler & Neuhaus (1998), which are activated by cAMP. The CNGC family has 20 members, of which the membrane locations are not yet known. It was hypothesised that cyclic nucleotides may be able to activate Ca^{2+}-release from cauliflower microsomes. To test this hypothesis cAMP and cGMP and their membrane permeable analogues, 8-Br-cAMP, 8-Br-cGMP and DT-cGMP were added to loaded vesicles. None of the nucleotides elicited any Ca^{2+}-release (Figure 4.16) suggesting an absence of cyclic nucleotide-gated Ca^{2+} mobilization pathways at endomembranes.

4.4.5.2. NAADP analogues

Two analogues of NAADP were tested for their ability to release Ca^{2+} from cauliflower vesicles. The nonphosphorylated analogue NAAD did not release significantly more Ca^{2+} than water at 1 μM final concentration. However, NADP mobilised 11.9 ± 2.6% of the accumulated Ca^{2+} from the vesicles (Figure 4.17). These results are consistent with Ca^{2+}-mobilisation experiments conducted on sea urchin homogenates with NAADP analogues. Limited release induced by NADP is thought to arise from the contamination of commercial preparations of NADP with trace amounts of NAADP (discussed in Lee, 1997).

4.4.5.3. $InsP_6$

Since the 1980's, when $InsP_6$ was confirmed as being present in animal cells, it has been attributed as having an array of diverse roles in cell function (for review see Shears, 2001). The presence of $InsP_6$ (phytic acid) in plants has been recognised for decades, but only recently has the compound been proposed to play a signalling role. Thus, $InsP_6$ has recently been reported to form part of the ABA signal transduction pathway in plants, inhibiting K^+_{in} channels in a Ca^{2+}-dependent manner, and with more potency than $InsP_3$ (Lemtiri-Chlieh *et al.*, 2000). An important question raised by the inhibition of K^+_{in}-channels by $InsP_6$ are: does $InsP_6$ act by causing $[Ca^{2+}]_c$ elevations? If so, does it act through the same pathway as $InsP_3$? Treating loaded cauliflower microsome vesicles with 100 μM $InsP_6$ released 10 ± 1.7 % of the accumulated Ca^{2+} (Figure 4.18). A T-test indicates that the release is not quite significant (P = 0.0562) in comparison to the release induced by water (control). Thus, it appears that if $InsP_6$ indeed acts as a mobiliser of internal Ca^{2+} stores in a similar manner to $InsP_3$ it is far less potent. Whether $InsP_3$ and $InsP_6$ act through the same signalling pathways has not been addressed in this study. As $InsP_6$ is unable to release as much Ca^{2+} as $InsP_3$, even when applied at a ten fold higher concentration, the data do not explain the potency of $InsP_6$ in inhibiting K^+_{in}-channels in guard cells. It is possible that $InsP_6$ acts more effectively through the ABA-sensitive hyperpolarisation-activated Ca^{2+} channels of the PM identified by Hamilton *et al.* (2000), as suggested by Lemtiri-Chlieh *et al.* (2000).

4.4.5.4. GSH

GSH is an abundant low molecular weight thiol. As a modulator of ligand-gated channels in animal cells it is considered in plants to be a sensor of stress and is involved in a variety of metabolic pathways including antioxidant defences. Initial experiments on the effects of GSH on the activity of ligand-gated Ca^{2+} release in plants indicated that GSH induced Ca^{2+}-release from cauliflower microsome vesicles. As levels of GSH have been found to be in the range of 2-3 mM in the roots of *Arabidopsis* (Fricker *et al.*, 2000) 1 mM GSH, which released 18.3 ± 3.2% of the total accumulated Ca^{2+}, is within the expected physiological range. The membrane integrity assay indicated that 1 mM GSH did not increase the 'leakiness' of the vesicles. Together these results suggest that GSH is activating a channel that is able to facilitate Ca^{2+} release. The nature of this putative channel, and whether it is specific for Ca^{2+}, is unknown and requires further examination, for example using electrophysiological approaches.

5. Mining the *Arabidopsis* genome for ligand-gated Ca^{2+} channels

5.1. Introduction

The data from various electrophysiological and biochemical studies indicates that plants possess a selection of Ca^{2+}-permeable channels including, those gated by stretch, voltage and ligands (Pineros & Tester, 1997; Sanders *et al.*, 1999; 2002). To date, however, a limited number of potentially Ca^{2+}-permeable channels has been cloned and functionally expressed. These include: (1) LCT1, a low-affinity cation transporter (and perhaps not a channel) from wheat (Schachtman *et al*, 1997); (2) AtTPC1, a voltage-activated PM channel from *Arabidopsis* (Furuichi *et al.*, 2001); (3) NtCBP4, a CNGC homologue from tobacco (Arazi *et al.*, 2000); and (4) AtCNGC2, from *Arabidopsis* (Köhler *et al.*, 2000; Leng *et al.*, 1999).

Biswas *et al.* (1995) detail the purification of an $InsP_3$-receptor from the hypocotyl of mung-bean (*Vigna radiata*) embryos. Although they identified and purified a microsomal/vacuolar 400 kDa protein, that when reconstituted in proteoliposomes demonstrated release with $InsP_3$, they did not ascertain any sequence data for the protein or the gene involved. Indeed, even though a large body of biochemical evidence for ligand-gated Ca^{2+} release channels in plants has been reported, there are no reports of any sequences that are homologous to the InP_3R or RyR of animals. The *Arabidopsis* genome sequencing project has provided a unique opportunity for searching for plant sequences with homologies to known proteins and has been utilised here to search for putative ligand-gated Ca^{2+} channels.

Skeletal and cardiac RyRs (RyR_1 and RyR_2) have been identified in animals that are twice as large as $InsP_3R$ As homotetrameric complexes with subunits exhibiting molecular sizes in excess of 500 kDa RyRs are among the largest proteins known (Lee, 1997). Despite their size RyR1 and RyR2 share 66% identity with each other and substantial structural and functional homology with $InsP_3Rs$ (Berridge, 1993). Structural and functional studies have shown that the structure of both RyRs and $InsP_3R$ can be roughly divided into a large N-terminal cytoplasmic arm that is thought to be responsible for ligand binding and regulation, a smaller C-terminal domain that is characterised by membrane-spanning regions surrounding a Ca^{2+} pore and short cytoplasmic tail (Zhao *et al.*, 1999; Michikawa *et al.*, 1994). A much

smaller isoform of RyR (RyR3), found in mammalian skeletal muscle, lacks the majority of the N-terminal and still functions as a Ca^{2+} channel that can be activated by cADPR (Giannini *et al.*, 1992; Sonnleitner *et al.*, 1998). An $InsP_3$ binding site has been identified that comprises an area of high homology in the sequences of the three isoforms of $InsP_3R$ so far identified (Yoshikawa *et al.*, 1996). This binding site is located at the N-terminal of $InsP_3Rs$. In between the $InsP_3$-binding site and the C-terminal membrane-spanning domains the sequences are dissimilar: the proteins are thought to contain domains related to more specific regulatory and transduction functions (Figure 5.1). Domains that have been used here to conduct homology searches in *Arabidopsis* are described in more detail below.

5.1.1. Ca^{2+}-channel domain

The area of sequence demonstrating the greatest degree of homology between $InsP_3Rs$ and RyRs is that of the C-terminus (Taylor & Traynor, 1995). In the C-terminus, membrane-spanning regions that are believed to form the Ca^{2+}-channel have been identified through: (1) hydropathy analysis; (2) mutagenesis and (3) comparisons with other Ca^{2+}-permeable ion-channels. The last two membrane-spanning domains (designated M3 and M4 in the RyR) are the most closely conserved between the receptors and probably reflect a common evolutionary origin. Part of the free C-terminal tail also demonstrates a region of high homology consisting of two cysteine residues and a 'TXCFICG' motif. The tail has been reported to act as a regulator of channel activity, moving to block/open the entrance to the pore region (Miyazaki *et al.*, 1992; Fadool & Ache, 1992), while the cysteine residues may be sites of thiol-reagent action (Berridge, 1993).

5.1.2. Ligand-binding domain

The region of the RyR2 responsible for binding cADPR has not yet been determined. A domain of 650 amino acid residues in $InsP_3Rs$ has been identified that has been reported to be responsible for the binding of $InsP_3$ (Mignery & Sudhof, 1990). This region is located in the N-terminal and is highly conserved among $InsP_3Rs$ from different species. The deletion of small areas of this region leads to a binding activity (Miyawaki *et al.*, 1991). Furthermore, heparin, an inhibitor of $InsP_3$-induced release, has been shown to also bind to this region.

5.1.3. EF-hand domain

EF-hand domains (named after the E and F regions of paravalbumin) are homologous sequences found within Ca^{2+}-binding proteins. The EF-hand is

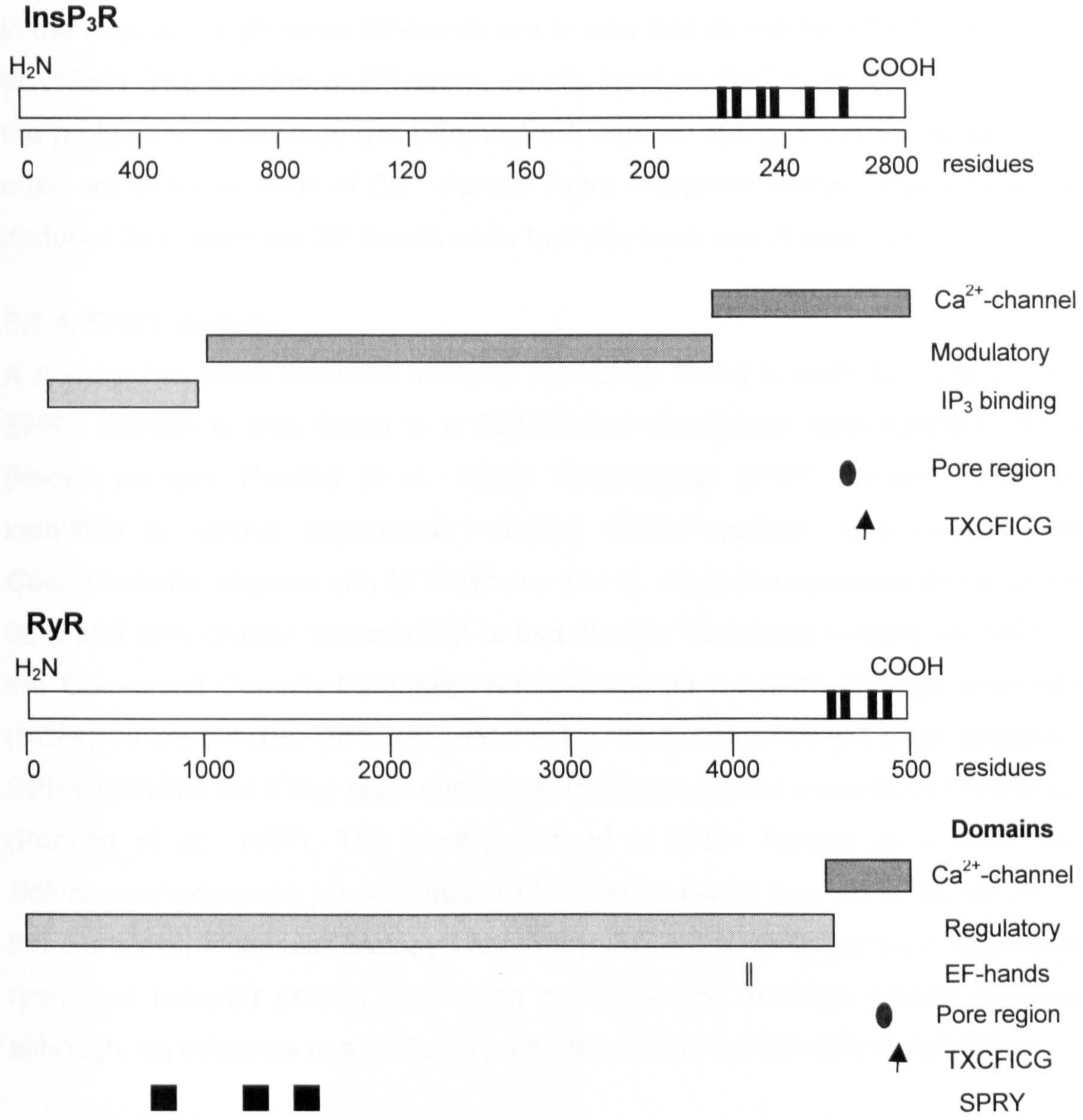

Figure 5.1. $InsP_3R$ and RyR domains

The $InsP_3R$ (type 1 isoform) and RyR (RyR2) are depicted. Black bars indicate the position of putative transmembrane spanning domains. Other domains discussed previously in this chapter are indicated: black lines for EF-hands, filled circles for pore regions, arrows for the conserved sequence 'TXCFICG' and filled squares for SPRY domains in the RyR. Figure based on Taylor & Trayner (1995).

approximately thirty amino acids long and is made up of two alpha-helical loops (Strynadka & James, 1989). In physiological conditions a Ca^{2+} ion will generally bind in the loop, although some EF-hands are known that do not bind Ca^{2+} (Van Eldik *et al.*, 1982). The function of EF-hands usually involves Ca^{2+}-dependent regulation of the proteins to which they are (Strynadka & James, 1991). Thus EF-hand proteins often act as transducers of Ca^{2+} signals. From sequence analysis RyRs have been deduced to contain two EF-hands while $InsP_3Rs$ have one (Figure 1.1).

5.1.4. SPRY domain

A domain has been identified in RyRs that is not found in $InsP_3Rs$. This so-called SPRY domain is also found in a *Dictostelium discoideum* dual-specificity kinase (known as spl1: Ponting *et al.*, 1997). Homologous SPRY domains have been identified in various organisms, including *Homo sapiens*, *Mus musculus* and *Caenorhabditis elegans* with *M. musculus* and *C. elegans* sequences demonstrating 98% and 53% identity, respectively, to that of man. Sequence lengths (as defined in the Conserved Domain Database; National Centre for Biotechnology Information (NCBI)) range between 200-300 amino acids. No function has yet been assigned to SPRY domains but it has been suggested that they may be involved in RNA-binding (Ponting *et al.*, 1997). The identification of a SPRY domain in a hypothetical *Schizosaccharomyces pombe* protein (382 amino acids) has led to its inclusion in the European Molecular Biology Laboratory (EMBL) data library as a hypothetical ryanodine receptor protein (Accession code: T41256 in NCBI protein database); although, no evidence has yet been produced to substantiate this classification.

The aim of the work presented in this chapter was to identify sequences within plant protein databases that contain homologies to the IP_3Rs and RyRs identified in animal cells and to assess their possible roles in plants. This was carried out by conducting BLAST searches of protein databases available over the internet for plant sequences, either experimentally-determined or deduced from the *Arabidopsis* and rice genome sequencing projects. One sequence in the *Arabidopsis* genome was identified that contained a SPRY domain homologous to that of the RyR. To investigate this putative protein further an attempt was made to identify a T-DNA insertion knockout mutant in the Wisconsin T-DNA transformed *Arabidopsis* lines. A yeast strain with a homologous gene knockout was also investigated.

5.2. Materials and Methods

5.2.1. Database searches

BLAST searches (see Altschul *et al.*, 1997) for plant sequences demonstrating homology to the ligand-gated Ca^{2+}-channels of animal cells were performed using protein sequences representing various domains of the IP_3Rs and RyRs (Table 5.1) and web-based database search tools and annotated databases supplied by The National Centre for Bioinformatics (NCBI: http://ncbi.nlm.gov/), The Institute for Genomic Research (TIGR: http://tigr.org/), Munich Information Centre for Protein Sequences (MIPS: http://mips.gsf.de/), SwissProt, Genbank, and The *Arabidopsis* Information Resource (TAIR: http://*Arabidopsis*.org/). The predicted sequences were obtained from the SwissProt database. Prediction of putative transmembrane spanning domains was performed using the program TMpred (Holfmann & Stoffel, 1993). Multiple alignments were carried out using the Multalin program (Corpet, 1988) or ClustalX (Thompson *et al.*, 1997). Unrooted tree diagrams were prepared via the neighbour-joining method using Clustal, PHYLIP (Felenstein, 1989) and 1000 bootstrap replicates. Graphical output of the trees was executed with TreeView (Page, 1996).

5.2.2. Chemicals and reagents

Purified *Arabidopsis thaliana* columbia DNA was a generous gift from Dr A. Amtmann (University of York). All other reagents are from Sigma unless otherwise stated.

5.2.3. Wisconsin knockout library screen

The University of Wisconsin T-DNA transformed *Arabidopsis* lines – described by Krysan *et al.* (1996; 1999) - were screened for T-DNA inserts within the SPRY domain encoding gene *At2g22020.* Oligonucleotide primers flanking the gene, Figure 5.1, were designed based on sequence data from the *Arabidopsis* genome database and synthesised by MWG Biotech (UK). The University of Wisconsin performed the initial screen of 62 polymerase chain reactions (PCR) (Krysan *et al.*, 1999). The PCR products were analysed by Southern blot: hybridising the blot with a probe made from PCR product amplified from wildtype *A. thaliana* columbia DNA, using primers designed to cover the beginning and end of the gene. Control reactions were performed with the primers designed here and supplied by Wisconsin. The University of Wisconsin tested the compatibility of the control primers with the primers designed here. All completed reactions were run out on a

Table 5.1. Templates used for homology searches

The sources of the sequences used for homology searches are indicated. The accession codes for the protein sequence entries in the Swiss-Prot database are given.

Search	Template	Sequence origin
Ryanodine receptor homologues		
RyR1	Entire sequence	P21817; *H. sapiens* O13054; *Makaira nigricans* P91905; *C. elegans* Q90984; *Gallus gallus* (fragment)
RyR2	Entire sequence	Q92736: *H. sapiens*
RyR3	Entire sequence	Q15413; *H. sapiens* Q90985; *G. gallus* (fragment)
RyR?	Entire sequence	Q24498; *D. melanogaster* Q82874; *Hemicentrotus pulcherrimus*
$InsP_3$ receptor homologues		
$InsP_3$R1	Entire sequence	Q14643; *H. sapiens*
$InsP_3$R2	Entire sequence	Q14571; *H. sapiens*
$InsP_3$R3	Entire sequence	Q14573; *H. sapiens*
$InsP_3$R?	Entire sequence	P29993; *D. melanogaster*
Homologous domains		
RyR/$InsP_3$R M3/M4 domain	RyR transmembrane domains M3 and M4	P21817; *H. sapiens* O13054; *Makaira nigricans* P91905; *C. elegans* Q24498; *D. melanogaster* Q82874; *Hemicentrotus pulcherrimus*
TXCIFCG	TXCIFCG	Conserved sequence (Berridge, 1993)
EF hand	Canonical EF hand sequence	As defined on the NCBI database
SPRY	Canonical SPRY domain	As defined on the NCBI database

Left1:	5'	AAG CGC GTT TGG TTC ACA ATC AAT GCC AT	3'
Left2:	5'	AGA CAG CCT ACG GGT TGG TAT GAT TTC AT	3'
Right1:	5'	TAC CAT GCG GAA TGT CTA ACA CAG TCC AT	3'
Right2:	5'	CCT TCT GGA GTT AAC GCA ATC CAT GAG TT	3'

Figure 5.2 Oligonucleoide primers used in the screen of the Wisconsin T-DNA knockout library for SPRY domain knockout mutants

The oligonucleotide primers used to screen the Wisconsin T-DNA knockout library for SPRY domain mutants are shown. The sequences were chosen to flank a gene on Chromosome 2 of *Arabidopsis*, *At2G22020,* which contains a SPRY domain.

1% (w/v) agarose gel for analysis. Where necessary DNA extractions from agarose gel were carried out using a Quiagen QIAquick ™ spin kit.

5.2.3.1 Hot start PCR

Hot start PCR conditions were used to produce DNA to use as a probe for *At2G22020* using primers Left1 and Right2 (Figure 5.1). 2 μl of genomic DNA (0.2 ng/μ)l was added to 4 μl 10X Ex-Taq buffer containing 4 μl dNTP mix, 1 μl of each primer (12 pmol/μl), and 28 μl water in PCR tubes. The reaction mix was covered with mineral oil and heated to 96 °C. Immediately upon reaching 96 °C 10 μl of enzyme mix (5 μl Ex-Taq buffer, 2.5 μl Ex-Taq polymerase [Bio Whittaker] and 42.5 μl water) was added. 36 heating cycles were carried out: 94 °C for 15 s, 65 °C for 30 s and 72 °C for 2 min. The temperature was then held at 72°C for 4 min before being cooled to 4 °C for storage.

5.2.3.2. Southern Blot

Following the first round of PCR performed by Wisconsin, the PCR products they supplied were run on a 1% (w/v) agarose gel. A Southern blot was prepared from the gel as follows. The agarose gel containing PCR products was incubated with 0.25 M HCl for 15 min, room temperature with gentle shaking to depurinate the DNA. Depurinated DNA was denatured by incubating the gel in 0.5 M NaOH, 1 M NaCl for 30 min at room temperature with gentle shaking. The gel was neutralised by incubating it in 5 M Tris-HCl (pH7.4), 3 M NaCl for 30 min, at room temperature with gentle shaking, and layered on top of three sheets of Whatman filter paper (3 MM) on a sponge soaked in 10x SSC buffer (1.5 M NaCl, 0.15 M Tri-sodium citrate, 5 M NaOH, pH 7.0), ensuring that no bubbles were trapped under the gel. The area around the gel was sealed with plastic-wrap, the surface of the gel was flooded with 10x SSC buffer and a pre-wetted Zeta-Probe GT membrane layered on top. The membrane was flooded with 10x SSC buffer and covered with two layers of Whatman filter paper (3 MM). Bubbles were removed at all stages. Paper towels were placed on top of the gel/membrane stack to a height of approximately 15 cm. An excess of buffer was placed into the tray below the gel and it was left to incubate for 24 h. The membrane was carefully removed from the gel, rinsed in 2x SSC buffer (0.3 M NaCl, 0.03 M Tri-sodium citrate, 1 M NaOH, pH 7.0), and allowed to air dry. Well positions were marked under UV light and the membrane was baked at 80 °C for 2 h.

5.2.3.3. Probe preparation

A probe for *At2G22020* was produced. 25 μg/ml *A. thaliana* columbia DNA was denatured by boiling for 3 min followed by rapid cooling in an ice bath for 5 min. 500 ng/ml denatured DNA was added to Labelling Buffer comprised of 20 μM dNTP mix, 400 μg/ml nuclease free BSA, 333 nM [α-^{32}P]dNTP, 100 U/ml DNA Polymerase I. The reaction mix was mixed gently and incubated at room temperature for 60 min. The reaction was terminated by heating to 100 °C for 2 min then cooling in an ice bath.

5.2.3.4. Hybridisation

The Southern blot was probed for the *At2G22020* gene by hybridising it with PCR product amplified from genomic *A. thaliana* columbia DNA. The Southern blot membrane was rolled inside two sheets of nylon mesh, inserted into a glass hybridisation tube, and covered with 100 ml of Hybridisation Solution containing (50% (v/v) formamide, 0.12 M $Na_2H_2PO_4$, 0.25 M NaCl and 7% (w/v) SDS). The probe was denatured by boiling it for 3 min then placing it directly into ice water for 5 min. Excess hybridisation solution was removed from the hybridisation tube and 10^6 cpm/ml of probe was added. The membrane was incubated for 4h at 42°C with stirring. The hybridisation fluid was replaced with 100 ml of High Stringency Wash Solution containing (0.1% SDS (w/v), 15 mM NaCl, 1.5 mM tri-sodium citrate and 50 mM NaOH (pH 7.0)) and incubated at 50 °C for 30 min. This wash was repeated twice. The washed membrane was analysed by exposure to Hyper-film (Amersham Life Sciences) for 48 h.

The identity of PCR products hybridising with the probes were confirmed by fluorescent DNA sequencing (Oxford DNA Sequencing Facility; Biochemistry Department, University of Oxford).

5.2.4. Yeast knockouts

5.2.4.1. Strains and mutants

The *Saccharomyces cerevisiae* strain BY4741 (*MATα, his3Δ1; leu2Δ0; met15Δ0, ura3Δ0*) was used as a wild type. YKL124w (*BY4741; MATα, his3Δ1; leu2Δ0; met15Δ0, ura3Δ0; YKL124w::kanMX4*) and YMR171c (*BY4741; MATα, his3Δ1; leu2Δ0; met15Δ0, ura3Δ0; YMR171c::kanMX4*) were knockout mutants of the wildtype with open reading frames homologous to *At2g22020* (YKL124w and YMR171c respectively) deleted. The wildtype and the mutants were purchased from

European *Saccharomyces cerevisiae* Archives for Functional Analysis (EUROSCARF, Johann Wolfgang Goethe-University, Frankfurt, Germany).

5.2.4.2. Yeast drop assay

The drop assay was used to test for differences in phenotype between the mutants and the wild type yeast strain. Cells were grown in YPD (10 g/l yeast extract, 20 g/l bactopeptone, 20 g/l glucose) at 37 °C until reaching an OD_{600} of 0.8. The cultures were serially diluted in steps of 10x and 2 ml of each sample was spotted onto a YPD agar plate (YPD media supplemented with 20 g/l agar) or a YPD agar plate containing 4, 5, 7.5 or 10 mM of the calcium chelator 1,2-Bis(2-amino-5-bromophenoxy)ethane-N,N,N',N'-tetraacetic acid (BAPTA). The plates were incubated at 37 °C for three days.

5.2.4.3. Yeast microsome preparation

The yeast wildtype strain and the two knockout mutants were grown up on YPD overnight, at 37 °C, to obtain colonies. Individual colonies were transferred to 200 ml AHC growth medium (2 g/l Yeast nitrogen base (Y-1250; Sigma), 6 g/l N-Z amine, 50 mM potassium dihydrogen phosphate and 2% (w/v) glucose supplemented with 20 mg/l L-histidine, 20 mg/l L-methionine, 60 mg/l L-leucine and 20 mg/l L-uracil; pH adjusted to 7.5 with KOH) and incubated at 30 °C for 48 h with shaking. The 200 ml inoculum was transferred to 800 ml of AHC growth medium and incubated for 48 h, at 30 °C with shaking. The culture was centrifuged at 3,000 rpm for 10 min in a Sorvall FS10C rotor and the pellets were resuspended in 500 ml of Pre-treatment (PT) solution (100 mM Tris, 10 mM DTT; pH adjusted to 9.5 with HCl) and incubated at 37 °C for 20 min with gentle shaking. The yeast suspension was centrifuged at 3,000 rpm for 10 min in a Sorvall SS34 rotor and the pellets were resuspended in 100 ml of Yeast Cell Wall Digestion Solution (YCWD) (1% (w/v) yeast extract, 2% (w/v) bactopeptone, 0.7 M sorbitol, 1% (w/v) glucose, 5 mM DTT, 100 mM Tris, pH adjusted to 7.5 with HCl supplemented with 7.5 mg/l zymolyase), prewarmed to 30 °C. The YCWD-yeast suspension was incubated for 1.5 h at 30 °C with gentle shaking and centrifuged at 6,000 rpm for 10 min in a Sorvall SS34 rotor. All further operations, including centrifugations, were carried out at 4 °C. The pellets were resuspended in Homogenisation Buffer (HB) (10% (w/v) glycerol, 1.5% (w/v) PVP-40, 5 mM EGTA and 50 mM Tris; the pH was adjusted to 7.5 with ascorbate) and homogenised with 4-5 strokes in a glass/Teflon homogeniser. The homogenate was centrifuged at 6,000 rpm for 10 min in a Sorvall SS34 rotor and the supernatant collected. The pellet was resuspended with HB solution, homogenised and

centrifuged as previously and the supernatant collected. The supernatants from the two steps were combined and centrifuged at 33,000 rpm in a Beckman Ti60 rotor for 40 min. The pellet was resuspended into Suspension medium (0.4 M glycerol, 5 mM BTP-MES (pH 7.4), 25 mM KCl and 30 mM $MgSO_4$ made up in Ca^{2+} free water), snap frozen in liquid nitrogen and stored at –80 °C.

5.2.5. Ca^{2+} uptake and release

Ca^{2+} uptake and release was performed as described for cauliflower microsomes in section 4.2.4, substituting yeast microsomes for cauliflower microsomes.

5.2.6. ADP-ribosyl cyclase assay

Yeast microsomes derived from wildtype and mutant strains were assayed for ADP-ribosyl cyclase activity as described in Chapter 2. Briefly, yeast microsomes (20 mg/ml total protein) were incubated with 20 – 500 μM NGD in buffered solution containing 20 mM Hepes, pH 7.2. The change in fluorescence was followed (excitation 300 nm; emission 410 nm, in a Perkin Elmer LS-5 luminescence spectrofluorimeter. A standard curve of cGDPR fluorescence as a function of cGDPR concentration was constructed, to enable quantification of cGDPR production by cauliflower extracts, as described in 2.2.6.

5.3. Results

5.3.1. Database searches

Recently initiatives such as the *Arabidopsis* genome sequencing project have resulted in a wealth of information regarding plant genes and the proteins they are believed to encode. The sequences of various isoforms of $InsP_3Rs$ and RyRs have been deduced for some time. Using the BLAST search engine the sequences of these receptors was compared to plant proteins available on databases through the internet. Because of the large size of these receptors, not only was the whole sequence of the receptor used as a template for the homology searches but also individual domains and canonical sequences of conserved domains. Initial searches indicated that there were no sequences in the database with high degrees of homology (over 30% identity over the entire sequence) to the receptors as a whole or to the conserved features of the Ca^{2+} channel or ligand-binding domains. A variety of plant sequences that possessed areas of homology to the receptors with less than 30% identity was identified (data not shown). Homologous sequences were assessed for putative transmembrane spanning domains using the TMpred program. Those predicted to have one or more transmembrane domains, and thus the potential to act as a Ca^{2+}-channel, were investigated in more detail and are listed in Table 4.2.

Domain searches for EF-hand domains and characteristic transmembrane spanning sequences common to Ca^{2+}-channels identified only a previously characterised Ca^{2+}-channel (AtTPC1). Searches using the SPRY domain as a template identified two hypothetical protein sequences: *At2G22020* and *At1G51450,* both were predicted to contain at least one transmembrane domain.

5.3.2. Analysis of *At2G22020*

The protein encoded by *At2G22020* contained a SPRY domain that aligned well with the SPRY domains of RyRs (Figure 5.3). As the transmembrane predicting program TMPred also indicated that the protein could contain between one and seven possible membrane spanning segments the protein was examined in greater detail. Analysis of EST data indicated that the actual reading frame encompassed not only the gene annotated *At2G22020* in the database but also *At2G22010* which is located adjacent to it on chromosome 2 (Dr B. Stanchev, University of York; personal communication). The phylogenetic tree in Figure 5.4 indicates that the proteins containing SPRY domains can be classified into several families including

Table 5.2. Plant sequences with homology to ligand-gated channels and putative transmembrane domains

BLAST searches for plant sequences demonstrating homology to the ligand-gated Ca^{2+}-channels of animal cells were performed using the entire sequence or various domains of mammalian RyRs and $InsP_3Rs$. Homologous sequences were analysed for putative transmembrane spanning domains using the program Tmpred, the number of spanning segments for the strongest model generated are indicated. Conserved domains are those defined on the NCBI database and are detailed below. Closest homologous known sequence refers to the most homologous protein of known function, as annotated in the NCBI database.

The domains are defined on the BLAST database as follows:

SPRY:	Domain of unknown function named from SPIa and the Ryanodine Receptor. Distant homologues are domains in butyrophilin/marenostrin/pyrin.
BT1:	BT1 family domain. BT1 family are transmembrane proteins including pteridine and biopterin transport proteins.
SMC_N, SMC_C:	Structural maintenance of chromosomes (SMC) superfamily N and C terminal domains involved in chromatin and DNA dynamics.
ABC transporter:	ABC transporters for a large family of proteins responsible for translocation of a variety of compounds across biological membranes.
Myosin tail:	A domain common to the myosin molecule, a fundamental contractile protein found in all eukaryote cell types.
PPR repeat:	This repeat is a domain of no known function. It occurs in PET309 and may be involved in RNA stabilisation. The family is greatly expanded in plants.
EF-hand:	EF-hands are calcium-binding motifs that occur at least in pairs. Each motif consists of a 12 residue loop flanked on either side by a 12 residue alpha-helix. EF-hands undergo a conformational change upon binding calcium ions.

Gene	Search	Length	Membrane spanning domains	Predicted domains	Closest homologous known sequence	Comment
At2G22020	RyR1, RyR2, RyR3, SPRY domain	796	1	SPRY	RyR	Hypothetical
At1G51450	RyR3	509	6	SPRY	ASH2	Hypothetical
At3G11080	RyR3	943	3	Leucine-rich repeat	Disease resistance protein	Putative
At3G11010	RyR3	957	7	Leucine rich repeat	Disease resistance protein	Putative
F19K16.31	RyR, M4 domain	497	11	BT1	Monocarboxylate transporter 3	Hypothetical
At2G27170	InP_3R	1166	1	Myosin tail, filament, SMC_N, SMC_C, ABC transporter	SMC family protein	Putative chromosome associated protein
F28P10.40	InP_3R, Ca^{2+}-channel domain	852	2	PPR repeat	PPR repeat protein	Putative
K9P8.12	InP_3R, InP_3-binding domain	619	2	-	Transport inhibitor response 1 protein	
At2G22530	Conserved sequence 'TXCIFCG'	897	12	-	Phosphatidylinositol glycan	Unknown
AtTPC1	Canonical EF hand	733	12	EF-hand	Voltage-gated Ca^{2+}-channel	Putative Ca^{2+}-channel

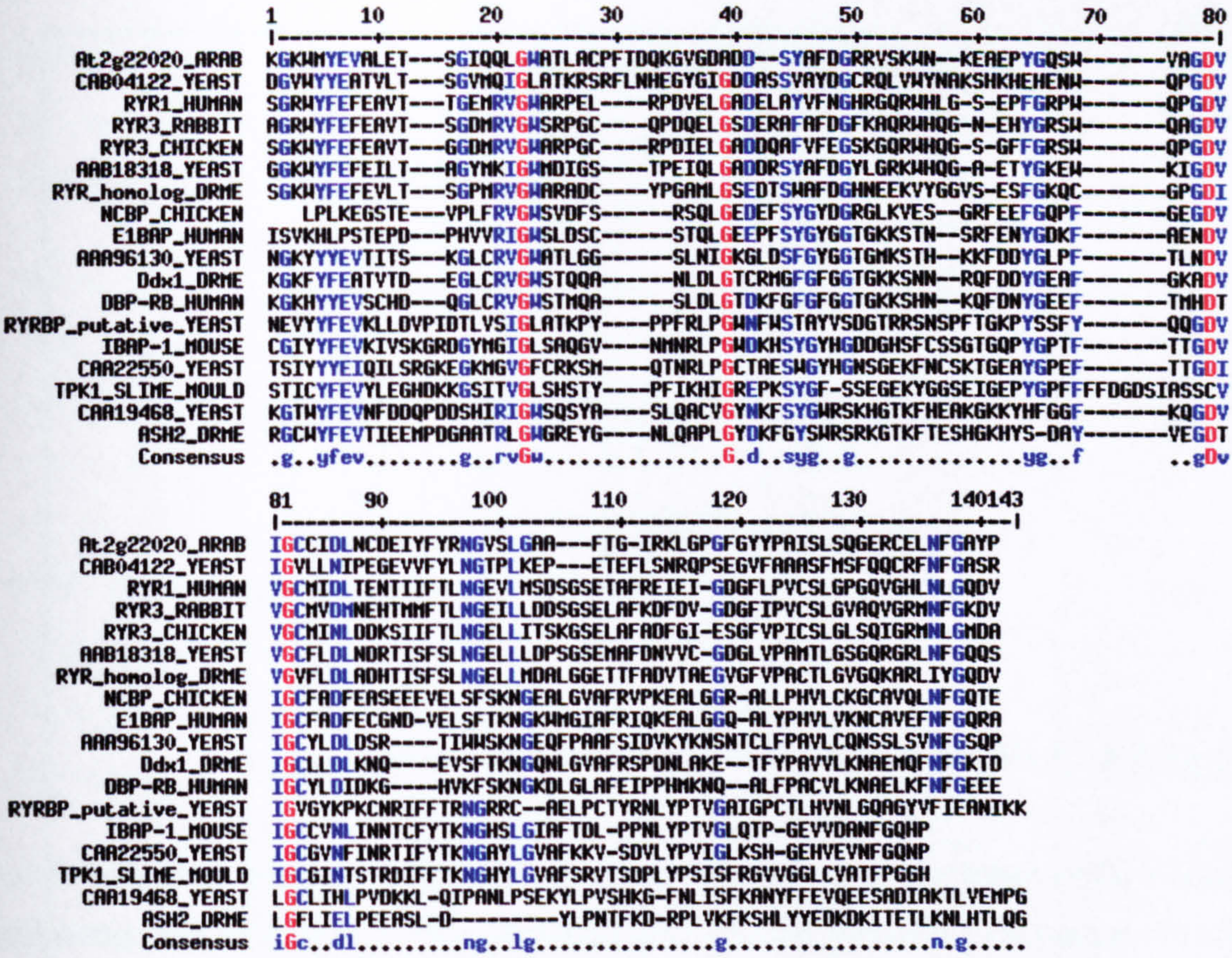

Figure 5.3. Multiple alignment of protein sequences containing SPRY domains

Protein sequences containing the SPRY domain, as defined by by the NCBI conserved domain database, were aligned with *At2g22020* using the Multalin program (Corpet, 1988). The 17 most similar sequences are displayed.

Figure 5.4. Phylogenetic tree of SPRY domain proteins

Multiple alignments were carried out using the ClustalX program (version 1.8) on protein sequences (including hypothetical proteins) with homology to the consensus SPRY domain sequence, as defined by the NCBI conserved domain database. The tree was constructed using the bootstrap neighbour-joining method with 1000 bootstrap trials.

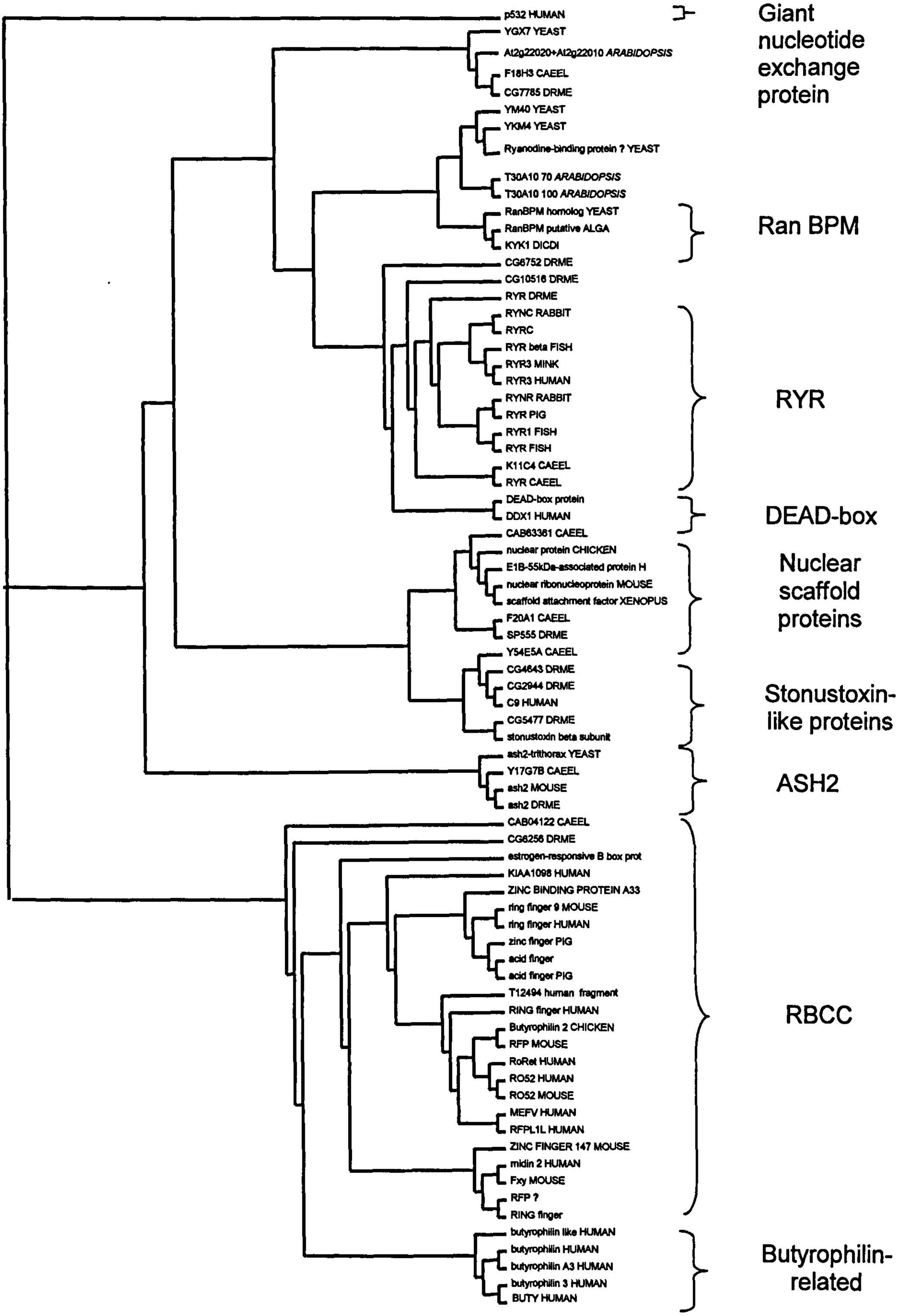
p532 HUMAN
YGX7 YEAST
At2g22020+At2g22010 ARABIDOPSIS
F18H3 CAEEL
CG7785 DRME
YM40 YEAST
YKM4 YEAST
Ryanodine-binding protein ? YEAST
T30A10 70 ARABIDOPSIS
T30A10 100 ARABIDOPSIS
RanBPM homolog YEAST
RanBPM putative ALGA
KYK1 DICDI
CG6752 DRME
CG10516 DRME
RYR DRME
RYNC RABBIT
RYRC
RYR beta FISH
RYR3 MINK
RYR3 HUMAN
RYNR RABBIT
RYR PIG
RYR1 FISH
RYR FISH
K11C4 CAEEL
RYR CAEEL
DEAD-box protein
DDX1 HUMAN
CAB63361 CAEEL
nuclear protein CHICKEN
E1B-55kDa-associated protein H
nuclear ribonucleoprotein MOUSE
scaffold attachment factor XENOPUS
F20A1 CAEEL
SP555 DRME
Y54E5A CAEEL
CG4643 DRME
CG2944 DRME
C9 HUMAN
CG5477 DRME
stonustoxin beta subunit
ash2-trithorax YEAST
Y17G7B CAEEL
ash2 MOUSE
ash2 DRME
CAB04122 CAEEL
CG6256 DRME
estrogen-responsive B box prot
KIAA1098 HUMAN
ZINC BINDING PROTEIN A33
ring finger 9 MOUSE
ring finger HUMAN
zinc finger PIG
acid finger
acid finger PIG
T12494 human fragment
RING finger HUMAN
Butyrophilin 2 CHICKEN
RFP MOUSE
RoRet HUMAN
RO52 HUMAN
RO52 MOUSE
MEFV HUMAN
RFPL1L HUMAN
ZINC FINGER 147 MOUSE
midin 2 HUMAN
Fxy MOUSE
RFP ?
RING finger
butyrophilin like HUMAN
butyrophilin HUMAN
butyrophilin A3 HUMAN
butyrophilin 3 HUMAN
BUTY HUMAN
Giant nucleotide exchange protein
Ran BPM
RYR
DEAD-box
Nuclear scaffold proteins
Stonustoxin-like proteins
ASH2
RBCC
Butyrophilin-related

butyrophilin related proteins, RBCC proteins, ASH2-like proteins and RyRs. The putative protein encoded by *At2G22020* and *At2g22010* is grouped with several proteins of unknown function in a clade separate to that of the RyRs.

5.3.3. Wisconsin knockout library screen

The Wisconsin T-DNA transformed *Arabidopsis* lines were screened for an insert into the At2G22020 gene. The control reaction indicated that the primers did not cross react and were suitable for the screen. The first round of PCR carried out by Wisconsin was analysed by probing a Southern blot of the PCR products with a PCR product amplified out of genomic *Arabidopsis* DNA using primers flanking the *At2G22020* gene. Several putatively positive hybridizations were identified; however, sequencing indicated that none of the products contained a T-DNA insert (data not shown).

5.3.4. Yeast deletion mutants

Two homologous genes to *At2G22020* were detected in *Sacchraromyces cerevisiae* (*YMR171C* and *YKL124W*) that were predicted to encoded protein sequences containing SPRY domains. To investigate further the role of these proteins strains of *S. cerevisiae* were purchased from EUROSCARF in which the open reading frame for these genes was deleted (YO4974 and YO6445). The effect of gene deletion was assessed by testing for differences in phenotype between the mutant and wildtype (Strain BY4741) in growth conditions with differing concentrations of calcium. Also, differences in calcium uptake and cADPR-induced Ca^{2+} release were assessed.

5.3.4.1. Yeast drop assay

The yeast drop assay was used to evaluate differences in growth of the three strains of yeast being assessed. Cultures of the three strains were diluted to equal optical densities and pipetted onto YPD agar plates containing 0, 5, 7.5 or 10 mM BAPTA in order to test for a Ca^{2+}-related phenotype. The growth of the yeast was assessed by evaluating the size of the drops after 3 days incubation at 30 °C. Figure 5.5 indicates that there was no discernable difference in growth between the knockout strains and the wildtype.

5.3.4.2. Yeast calcium uptake and release

Microsomes were prepared from the wildtype, and YMR171C and YKL124W deletion strains. The microsomes were tested for Ca^{2+}-uptake and cADPR-induced

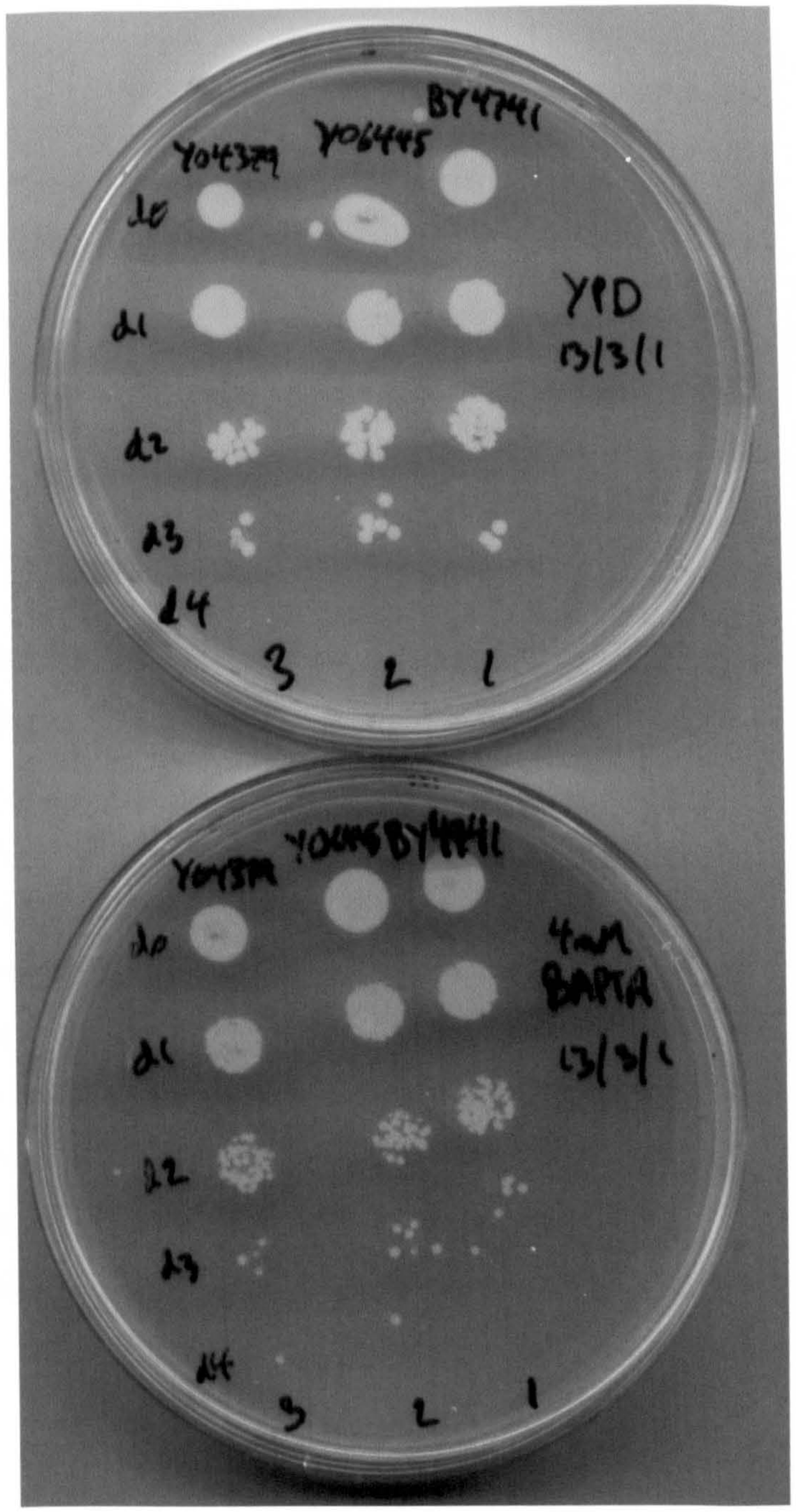

Figure 5.5. Growth of Yeast strains with SPRY gene deletions on BAPTA plates

Cultures of three strains of yeast 1) BY4741 – wildtype, 2) YO6445 – SPRY gene YKL124W deleted and 3) YO4974 – SPRY gene YMR171C deleted were diluted to equal densities and pipetted onto YPD agar plates containing 0 and 4 mM BAPTA. Growth on the plates was assessed after 3 days incubation at 30 °C.

release using the $^{45}Ca^{2+}$ radiometric flux filtration-assay. Figure 5.6A indicates that the microsomes were capable of sustaining Ca^{2+} uptake in the presence of ATP. An equal amount of Ca^{2+} was taken up by the three strains over 20 min, however, the wildtype microsomes initially accumulated Ca^{2+} more rapidly. Figure 5.6B shows that the microsomes derived from the YL124W knockout strain released significantly more Ca^{2+} than the other two strains over the time course of the assay both in the presence of cADPR and water. There was no difference between the amount of Ca^{2+} released from the microsomes of any of the strains, following ATP-driven loading, indeed by either cADPR or the negative control (water).

5.3.4.3. Yeast ADP-ribosyl cyclase assay

One indication that second messengers such as cADPR have a role in Ca^{2+}-signalling is the ability of that organism to metabolise them. The NGD assay was used to assess whether microsomes prepared from yeast displayed ADP-ribosyl cyclase activity and if deletion of SPRY domain genes affected this activity. Figure 5.7A illustrates that microsomes prepared from the wildtype strain of yeast demonstrate an increase in fluorescence when incubated with NGD consistent with the synthesis of cGDPR via ADP-ribosyl cyclase activity. Further experiments indicated that microsomes prepared from the three strains of yeast had no significant differences in the activity they demonstrated and that this activity could be abolished by boiling the microsomes for 1 h, see Figue 5.7B.

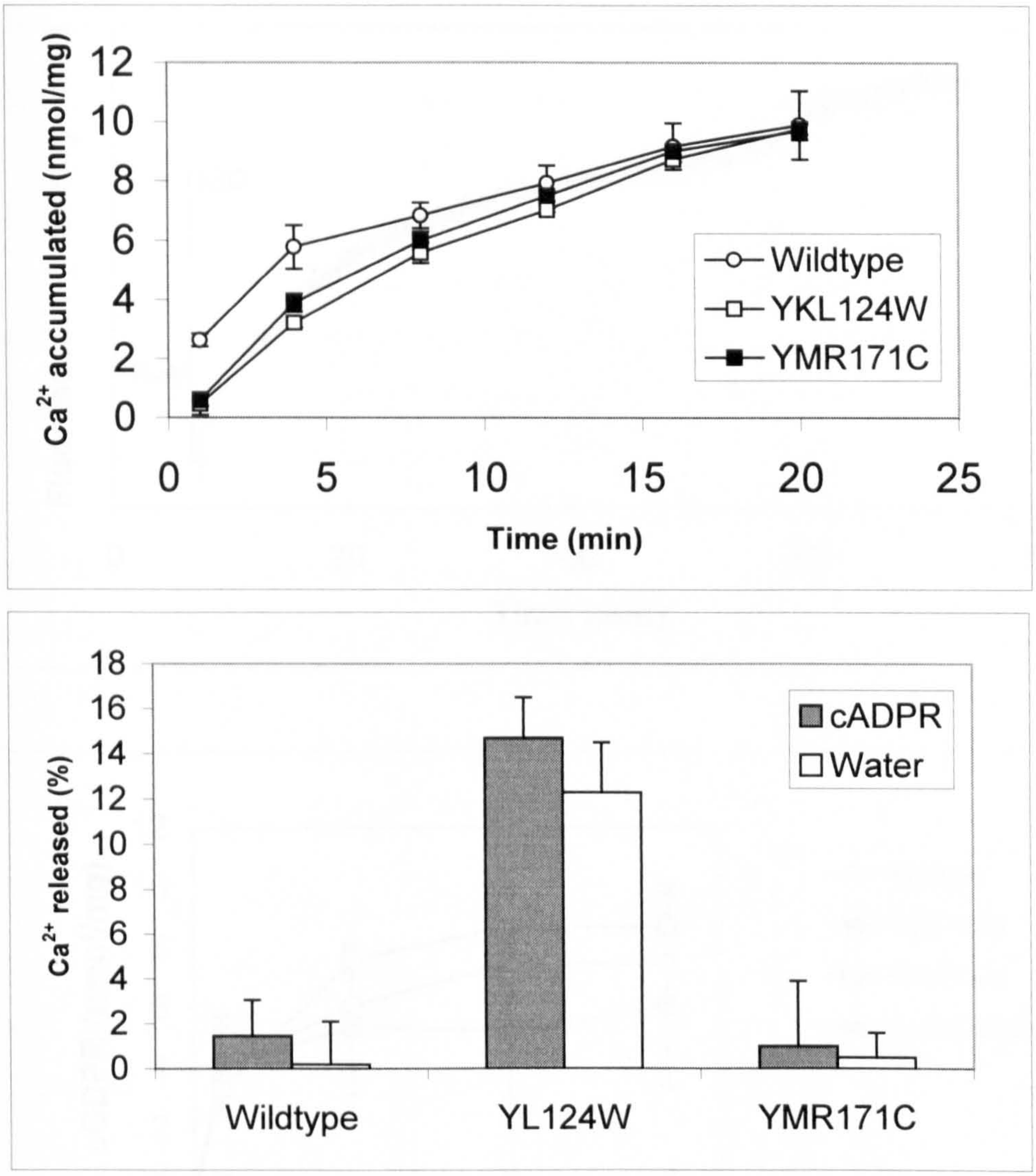

Figure 5.6. The uptake and release of Ca^{2+} from microsomes prepared from yeast with SPRY gene deletions

A. Yeast microsomes prepared from the wildtype strain BY4741 and two strains with SPRY genes YKL124W and YMR171C deleted were incubated with $^{45}Ca^{2+}$ in the presence of 3 mM ATP. **B.** Following loading of the vesicles with $^{45}Ca^{2+}$ to a steady state, further uptake was inhibited by the addition of the uncoupler FCCP (10 μM) and the P-type ATPase inhibitor Na_3VO_4 (250 μM) and data were standardised to this value. The Ca^{2+}-release agent cADPR was added to a final concentration of 10 μM and the total release over three minutes observed.

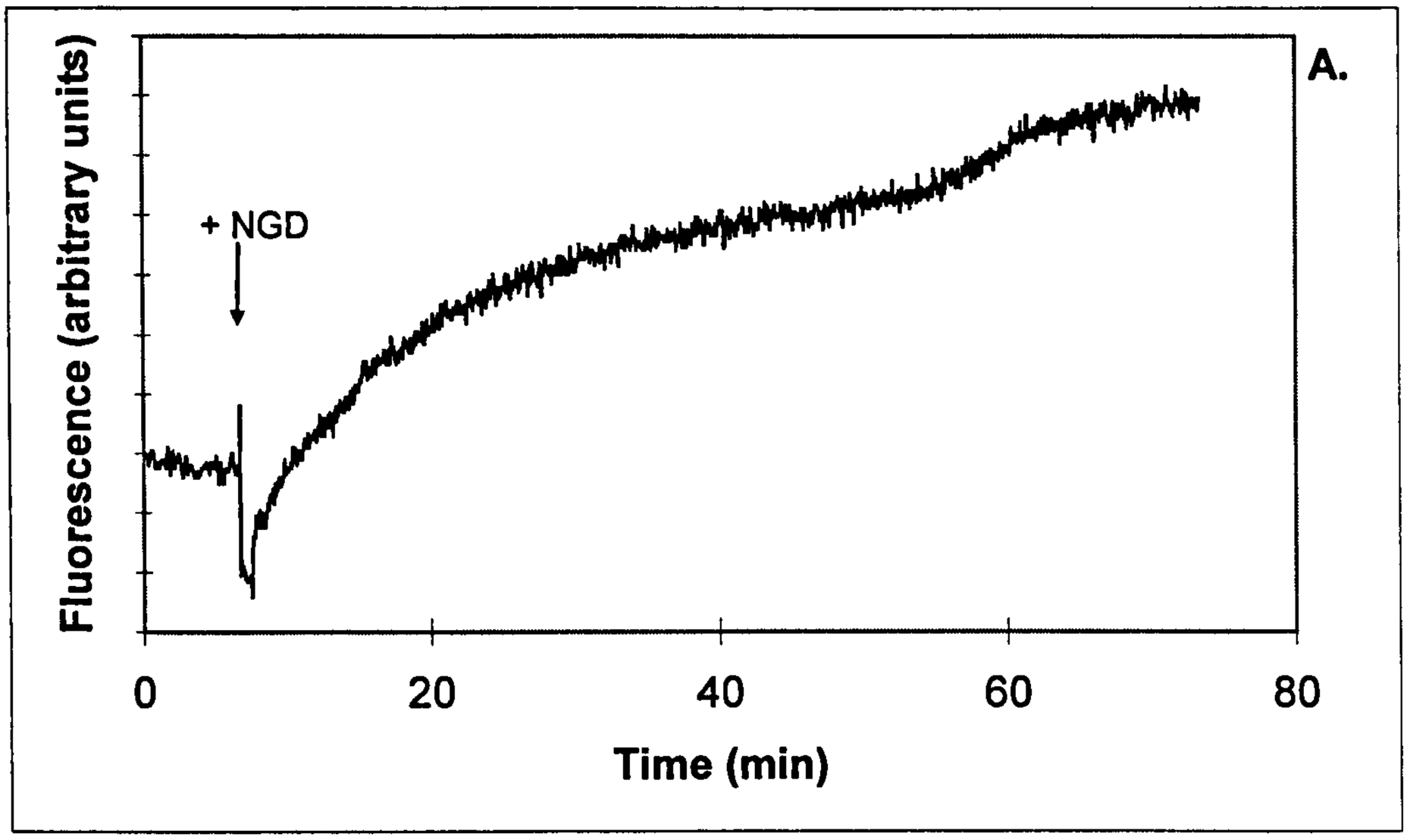

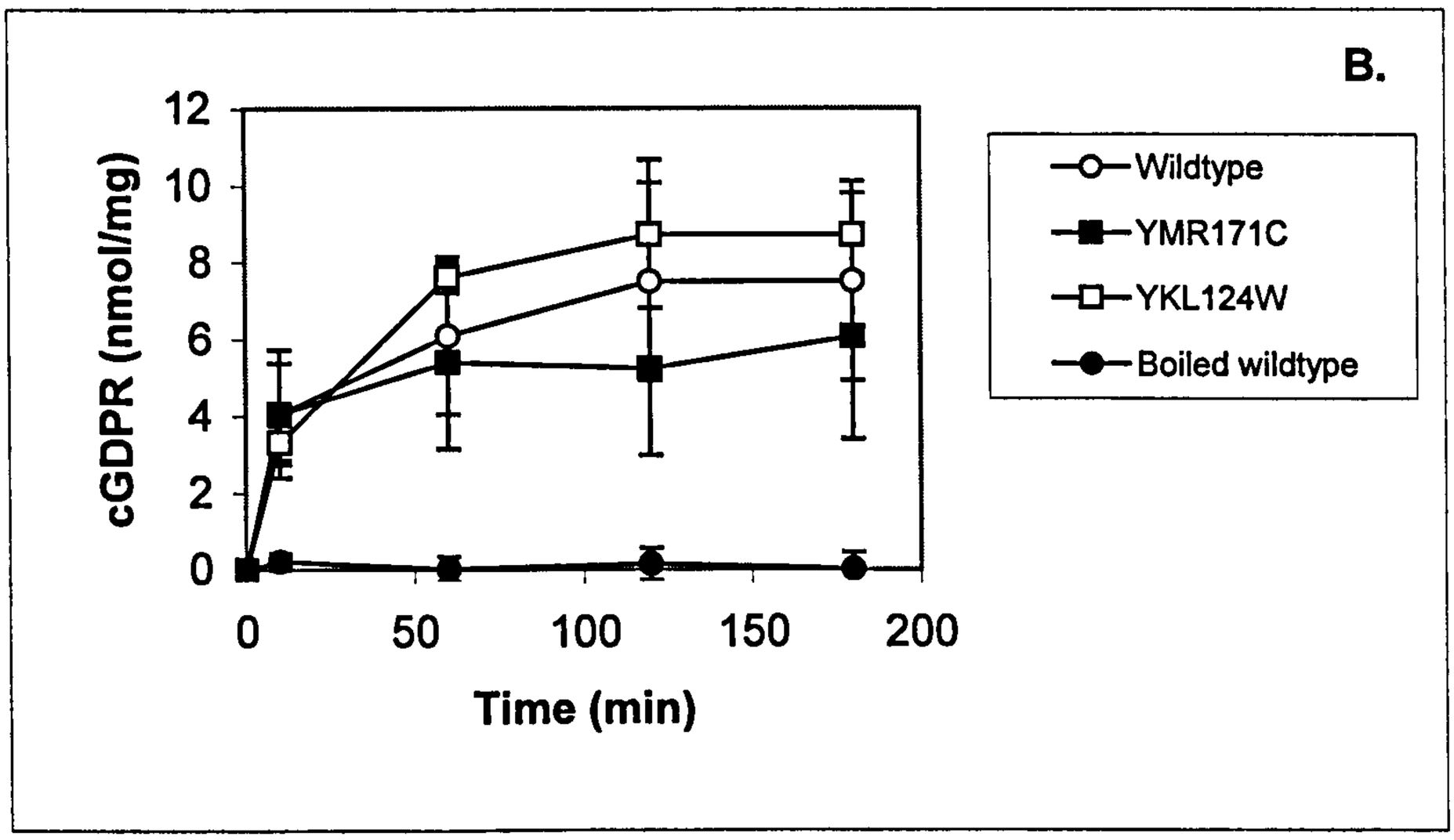

Figure 5.7. Yeast microsomes prepared from wildtype and SPRY gene deletion strains demonstrate ADP-ribosyl cyclase activity

Microsomes prepared from wildtype or mutant strains of yeast with SPRY genes YMR171C and YKL124W knocked were assayed for ADP-ribosyl cyclase activity by incubating them with 40 μM NGD as described. Changes in fluorescence were monitored with a luminescence spectrophotometer. Boiled microsomes were assayed as a negative control. **A.** Original recording of fluorescence produced by wildtype microsomes. **B.** Summary of results from three independent experiments on wildtype and mutant microsomes.

5.4. Discussion

BLAST searches of the available plant databases identified several protein sequences that contained both homologous regions to $InsP_3Rs$ and RyRs and putative membrane spanning domains (Table 5.2). The hypothetical proteins encoded by genes *At2G22020* and *At1G51450* were predicted to contain a SPRY domain (Figure 5.3) and at least one membrane-spanning domain. SPRY domains are found in all RyRs and although they are of unknown function they have been used in conjunction with EF-hand domains by bioinformaticists in the analysis of RyR sequences (Ponting *et al.*, 1997). Phylogenetic analysis of proteins containing SPRY domains indicate that the sequences included fall into three major groups: (1) Butyrophilin-related and RBCC proteins; (2) Human p532 and (3) ASH2, stonustoxin related proteins, nuclear scaffold proteins, RanBPM homologues, DEAD-box proteins and RyR. *At2G22020* falls in group 3 (Figure 5.4). The putative ryanodine-binding protein, T41256, identified in yeast also resides in group 3.

Although *At2G22020* did not appear to encode an EF-hand domain, as would be expected in a channel with high affinity for Ca^{2+}, its similarity to the SPRY domain and of RyR and possible membrane association prompted further analysis using knockout mutants. The Wisconsin T-DNA transformed *Arabidopsis* line was screened, however no T-DNA insert could be found in *At2G22020*. Yeast knockout mutants containing a deletion of homologues of *At2G22020* gene are commercially available and were used to search for differences in phenotype arising from the deletion. It was hypothesised that deletions affecting Ca^{2+} transport and homeostasis would affect mutant yeast growth during Ca^{2+} starvation more dramatically than the wildtype. However, no differences in phenotype could be detected when varying concentrations of the Ca^{2+}-chelator BAPTA were included in the growth media (Figure 5.5). There were also no differences in uptake of Ca^{2+} into microsomes prepared from wildtype and mutant strains of yeast (Figure 5.6). The ligand cADPR (10 μM) was unable to release significantly more Ca^{2+} from the microsomes than the negative control (water) suggesting the absence of Ca^{2+} channels responsive to cADPR.

Assaying yeast microsomes with the cGDPR fluorescence assay indicated, for the first time, that yeast may be capable ADP-ribosyl cyclase activity (Figure 5.7). The presence of cyclase activity suggests that yeast might use cADPR as a second messenger. If true, based on the evidence from other organisms, it is likely that

cADPR would be used in Ca^{2+}-homeostasis. Although the previous experiments indicated that cADPR was unable to elicit Ca^{2+}-mobilisation from yeast microsomes, it is possible that the microsome preparations used for the Ca^{2+}-transport studies were not suitable for the functional recovery of RyR homologues, and thus their existence in yeast can not be ruled out.

Considering the extensive biochemical and electrophysiological evidence for ligand-gated Ca^{2+} channels in plants, the absence of $InsP_3R$ and RyR homologues in the *Arabidopsis* genome is a surprise. One of the reasons *Arabidopsis* was initially chosen as a model plant for sequencing is due to its small nuclear genome size of approximately 125 megabases (of which 115.4 megabases have been sequenced; The *Arabidopsis* Genome Initiative, 2000). While this made it ideal for a genome sequencing project it seems likely that the *Arabidopsis* genome will not be representative of the majority of plants, especially as plant genomes are known to vary in size by several orders of magnitude, even within closely related species (Wendle *et al.*, 2002). Thus, it is possible that *Arabidopsis* may have lost ligand-gated channels from their repertoire of proteins while they still remain in other plants. Comparative analysis of the genomes of *Arabidopsis* and *C. elegans* has indicated that although *Arabidopsis* has a similar number of membrane transporters to *C. elegans* (~600 and ~700, respectively) it has 50% fewer channel proteins, approximately half of which are aquaporins (The *Arabidopsis* Genome Initiative, 2000). However, whether this deficit of channel proteins is an accurate reflection of the genomes of other plants is unknown.

One of the most intriguing discoveries of recent genome sequencing projects is that while essential intracellular processes, such as translation, appear to be conserved across kingdoms, organisms from different kingdoms use different sets of components to perform physiological processes. For example, comparative analysis between *Arabidopsis*, *C. elegans* and *Drosophila* demonstrates that plants have none of the components of several important signalling pathways found in *C. elegans* and *Drosophila* including receptor tyrosine kinase/Ras and nuclear steroid hormone receptors (The *Arabidopsis* Genome Initiative, 2000). As *Arabidopsis* has an abundance of MAP kinase (which lies downstream of the regulatory protein Ras) it has been proposed, by The *Arabidopsis* Genome Initiative (2000), that *Arabidopsis* (and other plants) may have evolved unique signalling pathways by combining a conserved MAP kinase cascade with new receptor types. Ligand-gated Ca^{2+}-release pathways may have undergone a similar transition, with the resulting

gene sequence divergence between RyRs and $InsP_3Rs$ and their functional equivalents in *Arabidopsis* being so extensive that they can not be identified by homology searches.

6. Concluding remarks and future work

The objective of this thesis was to investigate the characteristics and modes of control of ligand-gated Ca^{2+}-channels in higher plants, in an attempt to elucidate the mechanism by which plant cells are able to use Ca^{2+} as a signal for a diverse array of stimuli. Conclusions arising from the data have been discussed in previous chapters. In this chapter the conclusions are summarised and the direction future work should go in is considered.

6.1. *cADPR metabolism*

6.1.1. Summary

In Chapter 2 evidence indicating that the basal level of cADPR is in the low pmol/mg range (0.1-10 pmol/mg) and that plant tissue possesses ADP-ribosyl cyclase activity (with a rate of formation of cGDPR of 0.2-0.8 nmol/mh.h) was presented. These results argue in favour of cADPR having a physiological role in plant cells. In Chapter 3 the ADP-ribosyl cyclase activity of cauliflower was further characterised using the spectrophotometric assay for cGDPR and a radiometric assay monitoring the formation of [^{32}P]cADPR. The rate of formation of cGDPR was found to be dependent on the concentration of NGD in the assay, with a V_{max} of 2.8 μmol/g.h., and a K_m of 130.4 μM. Subcellular fractionation of cauliflower tissue indicated that the majority of the ADP-ribosyl cyclase activity was membrane bound. The activity of the soluble fraction was slightly activated by cGMP and demonstrated greater hydrolase activity than the membrane fraction. Other characteristics of the membrane bound cyclase activity, such as pH-dependence and lack of stimulation by ATP, are consistent with a monofunctional cyclase lacking hydrolase activity, similar to the ADP-ribosyl cyclase of *Euglena* (Masuda *et al.*, 1997). These results suggest that two forms of the enzyme may be present in cauliflower, membrane bound and soluble. Attempts to purify the activity from cauliflower microsomes resulted in a 49-fold increase in specific activity and the enrichment of a group of proteins (35-60 kDa).

6.1.2. Future work

The spectrophotometric assay provides a convenient means for monitoring ADP-ribosyl cyclase and hydrolase activity in plant tissue and should be used to further characterise these activities. Initial purification of ADP-ribosyclase activity indicates that a significant increase in specific activity can be achieved through sequential chromatographic steps. It is likely that this purification could be substantially improved through the inclusion of additional purification steps, such as affinity chromatography. The dye ligand Cibracon blue F3G-A is commonly used in the purification of enzymes interacting with NAD and NADP, due to its structural similarity with nucleotide cofactors, and may be useful in extracting ADP-ribosyl cylase activity from plant tissue. The low activity of ADP-ribosyl cyclase in cauliflower and other plant tissue presents difficulties when attempting to accurately measure the effects of metabolic regulators. A purified preparation could overcome problems with low activity and would also provide a means for obtaining sequence information.

Ziegler *at al.* (1997) successfully identified ADP-ribosyl cyclase in bovine liver mitochondria in a visualisation technique that combines SDS-PAGE electrophoresis and a variation of the spectrophotometric assay. Following separation of purified mitochondrial NADase by SDS-PAGE the gel was incubated with NAD or its fluorescent analogue, nicotinamide hypoxanthine dinucleotide (NHD). When viewing the gel on a UV-transilluminator with a 550 nm interference filter the authors observed the formation of fluorescent products, indicative of cyclase activity, allowing them to identify the proteins responsible. This assay could prove useful for identifying proteins with cyclase activity in purified plant preparations.

In animal systems basal cADPR levels have been measured at 100-200 nM (Walseth *et al.*, 1991) using a bioassay with sea urchin egg microsomes. Preliminary measurements of cADPR in plant tissue have been made with this assay (Bewell, 1999). This assay and/or HPLC could be used to further quantify cADPR metabolism in plant cells. The anion exchange resin AG MP-1 has been extensively used in the separation of nucleotides (Axelson *et al.*, 1981). These techniques would also prove useful in developing the quantitative assays necessary for monitoring metabolic changes in cADPR and NAADP in plants.

Results from NGD spectrophotometric assay indicate the yeast also possesses ADP-ribosyl cyclase activity (Chapter 5). Although *Pichia pastoris* has been used as an expression system for CD38 (Fryxell *et al.*, 1995) little is known about the role of ligand-gated Ca^{2+} channels (if any) in yeast or how they might metabolise ligands such as cADPR. As $InsP_3$ has been shown to release calcium from the vacuolar stores of *Saccharomyces cerevisiae* (Belde *et al.*, 1993) it is possible that yeast share similar mechanisms of Ca^{2+} homeostasis and signalling with plants. The results of the spectrophotometric assay support this proposition, however further studies are required. The spectrophotometric and HPLC techniques described above would prove useful in further characterising cyclase activity. As yeast possess sizeable vacuoles they may prove amenable to an electrophysiological approach similar to that carried out in plants.

6.2. Regulation of calcium release

6.2.1. Summary

Ligand-induced release of Ca^{2+} from cauliflower microsomes was monitored using a $^{45}Ca^{2+}$-radiometric flux assay. Ca^{2+} release was observed to be mediated by pH, redox agents, and, in the case of cADPR-induced release, by Ca^{2+}, indicating that these signal transduction components are capable of acting as endogenous modulators of $[Ca^{2+}]_c$ (Chapter 4).

The effect of pH on release was very similar to that seen with microsomes prepared from sea urchin eggs and may arise from a similar mechanism, possibly involving changes in ligand binding efficiency.

Oxidising agents, such as H_2O_2, have been demonstrated to activate the ligand-gated channels of animal cells over the concentration range used here (Favero *et al.*, 1995; Nam *et al.*, 2002). In plant cells H_2O_2 has also been show to activate PM Ca^{2+}-channels (Pei *et al.*, 2000). The biphasic effect of H_2O_2 observed here suggests that the channels responsible for the release of Ca^{2+} from internal stores can be activated by low levels of H_2O_2 while they are inhibited at higher concentrations. This raises the fascinating possibility that plant cells may use the redox state of the cell to determine whether increases in $[Ca^{2+}]_c$ arise from Ca^{2+}

originating from internal or external stores. Although biphasic regulation of ligand-channels through redox has been described in animal cells, i.e. in the modulation of $InsP_3$-induced release by thimerosal in cerebellar microsomes (Sayers *et al.*, 1993), the possibility that redox determines whether Ca^{2+} is of intra- or extra-cellular origin has not been extensively addressed.

Previously vacuolar ligand-gated Ca^{2+} release has been reported as being insensitive to changes in concentration of Ca^{2+}, indicating that these release pathways can not contribute to CICR in the manner witnessed in animal cells (see section 1.3.3.3). $^{45}Ca^{2+}$-flux experiments carried out here with microsomes prepared from meristematic tissue (enriched in ER and depleted in vacuolar membranes) indicate that, at normal physiological concentrations, ligand-induced Ca^{2+}-release is independent of Ca^{2+}. However, release of Ca^{2+} by cADPR in the presence of 1 mM $CaCl_2$ demonstrated an increase in activity. While this needs to be investigated further it raises the possibility that different populations of ligand-gated channels may exist in plant cells, with ones on the ER differentially regulated to those of the vacuolar membrane.

The $^{45}Ca^{2+}$-flux assay is also a powerful tool for screening for novel release agents. Release assays utilising cauliflower meristematic microsomes demonstrated that $InsP_6$ and GSH are potential Ca^{2+}-release agents in plants.

6.2.2. Future work

The regulation of ligand-gated Ca^{2+} release in animal cells has been characterised by following changes in binding of radio-labelled ligands after treatment with the regulator (Takasago *et al.*, 1991; Vanlingen *et al.*, 2000). This technique should be used to complement Ca^{2+}-release studies on plant microsomes. High-affinity binding sites for $InsP_3$ have previously been identified and partially characterised in red beet using [^{3}H]$InsP_3$ (Brosnan & Sanders, 1993) and it is likely that similar techniques using radio-labelled cADPR and NAADP can be developed. As the authors data indicate that the abundance of $InsP_3$-specific binding sites is very low (840 fmol/mg, 10- to 100- fold lower than reported in cerebellum) the use of higher activity radioisotopes (such as, ^{32}P with a specific radioactivity of 9128 Ci/mmol, compared to 28.7 Ci/mmol of ^3H) could facilitate binding studies.

One question arising from the study of regulators on Ca^{2+}-release from cauliflower microsomes is that concerning the mechanism of the biphasic effect of H_2O_2. One possibility is that H_2O_2 stimulates ligand-binding at low concentrations through a direct interaction with the ligand receptor and inhibits binding at high concentrations, possibly through peroxidation and destruction of the supporting membrane, in a similar manner to Ca^{2+}-relase channels isolated from skeletal muscle sarcoplasmic reticulum (Favero *et al.*, 1995). This proposition can be most effectively tested using a combined approach with both ligand-binding assays and electrophysiological techniques.

A second question arising from the study of regulators on Ca^{2+}-release is that of the differences in regulation of Ca^{2+}-permeable channels of different membranes. The biphasic regulation of Ca^{2+}-release by H_2O_2 and the activation of Ca^{2+}-release by Ca^{2+} observed in cauliflower microsomes contrast, respectively, with reports that H_2O_2 activates PM Ca^{2+}-permeable channels (Pei *et al.*, 2000) and that neither $InsP_3$ or cADPR gated currents across vacuolar membranes are activated by Ca^{2+} (Allen & Sanders, 1994b; Leckie *et al.*, 1998). Possible differences between ligand-gated Ca^{2+}-release pathways associated with specific membranes needs to be addressed using sucrose-density separated microsomes (as described in Navazio *et al.*, 1999) and comparing the effects of regulators on Ca^{2+} release from vesicles colocalising with ER or PM marker enzyme activity.

The ability of $InsP_6$ and GSH to mobilise Ca^{2+} from cauliflower microsomes needs to investigated in more detail. A recent report by Lemitri-Chlieh *et al.* (2000) indicates that $InsP_6$ modulates K^+ currents in guard cells through a Ca^{2+}-dependent mechanism (with a 100-fold greater potency than $InsP_3$) and may have a physiological role in the response of guard cells to ABA. Further studies using the $^{45}Ca^{2+}$-flux assay and electrophysiological approaches are necessary to determine if physiological concentrations of $InsP_6$ are capable of releasing Ca^{2+}. Cross desensitisation experiments analogous to those used for $InsP_3$ and cADPR (Allen *et al.*, 1995) would be beneficial in determining if $InsP_6$ acts through a separate pool of Ca^{2+} to other ligands. GSH has been identified as an inhibitor of Ca^{2+}-release channels and an activator of Ca^{2+}-pumps in animal

tissue (Belia *et al.*, 2000). Electrophysiological techniques should be employed to determine its role in plant cells.

6.3. Database search for RyR and $InsP_3R$ homologues

6.3.1. Summary

Sequence analysis of the *Arabidopsis* genome uncovered no sequences with extensive homology to $InsP_3R$ and RyR (Chapter 5). Two hypothetical protein sequences were identified that contained a SPRY domain homologous to those found in RyRs and putative transmembrane domains requisite of a channel protein. However, the predicted protein size of these sequences is far smaller than known RyRs. Furthermore, they do not demonstrate any homology with known Ca^{2+}-permeable pores. The lack of homology between these sequences and that of other Ca^{2+} channels indicates that if they are indeed involved in cADPR-release pathways they may either form novel Ca^{2+} channels, or be accessory proteins involved in the regulation of a Ca^{2+} channel.

6.3.2. Future work

For a comprehensive understanding of ligand-gated Ca^{2+} release pathways in plant cells it is imperative that the Ca^{2+} channels responsible are identified at a molecular level. Radio-labelled ligands have been used in the identification, and purification of ligand-gated Ca^{2+} channels in animals (Ferris *et al.*, 1989; Anderson *et al.* 1989). As computer searches of protein databases have failed to reveal RyR or $InsP_3R$ homologues similar methodologies need to be followed to identify receptors in plants. As mentioned above [^{3}H]$InsP_3$-binding proteins have already been identified in red beet. Scaling up this procedure should provide enough protein for in-gel micro-sequencing techniques which require 50-100 pmoles of protein (Küster *et al.*, 1997). Although initial [^{32}P]cADPR binding studies to plant microsomes have proven unsuccessful (A. Siddiquia, University of York; personal communication) preliminary binding indicated cauliflower meristematic microsomes are capable of binding [^{32}P]NAADP (data not shown). The pharmacology of NAADP-dependent release in cauliflower indicates that plants share a unique inactivation phenomenon with sea urchins (Navazio *et al.*,

2000). When microsomes are treated with a low nanomolar dose of NAADP (subthreshold in respect to Ca^{2+} release) prior to Ca^{2+}-release the release is fully inactivated. This is thought to arise from irreversible, or very slowly reversing, binding of NAADP to its receptor (Galione *et al.*, 2000) and is currently being used to tag NAADP receptors in sea urchin microsomes with [^{32}P]NAADP to aid recovery during purification. It is likely that tagging NAADP binding proteins in plant tissue in this manner could be used in a comparable purification strategy.

The nature of proteins containing SPRY domains in *Arabidopsis* remains to be determined. Preliminary searches of the recently sequenced rice genome (Goff, *et al.*, 2002; Yu *et al.*, 2002) gave comparable results to that of the *Arabidopsis* genome, i.e. several hypothetical SPRY domain proteins were identified but no RyR or $InsP_3R$ homologues (data not shown). Yeast mutant strains are commercially available that have had the genes for SPRY domain containing proteins deleted. Binding-studies comparing mutant and wildtype strains would be valuable for a preliminary determination of whether these proteins are acting as cADPR receptors. If binding is detected recombinant expression of SPRY containing proteins would allow further characterisation of the protein.

7. References

Aarhus, R., Graeff, R.M., Dickey, D.M., Walseth, T.F. & Lee, H.C. (1995). ADP-ribosyl cyclase and CD38 catalyze the synthesis of a calcium-mobilising metabolite from NADP. *J. Biol. Chem.* **270**: 30327-30333.

Adebanjo, O.A., Anandatheerthavarada, H.K., Koval, A.P., Moonga, B.S., Biswas, G., Sun, L., Soam, B.R., Bevis, P.J.R., Huang, C. L.-H., Epstein, S., Lai, F.A., Avadhani, N.G. & Zaidi, M. (1999). A new function for CD38/ADP-ribosyl cyclase in nuclear Ca^{2+} homeostasis. *Nature Cell Biol.* **1**: 409-414.

Airey, J.A., Beck, C.F., Tanksley, S.L., Murakami, K., Deerinck, T.J., Ellisman, M.H. & Sutko, J.L. (1991). Identification and localization of 2 triad junctional foot protein isoforms in mature avian fast twitch skeletal-muscle. *J. Biol. Chem.* **265**: 14187-14194.

Ajdic, D., McShan, W.M., Savic, D.J., Gerlach, D. & Ferretti, J.J. (2000). The NAD-glycohydrolase (*nga*) gene of *Streptococcus pyogenes*. *FEMS Microbiol. Lett.* **191**: 235-241.

Alexandre, J., Lassalles, J.P., Kado, R.T. (1990). Opening of Ca^{2+} channels in isolated red beet root vacuole membrane by inositol 1,4,5-trisphosphate *Nature* **343**:567

Allen, G.J. & Sanders, D. (1994a). Two voltage-gated, calcium release channels coreside in the vacuolar membrane of broad bean guard cells. *Plant Cell* **6**: 685-694.

Allen, G.J., & Sanders, D. (1994b). Osmotic stress enhances the competence of *Beta vulgaris* vacuoles to respond to inositol 1,4,5-trisphosphate. *Plant J.* **6**: 687-695.

Allen, G.J. & Sanders, D. (1995). Calcineurin, a type 2B protein phosphatase, modulates the Ca^{2+}-permeable slow vacuolar ion channel of stomatal guard cells. *Plant Cell* **7**: 1473-1483.

Allen, G.J. & Sanders, D. (1997). Vacuolar ion channels of higher plants. *Adv. Bot. Res.* **25:** 218-252.

Allen, G.J., Sanders, D. (1996). Control of ionic currents in guard cell vacuoles by cytosolic and luminal calcium. *Plant J.* **10**: 1055-1069.

Allen, G.J., Chu, S.P., Harrington, C.L., Schumacher, K., Hoffman, T., Tang, Y.Y., Grill, E., and Schroeder, J.I. (2001). A defined range of guard cell calcium oscillation parameters encodes stomatal movements. *Nature* **411**: 1053–1057

Allen, G.J., Chu, S.P., Schumacher, K., Shimazaki, C.T., Vafeados, D., Kemper, A., Hawke, S.D., Tallman, G., Tsien, R.Y., Harper, J.F., Chory, J., and Schroeder, J.I. (2000). Alteration of stimulus-specific guard cell calcium oscillations and stomatal closing in *Arabidopsis* det3 mutant. *Science* **289**, 2338–2342.

Allen, G.J., Kwak, J.M, Chu, S.P., Lloppis, J., Tsien, R.T., Harper, J.F. & Schroeder, J.I. (1999). Cameleon calcium indicator reports cytoplasmic calcium dynamics in *Arabidopsis* guard cells. *Plant* J. 19: 735-747.l

Allen, G.J., Muir, S.R. & Sanders, D. (1995). Release of Ca^{2+} from individual plant vacuoles by both $InsP_3$ and cyclic ADP-ribose. *Science* **268**: 735-737.

Altschul, J.M., Madden, T.L., Schaeffer, A.A., Zhang, J., Zhang, Z., Miller, W., Lipman, D.J. (1997). Gapped BLAST and PSI-BLAST: a new generation of protein database search programs. *Nucleic Acid Res* **25**: 3389-3402.

Amundson, J. & Clapham, D. (1993) Calcium waves. *Curr. Opinion. Neurobiolo.* **3:** 375-382.

Anderson, K., Lai, F.A., Liu, Q.Y., Rousseau, E., Erickson, H.P., Meissner, G. (1989). Structural and functional characterization of the purified cardiac ryanodine receptor-Ca^{2+} release channel complex. *J. Biol. Chem.* **264**: 1329-1335.

Andreev, I.G., Koren'Kov, Y.G. & Molotkovsky, Y.G. (1990).Calmodulin stimulation of Ca^{2+} - NH^{+} antiport across the vacuolar membrane of sugar-beet taproot. *Plant Physiol.* **136**: 3-7.

Anzai, K, Ogawa, K., Kuniyasu, A., Ozawa, T., Yamamoto, H. & Nakayama, H. (1998). Effects of hydroxyl radical and sulfhydryl reagents on the open probability of the purified cardiac ryanodine receptor channel incorporated into planar lipid bilayers. *Biochem Biophys Research Commun.* **259:**: 938-942.

The *Arabidopsis* Genome Initiative (2000). Analysis of the genome sequence of the flowering plant *Arabidopsis thaliana*. *Nature* **408**: 796-815.

Arazi, T. Kaplan, B. & Fromm, H. (2000). A high affinity calmodulin-binding site in a tobacco plasma-membrane channel protein coincides with a characteristic element of cyclic nucleotide-binding domains. *Plant Mol. Biol.* **42**: 591-601.

Arazi, T., Sunker, R., Kaplan, B., Fromm, H. (1999). A tobacco plasma membrane calmodulin-binding transporter confers Ni^{2+} tolerance and Pb^{2+} hypersensitivity in transgenic plants. *Plant J.* **20**: 171-182.

Armstrong, F., Leung, J., Grabov, A., Brearley, J., Giraudat, J. & Blatt, M.R. (1994). Sensitivity to abscissic acid of guard-cell K^{+} channels is suppressed by *abi-1*, a mutant *Arabidopsis* gene encoding a putative protein phosphatase. *Proc. Natl Acad. Sci. USA* **92**: 9520-9524.

Asada, K. (1994). Production and action of active oxygen species in photosynthetic tissues. In: Foyer CH, Mullineaux PM, eds. *Causes of photooxidative stress and amelioration of defense systems in plants*. Boca Raton, FL, USA: CRC Press, 77-104.

Assman, S.M. (1993). Signal transduction in guard cells. *Ann. Rev. Cell Biol.* **9**: 345-375.

Axelsen, K.B. & Palmgreen, M.G. (1998). Evolution of substrate specificities in the P-type ATPase superfamily. *J. Mol. Evol.* **46**: 84-101.

Axelson, J.T., Bodley, J.W., Walseth, T.F. (1981). A volatile liquid chromatography system for nucleotides. *Anal Biochem.* **116:** 357-360.

Bak, J., White, P., Timár, G., Missiaen, L., Genazzani, A.A. & Galione, A. (1999). Nicotinic acid adenine dinucleotide phosphate triggers Ca^{2+} release from brain microsomes. *Current Biol.* **9**: 751-754.

Balshaw, D.M., Xu, L., Yamaguchi, N., Pasek, D.A. & Meissner, G. (2001). Calmodulin binding and inhibition of cardiac muscle calcium release channel (ryanodine receptor). *J. Biol. Chem.* **276**:20144-20153.

Baluska, F., Samaj, J., Napier, R., & Volkmann, D. (1999). Maize calreticulin localizes preferentially to plasmadesmata in root apex. *Plant J.* **19**:481-488.

Baum, G., Chen, Y., Arazi, T., Takatsuji, H. & Fromm, H. (1993). A plant glutamate decarboxylase containing a calmodulin binding domain: Cloning, sequence and functional analysis. *J. Biol. Chem.* **268**: 19610-19617.

Belde, P.J., Vossen, J.H., Borst-Pauwels, G.W., Theuvenet, A.P. (1993).Inositol 1,4,5-trisphosphate releases Ca^{2+} from vacuolar membrane vesicles of *Saccharomyces cerevisiae*. *FEBS Lett.* 323:113-8

Berridge, M.J., Galione, A. (1988). Cytosolic calcium oscillators. *FASEB J.* **2**: 3074-3082.

Berridge, M.J. & Irvine, R.F. (1989). Inositol lipids and cell signalling. *Nature,* **341:** 197-205.

Berridge, M.J. (1993). Inositol trisphosphate and calcium signalling. *Nature* **361**: 315-325.

Berridge, M.J. (1997). Elementary and global aspects of calcium signalling. *J. Exp. Biol.* **200**: 315-319.

Berridge, M.J., Lipp. P. & Bootman, M.D. (2000). The versatility and universitality of calcium signalling. *Nature Rev Mol. Cell Biol.* **1**: 11-21.

Bers, D.M., Patton, C.W., Nuccitelli, R. (1994). A practical guide to the preparation of Ca^{2+} buffers. *Methods Cell Biol.* **40**: 3-29.

Bethk, P.C. & Jones, R.L. (1994). Ca^{2+}-calmodulin modulates ion channels activity in storage protein vacuoles of barley aleurone cells. *Plant Cell* **6**: 277-285

Bethke, P.C. & Jones, R.J. (1997). Reversible protein phosphorylation regulates the activity of the slow-vacuolar ion channel. *Plant J.* **11**: 1227-1235.

Bewell, M.A. (1999). Mechanisms of calcium homeostasis at higher plant endomembranes. Dphil Thesis, University of York.

Bewell, M.A., Maathius, F.J.M, Allen, G.J. & Sanders, D. (1999). Calcium induced calcium release mediated by a voltage-activated cation channel in vacuolar vesicles from red beet. *FEBS Letts.* **458**: 41-44.

Bezprozvanny, I., Ehrlich, B.E. (1993). ATP modulates the function of inositol 1,4,5-trisphosphate-gated channels at two sites. *Neuron* **10**: 1175-1184.

Biermann, B., Johnson, E.M. & Feldman, L.J. (1990). Characterization and distribution of a maize cDNA encoding a peptide similar to the catalytic region of second messenger dependent protein kinases. *Plant Physiol.* **94**: 1609-1615.

Biswas, G., Adebanjo, O.A., Freedman, B.D., Anandatheerthavarada, H.K., Vijayasarathy, C., Zaidi, M., Kotlikoff, M. & Avadhani, N.G. (1998). Retrograde Ca^{2+} signalling in C2C12 skeletal muocytes in response to mitochondrial genetic and metabolic stress: a novel mode of inter-organelle crosstalk. *EMBO J.* **18**: 522-533.

Biswas, S., Dalal, B., Sen, M. & Biswas, B. (1995). Receptor for *myo*-inositol trisphosphate from the microsomal fraction of *Vigna radiata*. *Biochem. J.* **306**: 631-636.

Blackbourn, H.D., Battey, N.H. (1993). Annexin-mediated secretory vesicle aggregation in plants. *Plant Physiol.* **89**: 27-32.

Blackford, S., Rea, P.A., Sanders, D. (1990). Voltage sensitivity of H^+/Ca^{2+} antiport in higher plant tonoplast suggests a role in vacuolar calcium accumulation. *J. Biol. Chem.* **265**: 9617-9620.

Blatt, M.R. & Armstrong, F. (1993). K^+ Channels of stomatal guard cells: abscissic acid evoked cpntrol of the outward rectifier mediated by cytoplasmic pH. *Planta* **191**: 330-341.

Blatt, M.R., Thiel, G., Trentham, D.R. (1990). Reversible inactivation of K^+ channels of Vicia stomatal guard cells following the photolysis of caged inositol 1,4,5-trisphosphate. *Nature* **345**: 766-769.

Blazev, R. & Lamb, G. D. (1999). Low [ATP] and elevated [Mg^{2+}] reduce depolarization-induced Ca^{2+} release in rat skinned skeletal muscle fibres. *Journal of Physiology* **520**: 203-215

Blume, B., Nurnberger, T., Nass, N. & Scheel, D. (2000). Receptor-mediated increase in cytoplasmic free calcium required for activation of pathogen defense in parsley. *Plant Cell* **12**:1425-1440.

Blumwald, E. and Poole, R.J. (1986). Kinetics of Ca^{2+}/H^+ antiport in isolated tonoplast vesicles from storage tissue of *Beta vulgaris* L. *Plant Physiol.* **80**: 727-731.

Blumwald, E. (1987). Tonoplast vesicles as a tool in the study of ion-transport at the plant vacuole. Physiol plantarum **69**: 731-734.

Bolwell, G.P. (1995). Cyclic AMP, the reluctant messenger in plants. *Trends Biochem. Sci.* **20**: 492-495.

Bonza, M.C., Morandini, P., Luoni, L., Geisler, M., Palmgren, M.G., De Michelis, M.I. (2000). At-ACA8 encodes a plasma membrane-localized calcium-ATPase of Arabidopsis with a calmodulin-binding domain at the N terminus. *Plant Physiol.* **123**: 1495-1506.

Bootman, M.D. & Berridge, M.J. (1995). The elemental principles of calcium signalling. *Cell* **83**: 675-678.

Bootman, M.D., Berridge, M.J. & Lipp, P. (1997). Cooking with calcium: The recipes for composing global signals from elementary events. *Cell* **91**: 367-373.

Bowler, C., Neuhaus, G., Yamagata, H., & Chua, N.H. (1994). Cyclic-GMP and calcium mediate phytochrome transduction. *Cell* **77:** 73-81.

Bowler, C., Van Montagu, M., & Inzé, D. (1992). Superoxide dismutase and stress tolerance. *Annu. Rev. Plant Physiol. Plant Mol. Biol.* **43**: 83-116.

Bradford, M.M. (1976). A rapid and sensitive method for the quantitation of microgram quantities of protein utilizing the principle of protein dye binding. *Anal. Biochem.* **72**: 258-256.

Brearley, C.A., Hanke, D.E. (2000). Metabolic relations of inositol 3,4,5,6-tetrakisphosphate revealed by cell permeabilization. Identification of inositol 3,4,5, 6-tetrakisphosphate 1-kinase and inositol 3,4,5,6-tetrakisphosphate phosphatase activities in mesophyll cells. *Plant Physiol.* **122**:1209-1216.

Brearley, C.A., Parmar, P.N. & Hanke, D.E. (1997) Metabolic evidence for PtdIns(4,5)P-2-directed phospholipase C in permeabilized plant protoplasts. *Biochem. J.* **324**: 123-131.

Brosnan, J.M. & Sanders, D. (1993). Identification and characterisation of high-affinity binding sites for inositol trisphosphate in red beet. *Plant Cell* **5**: 931-940.

Brown, E.G. & Newton, R.P. (1992). Analytical procedures for cyclic nucleotides and their associates enzymes in plant tissue. *Phytochem. Anal.* **3**:1-13.

Brownlee, C. & Wood, J.W. (1986). A gradient of cytoplasmic free calcium in growing rhizoid cells of *Fucus serratus*. *Nature* **320**: 624-626.

Bunney, T.D., Shaw, P.J., Watkins, P.A.C., Taylor, J.P., Beven, A.F., Wells, B., Calder, G.M. & Drøbak, B.K. (2000). ATP-dependent regulation of nuclear Ca^{2+} levels in plant cells. *FEBS Lett.* **476**: 145-149.

Burgess, G.M., Irvine, R.F., Berridge, M.J., McKinney, J.S. & Putney, J.W. Jr. (1984). Actions of inositol phosphates on calcium pools in guinea pig hepatocytes. *Biochem. J.* **224**: 741-746.

Bush, D.R. & Sze, H. (1986). Calcium-transport in tonoplast and endoplasmic-reticulum vesicles isolated from cultured carrot cells. *Plant Physiol.* **80**: 549-555.

Bush, D.R. (1995) Calcium regulation in plant cells and its role in signalling. *Annu. Rev. Plant Physiol.* **46:** 95-122.

Bush, D.S. & Jones, R.L. (1988). Cytoplasmic calcium and α-amylase secretion from barley aleurone protoplasts. *Eur. J. Cell Biol.* **46:** 466-469.

Bush, D.S. & McColl, J.D. (1987). Mass-action expressions of ion exchange applied to Ca^{2+}, H^{+}, K^{+} and Mg^{2+} sorbtion on isolated cell walls of leaves from *Brassica olercea*. *Plant Physiol.* **85**: 247-260.

Camacho, P. & Lechleiter, J.D. (1993). Increased frequency of calcium waves in *Xenopus laevis* oocytes that express a calcium ATPase. *Science* **260:** 226-229.

Cameron, A.M., Steiner, J.P., Sabatini, D.M., Kaplin, A.I., Walensky, L.D., Snyder, S.H. (1995). Immunophilin FK506 binding protein associated with inositol 1,4,5-trisphosphate receptor modulates calcium flux. *Proc Natl Acad Sci U S A.* **92**: 1784-1788.

Campell, A.K., Trewavas, A.J. & Knoght, M.R. (1996). Calcium imaging shows differential sensitivity to cooling and communications in luminous transgenic plants. *Cell Calc.* **19**: 211-218.

Cancela, J.M., Churchill, G.C. & Galione, A. (1999). Coordination of agonist-induced Ca^{2+}-signalling paterns by NAADP in pancreatic acinar cells. *Nature* **398**: 74-76.

Canut, H., Carrasco, A., Rossignol, M. & Ranjeva, R. (1993). Is the vacuole the richest store of inositol trisphosphate-mobilisable calcium in plant cells? *Plant Science* **90**: 135-143.

Carafoli, E. (1994). The phospholipid function of calcium and its regulation. *J. Hypertens. Suppl.* **12**:S47-56.

Carafoli, E. (1987). Intracellular calcium homeostasis. *Annu. Rev. Biochem.* **56**: 395-433.

Carpaneto, A., Cantu, A., Gambale, F. (1999). Redox agents regulate activity in vacuoles from higher plant cells. *FEBS Lett.* **442**: 129-132.

Carrion, A.M., Link, W.A., Ledo, F., Mellstrom, B & Naranjo, J.R. (1999). DREAM is a Ca^{2+}-regulated transcriptional repressor. *Nature* **398**: 80-84.

Cessna, S.G., Chandra, S. & Low, P.S. (1998). Hypo-osmotic shock of tobacco cells stimulates Ca^{2+} fluxes deriving first from external then internal Ca^{2+} stores. *J. Biol. Chem.* **273**: 27286-27291.

Chanson, A. (1991). A Ca^{2+}/H^{+} antiport system driven by the tonoplast pyrophosphate-dependent proton pump from maize roots. *J. Plant Physiol.* **137**: 471-476.

Chattaway, J.A., Drøbak, B.K., Watkins, P.A.C., Dawson, A.P., Letcher, A.J., Stephens, L.R. & Irvine, R.F. (1992). An inositol 1,4,5-trisphosphate-6-kinase activity in pea roots. *Planta* **187**: 542-545.

Chaudière, J., Ferrari-Iliou, R. (1999). Intracellular antioxidants: from chemical to biochemical mechanisms. *Food Chem Toxicol.* **37**:949-962.

Chen, X., Chang, M., Wang, B. & Wu, B. (1997). Cloning of a Ca^{2+}-ATPase gene and the role of cytosolic Ca^{2+} in the gibberelin-dependent signalling pathway in aleurone cells. *Plant J.* **11**: 363-371.

Cheng, H., Lederer, W.J., Cannell, M.B. (1993). Calcium sparks: elementary events underlying excitation-contraction coupling in heart muscle. *Science* **262**:740-744.

Cheng, S.H., Willmann, M.R., Chen, H.C., Sheen, J. (2002). Calcium □hospholip through protein kinases. The *Arabidopsis* calcium-dependent protein kinase gene family. *Plant Physiol.* **129**: 469-485.

Chin, D. & Means, A.R. (2000). Calmodulin: a prototypical calcium sensor. *Trends Cell Biol.* **10**: 322-328.

Chini, E.N., Liang, M. & Dousa, P. (1998). Differential effect upon cyclic-ADP-ribose and nicotinate-adenine dinucleotide phosphate-induced Ca^{2+} release systems. *Biochem J.* **335**: 499-504.

Clapham, D.E. (1995). Calcium signaling. *Cell* **27**:259-268.

Clarkson, D.T. & Hanson, J.B. (1980). The mineral nutrition of plants. *Anni. Rev. Plant Physiol.* **31**: 239-298.

Clayton, H., Knight, M.R., Knight, H., McAinsh, M.R. & Hetherington, A.M. (1999). Dissection of the ozone-induced calcium signature. *Plant J.* **17**: 575-579.

Cleland, R.E., Virk, S.S., Taylor, D. and Bjorkman, T. (1990). Calcium cell walls and growth. In *Calcium in Plant Growth and Developmen*t (ed. Hepler, P.K. & Leonard, R.T.), pp 9-16. Amer Soc. Plant Phsiol Symposium series, vol 4.

Clementi, R., Riccio, M., Sciorati, C., Nistico, G. & Meldolesi, J. (1996). The type 2 ryanodine receptor of neurosecretory PC12 cells is activated by cyclic ADP-ribose. Role of the nitric oxide/cGMP pathway. *J. Biol. Chem* **271**: 17739-17745.

Cohen P, & Cohen PT. (1989). Protein phosphatases come of age. *J Biol Chem.* **264**: 21435-21438.

Corpet F. (1988). Multiple sequence alignment with hierarchical clustering. *Nucleic Acids Res.* **16**: 10881-10890.

Connor, J.A. (1993). Intracellular calcium mobilization by Inositol 1,4,5-triphosphate: intracellular movements and compartmentalism. *Cell Calcium* **14**: 185-200.

Cosgrove & D.J. Hedrich, R. (1991). Stretch-activated chloride, potassium, and calcium channels coexisting in plasma-membranes of guard-cells of vicia-faba L. *Planta* **186**: 143-153.

Coté, G.C. & Crain, R.C. (1993). Biochemistry of phosphoinositides. *Ann. Rev. Physiol. Plant Mol. Biol.* **44**: 333-356.

Cote, G.C. & Crain, R.C. (1994). Why do plants have phosphoinositides? *BioEssays*, **16:** 39-46.

Coyaud, L., Kurddjian, A., Kado, R. & Hedrich, R. (1987). Ion channels and ATP-driven pumps involved in ion transport across the tonoplast of sugarbeet vacuoles. *Biocim. Biophys.Acta* **902**: 263-268.

Delledonne, M., Xia, Y., Dixon, R.A. & Lamb, C. (1998). Nitric oxide functions as a signal in plant disease resistance. *Nature* **394**: 585-588.

Delmer, D.P., Potikha, T.S. (1997). Structures and functions of annexins in plants. *Cell Mol Life Sci.* **53**:546-53.

DePass, A.L., Crain, R.C., Hepler, P.K. (2001). Inositol 1,4,5 trisphosphate is inactivated by a 5-phosphatase in stamen hair cells of *Tradescantia*. *Planta*. **213**: 518-524.

DePass, A.L. & Hepler, P.K. (1998). Delayed NAD^+ induced Ca^{2+} elevation in live plant cells: Evidence for cyclic ADP ribose synthesis. *Mol Biol Cell* **9**: 2800 Suppl. S, p483a.

DeWald, D.B., Torabinejad, J., Jones, C.A., Shope, J.C., Cangelosi, A.R., Thompson, J.E., Prestwich, G.D., Hama, H. (2001). Rapid accumulation of phosphatidylinositol 4,5-bisphosphate and inositol 1,4,5-trisphosphate correlates with calcium mobilization in salt-stressed signalling. *Plant Physiol.* **126**:759-769.

Ding, J.P. & Pickard B.G. (1993). Mechansensory calcium-selective cation channels in epidermal cells. *Plant J.* **3**: 83-110.

Downie, L., Priddle, J., Hawes, C. & Evans, D.E. (1998). A calcium pump at the higher plant nuclear envelope? *FEBS Lett.* **429**: 44-48.

Drøbak, B.K & Ferguson, I.B. (1985). Release of Ca^{2+} from plant hypocotyls microsomes by inositol 1,4,5-trisphsphate. *Biochem Biophys Res Comm.* **130**: 1241-1246.

Drøbak, B.K. & Watkins, P.A.C. (2000). Inositol (1,4,5)trisphosphate production in plant cells: an early response to salinity and hyperosmotic stress. *FEBS Letts.* **481**: 240-244.

Drøbak, B.K., Watkins, P.A.C., Chattaway, J.C., Roberts, K. & Dawson, A.P. (1991). Metabolism of inositol trisphosphate by a soluble enzyme fraction from pea roots. *Plant Phys.* **95**: 412-419.

Durner, J., Wenehenne, D. & Klessig, D.F. (1998). Defence gene induction in tobacco by nitric oxide, cyclic GMP and cyclic ADP-ribose.

Eager, K.R. & Dulhunty, A.F. (1999). Cardiac ryanodine receptor activity is altered by oxidising reagents in either the luminal or cytoplasmic solution. *J. Membrane Biol.* **167**: 205-214.

Ehrhardt, D.W., Wais, R. & Long, S.R. (1996). Calcium spiking in plant root hairs responding to *Rhizobium* nodulation signals. *Cell* **85:** 673-681.

Ehsan, H., Reichheld, J.P., Roef, L., Witters, E., Lardon, F., Vanbockstaele, D., Vanmontague, M. Inze, D. & Vanonckelen, H. (1998). Effect of indomethacin on cell cycle dependent cyclic AMP fluxes in tobacco BY-2 cells. *FEBS Letts.* **422**: 165-169.

Epstein, E. (1972). Mineral Nutrition of Plants: Principles and Perspectives. Wiley, New York.

Evans, N.H., McAinsh, M.R., Hetherington, A.M. (2001). Calcium oscillations in higher plants. *Curr Opin Plant Biol.* **4**: 415-420.

Evans, D.E. (1994). PM-type calcium pumps are associated with higher-plant cell intracellular membranes. *Cell Calcium* **15**: 241-246.

Evans, D.E., & Williams, L.E. (1998). P-type calcium ATPases in higher plants – biochemical, molecular and functional properties. *Biochemic. Biophysic. Acta* **1376**: 1-25.

Fadool, D.A., Ache, B.W. (1992). Plasma membrane inositol 1,4,5-trisphosphate-activated channels mediate signal transduction in lobster olfactory receptor neurons. *Neuron* **9**: 907-918.

Favero, T.G., Zable, A.C., Abramson, J.J. (1995). Hydrogen peroxide stimulates the Ca^{2+} release channel from skeletal muscle sarcoplasmic reticulum. *J. Biol. Chem.* **270**: 25557-25563.

Felenstein, J. (1989). PHYLIP: phylogeny inference package (Version 3.2). *Cladistics* **5**: 164-166.

Felle, H.H, Kondorosi, E., Kondorosi, A., Schultze, M. (2000). How alfalfa root hairs discriminate between Nod factors and oligochitin elicitors. *Plant Physiol.* **124**: 1373-1380.

Felle, H.H. (1989). Ca^{2+}-selective electrodes and their applications to plant cells and tissues. *Plant Physiol.* **91**: 1239-1242.

Felle, H.H. & Hepler, P.K. (1997). The cytosolic Ca^{2+} concentration of *Sinapsis alba* root hairs as revealed by Ca^{2+}-selective microelectrode tests and fura-dextran ration imaging. *Plant Phys.* **114**:39-45.

Ferris, C.D., Cameron, A.M., Bredt, D.S., Huganir, R.L., Snyder, S.H. (1992). Autophosphorylation of inositol 1,4,5-trisphosphate receptors.*J. Biol. Chem.* **267**: 7036-7041.

Ferris, C.D., Huganir, R.L., Bredt, D.S., Cameron A.M. & Snyder S.H. (1991). Inositol trisphosphate receptor – phosphorylation by protein-kinase-c and calcium calmodulin-dependent protein-kinases in reconstituted lipid vesicles. *Proc. Natl. Acad. Sci. USA* **88**: 2232.

Ferris, C.D., Huganir, R.L., Supattopne, S. & Snyder, S.H. (1989). Purified inositol 1,4,5-trisphosphate receptor mediates calcium flux in reconstituted lipid vesicles. *Nature* **342**: 87-89.

Folta, K.M. & Kaufman, L.S. (2000). Preparation of transcriptionally active nuclei from etiolated *Arabidopsis thaliana*. *Plant Cell Reports* **19**: 504-510.

Foyer, C. & Noctor, G. (2000). Oxygen processing in photosynthesis: regulation and signalling. *New Phytol.* **146**: 359-388.

Franklin-Tong, V.E., Drobak, V.E., Allan, A.C., Watkins, P.A.C. & Trewavas, A.J. (1996). Growth of pollen tubes of Papaver rhoeas is regulated by a slow-moving calcium wave propagated by inositol 1,4,5-trisphosphate. *Plant Cell* **8**: 1305-1321.

Fricker, M.D., May, M., Meyer, A.J., Sheard, N. & White, N.S. (2000). Measurement of glutathione levels in intact roots of *Arabidopsis*. *J. Microscopy* **198**: 162-171.

Fryxell KB, O'Donoghue K, Graeff RM, Lee HC, Branton WD. (1995). Functional expression of soluble forms of human CD38 in *Escherichia coli* and *Pichia pastoris*. **6**: 329-336.

Furuichi, T., Cunningham, K.W. & Muto, S. (2001). A putative two pore channel AtTPC1 mediates Ca^{2+} flux in *Arabidopsis* leaf cells. *Plant Cell Physiol.* **42**: 900-905.

Furuichi, T., Yoshikawa, S., Miyawaki, A., Wada, K., Maeda, M.,& Mikoshiba, K. (1989). Primary structure and functional expression of the inositol 1,4,5-trisphosphate-binding protein P_{400}. *Nature* **342**: 32-38.

Furuyama, T. & Dzelzkalns, V.A. (1999). A novel calcium-binding protein is expressed in *Brassica* pistils and anthers late in flower development. *Plant Mol. Biol.* **39**: 729-737.

Galione, A., Lee, H.C., Busa, W.B. (1991). Ca(2+)-induced Ca^{2+} release in sea urchin egg homogenates: modulation by cyclic ADP-ribose. *Science* **253**: 1143-1146.

Galione, A., McDougall, A., Busa, W.B., Willmott, N., Gilliot, I. & Whitaker, M. (1993). Redundant mechanisms of calcium-induced calcium release underlying calcium waves during fertilization of sea eggs. *Science* **261**: 348-352.

Galione, A., Patel, S. & Churchill, G.C. (2000). NAADP-induced calcium release in sea urchin eggs. *Biol. Cell.* **92**: 197-204.

Galione, A., White, A., Wilmott, N, Turner, M. & Potter, B.V. (1993). cGMP mobilizes intracellular Ca^{2+} in se urchin eggs by stimulating cyclic ADP-ribose synthesis. *Nature* **365**: 456-459.

Gehring, C.A., Irving, H.R. & Parish, R.W. (1990). Effects of auxin and abscissic acid acid on cytosolic calcium and pH in plant cells. *Proc. Natl Acad Sci.* **87**: 9645-9649.

Gehring, C.A., Irving, H.R., Kabbara, A.A., Parish, R.W., Boukli, N.M & Broughton, W.J. (1997). Rapid, plateau-like increases in intracellular free calcium are associated with Nod factor-induced root-hair deformation. *Mol. Plant-Microbe Interact.* **10**: 791-802.

Geisler, M., Frangne, N., Gomes, E., Martinoia, E. & Palmgren, M.G. (2000). The ACA4 gene of *Arabidopsis* encodes a vacuolar membrane calcium pump that improves salt tolerance in yeast. *Plant Physiol.* **124**: 1814-1827.

Geisler, M., Axelsen, K.B., Harper, J.F & Palmgren, M.G. (2000). Molecular aspects of higher plant P-type Ca^{2+}-ATPases. *Biocim. Biophys. Acta* **1465**: 52-78.

Gelli, A. & Blumwald, E. (1993). Calcium retrieval from vacuolar pools – characterization of a vacuolar calcium-channel. *Plant Physiol.* **102**: 1139-1146.

Gelli, A. & Blumwald, J. (1997). Hyperpolarization-activated Ca^{2+}-permeable channels in the plasma membrane of tomato cells. *J. Mem. Biol.* **155**: 35-45.

Genazzani, A. & Galione, A. (1997). A Ca^{2+} release mechanism gated by the novel pridine nucleotide, NAADP. *Trends Pharmacol. Sci.* **18**: 108-110.

Giannini, G., Clementi, E., Ceci, R., Marziali, G., Sorrentino, V. (1992). Expression of a ryanodine receptor-Ca^{2+} channel that is regulated by TGF-beta. *Science* **257**: 91-94.

Gidrol, X., Sabelli, P.A., Fern, Y.S., Kush, A.K. (1996). Annexin-like protein from *Arabidopsis thaliana* rescues delta oxyR mutant of Escherichia coli from H_2O_2 stress. *Proc Natl Acad Sci U S A.* **93**: 11268-11273.

Gilroy, S & Jones, RL (1992). Gibberellic acid and abscissic acid co-ordinately regulate cytoplasmic calcium and secretory activity in barley aleurone protoplasts. *Proc. Nat. Acad. Sci.* **89**: 3591-3595.

Gilroy, S., Fricker, M.D., Read, N.D. & Trewavas, A.J. (1991). Role of calcium in signal transduction of *Commelina* guard cells. *Plant Cell* **3**: 333-344.

Gilroy, S., Read, N.D. & Trewavas, A.J. (1990). Elevation of cytoplasmic calcium by caged inositol trisphosphate initiates stomatal closure. *Nature*, **346:** 769-771.

Goddard, H., Manison, N.F., Tomos, D., Brownlee, C. (2000). Elemental propagation of calcium signals in response-specific patterns determined by environmental stimulus strength. *Proc. Natl. Acad. Sci. U S A* **15**: 1932-1937.

Goff, S.A., Ricke, D., Lan, T.H., Presting, G., Wang, R., Dunn, M., Glazebrook, J., *et al.* (2002). A draft sequence of the rice genome (*Oryza sativa* L. ssp. japonica). *Science* **296**: 92-100.

Goldbeter, A., Dupont, G., Berridge, M.J. (1990). Minimal model for signal-induced Ca^{2+} oscillations and for their frequency encoding through protein phosphorylation. *Proc Natl Acad Sci U S A.* **87**:1461-1465.

Gong, M., Van de Luit, A.H., Knight M.R. & Trewavas, A.J. (1998). Heat-shock-induced changes in intracellular Ca^{2+} level in tobacco seedlings in relation to thermotolerance. *Plant Physiol.* **116:** 429-437.

Grabov, A. & Blatt, M.R. (1998a). Membrane voltage initiates Ca^{2+} waves and potentiates Ca^{2+} increases with abscisic acid in stomatal guard cells. *Proc. Natl Acad. Sci. USA* **95**: 4778-4783.

Grabov, A. & Blatt, M.R. (1998b). Co-ordination of signalling elements in guard cell ion channel control. *J. Exp. Bot.* **49**: 351-360.

Grabov, A., Blatt, M.R. (1999). A steep dependence of inward-rectifying potassium channels on cytosolic free calcium concentration increase evoked by hyperpolarization in guard cells. *Plant Physiol.* **119**: 277-288.

Graeff, R.M, Franco, L., De Flora, A. & Lee, H.C. (1998). Cyclic GMP-dependent and –independent effects on the synthesis of the calcium messengers cyclic ADP-ribose and nicotinic acid adenine dinucleotide phosphate. *J. Biol. Chem.* **273**: 118-125.

Graeff, R.M., Walseth, T.F, & Lee, H.C. (1997). Radioimmunoassay for measuring endogenous levels of cyclic ADP-ribose in tissues. *Methods. Enzymol.* **280:** 230-241.

Graeff, R.M., Walseth, T.F, Hill, H.K. & Lee, H.C. (1996). Fluorescent analogs of cyclic ADP-ribose: synthesis, spectral characterisation and use. *Biochem.* **35**: 379-386.

Graeff, R.M., Walseth, T.F., Fryxell, K., Branton, W.D., & Lee, C.L (1994). Enzymatic synthesis and characterisation of cyclic GDP-ribose. *J. Biol. Chem.* **48:** 30260-30267.

Gronwald, J.W. & Leonard, R.T. (1982). Isolation and transport properties of protoplasts from cortical cells of roots. *Plant Physiol.* **70**: 1391-1395.

Grzelak A, Rychlik B, Bartosz G. (2001). Light-dependent generation of reactive oxygen species in cell culture media. *Free Radic. Biol. Med.* **30**: 1418-1425.

Guse, A.H. (2002). Cyclic ADP-ribose (cADPR) and nicotinic acid adenine dinucleotide phosphate (NAADP): novel regulators of Ca^{2+}-signaling and cell function. *Curr Mol Med.* **2**:273-82.

Hakamata, Y., Nakai, J., Takeshima, H. & Imoto, K. (1992) Primary structure and distribution of a novel ryanodine receptor/release channel from rabbit brain. *FEBS Lett.* **312**: 229-235.

Hamilton, D.W., Hills, A., Kohler, B., Blatt, M.R. (2000). Ca^{2+} channels at the plasma membrane of stomatal guard cells are activated by hyperpolarization and abscisic acid. *Proc. Natl Acad Sci U S A.* **97**: 4967-4972.

Hardingham, G.E., Chawala, S., Johnson, C. & Balding. H. (1997). Distinct functions of nuclear and cytoplasmic calcium in the control of gene expression. *Nature* **385:** 260-264.

Harmon, A.C., Gribskov, M. & Harper, J.F. (2000). CDPKs – a kinase for every Ca^{2+} signal? *Trends Plant Sci.* **5**: 154-159.

Harmon, A.C., Putnam-Evans & Cormier, M.J. (1987). A calcium-dependent but calmodulin-independent protein kinase from soybean. *Plant Physiol.* **83**: 830-837.

Harper, J.F. (2001). Dissecting calcium oscillators in plant cells. *Trends Plant Sci.* **6**: 395-7.

Harper, J.F., Hong, B., Hwang, I., Guo, H.Q., Stoddard, R., Huang, J.F., Palmgren, M.G. & Sze, H. (1998). A novel calmodulin-regulated Ca^{2+}-ATPase (ACA2) from *Arabidopsis* with an N-terminal autoinhibitory domain. *J. Biol. Chem.* **273**: 1099-1106.

Hedrich, R. & Neher, E. (1987). Cytoplasmic calcium regulates voltage dependent ion channels in plant vacuoles. *Nature* **329:** 833-836.

Hedrich, R., Barbier-Brygoo, H., Felle, H.H., Flügge, U.I., Lüttge, U., Maathuis, F.J.M., Marx, S., Prins, H.B.A., Raschke, K., Schnabl, H., Schroeder, J.I. Struve, I., Taiz, L. & Ziegler P. (1988). General mechanisms for solute transport across the tonoplast of plant vacuoles: A patch clamp survey of ion channels and proton pumps. *Bot. Acta* **101**:7-13.

Heinz, E. & Weinstein, A.M. (1984). The overshoot phenomenon in cotransport. *Biochim. Biophys. Acta.* **776**: 83-91.

Hellmich, M.R. & Strumwasser, F. Purification and characterisation of a molluscan egg-specific NADase, a second messenger enzyme (1991). *Cell Regul.* **2**: 193-202.

Heo, W.D., Lee, S.H., Kim, M.C., Kim, J.C., Chung, W.S., Chun, H.J., Lee, K.J., Park, C.Y., Park, H.C., Choi, J.Y. & Cho, M.J. (1999). Involvement of specific calmodulin isoforms in salicyclic acid-independent activation of plant disease in resistance responses. *Proc. Natl Acad. Sci. USA* **19**: 766-771.

Hepler, P.K. & Wayne, R.O. (1985). Calcium and plant development. *Annual Rev. Plant Physiol.* **36**: 397-439.

Hirata, Y., Kimura, N., Sato, K.,Ohsugi, Y., Takasawa, S., Okamoto, H., Ishikawa, J., Kaisho, T., Ishihara, K. & Hirano, T. (1994). ADP-ribosyl cyclase activity of a novel bone marrow stromal cell surface molecule, BST-1. *FEBS Letts.i* **356**: 244-248.

Hirata, M., Suetmatsu, E., Hashimoto, T., Hamachi, T. & Koga, T. (1984). Release of Ca^{2+} from non-mitochondrial store sites in peritoneal macrophages treated with saponin by inositol 1,4,5-trisphosphate. *Biochem J.* **223**: 229-236.

Hirayama, T., Ohto, C., Mizoguchi, T., Shinozaki, K. (1995). A gene encoding a phosphatidylinositol-specific phospholipase C is induced by dehydration and salt stress in *Arabidopsis thaliana*. *Proc Natl Acad Sci U S A*. **92**:3903-3907.

Hirota, J., Michikawa, T., Natsume, T., Furuichi, T. & Mikoshiba, K. (1999). Calmodulin inhibits 1,4,5-triphosphate-induced calcium release through the purified and reconstituted inositol 1,4,5-triphosphate receptor type 1. *FEBS Letts.* **456**: 322-326.

Hirschi, K.D., Zhen, R.G., Cunningham, K.W., Rea, P.A. & Fink, G.R. (1996). CAX1, an H^+/Ca^{2+} antiporter from *Arabidopsis*. *Proc. Natl Acad. Sci. USA* **93**: 8782-8786.

Hofmann, K. & Stoffel, W. (1993). Tmbase – A database of membrane spanning proteins segments. *Biol. Chem.* **374**: 166

Holdaway-Clark, T.L., Feijo, J.A., Hackett, G.R., Kunkel, J.G. & Hepler, P.K. (1997). Pollen tube growth and the intracellular cytosolic calcium gradient oscillate in phase while extracellular calcium influx is delayed. *Plant Cell* **9**:1999-2010.

Holdaway-Clarke, T.L., Hackett, G.R., Kunkel, J.G., Hepler, P.K. & Feijo, J.A. (1998). Oscillations of cell expansion rate, cytoplasmic calcium, and calcium influx in the pollen tube. *J. Gen. Physiol.* **112:** 94.

Hoshi, T. (1995). Regulation of voltage dependence of the KAT1 channel by intracellular factors. *J. Gen. Physiol.* **105**: 309-328.

Howard, M., Grimaldi, J.C., Bazan, J.F., Lund, F.E., Santos-Argumedo, L., Parkhouse, R.M.E., Walseth, T.F. & Lee, H.C. (1993). Formation and hydrolysis of cyclic ADP-ribose catalysed by lymphocyte antigen CD38. *Science* **262**: 1056-1059.

Hsieh, W.L., Pierce, W.S. & Sze, H. (1991). Calcium-pumping ATPases in vesicles from carrot cells – stimulation by calmodulin or phosphatidylserine, and formation of a 120 kilodalton phosphoenzyme. *Plant Physiol.* **97**: 1535-1544.

Huan, C-H., Tate, B.F., Crain, R. & Coté, G.C. (1995). Multiple phosphoinositide-specific phospholipase C in oat roots: characterisation and partial purification. *Plant .J.* **8**: 257-267.

Huang, L., Berkleman, T., Franklin, A.E. & Hoffman, N.E. (1993). Characterisation of a gene encoding a Ca^{2+}-ATPase-like protein in the plastid envelope. *Proc. Natl Acad. Sci. USA* **90**: 10066-10070.

Inageda, K., Takahashi, K., Tokita, K., Nishina, H., Kanaho, Y., Kumimoto, I., Kontani, K., Hoshino, S. & Katada, T. (1995). Enzyme properties of *Aplysia* ADP-ribosyl cyclase: comparison with NAD glycohydrolases of CD38 antigen. *J. Biochem.* **117**: 125-131.

Irvine, R.F., Letcher, A.J., Dawson, R.M. (1980) Phosphatidylinositol phosphodiesterase in higher plants. *Biochem J.* **192**:279-283.

Irving, H. R., Gehring, C.A. & Parish, R.W. (1992). Changes in cytosolic pH and calcium of guard cells precede stomatal movements. *Proc. Natl Acad. Sci. USA* **89**: 1790-1794.

Irving, H., Gehring, C.A. & Parish, R.W. (1990). Effects of auxin and abscisic acid on cytosolic calcium and pH in plant cells. *Proc. Natl Acad. Sci.* USA **87:** 9645-9649.

Janystin, B. (1989). CAMP promoted protein phosphorylation of dialysed coconut milk. *Phytochemistry* **28**: 329-331.

Jayaraman, T., Ondriaš, Ondiašová, E. & Marks, A.R. (1996) Regulation of the inositol 1,4,5-trisphosphate receptor by tyrosine phosphorylation. *Science* **272**: 1492-1494.

Jennings, I. R., Rea, P.A., Leigh, R.A. and Sanders, D. (1988). Quantitative and rapid estimation of H^+ fluxes in membrane-vesicles – software for analysis of fluorescence quenching and relaxation. *Plant Phisiol (Betheseda)* **86**:1257-1263.

Johannes, E. & Sanders, D. (1995). Lumenal calcium modulates unitary conductance and gating of a plant vacuolar calcium-release channel. *J. Membr. Biol.* **146**: 211-224.

Johannes, E., Allen, G. & Sanders, D. In Blatt, M.R., Leigh, R.A. & Sanders, D. (Eds.) (1994). *Membrane Transport in Plants and Fungi: Molecular Mechanisms and Control.* Company of Biologists, Cambridge, 1994, pp 113-122.

Johannes, E., Brosnan, J.M. & Sanders D. (1992). Parallel pathways for intracellular Ca^{2+} release from the vacuole of higher plants. *Plant J.* **2**: 97-102.

Johansson, I., Larsson, C., Ek, B. & Kjellbom, P. (1996). The major integral proteins of spinach leaf plasma membranes are putative aquaporins and are phosphorylated in response to Ca^{2+} and apoplastic water potential. *Plant Cell* **8**: 1181-1191.

Jones, A.M. (2002). G-protein-coupled signalling in *Arabidopsis*. *Curr Opin Plant Biol.* **5**: 402-407.

Josefsson, L.G. & Rask, L. (1997). Cloning of a putative G-protein-coupled receptor from *Arabidopsis thaliana*. *Eur. J. Biochem.* **249**: 415-420.

Joseph, S.K., Rice, H.L. & Williamson, J.R. (1989). The effect of external calcium and pH on inositol trisphosphate-mediated release from cerebellum microsomal fractions. *Biochem J.* **258**: 261-265.

Karasawa, T., Takasawa, S., Yamakawa, K., Yonekura, H., Okamoto, H. & Nakamura, S. (1995). NAD^+-glycohydrolase from *Streptococcus pyogenes* shows cyclic ADP-ribose forming activity. *FEMS Microbiol. Lett.* **130**: 201-204.

Kasai, N. & Muto, S. (1990). Ca^{2+} pumps and Ca^{2+}/H^+ antiporter in plasma membrane vesicles isolated by aqueous two-phase partitioning from maize leaves. *J. Membr. Biol.* **114**: 133-142.

Kiegle, E., Haseloff, J. & Tester, M. (1998) in: Abstracts of the 11th International Workshop on Plant Membrane Biology, Cambridge. P198.

Kiegle, E., Moore, C., Hasseloff, J., Tester, M.A. & Knight, M.R. (2000). Cell type specific calcium responses to drought, salt and cold in the *Arabidopsis* root. *Plant J.* **23**: 267-278.

Kim H, Jacobson EL, Jacobson MK. (1993). Synthesis and degradation of cyclic ADP-ribose by NAD glycohydrolases. *Science* **261**: 1330-1333..

Kim HY, Cote GG, Crain RC (1996). Inositol 1,4,5-trisphosphate may mediate closure of K^+ channels by light and darkness in *Samanea saman* motor cells. *Planta* **198**: 279-287.

Klessig, D.F., Durner, J., Noad, R., Navarre, D.A., Wendehenne, D., Kumar, D., Zhou, J.M., Syah, J., Zhang, S., Kachroo, P., Trifa, Y., Pontire, D., Lam, E. & Silva, H. (2000). Nitric oxide and salicylic acid signalling in plant defense. *PNAS* **97**: 8849-8855.

Klüsener B, Weiler EW. (1999). A calcium-selective channel from root-Tip endomembranes of garden cress. *Plant Physiol.* **119**: 1399-1406.

Klüsener, B. Boheim., G., Liss, H., Engelberth, J. & Weiler, E.W. (1995). Gadolinium-sensitive, voltage-dependent calcium-release channels in the endoplasmic-reticulum of a higher plant mechanoreceptor organ. *EMBO J* **14:** 2708-2714.

Klüsener, B., Boheim, G. & Weiler, E.W. (1997). Modulation of the ER Ca^{2+} channel BCC1 from tendrils of *Bryonia diocia* by divalent cations, protons and H_2O_2. *FEBS Lett.* **407**: 230-234.

Knight, H., Knight, M. R. (1995) Recombinant aequorin methods for intracellular calcium measurement in plants. *Meth. Cell Biol.* **49**, 201-216.

Knight, H., Trewavas, A.J. & Knight, M.R. (1996) Cold calcium signalling in *Arabidopsis* involves two cellular pools and a change in calcium signature after acclimation. *Plant Cell* **8:** 489-503.

Knight, H., Trewavas, A.J. & Knight, M.R. (1997). Calcium signalling in *Arabidopsis thaliana* responding to drought and salinity. *Plant J.* **12:** 1067-1078.

Knight, M.R., Campbell, A.K., Smith, S.M. & Trewavas, A.J. (1991). Transgenic plant aequorin reports that the effects of cold shock and elicitors on cytoplasmic calcium. *Nature* **352:** 524-526.

Knight, MR, Smith, SM & Trewavas, AJ (1992). Wind-induced plant motion immediately increases cytosolic calcium. *Proc. Nat. Acad. Sci. USA* **89**:4967-4971.

Köhler, C. & Merkle, T.G. (1999). Characterization of a novel gene family of putative cyclic nucleotide- and calmodulin-regulated ion channels in *Arabidopsis thaliana*. *Plant J.* **18**: 97-104.

Köhler, C. & Neuhaus, G. (1998). Cloning and partial characterisation of two putative cyclic nucleotide-regulated ion channels from *Arabidopsis thaliana*, designated CNGC1 (Y16327) and CNGC2 (Y16328). *Plant Physiol.* **116**: 1604.

Köhler, C. & Neuhaus, G. (2000). Characteristation of calmodulin binding to cyclic nucleotide-gatde ion channels from *Arabidopsis* thaliana. *FEBS Lett.* **4710**: 133-136.

Komatsu, S. & Hirano, H. (1993). Protein kinase activity and protein phosphorylation in rice (*Oryza satvia* L) leaf. *Plant Sci.* **94**: 127-137.

Krysan, P.J., Young J.C., Tax F., Sussman M.R. (1996). Identification of transferred DNA insertions within Arabidopsis genes involved in signal transduction and ion transport. *Proc. Natl Acad. Sci.* **93**:8145.

Krysan, P.J., Young, J.K., & Sussman, M.R. (1999). T-DNA as an insertational mutagen in *Arabidopsis*. *Plant Cell,* **Vol II.**: 2283-2290.

Kudla, J., Xu, Q., Harter, K., Gruissem, W. & Luan, S. (1999). Genes for calcineurin B-like proteins in *Arabidopsis* are differentially regulated by stress signals. *Proc. Natl Acad. Sci USA* **96**: 4718-4723.

Kurosaki F, Kaburaki H, Nishi A. (1994). Involvement of plasma membrane-located calmodulin in the response decay of cyclic nucleotide-gated cation channel of cultured carrot cells. *FEBS Lett.* **340**:193-196.

Kuster, B., Wheeler, S.F., Hunter, A.P., Dwek, R.A., Harvey, D.J. (1997). Sequencing of N-linked oligosaccharides directly from protein gels: in-gel deglycosylation followed by matrix-assisted laser desorption/ionization mass spectrometry and normal-phase high-performance liquid chromatography. *Anal Biochem.* **250**: 82-101.

Laemmli, U.K. (1970). Cleavage of structural proteins during the assembly of the head of bacteriophage T4. *Nature* **227**: 680-685.

Laver, D.R., Lenz, G.K., Lamb, G.D. (2001). Regulation of the calcium release channel from rabbit skeletal muscle by the nucleotides ATP, AMP, IMP and adenosine. *J. Physiol.* **537**: 763-768.

Lawton, M.A., Yamamoto, R.T., Hanks, S.K. & Lamb, C.J. (1989). Molecular cloning of a plant transcript encoding protein kinase homologs. *Proc. Natl. Acad. Sci. USA* **86**: 3140-3144.

Lechleiter J, Girard S, Peralta E, Clapham D. (1991). Spiral calcium wave propagation and annihilation in *Xenopus* laevis oocytes. *Sience* **252**: 123-126.

Leckie, C.P., McAinsh, M.R., Allen, G.J., Sanders, D. & Hetherington, A.M. (1998). Abscisic acid-induced stomatal closure mediated by cyclic ADP-ribose. *Proc. Natl Acad. Sci. USA* **95**: 15837-15842.

Ledbetter MW, Preiner JK, Louis CF, Mickelson JR. (1994). Tissue distribution of ryanodine receptor isoforms and alleles determined by reverse transcription polymerase chain reaction. *J. Biol. Chem.* **269**: 31544-31551.

Lee HC, Aarhus R. (1993). Wide distribution of an enzyme that catalyzes the hydrolysis of cyclic ADP-ribose. *Biochim Biophys Acta.* **1164**: 68-74.

Lee, H.C. & Aarhus, R. (1991). ADP-ribosyl cyclase: an enzyme that cyclizes NAD^+ into a calcium-mobilizing metabolite. *Cell Regul.* **2**: 203-209.

Lee, H.C. & Aarhus, R. (1995). A derivative of NADP mobilizes calcium stores insensitive to inositol trisphosphate and cyclic ADP-ribose. *J. Biol. Chem.* **270**: 2152-2157.

Lee, H.C. (1997). Mechanisms of calcium signalling by cyclic ADP-ribose and NAADP. *Physiolo Rev.* **77**: 1133-1164.

Lee, H.C., Aarhus, R. & Graeff, R.M. (1995a). Sensitization of calcium-induced calcium release by cyclic ADP-ribose and calmodulin. *J. Biol. Chem.* **270**: 9060-9066.

Lee, H.C., Galione, A. & Walseth, T.F. (1994). Cyclic ADP-ribose: Metabolism and calcium mobilizing function. *Vitamins and Hormones.* **48**: 199-257.

Lee, H.C., Graeff, R. & Walseth, T.F. (1995b). Cyclic ADP-ribose and its metabolic enzymes. *Biochimie* **77**: 345-355.

Lee, H.C., Walseth, T.F., Bratt, G.T., Hayes, R.N. & Clapper, D.L. (1989). Structural determination of a cyclic metabolite of NAD^+ with intracellular Ca^{2+}-mobilzing activity. *J. Biol. Chem.* **264**: 1608-1615.

Legue, V., Blancaflor, E., Wymer, C., Perbal, G., Fantin, D. & Gilroy, S. (1997). Cytoplasmic free Ca^{2+} in *Arabidopsis* roots changes in response to touch but not gravity. *Plant Physiol.* **114**: 789-800.

Lemtiri-Chlieh, F., MacRobbie, E.A.C. & Brearly, C.A. (2000). Inositol hexakisphosphate is a physiological signal regulating the K^+-inward rectifying conductance in guard cells. *Proc. Natl. Acad. Sci USA* **97**: 8687-8692.

Leng Q, Mercier RW, Hua BG, Fromm H, Berkowitz GA. (2002). Electrophysiological analysis of cloned cyclic nucleotide-gated ion channels. *Plant Physiol.* **128**: 400-410.

Leng, Q., Mercier, R.W., Yao, Weizhe, Y. & Berkowitz, G. A. (1999). Cloning and first functional characterization of a plant cyclic nucleotide-gated cation channel. *Plant Phys.* **121**: 753-761.

Levine, A., Pennell, Alvarez, M.E., Palmer, R. & Lamb, C. (1996). Calcium-mediated apoptosis in a plant hypersensitive disease resistance response. *Curr. Biol.* **6**: 427-437.

Levitan, I.B. (1994). Modulation of ion channels by protein phosphorylation and dephosphorylation. *Annu. Rev. Physiol.* **56**: 193-212.

Lew, R.R., Briskin, D.P. & Wyse, R.E. (1986). Calcium uptake by endoplasmic reticulum from zucchini hypocotyls. *Plant Physiol.* **82**: 47-53.

Li, W., Luan, S., Schreiber, S.L. & Assmann, S.M. (1994). Evidence for protein phosphatase 1 and 2A regulaton of K^+ channels in two types of leaf cells. *Plant Physiol.* **106**: 963-970.

Liang, F., Cunningham, K.W., Harper, J.F. & Sze, H. (1997). ECA1 complements yeast mutants defective in Ca^{2+} pumps and encodes an endoplasmic reticulum-type Ca^{2+}-ATPase in *Arabidopsis thaliana*. *Proc. Natl Acad. Sci. USA* **94**: 8579-8584.

Lindberg & Strid, H. (1997). Aluminium induces rapid changes in cytosolic pH and free calcium and potassium concentrations in root protoplasts of wheat (*Triticium aestivum*). *Physiol. Plant* **99**: 405-414.

Lino, M. (1990). Biphasic Ca^{2+} dependence of inositol 1,4,5-trisphosphate-induced Ca^{2+} release in smooth muscle cells of the guinea pig taenia caeci. *J. Gen. Physiol.* **95**: 1103-1122.

Liu, J. & Zhu, J.K. (1998). A calcium sensor homolog required for plant salt tolerance. *Science* **280**: 1943-1945.

Lu, Y-T, Dharmasiri, M.A.N. & Harrington, H.M. (1995). Characterisation of a cDNA encoding a novel heat-shock protein that binds to calmodulin. *Plant Physiol.* **108**: 1197-1202.

Ma, H. (1994). GTP-binding proteins in plants: new members of an old family. *Plant Mol Biol.* **26**:1611-1636.

MacRobbie E.A.C. (1998). Signal transduction and ion channels in guard cells. *Philos Trans R Soc Lond B Biol Sci.* **353**: 1475-1488.

MacRobbie, E.A.C. (1997). Signalling in guard cells and regulation of ion channel activity. *J. Exp. Bot.* **48:** 515-528.

Maeshima M. (2001). Tonoplast Transporters: Organization and Function. *Annu Rev Plant Physiol Plant Mol Biol.* **52**:469-497

Mahló, R. & Trewavas, A.J. (1996). Localized apical increases of cytosolic free calcium control pollen tube orientation. *Plant Cell* **8**:1935-1949.

Malhó, R., Moutinho, A, Van der Lui, A. & Trewavas, A.J. (1998). Spatial characteristics of calcium □ignalling: The calcium wave as a basic unit in plant cell calcium signalling. *Philos. Trans. R. Soc. Lond.* B **353:** 1463-1473.

Malhó, R., Read, N.D., Pais, M.S. & Trewavas, A.J. (1994). Role of cytoplasmic free calcium in the reorientation of pollen tube growth. *Plant J.* **5**: 331-341.

Malmstrom, S., Askerlund, H.E. & Askerlund, P. (2000). Regulatory role of the N terminus of the vacuolar calcium-ATPase in cauliflower. *Plant Physiol.* **122**:517-526

Malmstrom, S., Askerlund, P. & Palmgren, M.G. (1997). A calmodulin-stimulated Ca^{2+}-ATPase from plant vacuolar membranes with a putative. Regulatory domain at its N-terminus. *FEBS Lett.* **400**: 324-328.

Marks AR. (1996). Immunophilin Modulation of Calcium Channel Gating. *Methods* **9**: 177-187.

Marschner, H. (1995). Mineral Nutrition of Higher Plants. Second Edition. Academic Press. New York.

Marshall, J., Corzo, A., Leigh, R.A., Sanders, D. (1994). Membrane potential-dependent calcium transport in right-side-out plasma membrane vesicles from *Zea mays* L. roots. *Plant J.* **5**: 683-694.

Martinoia, E. Locher, R. & Vogt, E. (1993). Inositol trisphosphate metabolism in subcellular fractions of barley mesophyll cells. *Plant Phys.* **102**: 101-105.

Maser, P., Thomine, S., Schroeder, J.I., Ward, J.M., Hirschi, K., Sze, H., Talke, I.N., Amtmann, A., Maathuis, F.J., Sanders, D., Harper, J.F., Tchieu, J., Gribskov, M., Persans, M.W., Salt, D.E., Kim, S.A., Guerinot, M.L. (2001). Phylogenetic relationships within cation transporter families of *Arabidopsis*. *Plant Physiol.* **126**: 1646-1667.

Masuda, W., Takenaka, S., Inegeda, K., Nishina, H., Takahashi, K., Katada, Tsuyama, S., Inui, H., Miyatake, K. & Nakano, Y. (1997). Oscillation of ADP-ribosyl cyclase activity during the cell cycle and function of cyclic ADP-ribose in a unicellular organism, *Euglena gracilis*. *FEBS letts.* **405:**104-106.

Masuda, W., Takenaka, S., Tsuyama, S., Inui, H., Miyatake, K. & Nakano, Y. (1999). Purification and characterisation of ADP-ribosyl cyclase from Euglena gracilis. *J. Biochem.* **125**: 449-453.

May, M.J., Vernoux, T., Leaver, C.J., Van Montagu, M. & Inzé, D. (1998). Glutathione homeostasis in plants: implications for environmental sensing and plant development. *J. Exp. Bot.* **49**: 649-667.

McAinsh, M.R., Brownlee, C. & Hetherington, A.M. (1990). Abscisic acid-induced elevation of guard cell cytosolic Ca^{2+} precedes stomatal closure. *Nature* **343:** 186-188.

McAinsh, M.R., Webb, A.A.R., Taylor, J.E. & Hetherington, A.M. (1995). Stimulus-induced oscillations In guard cell cytoplasmic free calcium. *Plant Cell* **7**: 1207-1219.

McAinsh, M.R. & Hetherington, A.M. (1998). Encoding specificity in Ca^{2+} signalling systems. *Trends Plant Sci.* **3:** 32-36.

McAinsh, M.R., Allen, G.J., Hetherington, A.M. & Sanders, D. (1996). The role of cyclic ADP-ribose in stomatal guard cells. *Plant Physiol* **111**: Special Supplement: 692.

McAinsh, M.R., Brownlee, C. & Hetherington, A.M. (1990). Abscisic acid-induced elevation of guard cell cytosolic Ca^{2+} precedes stomatal closure. *Nature* **343**: 186-188.

McAinsh, M.R., Brownlee, C. & Hetherington, A.M. (1992). Visualising changes in cytosolic-free Ca^{2+} during the response of stomatal guard cells to abscisic acid. *Plant Cell* **4:** 1113-1122.

McAinsh, M.R., Brownlee, C. & Hetherington, A.M. (1997). Calcium ions as second messengers in guard cell signal transduction. *Physiol Plant* **100**: 16-29.

McCarty, D.R., Chory, J. (2000). Conservation and innovation in plant signalling pathways. *Cell* 103:201-209

McPhalen, C.A., Strynadka, N.C. & James, M.N.G. (1991). Calcium-binding sites in proteins: A structural perspective. *Adv. Prot. Chem.* **42**: 77-41.

Mehta K, Shahid U, Malavasi F. (1996). Human CD38, a cell-surface protein with multiple functions. *FASEB J.* **10**: 1408-1417.

Mészáros, L.G., Bak, J., Chu, A.. (1993). Cyclic ADP-ribose as an endogenous regulator of the non-skeletal type ryanodine receptor Ca^{2+} channel. *Nature* **364**: 76-79.

Meyer, T. (1991). Cell signalling by second messenger waves. *Cell* **64**: 675-678.

Michalak, M., Mariani, P., & Opas, M. (1998). Calreticulin, a multifunctional Ca^{2+} binding chaperone of the endoplasmic reticulum. *Bioch. Cell Biol.* **76**: 779-785.

Mignery, G.A & Südhof, T.C. (1990). The ligand binding site and transduction mechanism in the inositol-1,4,5-triphosphate receptor. *EMBO J.* **9**: 3893-3898.

Mignery, G.A., Südhof, T.C., Takei, K. & De Camilli, P. (1989). Putative receptor for inositol 1,4,5-trisphosphate similar to ryanodine receptor. *Nature* **342**: 192-195.

Mikami, K., Katagiri, T., Luchi, S., Yamaguchi-Shinozaki, K., Shinozaki, K. (1998). A gene encoding phosphatidylinositol-4-phosphate 5-kinase is induced by water stress and abscisic acid in *Arabidopsis thaliana. Plant J.* **15**:563-568.

Miller, A.J. & Sanders, D. (1987). Depletion of cytoplasmic free calcium induced by photosynthesis. *Nature* **326**: 397-400.

Miller, D., Callaham, D.A., Gross, D.J. & Hepler, P.K. (1992). Free Ca^{2+} gradient in growing pollen tubes of *Illium*. *J. Cell Sci.* **101**: 7-12.

Miyawaki, A., Furuichi, T. & Ryou, Y. (1991). Structure function relationships of the mouse inositol 1,4,5-trisphosphate receptor. *Proc. Natn Acad. Sci. USA* **88**: 4911-4915.

Miyazaki, S. (1995). Inositol trisphosphate receptor mediated spatiotemporal calcium signalling. *Curr Opin Cell Biol.* **7**: 190-196.

Miyazaki, S., Yuzaki, M., Nakada, K., Shirakawa, H., Nakanishi, S., Nakade, S., Mikoshiba, K. (1992). Block of Ca^{2+} wave and Ca^{2+} oscillation by antibody to the inositol 1,4,5-trisphosphate receptor in fertilized hamster eggs. *Science* **257**: 252-255.

Morsomme, P. & Boutry, M. (2000). The plant plasma membrane H^+-ATPase: structure, function and regulation. *Biochim. Biophys. Acta* **1465**:1-16.

Muir, S., Bewell, M., Sanders, D. and Allen, G.J. (1997). Ligand-gated Ca^{2+} channels and Ca^{2+} signalling in higher plants. *J. Exp. Bot.* **48**: 589-597.

Muir, S.R. & Sanders, D. (1996). Pharmacology of Ca^{2+} release from red beet microsomes suggests the presence of ryanodine receptor homologs in higher plants. *FEBS Letts* **395**: 39-42.

Muir, S.R. & Sanders, D. (1997). Inositol 1,4,5 trisphosphate-sensitive Ca^{2+} release across non-vacuolar membranes in cauliflower. *Plant Physiol.* **114**: 1511-1521.

Munnik T, Irvine RF, Musgrave A. (1998). Phospholipid signalling in plants. *Biochim Biophys Acta.* **1389**: 222-272.

Musgrave, A., Kuin, H., Jongen, M., de Wildt, P., Schuring, F., Klerk, H., van der Ende, H. (1992). Ethanol stimulates phospholipids turnover and inositol 1,4,5 trisphosphate production in *Chlamydomonas eugametos* gametes. *Planta* **186**: 442-449.

Muto, S. & Miyachi, S. (1977). Properties of a protein activator of NAD kinase from plants. *Plant Physiol.* **59**: 55-60.

Nakai, J., Imagawa, T., Hakamata, Y., Shigekawa, M., Takeshima, H. & Numa, S. (1990). Primary structure and functional expression from cDNA of the cardiac ryanodine receptor/calcium release channel. *FEBS Lett.* **271**: 169-177.

Nam, S.H., Jung, S.Y., Yoo, C.M., Ahn, E.H., Suh, C.K. (2002). H_2O_2 enhances Ca^{2+} release from osteoblast internal stores. *Yonsei. Med. J.* **43**: 229-235.

Navazio, L. Bewell, M.A., Siddiqua, A., Dickinson, G.D., Galione, A. & Sanders, D. (2000). Calcium release from the endoplasmic reticulum of higher plants elicited by the NADP metabolite nicotinic acid dinucleotide phosphate. *Proc. Nat. Acad. Sci.* **97**: 8693-8698.

Navazio, L., Mariani, P. & Sanders, D. (2001). Mobilization of Ca^{2+} by cyclic ADP-ribose from the endoplasmic reticulum of cauliflower florets. *Plant Physiol.* **125**: 2129-2138.

Neuhaus, G., Bowler, C., Hiratsuka, K., Yamagata, H. & Chua, N.H. (1997). Phytochrome-regulated expression of gene expression requires calcium and cGMP. *EMBO J.* **16:** 2554-2546.

Nishimura, H. Hayamizu T., & Yanagisawa, Y. (1986). Reduction of NO_2 to NO by rush and other plants. *Environ. Sci. Technol.* **20**: 413-416.

Nobiling, R. & Reiss, H-D. (1987). Quantitative analysis of calcium gradients and activity in growing pollen tubes of *Lilium longiflorum*. *Protoplasma* **139**: 20-24.

Noctor G, Veljovic-Jovanovic S, Foyer CH. (2000). Peroxide processing in photosynthesis: antioxidant coupling and redox signalling. *Philos Trans R Soc Lond B Biol Sci.* **355**: 1465-1475.

Noctor, G. & Foyer, C.H. (1998). Ascorbate and glutathione: keeping active oxygen under control under control. *Ann. Rev. Plant Physiol.* **49**: 249-279.

Nunn, D.L., Taylor, C.W. (1990). Liver inositol, 1,4,5-trisphosphate-binding sites are the $Ca^{2(+)}$-mobilizing receptors. *Biochem J.* **270**: 227-232.

Oba, T., Ishikawa, T., Murayama, T., Ogawa, Y. & Yamaguchi, M. (2000). H_2O_2 and ethanol act synergistically to gate ryanodine receptor/calcium-release channel. *Am. J. Physiol.* **279**: C1366-C1374.

Orr, I., Shoshan-Barmatz, V. (1996). Modulation of the skeletal muscle ryanodine receptor by endogenous phosphorylation of 160/150-kDa proteins of the sarcoplasmic reticulum. *Biochim. Biophys. Acta.* **1283**:80-88.

Page, R.D. (1996). TreeView: an application to display phylogenetic trees on personal computers. *Comput. Appl. Biosci.* **12**: 357-358.

Parker I, Yao Y. (1996). Ca^{2+} transients associated with openings of inositol trisphosphate-gated channels in *Xenopus oocytes*. *J. Physiol.* **491**: 663-668.

Patel, S., Joseph, S.K., Thomas, A.P. (1999). Molecular properties of inositol 1,4,5-trisphosphate receptors. *Cell Calcium* **25**: 247-264.

Patel, S., Morris, S.A., Adkins, C.E., O'Beirne, G., Taylor, C.W. (1997). Ca^{2+}-independent inhibition of inositol trisphosphate receptors by calmodulin: redistribution of calmodulin as a possible means of regulating Ca^{2+} mobilization. *Proc. Natl. Acad. Sci. U S A.* **94**: 11627-11632.

Patharkar, O.R., Cushman, J.C. (2000). A stress-induced calcium-dependent protein kinase from *Mesembryanthemum crystallinum* phosphorylates a two-component pseudo-response regulator. *Plant J.* **24**: 679-691.

Pawlikowska, L., Cottrell, S.E., Harms, M.B., Li, Y. & Rosenberg, P.A. (1996). Extracellular synthesis of cADP-ribose from nicotinamide-adenine dinucleotide by rat cortical astrocytes in culture. *J. Neurosci.* **16:** 5372-5381.

Pei, Z.-M., Schroeder, J.I. & Schwarz, M. (1998). Background ion channel activites in *Arabidopsis* guard cells and review of ion channel regulation by protein phosphorylation events. *J. Exp. Bot.* **49**: 319-328.

Pei, Z.M., Ward, J.M. & Schroeder, J.I. (1999). Magnesium sensitizes slow vacuolar channels to physiological cytosolic calcium and inhibits fast vacuolar channels in fava bean guard cell vacuoles. *Plant Physiol.* **121**: 977-986.

Pei, Z-M, Murata, Y., Benning, G., Thomine, S., Klüsner, B., Allen, G.J., Grill, E. & Schroeder, J.I. (2000). Calcium channels activated by hydrogen peroxide mediate abscissic acid signalling in guard cells. *Nature* **406**: 731-734.

Penson, S.P. Schuurink RC, Fath A., Gubler F., Jacobsen J.V. & Jones R.L. (1996). cGMP is required for gibberelic acid-induced gene expression in barley aleurone. *Plant Cell* **8**: 2325-2333.

Perez-Prat, E., Narashimhan, M.L., Binzel, M.L., Botella, M.A., Chen, Z., Valpuesta, V., Bressan, R.A. & Hasegawa, P.M. (1992). Induction of a putative Ca^{2+}-atpase messenger-RNA in NaCl-adapted cells. *Plant Physiol.* **100**: 1471-1478.

Pessah, I.N., Waterhouse, A.L., Casida, J.E. (1985). The calcium-ryanodine receptor complex of skeletal and cardiac muscle. Biochem Biophys Res Commun. **128**: 449-456.

Pfeiffer, S., Janistyn B., Jessner G., Pichorner H. & Ebermann R. (1994). Gaseous nitric oxide stimulates guanosine-3',5'-cyclic monophosphate (cGMP) formation in spruce needles. *Phytochemisty* **36**: 259-262.

Pineros, M. & Tester, M. (1997). Calcium channels in higher plant cells: sectivity, regulation and pharmacology. *J. Exp. Bot.* **48**:551-577.

Pittman, J.K., Hirschi, K.D. (2001). Regulation of CAX1, an *Arabidopsis* $Ca(^{2+})/H^{+}$ antiporter. Identification of an N-terminal autoinhibitory domain. *Plant Physiol.* **27**:1020-1029.

Pollard HB, Guy HR, Arispe N, de la Fuente M, Lee G, Rojas EM, Pollard JR, Srivastava M, Zhang-Keck ZY, Merezhinskaya N, *et al.* (1992). Calcium channel and membrane fusion activity of synexin and other members of the Annexin gene family. *Biophys J.* **62**:15-18

Ponting, C., Schultz, J. & Bork, P. (1997). SPRY domains in ryanodine receptors (Ca^{2+}-release channels). *TIBS* **22**: 193-194.

Pottosin, I.I., Tikhonova, L.I., Hedrich, R. & Schonknecht, G. (1997). Slowly activating vacuolar channels cannot mediate Ca^{2+} induced Ca^{2+} release. *Plant J.* **12**: 1387-1398.

Prasad, T.K., Anderson, M.D., Martin, B.A., Stewart, C.R. (1994). Evidence for chilling-induced oxidative stress in maize seedlings and a regulatory role for hydrogen peroxide. *Plant Cell* **6**: 65-74.

Price, A.H., Taylor, A., Ripley, S.J., Griffiths, A., Trewavas, A.J. & Knight, M.R. (1994). Oxidative signals in tobacco increase cytosolic calcium. *Plant Cell* **6**:1301-1310.

Racay, P., Kaplan, P., Mezesova, V. & Lehotsky, J. (1997). Lipid peroxidation both inhibits Ca^{2+}ATPases and increases Ca^{2+} permeability of endoplasmic reticulum membrane. *Biochem. Mol. Biol. Int.* **41**:647-655.

Ranjeva, R., Carrasco, A. & Boudet, A.M. (1988). Inositol trisphosphate stimulates the release of calcium from intact vacuoles isolated from *Acer* cells. *FEBS Lett.* **230**: 137-141.

Ranjeva, R., Refuao, G., Boudet, A.M. & Marone, D. (1983). Activation of plant quinate: NAD^{+} 3-oxidoreductase by Ca^{2+} and calmodulin. *Proc. Nat. Acad. Sci. USA.* **50:** 5222-5224.

Raschke, B.C. & Wolf, A.H. (1996). Molecular cloning of a p-type $Ca2^{+}$-ATPase from the halotolerant alga *Dunaliella bioculata. Planta* **200**: 78-84.

Rathore KS, Cork RJ, Robinson KR. (1991). A cytoplasmic gradient of Ca^{2+} is correlated with the growth of lily pollen tubes. *Dev Biol.* **148**: 612-619.

Raynal P, Pollard HB. (1994). Annexins: the problem of assessing the biological role for a gene family of multifunctional calcium- and phospholipid-binding proteins. *Biochim Biophys Acta.* **1197**: 63-93.

Read, N.D., Shacklock, P.S., Knight, M.R. & Trewavas, A.J. (1993). Imaging calcium dynamics in living plant cells and tissues. *Cell Biol. Int.* **17**: 111-125.

Reddy, A.S.N. (2001). Calcium: silver bullet in signalling. *Plant Sci.* **160**: 381-404.

Reddy, V.S., Ali, G.S., Reddy, A.S. (2002). Genes encoding calmodulin-binding proteins in the *Arabidopsis* genome. *J Biol Chem.* **277**: 9840-9852.

Reyes-Harde, M., Potter, B.V.L., Galione, A. & Stanton, P.K. (1999). Induction of hippocampal LTD requires nitric-oxide stimulated PKG activity and Ca^{2+} release from cyclic ADP-ribose-sensitive stores. *J. Neurophysiol.* **82**: 1569-1576.

Roberts, S.K. & Snowman, B.N. (2000). The effects of ABA on channel-mediated K(+) transport across higher plant roots. *J. Exp. Bot.* **51**:1585-94.

Rodney, G.G., Williams, B., Y., Strasburg, G., M., Beckingham, K. & Hamilton, S.L. (2000). Regulation of RYR1 activity by Ca^{2+} and calmodulin. *Biochem.* **39**:7807-7812.

Ross, C.A., Danoff, S.K., Schell, M.J., Snyder, S.H. & Ullrich, A. (1992). Inositol 1,4,5-trisphosphate receptors – distinct neuronal and nonneuronal forms derived by alternative splicing differ in phosphorylation. *Proc. Natl Acad. Sci. USA* **89**: 4265-4269.

Rudd, J.J., and Franklin-Tong, V.E. (2001). Unravelling response-specificity in Ca^{2+} signalling pathways in plant cells. *New Phytol.* **151**: 7–33

Sanders, D., Brownlee, C., & Harper, J.F. (1999). Communicating with calcium. *Plant cell.* **11**:691-706.

Sanders, D., Muir, S.R. & Allen, G.J. (1995). Ligand- and voltage- gated calcium release channels at the vacuolar membrane. *Trans. Biochem Soc.*

Sanders, D., Pelloux, J., Brownlee, C., Harper, J.F. (2002). Calcium at the crossroads of signalling. *Plant Cell* **14** Suppl: S401-417.

Sayers, L.G., Brown, G.R., Michell, R.H. & Michelangeli, F. (1993). The effects of thimerosal on calcium uptake and inositol 1,4,5-triphosphate-induced calcium release in cerebellar microsomes. *Biochem J.* **289**: 883-887.

Schachtman, D.P., Kumar, R., Schroeder, J.I. & Marsh, E.L. (1997). Molecular and functional characterisation of a novel low-affinity cation transporter (LCT1) in higher plants. *Proc. Natl Acad. Sci. USA* **94**: 11079-11084.

Schmidt, C., Schelle, I., Liao, Y-J. & Schroeder, J.I. (1995). Strong regulation of slow anion channels and abscissic acid signalling in guard cells by phosphorylation and dephosphorylation events. *Proc. Natl Acad. Sci. USA* **92**: 9535-9539.

Schumacher, K., Vafeados, D., McCarthy, M., Sze, H., Wilkins, T., Chory, J. (1999). The Arabidopsis det3 mutant reveals a central role for the vacuolar H(+)-ATPase in plant growth and development. *Genes* **13**:3259-3270.

Schumaker, K.S. & Sze, H. (1987). Inositol 1,4,5-trisphosphate releases Ca^{2+} from vacuolar membrane vesicles of oat roots. *J. Biol. Chem.* **262**: 3944-3946.

Schumaker, K.S. & Sze, H. (1990). Solubilization and reconstitution of the oat root vacuolar H^+/Ca^{-2+} exchanger. *Plant physiol.* **92**: 340-345.

Schuurink, R.C., Shartzer, S.F., Fath, A. & Jones, R.L. (1998). Characterization of a calmodulin-binding transporter from the plasma membrane of barley aleurone. *Proc. Natl Acad. Sci. USA* **95**: 1944-1949.

Sedbrook, J.C., Kronebusch, P.J., Borisy, G.G., Trewavas, A.J., Masson, P.H. (1996). Transgenic AEQUORIN reveals organ-specific cytosolic Ca^{2+} responses to anoxia and Arabidopsis thaliana seedlings. *Plant Physiol.* **111**: 243-257.

Shacklock, P.S., Read, N.D., & Trewavas, A.J. (1992). Cytosolic free calcium mediates red light induced photomorphogenesis. *Nature* **358:** 153-155.

Shears, S.B. (2001). Assessing the omnipotence of inositol hexakisphosphate. *Cellular Signalling* **13**: 151-158.

Shi, J., Kim, K.-N., Ritz, O., Albrecht, V., Gupta, R., Harter, K., Luan, S. & Kudla, J. (1999). Novel protein kinases associated with calcineurin B-like calcium sensors in *Arabidopsis*. *Plant Cell*, **11**: 2393–2405.

Shigaki T, Cheng NH, Pittman JK, Hirschi K. (2001) Structural determinants of Ca^{2+} transport in the *Arabidopsis* H^+/Ca^{2+} antiporter CAX1.

Sienaert, I., Missiaen, L., De Smedt, H., Parys, J.B., Sipma, H., Casteels, R. (1997). Molecular and functional evidence for multiple Ca^{2+}-binding domains in the type 1 inositol 1,4,5-trisphosphate receptor. *J Biol Chem*. **272**: 25899-25906.

Sitsapesan, R. & Williams, A.J. (1995). cADPR and related compounds activate sheep skeletal sacroplasmic reticulum Ca^{2+} -release channel. *Am. J. Physiol.* **268**: 1235-C1240.

Sonnleitner, A., Conti, A., Bertocchini, F., Schindler, H., Sorrentino, V. (1998). Functional properties of the ryanodine receptor type 3 (RyR3) Ca^{2+} release channel. *EMBO J.* **17**: 2790-2798.

Sorrentino, V. (1995). The ryanodine receptor family of intracellular calcium release channels. *Adv Pharmacol.* **33**: 67-90.

Staxen, I., Montgomery, L., Hetherington, A.M. & McAinsh, M.R. (1996). Do oscillations in cytoplasmic free calcium encode the ABA signal in stomatal guard cells? *Plant Physiol.* **111**: S151.

Staxen, I., Pical, C., Montgomery, L.T., Gray, J.E., Hetherington, A.M. & McAinsh, M.R. (1999). Abscisic acid induces oscillations in guard-cell cytosolic free calcium that involve phosphoinositide-specific phospholipase C. *Proc. Natl Acad. Sci. USA* **96**: 1779-1784.

Strand, M., Louis, C. & Mickelson, J. (1993). Phosphorylation of the porcine skeletal and cardiac muscle sarcoplasmic reticulum ryanodine receptor. *Biochim. Biophys. Acta* **1175**: 319-326.

Strynadka, N.C., James, M.N. (1989). Crystal structures of the helix-loop-helix calcium-binding proteins. *Annu Rev Biochem.* **58**: 951-998.

Strynadka, N.C., James, M.N. (1991). Calcium-binding sites in proteins: a structural perspective. *Adv Protein Chem.* **42**: 77-144.

Subbaiah, C.C., Bush, D.S. & Sachs, M.M. (1994). Elevation of cytosolic calcium precedes anoxic gene expression in maize suspension-cultured cells. *Plant Cell* **6**: 1747-1762.

Südhof, T.C., Newton, C.L., Archer, III, B.T., Ushkaryov, Y.A. & Mignery, G.A. (1991). Structure of a novel Insp3 receptor. *EMBO J.* **10**: 3199-3206.

Supattapone, S., Worley, P.F., Baraban, J.M. & Snyder, S.H. (1988). Solubilization, purification and characterization of an inositol trisphosphate receptor. *J. Biol. Chem.* **263**: 1530-1534.

Takahashi, A., Camacho, P., Lechleiter, J.D., Herman, B. (1999) Measurement of intracellular calcium. *Physiol. Rev.* **79**: 1089-1125.

Takahashi, K., Kukimoto, I., Tokita, K, Inageda, K., Ionue, S, Kontani, K., Hoshino, S, Nishina, H., Kanaho, Y., & Katada, T. (1995). Accumulation of cyclic ADP-ribose measured by a specific radioimmunoassay in differentiated human leukemic HL-60 cells with all-*trans*-retinoic acid. *FEBS lett.* **371:** 204-208.

Takasago, T., Imagawa, T., Furukawa, K., Ogurusu, T. & Shigekawa, M. (1991). Regulation of the cardiac ryanodine receptor by protein kinase-dependent phosphorylation. *J. Biochem.* **109**: 163-170.

Takasawa, S., Tohgo, A., Noguchi, N., Koguma, T., Nata, K., Sugimoto, T., Yonekura, H. & Okamoto, H. (1993). Synthesis and hydrolysis of cyclic-ADP-ribose by human leukocyte antigen CD38 and inhibition of the hydrolysis by ATP. *J. Biol. Chem.* **268**: 26052-26054.

Takeshima, H., Nishimura, S., Matsumoto, T., Ishida, H., Kangawa, K., Minamino, N., Matsuo, H., Ueda, M., Hanaoka, Hirose, T. & Numa, S. (1989). Primary structure and expression from complementary DNA of skeletal muscle ryanodine ryceptor. *Nature* **339**: 439-445.

Tate, B.F., Schaller, G.E., Susman, M.R. & Crain, R.C. (1989). Characterisation of a polyphosphoinositide phospholipase C from the plasma membrane of *Avena sativa*. *Plant Physiol.* **91**: 1275-1279.

Taylor, A.R., Manison, N.F.H., Fernandez, C., Wood, J.W. & Brownlee, C. (1996). Spatial organization of calcium signalling involved in cell volume control of the Fucus rhizoid. *Plant Cell* **8**: 2015-2031..

Taylor, C.W. & Traynor, D. (1995). Calcium and inositol trisphosphate receptors. *J. Membrane. Biol.* **145**: 109-118.

Thiel, G., MacRobbie, E.A., Hanke, D.E. (1990). Raising the intracellular level of inositol 1,4,5-trisphosphate changes plasma membrane ion transport in characean algae. *EMBO J.* **9**: 1737-1741.

Thiel, G. & Blatt, M.R. (1994). Phosphatase antagonist okadaic acid inhibits steady-state K^+ currents in guard cells. *Plant J.* **5**: 727-733.

Thion, L., Mazars, C., Nacry, P., Bouchez, D., Moreau, M., Ranjeva, R. & Thuleau, P. (1998). Plasma membrane depolarization-activated calcium channels, stimulated by microtubule-depolymerizing drugs in wild-type *Arabidopsis thaliana* protoplasts, display constitutively large activities and a longer half-life in *ton2* mutant cells affected in the organization of cortical microtubules. *Plant J.* **13**: 603-610.

Thomas, A.P., Renard, D.C., Rooney, T.A. (1991). Spatial and temporal organization of calcium signalling in hepatocytes. *Cell Calcium* **12**:111-26

Thomas, J.A., Poland, B., Honzatko, R. (1995). Protein sulfhydryls and their role in the antioxidant function of protein S-thiolation. *Arch Biochem Biophys.* **319**: 1-9.

Thomashow, M.F. (1998). Role of cold-responsive genes in plant freezing tolerance. *Plant Physiol.* **118**: 1-8.

Thompson, J.D., Gibson, T.J., Plewniak, F., Jeanmougin, F. & Higgins, D.G. (1997). The CLUSTALX windows interface: flexible strategies for multiple sequence alignment aided by quality analysis tools. *Nucleic Acids Res.* **25**: 4876-4882.

Thuleau, P., Moreau, M., Schroeder, J.I., Ranjeva, R. (1994). Recruitment of plasma membrane voltage-dependent calcium-permeable channels in carrot cells. *EMBO J.* **13**:5843-5847.

Thuleau, P., Schroeder, J. & Ranjeva, R. (1998). Recent advances in the regulation of plant calcium channels: evidence for regulation by G-proteins, the cytoskeleton and second messengers. *Current Opinion Cell Biol.* **1**: 424-427.

Trewavas, A. (1999). Le Calcium, C'est la vie: Calcium makes waves. *Plant Physiol.* **120**: 1-6.

Trump, B.F., Berezesky, I.K. (1995). Calcium-mediated cell injury and cell death. *FASEB J.* **9**:219-228.

Van Camp, W., van Montagu, M., Inze, D. (1998). H_2O_2 and NO: redox signals in disease resistance. *Trends Plant Sci.* **3**: 330-334.

Van Eldik, L.J. & Watterson, D.M. (1998). *Calmodulin and Signal Transduction.* New York, USA: Academic Press.

Van Eldik, L.J., Zendegui, J.G., Marshak, D.R., Watterson, D.M. (1982). Calcium-binding proteins and the molecular basis of calcium action. *Int Rev Cytol.* **77**: 1-61.

Vanlingen, S., Sipma, H., Missiaen, L., De Smedt, H., De Smet, P., Casteels, R. & Parys, J.B. (1999). Modulation of type 1,2 and 3 inositol 1,4,5-triphosphate receptors by cyclic ADP-ribose and thimerosal. *Cell Calcium* **25**: 107-114.

Veena, V.S., Reddy, S.K. & Sopory, A. (1999). Glyoxalase I from *Brassica juncea*: molecular cloning, regulation and its over-expression confer tolerance in transgenic tobacco under stress. *Plant J.* **17**: 385-395.

Very, A.A., Davies, J.M. (2000). Hyperpolarization-activated calcium channels at the tip of Arabidopsis root hairs. *Proc Natl Acad Sci U S A*. **97**: 9801-9806.

Volotovski, I.D., Sokolovsky, S.G., Molchan, O.V., Knight, M.R. (1998). Second messengers mediate increases in cytosolic calcium in tobacco protoplasts. *Plant Physiol.* 117:1023-1030.

Wagenknect, T., Grassucci, R., Frank, J., Saito, A., Inui, M. & Fleischer, S. (1989). Three-dimensional architecture of the calcium channel/foot structure of the sarcoplasmic reticulum. *Nature*: **338**: 167-170.

Walseth, T.F. & Lee, H.C. (1993). Synthesis and characterisation of antagonists of cyclic-ADP-ribose-induced Ca^{2+} release. *Biochim Biophys. Acta.* **1178**: 235-242.

Walseth, T.F., Aarhus, R, Zeleznikar, R.J. Jr, Lee, H.C. (1991) Determination of endogenous levels of cyclic ADP-ribose in rat tissue. *Biochimica et Biophysica Acta* **1094:** 113-120.

Walton, T.J. (1995). Inositol lipid signal transduction in phytoalexin elicitation. *Biochem Soc Trans.* **23**: 862-867.

Wang XQ, Ullah H, Jones AM, Assmann SM. (2001). G protein regulation of ion channels and abscisic acid signaling in *Arabidopsis* guard cells. *Science* **292**: 2070-2072.

Ward, J.M. & Schroeder, J.I. (1994). Calcium-activated K^+ channels and calcium-induced calcium release by slow vacuolar channels in guard cells implicated in the control of stomatal closure. *Plant Cell* **6:** 669-683.

Watras, J., Bezprozvanny, I. & Ehrlich, B.E. (1991). Inositol 1,4,5-trisphosphate-gated channels in cerebellum: presence of multiple subconductance states. *J. Neurosci.* **11**: 3239-3249.

Webb, A.A.R., Larman, M.G., Montgomery, L.T., Taylor, J.E., and Hetherington, A.M. (2001). The role of calcium in ABA-induced gene expression and stomatal movements. *Plant J.* **26**: 351–362.

Webb, A.A.R., McAinsh, M.R., Taylor, J.E. & Hetherington, A.M. (1996). Calcium ions as intracellular second messengers in higher plants. *Advances in Botany Research.* **22**: 45-96.

Wendel, J.F., Cronn, R.C., Johnston, J.S., Price, H.J. (2002). Feast and famine in plant genomes. *Genetica*. **115**:37-47.

White, P., Bowen, H., Demidchik, V., Nichols, C., Davies, J. (2002). Genes for calcium-permeable channels in the plasma membrane of plant root cells. *Biochim Biophys Acta*. **1564**: 299.

White, P.J. (1993). Characterization of a high-conductance, voltage-dependent cation channel from the plasma membrane of rye roots in planar lipid bilayers. *Planta* **191**: 541-551.

White, P.J. (1994). Characterisation of a voltage-dependent cation channel from the plasma membrane of rye (*Secale cereale* L.) roots in planar lipid bilayers. *Planta* **193:** 186-193.

White, P.J. (1998). Calcium channels in the plasma membrane of root cells. *Ann. Bot.* **81:** 173-183.

White, P.J. (2000). Calcium channels in higher plants. *Biochim. Biophys. Acta* **1465**: 171-189.

Williamson, RE & Ashley C.C. (1982). Free Ca^{2+} and cytoplasmic streaming in in the alga *Chara. Nature* **296**: 647-651.

Wilmott, N., Sethi JK, Walseth TF, Lee HC, White AM, Galione A. (1996). Nitric oxide-induced mobilization of intracellular calcium via the cyclic ADP-ribose pathway. *J. Biol. Chem.* **271**: 3699-3705.

Wimmers, L.E., Ewing, N.N. & Bennet, A.B. (1992). Higer plant Ca^{2+}-ATPase: Primary structure and regulation of mRNA abundance by salt. *Proc. Natl Acad. Sci. USA.* **89**: 9205-9209.

Wu, Y., Kuzma, J., Maréchal, Graeff, Lee, H.C., Foster, R. & Chua, N-H. (1997). Abscisic acid signalling through cyclic ADP-ribose in plants. *Science* **278**: 2126-2129.

Wymer, C.L., Bibikova, T.N. & Gilroy, S. (1997). Cytoplasmic free calcium distributes during the development if root hairs of *Arabidopsis thaliana. Plant J.* **12:** 427-439.

Yoshida, A., Takahashi, M., Imagawa, T., Shigekawa, M., Takisawa, H. & Nakamura, T. (1992). Phosphorylation of ryanodine receptors in rat myocytes during beta-adrenergic stimulation. *J. Biochem.* **111**: 186-190.

Yoshikawa, F., Morita, M., Mankawa, T., Michikawa, T., Furuichi, T. & Mikoshiba, K. (1996). Mutational analysis of the ligand binding site of the inositol 1,4,5-trisphosphate receptor. *J. Biol. Chem.* **271**: 18277-18284.

Yu, J., Hu, S., Wang, J., Wong, G.K., Li, S., Liu, B., Deng, Y., Dai, L., Zhou, Y., *et al.* A draft sequence of the rice genome (*Oryza sativa* L. ssp. indica). *Science* **296**: 79-92.

Zaidi, A. & Michaelis, M.L. (1999). Effects of reactive oxygen species on brain synaptic plasma membrane Ca^{2+}-ATPase. *Free Rad. Biol. Med.* **27**: 810-821.

Zhang, B.-X., Zhao, H. & Muallem, S. (1993). Ca^{2+}-dependent kinase and phosphatase control inositol 1,4,5-triphosphate-mediated Ca^{2+} release. *J. Biol. Chem.* **268**: 10997-11001.

Zhang, P., Toyoshima, C., Yonekura, K., Green, N.M & Stokes, D.L. (1998). Structure of the calcium pump from sarcoplasmic reticulum at 8-angstrom resolution. *Nature* **392**: 835-839.

Zhao, M., Li., P., Li, X., Zhang, L., Winkfein, R.J. & Chen, S.R.W. (1999). Molecular identification of the ryanodine receptor pore forming segment. *J. Biol. Chem.* **274**: 25971-25974.

Ziegler, M., Jorcke, D., Schweiger, M. (1997) Identification of bovine liver mitochondrial NAD^+ glycohydrase as ADP-ribosyl cyclase. *Biochem J.* **326:** 401-405.

Zielinski, R.E. (1998). Calmodulin and calmodulin-binding proteins in plants. *Ann. Rev. Plant Physiol. Plant Mol. Biol.* **49**: 697-725.

Zimmermann, S., Nurnberger, T., Franchisse, J-M, Writz, W., Guern, J., Hedrich, R. & Scheel, D. (1997). Receptor-mediated activation of a plant Ca^{2+}-permeable ion channel involved in pathogen defense. *Proc. Natl Acad. Sci. USA* **94**: 2751-2755.